Orbital Control and Selectivity in Addition Reactions

A thesis

submitted in partial fulfilment

of the requirements for the Degree

of

Doctor of Philosophy in Chemistry.

in the

University of Canterbury.

by

Dugald Quentin McDonald

University of Canterbury

1991.

Contents

Abstract 1

Part I

1. The Application of Molecular Orbital Theory to the Diels-Alder Reaction 5
2. Semi-empirical Molecular Orbital Methods. 27
3. Diastereofacial Selectivity in the Diels-Alder Reaction. 51

Part II

4. The Application of Molecular Mechanics to Investigate Steric Influences in Determining Facial Selectivity. 87
5. Diastereofacial Selection in Diels-Alder reactions to a Cage Diol 97
6. Diastereofacial Selection in Diels-Alder Reactions of Mono and Dimethylidene Substituted Cage Dienes. 105
7. Synthetic Studies on Cage Compounds 115

Part III

8. The Application of Semi-empirical Methods to the Study of Reaction Pathways. 127
9. AM1 and PM3 Studies of the Diels-Alder Reactions of Acetylene. 133
10. AM1 Calculations of Acetylene Additions to Cage-fused Dienes 147
11. Orbital Mixing in Cage-fused Dienes and the Consequences for Diastereofacial Selection in Diels-Alder Reactions 157
12. Cycloaddition Reactions of Diimide 169
13. The "Cieplak" Effect. Direction of Reaction at Facially Dissymmetric π Systems by Hyperconjugative Interactions 185

Experimental 197

Crystallography 217

Computer Software 227

References 257

Acknowledgments 269

Abstract.

Several topics which are relevant to the results and methods in this thesis are examined in Part I. Recent developments in the application of molecular orbital theory to the Diels-Alder reaction and the history and development of semi-empirical molecular orbital methods are reviewed. A survey of the major developments in understanding diastereofacial selection in the Diels-Alder reaction is also included in Part I.

In Part II experimental and molecular mechanics studies are described for the addition of several azo, acetylenic and alkene dienophiles with four cage-fused dienes. Reactions of a dihydroxy substituted cage diene were found to proceed with complete selectivity for reaction from the face of the diene *anti* to the cyclobutane group, with the exception of the reaction of nitrosobenzene which was determined to be reversible. For most of the dienophiles, however, molecular mechanics calculations of the products in the reactions confirm that the relative stability of the adducts does not control the diastereofacial selection in the reaction. With a series of mono- and dimethylidene substituted cage-fused dienes, reactions of alkene dienophiles showed a strong preference for reaction from the *anti* face of the diene and this is successfully rationalized by a transition state model based on molecular mechanics. A series of mono and dimethylidene substituted cage dienes showed an opposing trend in facial selectivity, upon reaction with acetylenic dienophiles, to that observed with azo dienophiles. The selectivity observed for the reactions of acetylenic dienophiles cannot be rationalised by the "steric only" molecular mechanics based transition state models and this is interpreted as pointing to the importance of direct interactions between the substituents on the cage diene and the approaching dienophile. Several studies on the chemistry of cage-fused dienes are described with emphasis on the importance of transannular interaction during attempts to effect functional group interconversions of the cage substituents.

Part III of this thesis reports studies using the AM1 and PM3 molecular orbital methods to examine several systems where orbital control may be important in determining facial selection. The reaction of acetylene with both simple dienes and cage-fused dienes is

examined by application of the AM1 and PM3 methods. The reactions of acetylene with all the dienes studied are predicted to occur in reactions which are both concerted and synchronous. A detailed analysis of the energy changes in the molecular orbital energy levels during the reactions revealed destabilizing interactions involving the "orthogonal" HOMO of acetylenic dienophiles. These are important in determining the diastereofacial selection of reactions of acetylenic dienophiles with cage-fused dienes when there are suitably placed lone pairs on terminal substituents. The extent of σ/π interaction, determined by AM1 calculations for several cage-fused dienes, is shown to vary considerably with the nature of the cage substituents, but this is not considered to be an important factor in determining facial selection. As a model for substituted azo dienophiles, the Diels-Alder reactions of diimide (N_2H_2) have been studied by the PM3 method. This reaction is predicted to be both concerted and synchronous for the reaction of Z-diimide and butadiene in the *exo* mode but for the reaction of Z-diimide in the *endo* mode, the reaction is predicted to proceed via an unsymmetrical transition structure although still in a concerted reaction. The reaction of E-diimide with butadiene is considerably more complicated and three stationary points were located on the potential energy surface. The energy of aziridinium imide intermediates in possible two-step reactions of diimide and butadiene were evaluated by the PM3 method and determined to be approximately the same as the energy of the transition structures in the concerted reactions and so this precludes the involvement of these species in the reaction pathway. Finally the AM1 method was applied to examine the effect of substituents in determining the facial selection in the addition of methanol to 2,3-disubstituted-7-norbornanones and of ethylene to 5-substituted cyclopentadienes. Both of these systems have been proposed to show diastereofacial selection influenced by hyperconjugative stabilization. However, the AM1 method was not able to reproduce the observed facial selection in these reactions.

The operation and function of several computer programs developed during the course work for the graphical analysis of the results of molecular mechanics and molecular orbital calculations and for quantifying σ/π interaction in dienes are described in the appendix.

Part I.

Introduction.

1. The Application of Molecular Orbital Theory to the Diels-Alder Reaction.

A review of the major applications of variational and perturbational molecular orbital theory to understanding the mechanism and stereochemistry of the Diels-Alder reaction.

2. Semi-empirical Molecular Orbital Methods.

The history and theoretical basis of modern semi-empirical molecular orbital methods.

3. Diastereofacial Selectivity in the Diels-Alder Reaction.

A review of the Diels-Alder reactions of facially dissymmetric dienes and dienophiles with particular emphasis on the steric and electronic interactions which have been proposed to be important in determining diastereofacial selectivity.

Chapter 1.

The Application of Molecular Orbital Theory to the Diels-Alder Reaction.

In the time since the [π2 + π4] cycloaddition was first reported[1] by Diels and Alder in 1928, this reaction has been of considerable interest to synthetic organic chemists. This interest has not diminished in recent years; an examination of the number of abstracts listed with the Chemical Abstracts service which list the words "Diels-Alder" in the period 1967-1990 shows that the number of such references has at least kept pace with the total number of articles abstracted (Figure 1).

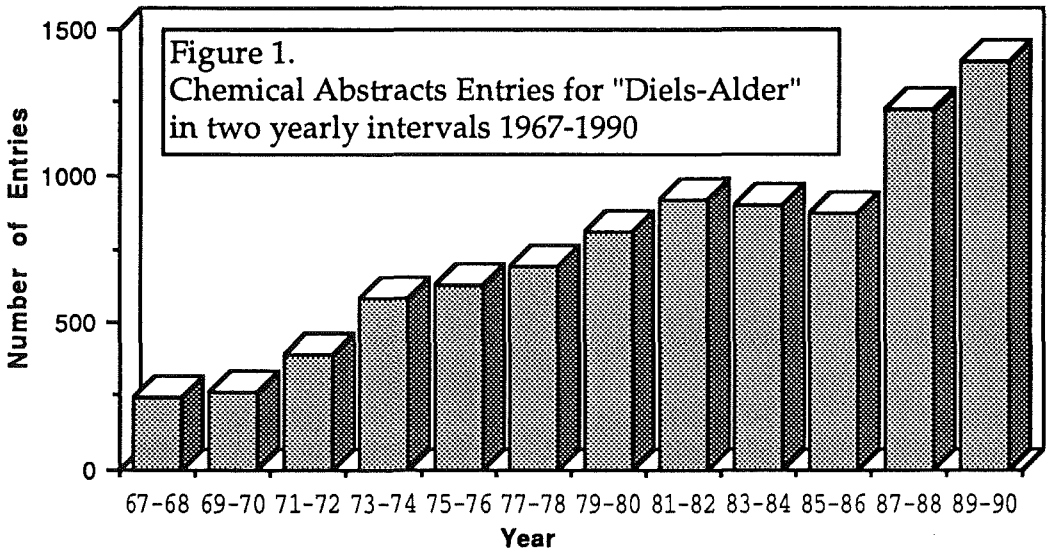

In addition to having tremendous synthetic utility, the apparent simplicity of the reaction, the fact that it is little influenced by external effects such as solvent, and the desire to understand and therefore gain greater control over the application of this reaction has been the impetus for a large volume of research into the mechanism. Because the limitations of experimental methods for elucidating the mechanism quickly became apparent, molecular orbital theory, in both quantitative and semi-quantitative forms, has played a vital role in developing an understanding, not only of the mechanism of the reaction but also of the regiochemistry.

By the beginning of the 1960's, two possible pathways had been delineated for the Diels-Alder reaction.[2] These two possible pathways are shown in Figure 2.

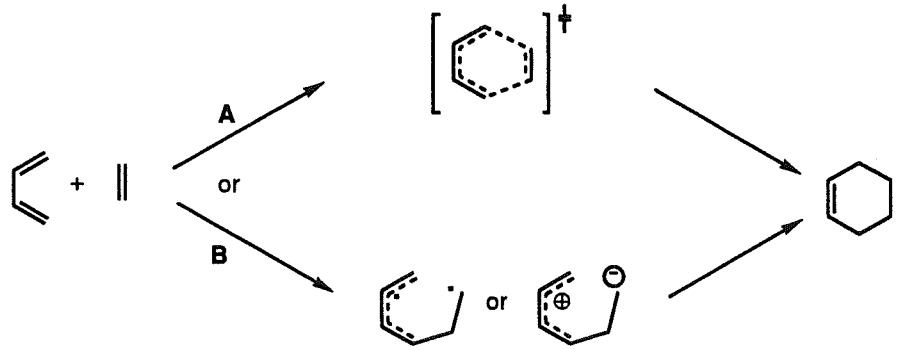

Figure 2. The two possible reaction mechanisms for the Diels-Alder reaction of ethylene and butadiene.

Route **A** in Figure 2 represents the formation of both of the new bonds of the reaction in one kinetic step without the intervention of any intermediate species.* The transition state for such a species is considered to be analogous to benzene and thus would be expected to be stabilized by aromaticity. The contrasting proposal is shown as route **B** in Figure 2 and involves the step-wise formation of each bond and the intermediacy of either a radical or zwitterionic species, before the formation of the second bond. While there was at the time the larger volume of evidence for the concerted process[3], some experimental evidence, particularly for unsymmetrical dienophiles, supported a mechanism with at least some degree of asynchronicity.[4] The apparently contradictory early experimental evidence opened the way for a number of molecular orbital based experimental studies which have proven to be important in elucidating the detailed mechanism of the reaction.

The application of molecular orbital theory to the Diels-Alder reaction has taken two main forms. The first is that based on a perturbational molecular orbital (PMO) approach, where quantitative and semi-quantitative procedures have been developed, largely to assist in understanding and predicting the stereochemistry of the reaction. These approaches are

* The following terms will be used in this section and these definitions will be used as given by Dewar[5];
- A *concerted* reaction takes place in a single kinetic step.
- A *two-step* reaction takes place in two distinct steps via a stable intermediate.
- A *synchronous* reaction is one in which all the bond-making and bond-breaking processes have proceeded to equal extents at the transition state.
- A *two stage* reaction is concerted, but not synchronous, thus some bonding changes occur mostly before the transition state and some mostly after the transition state.

usually based on assumptions about the mechanism of the reaction. The other area of development has concerned variational molecular orbital approaches. These range from early simple semi-empirical models to the more recent "state of the art" *ab initio* calculations. Such variational molecular orbital treatments have been of particular value in modelling the mechanism of the Diels-Alder reaction. A discussion of the major developments in each of these two area will be the subject of the remainder of this section.

Perturbational methods have the following basis:[6] For a time independent Hamiltonian H which cannot be solved by the expression

$$H\Psi_n = E_n\Psi_n \qquad 1$$

one considers a related system or systems which have a Hamiltonian H^0 which can be solved. The difference between the two Hamiltonians is a further Hamiltonian H' which is represented as follows:

$$H = H^0 + \lambda H' \qquad 2$$

where λ is a parameter which ranges from 0 to 1 and allows increasing perturbation of the zero-order H^0 system. If Ψ^0 is the wave function of the unperturbed system with energy E^0, and Ψ_n is the perturbed wave function then:

$$(H^0 + \lambda H')\Psi_n = E_n\Psi_n \qquad 3$$

and now E_n and Ψ_n depend on the degree of perturbation. The expressions for the required wavefunction E_n and Ψ_n can be expanded as a Taylor series in powers of λ such that

$$\Psi_n = \Psi_n^{(0)} + \lambda\Psi_n^{(1)} + \lambda^2\Psi_n^{(2)} + \lambda^3\Psi_n^{(3)} + \ldots + \lambda^k\Psi_n^{(k)} \qquad 4$$

$$E_n = E_n^{(0)} + \lambda E_n^{(1)} + \lambda^2 E_n^{(2)} + \lambda^3 E_n^{(3)} + \ldots + \lambda^k E_n^{(k)} \qquad 5$$

Thus the perturbation can be carried to any order k and will eventually converge to give the required wavefunction Ψ_n and energies E_n. Pauling[7] and Coulson[8] were the first to develop perturbation methods in the framework of molecular orbital theory and apply them to problems in organic chemistry. Their work was extended by Pople[9] who developed the theory in terms of LCAO molecular orbitals and applied it to the study of charge distributions in conjugated molecules.[10] McWeeny[11] later developed a procedure where the perturbation is applied directly to the Fock density matrix in a procedure known a self consistent perturbation theory. Since that time several schemes have been developed where the zero-order wavefunctions of the dienes and dienophiles are considered in a perturbation

treatment, usually to second order (k=2), as an approximation to the wavefunction for the transition state in the Diels-Alder reaction.

The most widespread application of perturbation theory to the Diels-Alder reaction has been based on the work of Fukui[12] which taken in conjunction with the "orbital symmetry" rules of Woodward and Hoffmann[13] provide a simple procedure which considers in a semi-quantitative manner the orbital interaction between two reacting species in a number of pericyclic reactions. This can be done without detailed calculations of the transitional species involved in the reaction. For the Diels-Alder reaction this theory is usually applied with the assumption that the most important stabilizing interaction during the reaction course is the two electron interaction involving the "frontier orbitals", the highest occupied molecular orbital (HOMO) with the lowest unoccupied molecular orbital (LUMO). In particular for the reaction of an electron deficient dienophile with a electron rich dienophile (the usual situation) the interaction of the $HOMO_{diene}$-$LUMO_{dienophile}$ is considered to be the most important interaction. The theoretical basis for the exclusion from consideration of the other possible symmetry allowed orbital interaction is discussed in the section on quantitative perturbational methods. It should be noted that the "frontier orbital" theory (FMO) is usually applied with the assumption that the Diels-Alder reaction takes place with a concerted mechanism. The frontier orbital theory itself cannot however be used to demonstrate that the reaction is concerted.

Frontier orbital theory, together with the Woodward-Hoffmann rules has most successfully been applied to the understanding of the regiochemistry of the Diels-Alder reactions of unsymmetrically substituted dienes and dienophiles.[14] This problem is shown in Figure 3. Houk[15] and others[16] have proposed a simple treatment for understanding

Figure 3. Regiochemical possibilities in the Diels-Alder reaction of a 1-substituted diene and a 1-substituted alkene.

and predicting the regiochemistry of such reactions based on experimentally determined and calculated orbital energies and calculated orbital coefficients for the frontier orbitals of

substituted dienes and dienophiles. Houk noted that conjugating substituents compress the HOMO/LUMO separation, electron releasing substituents raise both frontier orbitals while electron withdrawing substituents lower both frontier orbitals. With a knowledge of these factors, a prediction of the effect of substitution in the reactants on reaction regiochemistry becomes possible. For example, many Diels-Alder reactions are between dienes with electron rich substituents and dienophiles with electron withdrawing or conjugating substituents, and an example of this is the reaction of 1,3-pentadiene and acrolein (Figure 4).

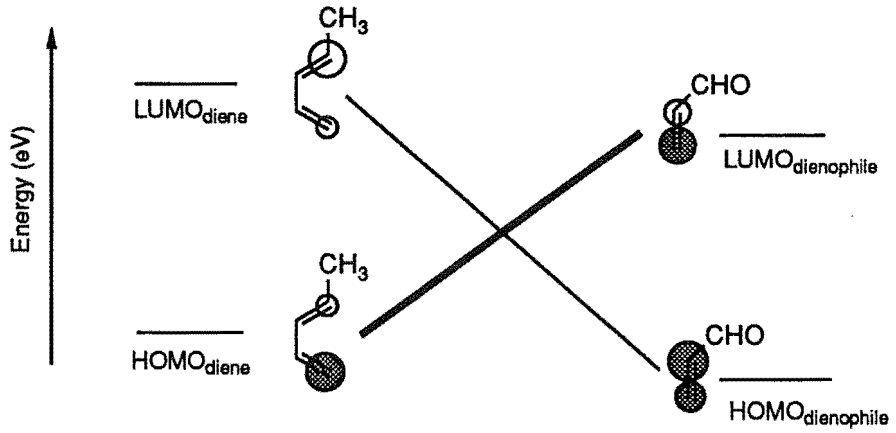

Figure 4. Schematic view of frontier orbital interactions for the Diels-Alder reaction of 1,3-pentadiene with acrolein. Circle sizes represent the magnitude of the orbital lobes at the termini.

FMO theory states that the strongest interaction will occur between the HOMO/LUMO pair which are closest in energy; in Figure 4 this is the $HOMO_{diene}$ and the $LUMO_{dienophile}$. In addition to this Houk pointed out that the reaction will occur so as to bring the large terminal atomic orbital coefficient in each species together. For the reactants shown in Figure 4 this would be the "ortho" reaction, and this is borne out by experiment.

While FMO theory is simple to apply and therefore popular with those who are primarily experimentalists, there are situations where it will fail in an unpredictable manner. Dewar,[17] has recently critically reviewed FMO theory and concluded that it "does not have a good basis in quantum mechanics". He proposes instead his own "PMO" theory of reactivity which he states can be applied with greater success.[18]

Perturbation theory has also been applied to the Diels-Alder reaction in a number of more quantitative treatments which consider not only the "frontier" orbital interactions, but all symmetry allowed orbital interactions between the two reacting species. The first

application of a quantitative perturbation theory to the Diels-Alder reaction was by Herndon and Hall[19] who used Hückel and extended Hückel molecular orbital methods to calculate the zero-order wavefunctions for a number of substituted butadienes and dienophiles. They found that consideration of only the HOMO/LUMO energy interactions was in fact satisfactory to predict the experimentally observed regiochemistry in the reactions they examined. In a later study Herndon[20] suggested that in reactions of cyano substituted dienophiles, biradical intermediates may be important because their Hückel-based quantitative perturbational calculations were successful in predicting the reaction partitioning in reactions such as **1** with butadiene to form **2** and **3**.

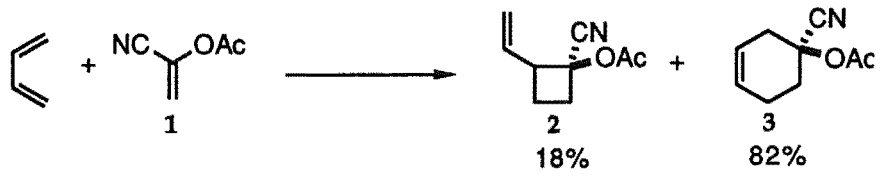

In contrast to the orbital perturbation theory used by Herndon, Sustmann et al.[21] extended the self-consistent perturbation methodology first developed by McWeeny[11] to a general form for two interacting systems and applied[22] it to the Diels-Alder reaction of cyclopropene and cyclopentadiene using the semi-empirical variational procedure MINDO/1 to calculate the zero-order wave functions of the reacting species. This reaction can occur with *endo* or *exo* stereochemistry as shown in Figure 5. The perturbation

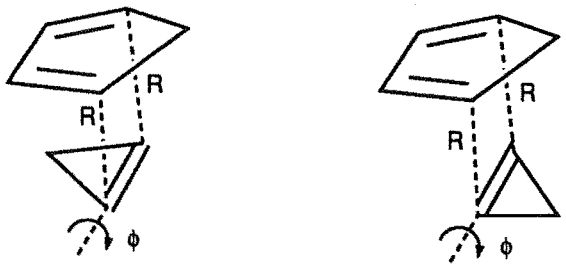

Figure 5. Geometry of *endo* and *exo* modes of addition for the reaction of cyclopropene with cyclopentadiene.

calculations were performed with the reaction distance R of 3 and 4 Å and with the angle ϕ between the planes of the reacting species varied over the range 0-130°. With R=4.0Å and ϕ=0° (parallel approach), the *endo* approach was calculated to be 6.9 kJ mol^{-1} more stable than the *exo* and this difference increased sharply with the closer approach of the two reactants in line with the experimentally observed preference for this reaction to occur in the *endo* mode. Cyclopropene has no "secondary" π system to undergo orbital overlap with the

diene so this commonly tendered explanation for the *endo* preference in such reactions is not applicable in this case. These perturbation calculations of Sustmann et al. were, however, unable to identify any one particular interaction as being important for the predicted *endo* selectivity.

The SCF perturbation method is of limited accuracy (especially when compared to comparable variational molecular orbital calculations) for the determination of total energies and does not allow easy interpretation of the results in terms of orbital interactions. The work of Salem[23] and Klopman[24] resulted in the development of a general treatment of chemical reactivity, which, while more quantitative than simple FMO theory, retains the advantages of all orbital perturbation techniques in that the results are easily interpreted in terms of the orbitals interactions with which organic chemists are familiar. Sustmann and Sicking have extended[25] these ideas in the framework of the MINDO/3 formulation and applied it to the Diels-Alder reactions of 2,3-bis(methylene)norbornane (4).

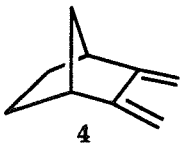

4

Their formulation is typical of PMO treatments and so will be discussed in some detail. Sustmann and Sicking[25] considered the perturbation to second order so the total perturbation energy (ΔE) is the sum of the first order ($\partial E^{(1)}$) and second order energy terms ($\partial E^{(2)}$) terms. Within the MINDO/3 formalism (see Chapter 2) the expressions for $\partial E^{(1)}$ and $\partial E^{(2)}$ are:

$$\partial E^{(1)} = \sum_k \sum_l (q_k q_l \gamma_{kl} + (\gamma_{N_k N_l} - \gamma_{kl}) C_k C_l f(R_{kl})) \qquad 6$$

for all atoms k on one system and l on the other with separation R_{kl}; total atomic charges q_k and q_l, core charges C_k and C_l ,total point charge repulsion between the atoms γ_{kl} and $\gamma_{N_k N_l}$ as the core-core repulsion integral. The second order energy term was considered as

$$\partial E^{(2)} = -2 \sum_U^{occ} \sum_P^{unocc} \frac{\left[\sum_\mu \sum_\lambda C_{U\mu} C_{P\lambda} \beta_{\mu\lambda} \right]^2}{E_U - E_P}$$

$$-2 \sum_P^{occ} \sum_U^{unocc} \frac{\left[\sum_\mu \sum_\lambda C_{P\mu} C_{U\lambda} \beta_{\mu\lambda} \right]^2}{E_P - E_U} \qquad 7$$

In equation 7 U denotes a molecular orbital on one system and P a molecular orbital on the other, with E_U and E_P as the one-electron orbital energies, $C_{U\mu}$ and $C_{P\lambda}$ as the molecular orbital coefficients for the atomic orbital μ in MO(U) on one system of the interacting pair and atomic orbital λ in MO(P) on the other. The term $\beta_{U\lambda}$ is the resonance integral between the two atomic orbitals on the different systems, which with the MINDO/3 approximation is a function of the overlap between those two atomic orbitals. The summation is over all the filled orbitals of the first system with all the unfilled orbitals of the second, and then all the unfilled orbitals of the first system with all the filled orbitals of the second. Equations (6) and (7) illustrate the basis for the consideration in simple FMO of only the HOMO/LUMO interactions. The first order perturbation is not considered in FMO because it is considered that for the reaction of two neutral species this term which depends on the atomic charge will be constant for most reactions. The second order term is simplified to just a consideration of the HOMO/LUMO interactions because the denominator in equation 7 is the energy difference of the filled and unfilled molecular orbitals in each system. This energy difference will be smallest for the HOMO/LUMO interaction and thus their contribution to the second order energy will be greatest.

Using expressions 6 and 7 and zero order wavefunctions calculated by the MINDO/3 or MNDO methods based on MNDO geometries, Sustmann and Sicking[25] calculated the interaction energy between diene **4** and several dienophiles at a separation of 2.5Å and planar with each face of the diene. The interactions were interpreted as the sum of three terms: charge and steric interaction (Eq. 6) and covalent interaction (Eq. 7). As expected, the charge interaction was not significant for the largely non-polar dienophiles which were examined, and the balance between the steric and covalent interactions was considered most important for determining the relative reactivity of the dienophiles consistent with experimental observations.

Sustmann et al.[26] later applied this method to the investigation of the prototype Diels-Alder reaction of ethylene and butadiene. They determined in this study that the geometry at which the PMO calculation is performed had a large influence on the relative importance of the various orbital interactions between the diene and the dienophile. For example when the geometry was performed for the geometry **A** shown in Figure 6, the

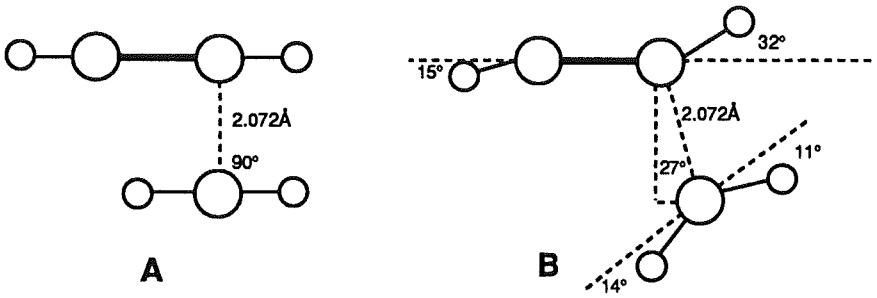

Figure 6 Side view of the geometries used in the PMO calculations for the reaction of ethylene and butadiene.

$HOMO_{diene}$-$LUMO_{dienophile}$ interaction was ca. 10 times bigger than the $HOMO_{dienophile}$-$LUMO_{diene}$ while for geometry **B**, these two interactions were of comparable magnitude as expected for this "neutral" Diels-Alder reaction. When the sum of the MINDO/3 calculated perturbation energy (Eq 6 + 7) was added to the MINDO/3 calculated heat of formation for ethylene and butadiene, it was approximately the same as the MINDO/3 calculated heat of formation for the complex **B** in Figure 6, demonstrating that evaluation of expressions 6 and 7 is an accurate method of estimating the interaction energy in such a reaction. In these quantitative studies the "frontier" orbital interactions dominate the second order term (Eq 7). This adds support for the use of the simpler semi-quantitative FMO methods as discussed earlier, especially in reactions where the coulombic interactions (Eq 6) are likely to be small.

The application of variational molecular orbital treatments to the Diels-Alder reaction has been limited by the ability to compute complete wavefunctions and energies for all the species involved, as the minimum reaction system has at least 32 valence electrons. Semi-empirical molecular orbital procedures have therefore played an important role. The earliest variational molecular orbital calculation for the Diels-Alder reaction was by Brown[27] who applied Hückel molecular orbital theory to an examination of the Diels-Alder reactions of a number of polycyclic aromatic hydrocarbons with maleic anhydride. He assumed that such reactions proceed in a concerted manner with simultaneous formation of the two new σ bonds and that the ease of formation of an adduct depends only on the energy required to localize two of the π-electrons of the diene. This allows the definition of a quantity known as the para-localization energy:

$$P = E_r - E + 2\alpha \qquad 8$$

where E is the Hückel π electron energy of the original conjugated system, 2α is the energy of the two localized electrons and E_r is the Hückel energy of the final non-conjugated isolated π systems. Brown calculated these values for a number of aromatic systems only some of which were known to undergo reaction with maleic anhydride and determined that the reaction will only occur if the localization energy P is less than 3.6. So benzene with a P value of 4.00 will not react, whereas anthracene with the 9,10 para value of 3.31 will react (Figure 7).

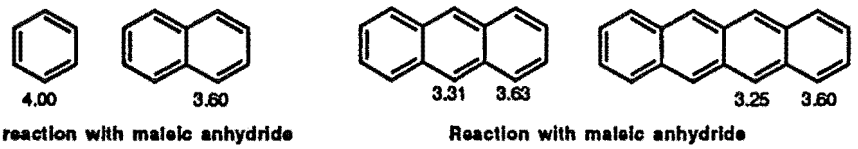

Figure 7. Paralocalisation energies for polycyclic aromatic hydrocarbons calculated by Brown[27]

These results allowed satisfactory prediction of the reactivity and position of reaction for a number of polycyclic aromatic hydrocarbons which had not previously been studied and Brown went on to extend the generality of this procedure by studying the effect of heteroaromatic substitution on the localization energy.[28] Hopff and Schweizer[29] also used the concept of localization energy in polycyclic aromatic hydrocarbons as an index of reactivity. By using an approximate method for determining the localization energy they were able to consider a number of large polycyclic hydrocarbons in reactions with maleic anhydride, benzoquinone, dimethyl acetylenedicarboxylate, and maleic ester and their predictions of reactivity were in good agreement with experiment. Streitwieser[30] later tried to extend the localization theory to predict the regiochemistry of Diels-Alder reactions by considering a different localization value for each carbon of the bonds which are formed during the reaction. While he had some success in reproducing experimental observations for conjugated systems, the method suffered from the limitations of the Hückel method (see Chapter 2) in that results were highly dependant on the choice of Hückel parameters.

The development of the "all-valence" SCF-MO method CNDO/2 allowed Kikuchi[31] to calculate the interaction energy, molecular and electronic structure and geometrical relationships of the reactants along the reaction path of ethylene and butadiene. In these calculations Kikuchi considered only the concerted, synchronous reaction with the length of each of the forming σ bonds held the same at all points along the reaction path, but he found no maximum in energy corresponding to a transition state for the reaction, and this was

considered as a deficiency of the CNDO/2 procedure. The CNDO/2 calculation however indicated that while the reactants may approach in a coplanar arrangement in the early stages of the reaction, the angle between the planes of the reactants changes to maximize orbital overlap between the termini of the reactants in the later stages of reaction. He also stated that σ-orbitals have to be considered in the molecular orbital correlation diagrams for the reactions because of the strong mixing of the π and σ orbitals during the reaction.

Ab initio molecular orbital theory was first applied to the Diels-Alder reaction by Burke et al.[32] in their study of the reaction of ethylene and butadiene. They used only a minimal STO-3G basis set to examine the reaction based on the variation of a small number of geometrical parameters and found a symmetrical structure corresponding to a maximum in energy which they reported was 87.0 kJ mol^{-1} above the energy of the reactants. The later study of Townshend et al[33] was more complete as they used a STO-3G basis set to thoroughly scan the potential energy surface and locate any energy extrema, including unsymmetrical species and then these stationary points were recalculated using the extended 4-31G basis set. In order to account for the effects of electron correlation they applied a 3X3 configuration interaction (CI) procedure and first calculated an energy difference between the products and reactants in the reaction of ethylene and butadiene of 143.9 kJ mol^{-1} at the 4-31G level of theory and this compared well with the experimental enthalpy of reaction of 135.4 kJ mol^{-1}. Complete optimization was not performed for all the geometrical variables involved in the reaction but they instead employed a coordinate system which they considered to be flexible enough to accommodate all conformations of interest, but in which all the C-H bond distances were held at standard values. Their detailed study of the reaction surface revealed that at both the STO-3G and extended 4-31G 3X3CI levels of theory the synchronous concerted reaction path with a symmetrical transition state was favoured. The geometry obtained for this transition structure is shown in Figure 8 and the calculated activation energy for the reaction was 178.2 kJ mol^{-1} at the 4-31G 3X3 CI level. They also located two other pathways on the 4-31G 3X3 CI potential energy surface, one where one of the σ bonds is first formed completely without participation from the other

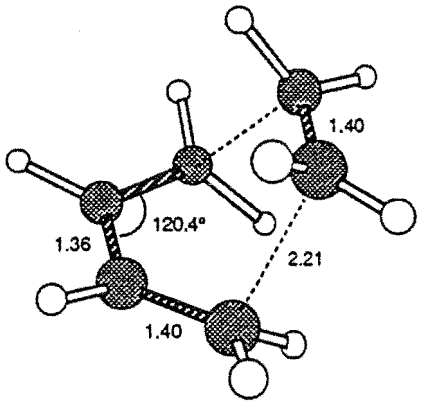

Figure 8. Main geometrical parameters from the 4-31G 3X3CI calculation by Townshend et al.[33] for the symmetrical transition structure in the Diels-Alder reaction of ethylene and butadiene.

terminus, and another in which the reaction follows a near concerted path until the reactants approach within about 2.2 Å then an antisymmetric bond rearrangement occurs. Both of these unsymmetrical paths were determined to be higher in energy relative to the concerted pathway.

While these *ab initio* calculations supported the existence of a concerted mechanism for the Diels-Alder reaction, at least for that of the reaction of ethylene and butadiene, the authors acknowledge that reactions with substituted dienes and dienophiles may proceed via the unsymmetrical, biradical pathway, which for the reaction of ethylene and butadiene is only ca. 8.4 kJ mol^{-1} higher than the concerted pathway. They also pointed out that the activation barrier for the reaction was largely due to the interaction of the filled π-orbital of the ethylene with the ψ_1 orbital of butadiene and that the stabilizing two electron interactions which are the basis of FMO theory may begin to contribute only at the region of the transition state with repulsive forces dominating until that point.

In contrast to these *ab initio* calculations the semi-empirical calculations of the time predicted that the reaction would proceed in preference via a two stage mechanism. McIver[34] performed MINDO/2 calculations on a C_S symmetry stationary point for the Diels-Alder reaction of butadiene and ethylene and determined that it was not a true transition state as there were two negative eigenvalues in the force constant matrix. The less negative of these roots corresponded to an unsymmetrical movement of the reactants leading towards an unsymmetrical transition structure of lower energy. He made no attempt to characterize

any possible unsymmetrical species with this method but rather argued on the basis of symmetry considerations and by analogy to the known stretching constants of stable molecules, that the transition structure in this reaction is unlikely to be symmetrical. Dewar[35] later reported a MINDO/3 calculation which came to the same conclusion as McIver regarding the symmetrical transition species being a second order stationary point which is higher in energy than the "true" unsymmetrical transition structure. With the inclusion of 2X2 CI the calculated activation energy for the reaction based on this unsymmetrical species was 117.8 kJ mol^{-1} which is in better agreement with the experimentally determined value of 115.1 kJ mol^{-1} than that obtained by the *ab initio* calculations for a symmetrical transition structure. No biradical intermediates were located with the MINDO/3 method and the reaction was concluded to be of the two-stage type[5] similar to that proposed by Woodward and Katz.[4]

Dewar[36] later extended his MINDO/3 CI results with a UHF-MINDO/3 study which used the unrestricted Hartree-Fock method to scan the potential energy surface and then recalculated the stationary points found with a MINDO/3 3X3 CI procedure. On the basis of these calculations he proposed that the reaction occurs with two transition states and an intermediate with considerable biradical character. The UHF-MINDO/3 potential energy surface for the reaction of ethylene and butadiene is shown schematically in Figure 9.

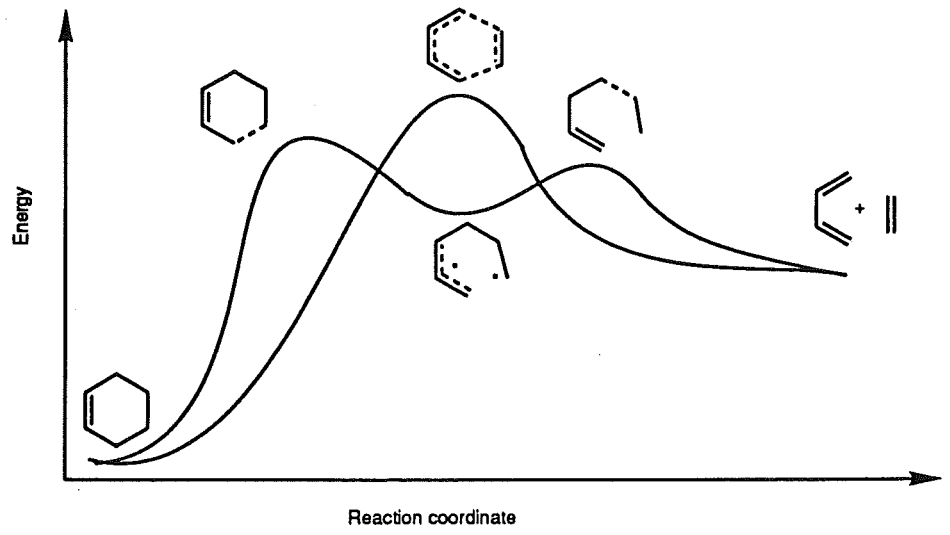

Figure 9. Schematic representation of the UHF-MINDO/3 potential energy surface for the retro Diels-Alder reaction of cyclohexene into butadiene and ethylene.

The MINDO/3 calculations of Dewar were also able to successfully reproduce the

experimentally observed kinetic isotope effects in the retro-Diels-Alder reaction of the bicyclo[2.2.2]octadiene **5** to anthracene **6**. These kinetic isotope effects had been previously

5 **6**

considered as evidence for the reaction occurring in a concerted synchronous manner, but Dewar was able to reproduce them based on calculations which predict an asynchronous reaction.

On the basis of his MINDO/3 study Dewar concluded that the use of such semi-empirical molecular orbital methods was more appropriate for this study than the *ab initio* procedure which has been applied by Burke et al.[32] and Townshend et al.[33] because the use of the less time intensive MINDO/3 method allows full optimization of all the geometric variables and thus a full exploration of the potential energy surface for the reaction. The *ab initio* calculations were carried out by a cyclic variation of only a selected number of geometrical co-ordinates and this is an unsatisfactory procedure for all but the smallest multi-atom systems. Furthermore, neither of the groups using the *ab initio* methods, Burke et al.[32] and Townshend et al.[33], had attempted to calculate and diagonalize the force constant matrix for the stationary points and were therefore unable to establish whether these points were true maxima or minima on the potential energy surface. Dewar contended that if they had applied these procedures with the *ab initio* methods then their conclusions may have been in agreement with the MINDO/3 results. Dewar later went on to generalize his conclusions from the MINDO/3 studies of the Diels-Alder reaction and reported his view that "Multi-bond reactions cannot normally be synchronous".[37]

Although the results of the *ab initio* and semi-empirical molecular orbital calculations are apparently at variance they both in fact report a potential energy surface with largely the same gross features; a concerted pathway with a symmetrical transition structure and an asynchronous pathway with two transition states and an intermediate with some biradical character (Figure 9). These two pathways have been predicted by both methods to be close in energy but the relative energetic ordering of each possibility is dependent on the method. To distinguish between two possible pathways which are close

(ca. 8.4 kJ mol^{-1} difference) in energy is a demanding test for any molecular orbital method. The key discrepancy is in the relative stabilization which each of the main types of procedure predicts for species with significant biradical procedure. The UHF-MINDO/3 method may in fact overestimate the stability of such species[38] as the effects of electron correlation are already included in the parameterization of MINDO/3 where the parameters are adjusted to reproduce experimental data. In contrast the *ab initio* methods of Townshend et al.[33] do not fully include the effects of electron correlation and may have seriously underestimated the stability of species with some biradical character. Ortega[39] performed a series of calculations which showed that the inclusion of correlation energy by a perturbation treatment to third order (MP3) in *ab initio* calculations favoured the asynchronous reaction path, but these calculations were not performed with full geometry optimization and no stationary points were characterized.

Only recently has an increase in computation power allowed geometry optimization for systems such as the reaction of ethylene and butadiene to be carried out with complete optimization of all geometrical variables. In addition to this recent advances in semi-empirical methods allow a more realistic evaluation of the energy of species with biradical character.

The first *ab initio* calculation of the symmetrical reaction pathway for the Diels-Alder reaction of ethylene and butadiene with complete optimization of all geometrical variables was performed at the STO-3G level of theory by Houk and Brown.[40] They confirmed that this structure is an authentic transition state on the STO-3G potential energy surface as it had exactly one imaginary vibrational frequency. The activation energy was calculated to be 150.6 kJ mol^{-1} , the geometry of the C_s stationary point is shown in Figure 10. The effect of a gradient optimization on all geometrical variables was to produce a geometry which reveals several structural features of the transition state which were not identified in the earlier *ab initio* calculations. For instance the hydrogens at C2 and C3 of the diene are bent out of the plane of the diene by 14.0°, towards the approaching dienophile. Houk considered that this bending occurs in order to maintain overlap with the terminal diene methylene groups (C1 and C4), which themselves have rotated in order to obtain the best possible overlap with the approaching dienophile and that this bending may have

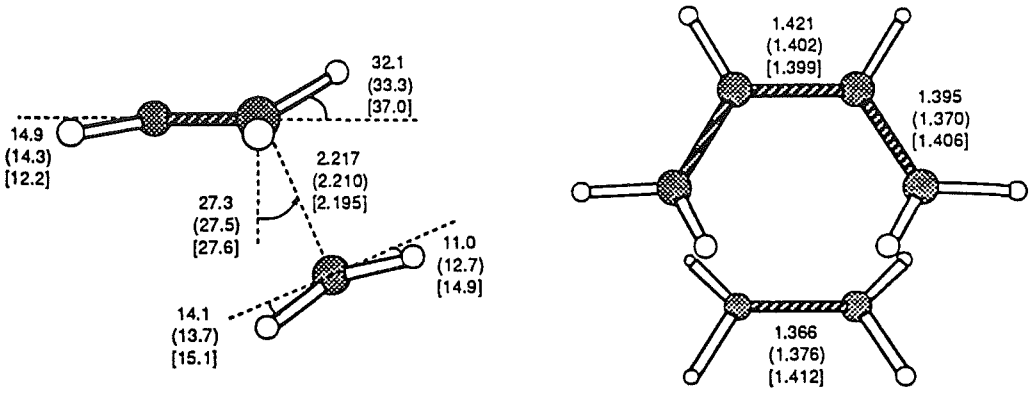

Figure 10. Transition state geometries calculated by Houk et al.[40,41] for the symmetrical transition structures in the Diels-Alder reaction of ethylene and butadiene. Parameters are from STO-3G, RHF 3-21G (parenthesis) and UHF 3-21G [square brackets] calculations.

important consequences for determining the facial selectivity in the reactions of dienes which are fused to norbornane skeletons (See Chapter 3). Houk later[41] re-investigated this transition structure using a split valence basis set, 3-21G in both restricted (RHF) and unrestricted (UHF) HF methods. The geometries obtained in these studies are also shown in Figure 10, and the calculated activation energies are as follows: 150.2 kJ mol^{-1} (RHF/3-21G) and 116.3 (UHF/3-21G). Although the UHF value for activation energy gives better agreement with experiment than the RHF one, the UHF/3-21G stationary point was calculated to have two imaginary frequencies, indicating the existence of a lower energy unsymmetrical transition state on the potential energy surface at that level of theory. Houk, however, considered that the UHF calculations are biased towards species with a biradical character since the UHF wavefunction is approximately 50% triplet.

In order to be able to quantify which of the two reaction pathways will be favoured for the prototype reaction of ethylene with butadiene, Bernardi et al.[42] carried out an extensive survey of the potential energy surface using the multi-configurational self-consistent field method (MCSCF). A complete active space (CAS) wavefunction was used which involved either Ψ_2 and Ψ_3 of the butadiene and π and π^* of the ethylene (CAS1) or all four π molecular orbitals of the butadiene and the π and π^* orbitals of ethylene (CAS2). They considered, on the basis of analogous studies of related cycloadditions[43] that this method would allow for a reliable evaluation of both the biradical species in the unsymmetrical pathway and the closed shell transition state for the concerted process. They used both minimal (STO-3G) and extended (4-31G) basis sets with gradient optimization for

all geometrical variables. A transition structure for the symmetrical reaction pathway was located and the geometry is shown in Figure 11. The calculated activation energy for

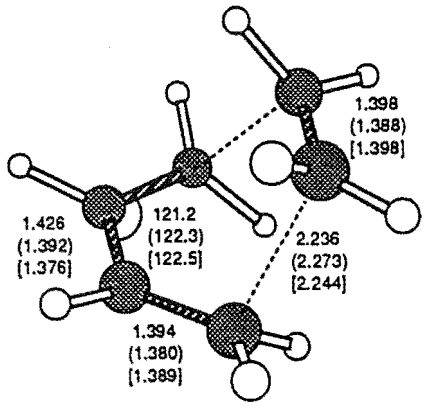

Figure 11. Main geometrical parameters from the MC-SCF calculations by Bernardi et al. for the transition structure in the Diels-Alder reaction of ethylene and butadiene. Parameters are from CAS1 STO-3G, CAS2 STO-3G (parenthesis) and CAS1 4-31G [square brackets] calculations.

the 4-31G CAS concerted pathway was found to be 139.3 kJ mol^{-1} which was 8.4 kJ mol^{-1} lower than the lowest energy transition state on the alternative unsymmetrical pathway. While they point out that the 8.4 kJ mol^{-1} may not be significant at the level of theory used, they suggest on the basis of results obtained with calculations for 1,3 dipolar additions that the inclusion of dynamic electron correlation would favour the synchronous path. They do, however, concede that substituents on the dienophile or diene may result in a different potential energy surface for the reaction and the asynchronous mechanism may be important for these cases.

Recent *ab initio* calculations by Bach et al.[44] for the reaction of ethylene and butadiene utilized the RHF method, but employed large basis sets including polarization functions and used Møller-Plesset (MP) perturbation theory to estimate the effects of electron correlation. Only the symmetrical pathway was examined and the transition structure obtained was similar to that obtained by Bernardi et al.[42] as shown in Figure 11. The calculated activation energy at the highest level of theory used (106.3 kJ mol^{-1}, MP4SDTQ/6-31G*) compares favourably with the experimental value of 115.1 kJ mol^{-1}. Bach et. al.[44] analyzed the orbital changes during the reaction and concluded that the activation energy is mainly due to closed-shell repulsions between the filled orbitals of the

reactants. Surprisingly, they determined that not only four-electron, but also two-electron interactions at the transition state are net destabilizing. This has important ramifications for FMO theory as one of the most important assumptions of this theory is that such two electron interactions at the transition state are the major stabilizing interactions of the reaction. Coxon et al.[45] have reported a related calculation for the reaction of acetylene and butadiene and concluded that the higher activation barrier (119.7 kJ mol^{-1}, MP4SDQ/4-31G//HF/4-31G) for the reaction of acetylene and butadiene with respect to that calculated for the reaction of ethylene is the result of the increase in energy of the filled π orbital of the acetylene which is not undergoing bonding changes during the reaction.

While the prototype Diels-Alder reaction of ethylene and butadiene has been the subject of most applications of variational molecular orbital calculations to understanding this reaction, recent advances in computer power and the development of reliable semi-empirical molecular orbital methods have made possible the study of the Diels-Alder reaction of substituted dienophiles and dienes by molecular orbital calculations. These substituted cases are particularly important as there is a greater volume of experimental data for comparison purposes for the reactions of substituted dienophiles compared with the reaction of ethylene, and calculations for substituted systems will allow investigation of the influence of substituents on reaction regiochemistry and stereochemistry.

Dewar reported[5] application of his AM1 and MNDO semi-empirical methods to the reaction of butadiene with ethylene and cyanoethylenes **7-11**. While the results obtained

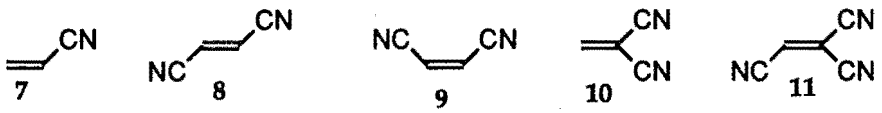

with the MNDO method continue to predict that an asynchronous reaction pathway would be favoured, the newer AM1 method is the first semi-empirical method which favours the synchronous, concerted pathway with the geometry of the AM1 calculated transition structure for the reaction of ethylene similar to those obtained by the high level *ab initio* calculations and only small deviations from complete symmetry obtained for the reactions of the unsymmetrical cyanoalkenes **8**, **10** and **11**. Dewar, however, has stated his belief, that AM1, bring a RHF procedure, underestimates the stability of the biradical-like species in the unsymmetrical pathway and therefore erroneously favours the synchronous pathway.

The AM1 calculations also failed to reproduce the experimentally observed greater reactivity of the cyanoalkenes, predicting **7-11** to be considerably *less* reactive than ethylene towards butadiene. He believes that calculations using the UHF versions of AM1 and MNDO and those including a 3X3 configuration interaction are suitable for the study of the Diels-Alder reaction. These methods produce results similar to those from MINDO/3 as discussed earlier, favouring a reaction pathway with two unsymmetrical transition states and a biradical intermediate. These conclusions were paralleled in a RHF and UHF AM1 study of the potential energy surface for the reactions of cyano-substituted ethylenes and substituted butadienes by Choi and Lee.[46] In this case the RHF-AM1 method consistently predicted a concerted reaction pathway with a symmetrical (or near symmetrical) transition structure but like the results of Dewar, the RHF-AM1 calculated activation barriers were at variance with experimental observations in that alkenes with electron withdrawing substituents were predicted to be less reactive towards butadiene than ethylene and the reactions of all dienophiles with cyclopentadiene were predicted to occur with a greater barrier than with butadiene. With the UHF-AM1 method a detailed search of the potential energy surface was carried out and four transition structures (two of which had been identified by Dewar) and two intermediates with a biradical character were predicted to occur along the asynchronous reaction path of ethylene and butadiene. The substituent effects calculated with the UHF AM1 method were in better agreement with experiment than the RHF-AM1 results and this was considered as evidence that the Diels-Alder reaction will have an asynchronous mechanism.

Houk[47] has re-investigated by the application of *ab initio* methods some of the reactions of cyano-substituted alkenes which were studied with semi-empirical methods as described above. He obtained symmetrical or near symmetrical transition structures at the RHF 3-21G level of theory for the reaction of cyanoalkenes **7-11** with butadiene for which, while the transition state geometries obtained were similar to the AM1 results reported by Dewar, the variation of calculated activation energy with increasing cyano substitution is more in line with the experimental observation that cyanoalkenes are more reactive towards butadiene than ethylene. Houk also examined the 3-21G and AM1 transition structures for the reactions of ethylene and acrylonitrile with cyclopentadiene and again

only the *ab initio* calculation was able to correctly predict the greater reactivity of cyclopentadiene relative to butadiene. Neither method of calculation was however able to correctly predict the experimentally observed preference for the addition of acrylonitrile to butadiene and cyclopentadiene in the *endo* mode, with both 3-21G and AM1 methods predicting that the *exo* mode would be favoured by ca. 1.3 kJ mol^{-1}.

In order to investigate the influence of Lewis acid catalysis on reactivity and stereochemistry in the Diels-Alder reaction, Houk[48] has performed calculations at the 3-21G level of *ab initio* theory for the reaction of butadiene with an acrolein-BH_3 complex.

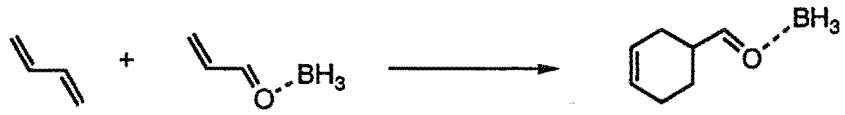

The transition structures for each of the four possible modes of reaction showed a considerably greater degree of asymmetry than those calculated for the uncatalysed reaction but the reaction was considered to be still concerted for all possible modes. Single-point calculations were performed at the higher 6-31G* level on the 3-21G optimized geometries, and from these calculations the *endo* mode of addition was predicted to be more favoured when the BH_3 is coordinated to the acrolein than for the uncatalysed reaction, consistent with the experimentally observed increased *endo* preference with Lewis acid catalysis of this reaction. Houk examined the differences in a number of calculated properties between the transition structures for the catalyzed and uncatalysed reaction and concluded that both increased frontier orbital interaction and the resulting charge separation and dipole interaction are important in lowering the activation energy and enhancing the *endo* selectivity of the catalyzed reaction.

Molecular orbital theory in a number of forms ranging from simple FMO theory to high level *ab initio* calculations have therefore played an important role in focussing attention on the mechanistic detail of the Diels-Alder reaction which if understood would improve our ability to utilize this reaction in chiral and stereoselective syntheses. While the perturbation theory approaches may be useful if carefully applied to the prediction of reaction regiochemistry, the information which these simple treatments can provide about the nature of the mechanism of the Diels-Alder reaction is limited.

With the recent increase in computer power it is becoming increasingly possible to

apply variational molecular orbital calculations to explore transition state geometry and energy rather than taking ground state arguments and parameters to estimate qualitatively relative transition state energies. The most recent high level *ab initio* calculations strongly support a synchronous concerted mechanism with a single symmetrical or near symmetrical transition state. This is also the conclusion drawn from the most recent measurements of kinetic isotope effects for the reaction of isoprene with a number of deuterium substituted dienophiles.[49] Modern semi-empirical calculations such as those using the AM1 method predict a similar concerted reaction mechanism to that from *ab initio* calculations but are less successful in reproducing experimentally observed effects on reactivity of substitution in the diene or dienophile. There are however still many aspects of the Diels-Alder reaction which remain to be rationalized, most notably the diastereoselection observed with many facially dissymmetric dienes, and molecular orbital theory will no doubt play an important role in future research directed towards elucidating the details of such processes.

Chapter 2.

Semi-empirical Molecular Orbital Methods.

Semi-empirical methods are those which combine simplified quantum theory and experimentally derived parameters with the aim of allowing the computation of molecular properties (energies, geometries, electronic structure etc) to a high degree of accuracy and with minimal computational effort. This section will be devoted to a discussion of the development of some widely used semi-empirical molecular orbital methods, with particular emphasis on those which contributed to the development of the modern methods which have been utilized in this work.

Where it all began.

Semi-empirical methods have a foundation in common with all quantum chemistry, namely the work of Erwin Schrödinger which was carried out in the early part of this century. He built on the wave mechanics of de-Broglie and the atomic structure proposed by Bohr to develop the quantum mechanical description of a set of interacting particles - the nuclei and electrons in a molecule. This is succinctly represented by the time independent Schrödinger wave equation (SWE).

$$\{ T + V \} \Psi = E \Psi \qquad 9$$

Here **T** and **V** are linear operators for kinetic and potential energy respectively and Ψ is the "wave function" which describes the spatial distribution of the particles.

A direct solution of the SWE is only possible for one electron systems such as the hydrogen atom. In order to apply this theory to multi-electron systems a series of approximate theoretical treatments are applied. The basis of these is the Hartree-Fock approximation. Here the total energy of a system can be described as the sum of a number of terms:

$$E = \sum_{i}^{n} h_i + \frac{1}{2} \sum_{i\,j}^{n} (J_{ij} - K_{ij}) + \sum_{\kappa\,\lambda}^{n} Z_\kappa Z_\lambda / (R_\kappa - R_\lambda) \qquad 10$$

The h_i term represents the kinetic energy of the electron and the interaction with the nucleus

and is given by

$$h_i = \int \phi_i(k) \left(-\frac{1}{2}\nabla^2_k - \Sigma Z_k/(r - R_k) \right) \phi_i(k)\, d\tau \qquad 11$$

The J term represents the classical representation of the electrostatic charge repulsion between the two charge distributions and is given by:

$$J_{ij} = \int\int \phi^*_i(k)\, \phi_i(k)\, (R_k - R_l)^{-1}\, \phi^*_j(l)\, \phi_j(l)\, d\tau\, d\tau \qquad 12$$

This classical repulsion is modified by the K_{ij} term which represents the "exchange integral":

$$K_{ij} = \int\int \phi^*_i(k)\, \phi_j(k)\, (R_k - R_l)^{-1}\, \phi^*_j(l)\, \phi_i(l)\, d\tau\, d\tau \qquad 13$$

This represents the bonding contribution between electron distributions.

Values for ϕ_i can be established by minimizing the energy with respect to variations in ϕ_i which by the "variation principle" will give the best possible set of ϕ - this is the Hartree-Fock wavefunction. The minimization of the energy can be expressed in terms of n simultaneous equations of the form:

$$F(k)\, \phi_i(k) = \varepsilon_i \phi_i(k) \qquad 14$$

Here F(k) is the Fock operator and is the sum of a one-electron term, H(k), and a multielectron term G(k). Generally the solution of ϕ_i is determined by assuming some form of the starting orbitals, substituting the appropriate calculated values into equation 8 to obtain a further set and repeating in an iterative process until no change is observed in the orbitals; the system has then become "self-consistent" and this method is known as the Self Consistent Field (SCF) method. Thus the detailed treatment of the repulsions of every pair of electrons required in the SWE has been approximated by a treatment that considers the average field that each electron exerts on all other electrons. This process however makes no allowance for the fact that the in multielectron systems electron motion is not independent but rather the motion of the electrons is correlated in order to ensure that the inter-electron repulsion is kept to a minimum. The SCF procedure can not therefore be used accurately to calculate the total energy of a system - the value obtained will always be in error by an amount that is, by definition, the correlation energy of the system. Semi-empirical methods

correct for this correlation by the inclusion of parameters in the expressions for H and G which are derived from experimentally derived quantities. In this way the effect of electron correlation can be "compensated".

The Hartree-Fock equation can be solved numerically for atoms but in molecular systems with lower symmetry this is not practical. A milestone in quantum chemistry was reached in the early 1950's when Roothaan[50] and Hall[51] independently developed an implementation of the variation method which involves the use of the atomic orbitals, ϕ, in a molecule as the basis functions Φ. This treatment is known as the Linear Combination of Atomic Orbitals - Self Consistent Field (LCAO-SCF) method. In a molecule the electrons are considered to occupy, in pairs, a set of molecular orbitals ψ_j. First we consider that the electrons μ and υ reside in atomic orbitals ϕ_μ and ϕ_υ centered on atom A and λ and σ reside in ϕ_λ and ϕ_σ on atom B. So with this notation for n atomic orbitals:

$$\psi_i = \sum_i^n \phi_\upsilon C_{\upsilon i} \qquad 15$$

and $$\sum C_i(F_{\mu\upsilon} - S_{\mu\upsilon}\varepsilon_i) = 0 \qquad 16$$

The term $S_{\mu\upsilon}$ is known as the "overlap integral" and is defined as :

$$S_{\mu\upsilon} = \int \phi_\upsilon^* \phi_\mu \, d\tau \qquad 17$$

The multi-electron Fock matrix $F_{\mu\upsilon}$ can be considered the sum of a one electron term and a two electron term as discussed above. So

$$F_{\mu\upsilon} = H_{\mu\upsilon} + G_{\mu\upsilon} \qquad 18$$

$H_{\mu\upsilon}$ is the matrix element of the one-electron Hamiltonian which includes the kinetic and potential energy for electrons in the field of the core. So

$$H_{\mu\upsilon} = \int \phi_\mu [-\tfrac{1}{2}\nabla^2 - \Sigma V_a(R)] \phi_\upsilon \, d\tau \qquad 19$$

$G_{\mu\upsilon}$ is the matrix element which depends on the other valence electrons and so is written

$$G_{\mu\upsilon} = \sum_{\lambda\,\sigma} P_{\lambda\sigma} [(\mu\upsilon/\lambda\sigma) - \tfrac{1}{2}(\mu\sigma/\mu\lambda)] \qquad 20$$

$G_{\mu\upsilon}$ depends on the molecular orbitals as indicated by the presence of the density matrix $P_{\lambda\sigma}$ in equation 20.

$$P_{\lambda\sigma} = 2 \sum_i C_{i\lambda} C_{i\sigma} \qquad 21$$

The two electron integrals are defined as

$$(\mu\upsilon/\lambda\sigma) = \int\int \phi_\upsilon(1)\,\phi_\mu(1)\,\frac{1}{R_{12}}\,\phi_\lambda(2)\,\phi_\sigma(2)\;d\tau \qquad 22$$

There is a large number of such two-electron multi-dimensional integrals to evaluate in most calculations on polyatomic species. Consequently these are always prime targets for approximation in semi-empirical treatments.

Finally the electronic energy of a system is given by

$$E_{el} = \frac{1}{2}\sum_{\mu\,\upsilon} P_{\mu\upsilon}\,(F_{\mu\upsilon} + H_{\mu\upsilon}) \qquad 23$$

and the total energy is the sum of the electronic energy and the total repulsion energy between the cores.

$$E_{tot} = E_{el} + \sum_{A}^{N}\sum_{B}^{N} Z_A\,Z_B\,/\,R_{AB} \qquad 24$$

So with the development of this Roothaan-Hall formalism it was now possible to begin direct meaningful calculations of the wavefunction (and consequently the properties) of a molecular system. And it was soon after that what was described by Robert Parr[52] as a "fundamental dichotomy" arose. The elements of the Fock matrix in equation 18 can be calculated from a knowledge of the basis functions - the atomic orbitals. This purely theoretical approach became known as the *ab initio* (meaning quite literally "from the start") approach, the calculation of molecular properties from the fundamental constants of physics. It would seem that this approach should be the aim of everyone attempting to use calculations for chemical applications. There are however two important problems. The first is that *ab initio* calculations are still dependent on the LCAO-SCF method and so their accuracy is bound by the limits of this approximation. Consequently the results of *ab initio* calculations are often not accurate enough to be chemically useful, particularly if a minimal basis set of atomic orbitals is used. More importantly the time taken for *ab initio* calculations is considerable as a large number of electron interaction integrals must be evaluated. For this reason the calculations before the development of high speed computers were limited to simple diatomic molecules. There was still, however, a demand from chemists to be able to calculate the properties of a wide range of molecules, with reasonable accuracy and at modest cost. Consequently methods were developed which use less rigorous approximations in the Roothaan-Hall treatment, but include the use of experimentally derived parameters to allow calculations to proceed economically and with useful accuracy.

These are the semi-empirical molecular orbital methods and will be the topic of the remaining discussion.

The Hückel Molecular Orbital Theory. (HMO)

The Hückel molecular orbital theory[30,53] is the oldest semi-empirical molecular theory dating back to the 1930's. It is suitable in its most basic form only for large, planar, conjugated molecules as central to the Hückel theory is the concept that in these molecules the interaction between the π electrons and the σ electrons is small. If this is so then the π-electrons may be treated as a loosely bound group of electrons moving in the field of a core made up of the σ electrons and the nuclei. This is essentially a one-electron treatment with the multielectron matrix element F_{ij} in equation 18 being approximated by a one-electron term H_{ij}^{π}. In its most basic form the HMO theory applies four approximations during the evaluation of the one electron matrix. The first is that of zero differential overlap. That is to say the overlap integral S_{ij} as defined in equation 17 is simply treated as

$$S_{ij} = \delta_{ij} \qquad 25$$

where δ_{ij} is known as the Kronecker delta and $\delta_{ij}=1$ if i=j and $\delta_{ij}=0$ if i≠j.

Secondly the diagonal terms H_{ii}^{π} which represent the coulombic integrals in the molecule are set to a common value for every equivalent center in the molecule so

$$H_{ii}^{\pi} = (\phi_i / H^{\pi} / \phi_j) = \alpha \qquad 26$$

The resonance integral is also set to a standard value when the atomic orbitals are on neighboring atoms

$$H_{ij}^{\pi} = (\phi_i / H^{\pi} / \phi_j) = \beta \qquad \text{if i,j are adjacent atoms} \qquad 27$$

The fourth and final approximation is that the off diagonal terms are set to zero if the atomic orbitals in the basis set are not located on neighboring atoms.

$$H_{ij}^{\pi} = 0 \qquad \text{if i,j not adjacent atoms.} \qquad 28$$

Although it may appear that the quantities α and β may be evaluated explicitly from the above expressions this is not the case as the Hamiltonian H^{π} is not well defined. Instead the secular equation which results with these quantities is solved to give values of the roots (the orbital energies) in terms of the parameters α and β. These parameters can then be

adjusted to fit experimental orbital energies obtained from spectroscopic or polarographic experiments. Once suitable values of α and β are determined, the coefficients C_{ij} can be established. This results in an approximate description of the wavefunction for the π system. There is however very little in the HMO theory that can be described as theoretically sound. The neglect of π/σ interaction, antisymmetrization and overlap influences means that it is really only useful for correlative purposes. Furthermore the Hückel approach is best in the situation where there is a large number of compounds of a similar type to allow accurate parameterization. For this reason heteroaromatic compounds prove a particularly difficult problem; not only do they require a larger number of parameters, but there are smaller numbers of heteroaromatic compounds available to provide the necessary experimental data for parameterization. Not withstanding the deficiencies of the HMO method, it paralleled the picture of molecular orbitals held by organic chemists of the time and so it was highly utilized until the early 1960's. At that time Hoffmann[54] commented that "The steady pursuit of correlations between theoretically calculated π electron properties and measurables has unfortunately cast a shadow of unreality on the σ framework". A need for a more general semi-empirical treatment was evident and these have formed the basis for the development of modern semi-empirical methods.

Extended Hückel molecular orbital theory.

The logical progression from the simple HMO theory was to attempt to increase its generality of application while maintaining the ease of calculation - the development which is known as the extended Hückel molecular orbital theory[30,55] was in fact based on earlier work by Mulliken, Wolfsberg and Helmholtz. HMO was extended to allow calculations on aromatic and aliphatic, organic and inorganic systems, with one simple parameterization. In the extended Hückel molecular orbital theory the zero differential overlap approximation is no longer applied. Instead the overlap integral is evaluated exactly using Slater type orbitals for a valence only basis set. The critical difference is, however, that although it is still essentially a one-electron approximation to the full Fock matrix, the matrix elements representing coulombic repulsion, H_{ii}, are evaluated directly

from experimental values for the valence state ionization potentials (VOIP) so that H_{ii}(H1s) = -13.6eV, H_{ii}(C2s) = -21.4eV and H_{ii}(C2p) = -11.4eV. The off-diagonal terms (the resonance integrals) are approximated by a function of the coulombic terms and the overlap integral:

$$H_{ij} = 0.5K(H_{ii} + H_{jj})\, S_{ij} \quad \text{where } K=1.75 \qquad 29$$

This treatment was therefore one of the first to apply systematic parameters in an early stage of the calculation. With a computer implementation the Hückel energy of a molecule could be evaluated quickly, allowing the study of the variation of potential energy with geometry. An example is the C-H bond of methane where the potential energy curve has the correct form but the minimum in the potential well occurs at about 1.0Å which is too short for a C-H bond. This highlights the problems of such a one-electron treatment in that it could not correctly predict bond lengths, binding energies and molecular orbital energies. If, however, idealized bond lengths were assumed the extended HMO treatment was successful in predicting the conformational preferences for cyclohexane and obtaining a value close to the experimental value for the barrier to rotation in ethane.

Subsequent work on the extended HMO theory has attempted to refine the parameters by adjustment to mimic *ab initio* calculations.[55] This however has not been able to extend the accuracy of such procedures to match the *ab initio* calculations and it was apparent that a different approach to simplification of the secular equation 16 was required.

Complete Neglect of Differential Overlap (CNDO).

In 1965 Pople and co-workers, recognizing the limitations of the Hückel based approaches, developed the Complete Neglect of Differential Overlap (CNDO) scheme.[56]. This is a more sophisticated attempt to introduce parameters into quantum theory and was the basis for the line of research which led directly to today's modern semi-empirical molecular orbital methods. The Pople CNDO method of the mid-1960's was based on the earlier π-only treatment of Pariser, Pople and Parr[57] which did allow for some two-electron interaction. In fact this earlier theory was the first "CNDO" treatment as it neglected all two electron integrals which depend on overlap of charge in different orbitals, the

the remaining integrals being calculated by the use of semi-empirical expressions. This approach was successful in prediction of electronic spectra[58] and the calculation of some molecular properties, but for planar unsaturated molecules only. While it was definitely an improvement on simple Hückel theory it was still not generally applicable to problems of wider chemical interest.

Pople recognized that any approximation with the intention of simplifying the quantities in equation 16 must retain invariance with respect to transformation of the atomic orbitals used in the basis sets. So the results of a calculation must be the same after the changing of the local axes - that is a rotational invariance. The results must also be invariant to the transformations involving mixing of S and P orbitals. With these conditions in mind he proposed the CNDO method for approximate calculation of the quantities listed in equations 17-22. There are essentially five approximations central to the CNDO theory.

1) Complete neglect of differential overlap, so the atomic orbitals are treated as an orthonormal set with $S_{\mu\upsilon} = \delta_{\mu\upsilon}$ as in the Hückel treatment. The result of this is that the coefficients form an orthogonal matrix :

$$\sum_{\mu} C_{\mu i}\, C_{\mu j} = \delta_{ij} \qquad 30$$

For different orbitals on the same atom the overlap is already zero, but for different orbitals on different atomic centers this is a severe approximation.

2) All the two electron integrals which depend on overlap of charge densities of different basis orbitals are neglected so

$$(\mu\upsilon/\lambda\sigma) = 0 \qquad \text{unless } \mu=\upsilon \text{ and } \lambda=\sigma \qquad 31$$

The non-zero values are given a common value

$$\gamma_{\lambda\mu} = (\lambda\lambda/\mu\mu) \qquad 32$$

This approximation does not satisfy the requirement for rotational invariance. To satisfy that a third approximation is required.

3) $\gamma_{\lambda\mu}$ is assumed to depend only on the type of atoms to which ϕ_μ and ϕ_λ belong and not on the type of orbital. So the quantity γ_{AB} measures the average electron repulsion between an electron on atom A and an electron on atom B. This averaging of the repulsion restores the rotational invariance. γ_{AB} is calculated from the use of Slater S atomic orbitals for atoms A

and B in the following expression

$$\gamma_{AB} = \int\int S_A^2(1)\ \frac{1}{R_{AB}}\ S_B^2(2)\ d\tau \qquad 33$$

With these approximations the expression for the diagonal elements of the Fock matrix becomes

$$F_{\mu\mu} = H_{\mu\mu} - P_{\mu\mu}\gamma_{AA} P_{AA}\gamma_{AB} + \sum_{A\neq B} P_{BB}\gamma_{AB} \qquad 34$$

P_{BB} is the total valence electron density on B and $H_{\mu\mu}$ is defined as:

$$H_{\mu\mu} = (\mu / -\tfrac{1}{2}\nabla^2 - V_a / \mu) - (\mu / V_B / \mu)$$

$$= U_{\mu\mu} - \Sigma(\mu / V_B / \mu) \qquad 35$$

$U_{\mu\mu}$ is an atomic parameter and can be derived from experimentally measurable values for atomic energy levels.

4) The quantity $(\mu / V_B / \mu)$ represents the interaction of ϕ_μ with the core of all other atoms. In the CNDO treatment it is set to a value which is the same for all the valence atomic orbitals. So

$$(\mu / V_B / \mu) = V_{AB} \qquad 36$$

The quantity V_{AB} is calculated directly from the integral

$$V_{AB} = \int S_A^2(1)\ Z_B / R_{AB}\ d\tau \qquad 37$$

which is based on a classical point charge treatment (S_A is the Slater S-type atomic orbital on atom A) and so

$$H_{\mu\mu} = U_{\mu\mu} - \sum_{B(\neq A)} V_{AB} \qquad 38$$

5) Finally the off-diagonal one electron terms are the subject of the fifth approximation. If μ and υ are on the same atom then $H_{\mu\upsilon}$ is set to zero. If they are on different atoms then this represents the interaction of the charge distribution $\phi_\mu\phi_\upsilon$ with adjacent cores - this bonding contribution is known as the "resonance integral". In the CNDO treatment resonance integral is considered only to depend on the local environment so

$$H_{\mu\upsilon} = \beta_{\mu\upsilon} = \beta_{AB}^\circ\ S_{\mu\upsilon} \qquad 39$$

where β_{AB}° is a parameter for each bond type. This parameter was determined by a trial and error method to give the best fit to the results of full LCOA-SCF calculations.

Calculations using the CNDO method were carried out[59] initially on a range of diatomic and small polyatomic molecules. In general the results were disappointing with

unsatisfactory calculation of bond lengths and dissociation energies. These failings suggest that the errors introduced in the neglect of differential overlap are themselves a function of internuclear distance. Better results were obtained in the calculation of equilibrium bond angles. Here there seems to be less dependence on the neglect of differential overlap and the CNDO method is able to predict the correct stereochemistries for methanol and ethanol. The main success of the CNDO method has been that it was a good starting point for the development of a truly useful semi-empirical method and it demonstrated that such methods require considerably less computational effort than a full LCAO-SCF calculation.

A small modification to the CNDO scheme, known as CNDO/2,[60] was introduced by Pople the following year. This involves the neglect of the so-called penetration integrals. In the original CNDO the diagonal terms in the Fock matrix could be written

$$F_{\mu\mu} = U_{\mu\mu} + (P_{AA} + \frac{1}{2}P_{\mu\mu})\gamma_{AA} + \sum_{B(\neq A)} (P_{BB} - Z_B)\gamma_{AB} + \sum_{B(\neq A)} (Z_B\gamma_{AB} - V_{AB}) \qquad 40$$

The final term in equation 40 represents the effect of electrons in one orbital penetrating those of another orbital leading to a nett attraction. As CNDO/1 binding energies are too large and bond lengths too short an attempt was made to correct this in CNDO/2 by setting V_{AB} equal to $Z_B\gamma_{AB}$ and thus eliminating the term representing the penetration effects. A further correction involved a superior method of estimating $U_{\mu\mu}$ from atomic data such that:

$$U_{\mu\mu} + (Z_A - \frac{1}{2})\gamma_{AA} = \frac{1}{2}(I_\mu + A_\mu) \qquad 41$$

where I_μ is the atomic ionisation potential and A_μ the electron affinity for the atomic orbital ϕ_μ.

With the CNDO/2 method, only a slight improvement in the calculations was possible, with long-range interactions and angular dependence the only molecular properties being properly treated. In fact there are serious deficiencies in the CNDO method. For example there is no separation in open shell systems of states arising from the same configuration - methylene therefore shows no separate singlet and triplet states. Furthermore in many situations and, in particular, planar aromatic molecules no spin density is calculated in the σ orbitals. This is clearly the result of the complete neglect of one-centre exchange integrals and was realized independently by Pople[61] and Dixon[62] who both proposed an improved method in 1967. Essentially their treatments are identical and for the

sake of continuity, only the Pople scheme will be discussed in detail.

Intermediate Neglect of Differential Overlap. (INDO).

Here a limited number of one-centre exchange products are evaluated using a semi-empirical expression. The method involves the assumption that the 2s and 2p orbitals have the same radial parts. Given this, the expressions of Slater are used to evaluate the integrals:

$$(ss/ss) = F^0 = \gamma_{AA} \text{ as before} \qquad 42$$

$$(sx/sx) = 1/3\, G^1 \qquad 43$$

$$(xx/xx) = 3/25\, F^2 \qquad 44$$

and similar expressions to evaluate (yy/yy) etc. The Slater parameters F^0, G^1, and F^1 were derived from experimental atomic data. This method was originally applied to a range of AB and AB_2 molecules and was successful in correcting the worst deficiencies of the CNDO method which were due to the neglect of the one-centre exchange integrals. For example Figure 12, shows the correct triplet-singlet separation for methylene as calculated by the INDO method. INDO also showed improvement in the treatment of spin densities

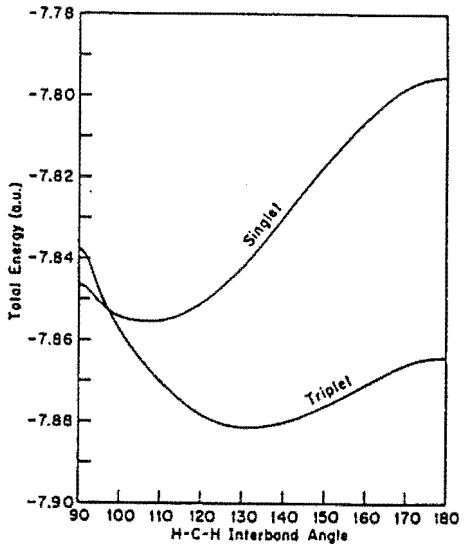

Figure 12. Calculated total INDO energy vs H-C-H interbond angle for methylene.

and in a study of the ethyl and methyl radicals it was possible to calculate hyperfine coupling constants which were in good agreement with experiment. The greatest limitation, however, of the INDO approach was that, while some atomic experimentally derived

parameters were used, other adjustable parameters were fitted so as to reproduce the results of *ab initio* calculations. There are two problems with this approach. Firstly these calculations were limited at the time to diatomic and small polyatomic molecules and so the large group of molecules needed for complete parameterization was not available. Secondly, *ab initio* calculations are themselves limited by the accuracy of the RH method and any treatment attempting to mimic these results will be limited in a similar way and the power of introducing parameters will therefore be limited. A decided change in the philosophy of semi-empirical molecular orbital methods is discernible when in 1968 Dewar took the INDO treatment and introduced a system where parameters were introduced with the sole purpose of reproducing experimental results.

The MINDO approach ('Modified INDO').

Between 1968 and 1975 the MINDO approach was developed by the research group led by M.J.S Dewar. Here, as noted earlier, the primary objective was to calculate with chemical accuracy (± 5.0kJ mol^{-1}) the ground state equilibrium heat of formation at 25°C. It was also the aim to be able to determine other useful molecular properties such as geometry , dipole moments and ionization potentials. Dewar envisaged a "computational spectrometer" - he wished to make computational chemistry as much a part of the everyday work of chemists as NMR or infrared spectroscopy.

The original MINDO approach[63] retained the essence of the INDO method but introduced more parameters in order to try to reproduce experimental results. The major differences are in the evaluation of the two-centre electron repulsion and the resonance integrals. As in the INDO method the two-centre integrals between atomic orbitals on a given pair of atoms is assigned the value γ_{AB}. But instead of evaluating these integrals by evaluation of equation 33 using the Slater-Zener s-orbital functions, a parameterized function was used for the evaluation of these quantities. The function has to meet the conditions that it goes to the classical e^2/R_{AB} at infinite separation and it should go the average one-center value, $\frac{1}{2}(F^0_A + F^0_B)$ as R_{AB} tends to zero. The expression chosen was:

$$\gamma_{AB} = -14.399\ [\ ((R_{AB})^2 + \rho_A + \rho_B\ )^2\ ]^{1/2} \quad \text{where } \rho_X = -7.1995/F^0_X \qquad 45$$

The advantage of evaluating the resonance integral by a semi-empirical expression

involving experimentally derived parameters is that the effect of electron correlation will implicitly be allowed for in the parameterization. The integrals calculated in this manner are consistently smaller than the corresponding values calculated by the direct evaluation of expression 27.

The resonance integrals are also evaluated from a semi-empirical function:

$$\beta_{\mu\upsilon} = S_{\mu\upsilon} \; (I_\mu^A + I_\upsilon^B) \, f(R_{AB}) \qquad 46$$

where I_μ is the ionization potential for removal of an electron from the appropriate atomic orbital, $S_{\mu\upsilon}$ is the overlap integral and $f(R_{AB})$ is a parameterized function which displays the correct dependence on the inter-center distance R_{AB}. It has the form

$$f(R_{AB}) = \beta_{cc}^I + (\beta_{cc}^I / R_{AB}) \qquad 47$$

for carbon carbon bonds and

$$f(R_{AB}) = \beta_{xx}^I \qquad 48$$

for other bonds, where β^I and β^{II} are adjustable parameters.

Finally the total core-core repulsion was set equal to the total electron-electron repulsion. This means that the total coulombic interaction between two neutral atoms is zero.

MINDO was implemented in a computer program and a number of parameterization schemes investigated. Because of the setting of the total core-core repulsion to the total electron-electron repulsion, it was not possible to determine a single set of parameters which would correctly reproduce experimental bond lengths and heats of formations. Consequently all MINDO results were for systems with the geometries fixed at their experimental values. Calculations were carried out for a range of hydrocarbons and compounds containing nitrogen and oxygen. The RMS error in the calculated heat of formations was ca. 4.8 kJ mol^{-1}, but the necessity of using fixed experimental geometries severely limited the usefulness of the method. This was not the case in the next development in the MINDO series.

MINDO/2[64] evaluated the one- and two-center integrals in the same manner as in MINDO/1, but in this more advanced method the total core-electron attractions are set to equal the negative of the total electron-electron repulsions. The resonance integrals and the core-core repulsions are evaluated by semi-empirical expressions that depend on the inter-nuclear separation, for the resonance integrals:

$$\beta_{\mu\upsilon} = B\, S_{\mu\upsilon}\, (I_\mu + I_\upsilon)\, f_1(R_{AB}) \qquad 49$$

where I is the atomic ionization potential and B is an adjustable parameter.

The core-repulsion between two atoms CR_{AB} was evaluated as :

$$CR_{AB} = ER_{AB} + (Z_A Z_B e^2 / R_{AB} - ER_{AB})\, f_2(R_{AB}) \qquad 50$$

where ER_{AB} is the total electron-electron repulsion between atoms A and B and Z_X is the core charge of X (defined as the difference between the atomic number and the number of valence electrons). The function $f_2(R_{AB})$ must tend to zero at infinite separation (i.e. no bonding) and to unity as the separation approaches zero.

In order to find suitable functions for $f_1(R_{AB})$ and $f_2(R_{AB})$ over 150 combinations were tried. The best results were obtained with $f_1 = 1$ and $f_2 = \exp(-\alpha R_{AB})$. So for every atom pair there are two parameters α and β. Systematic optimization of these parameters resulted in a method which could produce the best agreement with experiment of any of the semi-empirical methods previously, although "chemical accuracy" was not achieved.

More significant improvement was found with the introduction of the final MINDO scheme MINDO/3[65,66] which is still in use today.[67] In MINDO/3 a different method is utilized for the evaluation of the one-center integrals $g_{\mu\upsilon}$ and $h_{\mu\upsilon}$. Instead of using the Slater-Condon parameters (42-44) a method is used which allows independent evaluation of these quantities from atomic data. MINDO/3 also uses a slightly different method for the core-core repulsion function in the case of N-H and O-H bonds.

$$f_2(R_{AB}) = \alpha_{HX}\, e^{-Rab} \qquad 51$$

It was however the method of parameterization and its implementation that has meant that MINDO/3 performs better than any other MINDO scheme. The choice of parameters was carried out almost automatically using a computer program and an iterative least-squares method. Furthermore MINDO/3 was the first semi-empirical method to take full advantage of the techniques for determination of equilibrium geometries by the optimization of geometrical variables in order to minimize the energy of the molecule. The most efficient methods for doing this require not only the evaluation of the energy for each geometry but also the evaluation of the derivative of the energy with respect to geometrical variables. This latter quantity is easily calculated in the MINDO approximation and thus full geometry optimizations of quite large molecules, for example LSD[68] (144 independent

variables) can be carried out without any assumptions being made about the geometry. The MINDO/3 method gives good results for heats of formations. Figure 13 shows a correlation between experimental and calculated heats of formation for 193 compounds. The geometries

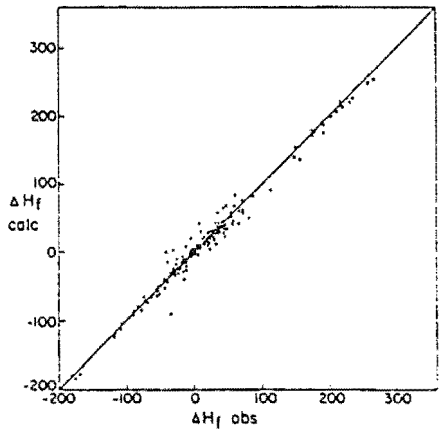

Figure 13 Plot of calculated (MINDO/3) vs observed heats of formation (25°) for 193 compounds derived from C, H, N, O, F, Si, P, S and Cl

and dipole moments calculated by MINDO/3 show a reasonable agreement with experiment. The latter are particularly interesting as dipole moments were not explicitly included in the parameterization. MINDO/3 was therefore the first semi-empirical method to show genuine utility for the calculation of ground state molecular properties. Furthermore because many possible geometries could be calculated quickly, it soon began to be used for the study of transient species in chemical reactions, where the study of potential surfaces for a molecule or reacting system may require thousands of calculations.

There are however some known problems with the MINDO/3 method which any potential user must be aware of. Molecules containing triple bonds are predicted to be too stable, while strain energy is often underestimated in calculations involving the MINDO/3 method. Furthermore the results for molecules such as $H_2N\text{-}NH_2$ where there are unshared lone pairs on adjacent atoms are often poor. It is apparent that any method based on the INDO approximation, with the neglect of one-centre differential overlap will not be able to achieve the high degree of accuracy required by experimental chemists.

An alternative, more rigorous, scheme was proposed by Pople in 1968, at the same time as INDO. This was based on the neglect of diatomic differential overlap (NDDO).[59] In the INDO approximation the integrals $(\mu\mu/\sigma\sigma)$ are set equal to some common value γ_{AB} regardless of whether ϕ_μ and ϕ_υ are of the s, pσ or pπ type. In fact they are not equal and in

the NDDO approximation additional bicentric integrals are evaluated which are neglected in the INDO and CNDO schemes. For a pair of dissimilar first row elements there are in fact 22 bicentric integrals to be calculated, not one as in the simpler treatments. Early implementations of the NDDO approximation[69] attempted to calculate the additional bicentric orbitals from direct quadrature of Slater-Zener atomic orbitals. This was not only computationally difficult but also made no allowance for the effects of electron correlation and so gave unacceptable results. A full NDDO implementation was not possible until 1977 when Dewar and co-workers developed a method for evaluation of these integrals that was both economic and allowed for electron correlation because it was based on an expression which included experimentally derived parameters.

Modified Neglect of Diatomic Overlap. (MNDO).

In the MNDO approximation the one-center integrals are derived from experimental (atomic) data using the method as in MINDO/3 which continues to allow for the effects of electron correlation. The core-core repulsion, core-electron attraction and resonance integrals are all evaluated by the use of semi-empirical expressions:

$$V_{\mu\upsilon,B} = -Z_B (\mu^A \upsilon^B / S^A S^B) + f_2(R_{AB}) \qquad 52$$

$$CR_{AB} = Z_A Z_B (S^A S^A / S^B S^B) + f_3(R_{AB}) \qquad 53$$

If $f_2(R_{AB}) = f_3(R_{AB})$ then the core-electron attraction (52) and the core-core repulsion (53) functions nearly cancel. During the parameterization it was assumed that $f_2(R_{AB}) = 0$ and various functions were tried for $f_3(R_{AB})$.

The resonance integrals are determined by :

$$\beta_{\mu\upsilon} = f_4 (R_{AB}) S_{\mu\upsilon} \qquad 54$$

The functions f_1-f_4 (f_1 is involved in the expression for the bicentric integrals) were determined by trial and error using a wide variety of functions which satisfied the boundary conditions. After extensive trials it was found that

$$f_3(R_{AB}) = Z_A Z_B (S^A S^A / S^B S^B) [e^{-\alpha_a R_{ab}} + e^{-\alpha_b R_{ab}}] \qquad 55$$

and

$$f_4(R_{AB}) = \frac{\beta_\mu{}^A + \beta_\lambda{}^B}{2} \qquad 56$$

are the best forms for these functions. The parameters α and β are, in the MNDO approximation, treated as atomic quantities rather than the bond or atom pair quantities as in MINDO. This causes no loss of accuracy and has some advantages - it means fewer parameters are required overall for three or more atoms parameterized, only five additional parameters are required for each additional atom and the atomic parameters are periodic allowing cautious extrapolation or interpolation to be applied in the determination of parameters for atoms where experimental data is scarce or unreliable. The parameters α and β were determined by an iterative least squares method which involved full geometry optimization of the 10 molecules in each of the standard sets for CH, CHN and CHO compounds.

For completeness the expressions for the Fock matrix elements in the MNDO expression are shown below.

$$F_{\mu\mu} = U_{\mu\mu} + \sum_{B} V_{\mu\mu,B} + \sum_{\upsilon}^{A} P_{\mu\upsilon}[(\mu\mu/\upsilon\upsilon) - \frac{1}{2}(\mu\upsilon/\mu\upsilon)] + \sum_{B}\sum_{\lambda\sigma}^{B} P_{\lambda\sigma}(\mu\upsilon/\lambda\sigma) \qquad 57$$

$$F_{\mu\upsilon} = \sum_{B} V_{\mu\upsilon,B} + \frac{1}{2} P_{\mu\upsilon}[3(\mu\upsilon/\mu\upsilon) - (\mu\mu/\upsilon\upsilon)] + \sum_{B}\sum_{\lambda\sigma}^{B} P_{\lambda\sigma}(\mu\upsilon/\lambda\sigma) \qquad 58$$

$$F_{\mu\lambda} = \beta_{\mu\upsilon} - \frac{1}{2}\sum_{\upsilon}^{A}\sum_{\sigma}^{B} P_{\mu\sigma}(\mu\upsilon/\lambda\sigma) \qquad 59$$

The quantities in the above three expressions can all be evaluated from the semi-empirical expressions given previously and this produces a Fock matrix which is a closer approximation to the full Fock matrix than any previous treatment could achieve as it includes all the two-centre terms involving monoatomic differential overlap. The result is a method which is superior in its ability to calculate ground state properties (especially those involving angular dependence) and the absolute mean error in the calculation of ground state properties with MNDO is only about one half that in the MINDO/3 method, while this is achieved with only a 20% increase in computing time. An improvement of this magnitude must be attributed to a better theoretical basis rather than simply an improved parameterization. There are four specific areas of improvement in the MNDO method over earlier schemes. Firstly there is a better treatment of aromatic hydrocarbons and triple bonds. Because one-centre overlap is no longer neglected there is better treatment for bonds between atoms with unshared lone pairs and, related to this, improved bond angles because

of the better treatment of angular dependence in the NDDO approximation. Finally the energetic ordering of molecular orbitals is much better than in the MINDO/3 method (where spurious high lying σ orbitals were predicted) and is now in good agreement with photoelectron spectroscopy because of a better theoretical description of the difference between π and σ electrons. MNDO, however, also contained some areas where the performance was unsatisfactory - poor activation energies for many simple reactions, underestimation of the stability for molecules which are "crowded" (e.g. cubane) and an inability to reproduce hydrogen bonds. These problems have been addressed in a "state-of-the-art" NDDO method - AM1.

Austin Model 1. (AM1).

AM1[70] was introduced by the Dewar group (situated at the University of Texas in *Austin*) in 1985 after it was recognized that the deficiencies in MNDO resulted from an inappropriate form for the core-repulsion function (eq. 53) - this leads to an overestimation of the repulsion of atoms separated by their Van der Waals distance. In AM1 (so named to avoid any connection with the poorly performing CNDO/INDO based methods) the core-repulsion function has additional Gaussian terms containing adjustable parameters, so

$$CR_{AB} = Z_{AB}\,\gamma_{ss}\,[\,1 + F(A) + F(B)\,] \qquad 60$$

where

$$F(A) = \exp(-\alpha_a R_{AB}) + \sum_{i}^{4} K_{Ai} \exp[L_{Ai}\,(R_{AB} - M_{Ai})^2] \qquad 61$$

$$F(B) = \exp(-\alpha_b R_{AB}) + \sum_{j}^{4} K_{Bi} \exp[L_{Bi}\,(R_{AB} - M_{Bi})^2] \qquad 62$$

The K parameter was found not to be critical and so only the L and M parameters were included for optimization.

AM1 also represents an improvement over MNDO because of the manner in which the parameters were determined. The optimizable parameters define a "hypersurface" for any given molecular system. The great number of possible values for the parameters make it difficult to determine a set which gives the result which shows the best agreement with observed values. During the development of AM1 a new method allowed a full search of the

parameter "hypersurface" to be carried out and so it is believed that the parameters represent a global minimum and possibly the best set for any NDDO based method.

The improvement in performance of AM1 over MNDO and MINDO/3 methods is shown in Table 1.

Table 1.
Comparison of Mean Absolute Errors for AM1, MNDO and MINDO/3 (for hydrocarbons only.)[70]

Average error in:	number of compounds	AM1	MNDO	MINDO/3
Heat of formation (kJ mol^{-1})	58	21.21	24.56	40.58
Dipole Moments (D)	11	0.17	0.25	0.26
Ionization Energies (eV)	22	0.29	0.39	0.31

Other improvements are a correct treatment of hydrogen bonds because of the modified core-repulsion function and better values for activation energies in simple reactions because of the optimal values obtained for the exponents of the Slater-Zener orbitals used in the basis set. These improvements, in particular over MNDO, are achieved without any increase in computation time. This level of accuracy, while retaining economy of calculation means that AM1 is a useful method and closer to a "computational spectrometer" than any previous method.

MNDO-PM3 (MNDO -Parametric Method 3)

The most recently developed semi-empirical method to date is the PM3 method which was developed by Stewart.[71] The theoretical framework of the PM3 method is identical to that for the AM1 method described earlier, but the development of new methods for optimizing the MNDO parameters combined with the availability of greatly increased computer power together allowed the MNDO parameters to be re-optimized to obtain a set which performed largely better in prediction of all molecular properties than the original set. The PM3 method shows particular improvements in the calculation of the heats of formation of hypervalent compounds : the average error of 106 hypervalent compounds was 56.9 kJ mol^{-1} compared with 317.1 kJ mol^{-1} for MNDO.

The value of the PM3 parameterization has, however, been questioned by Dewar.[72] He has stated his belief that the PM3 method does not provide a sufficient improvement over AM1 to justify its widespread use and distribution and that the comparisons made in relative heats of formation for hypervalent compounds as calculated by each method were erroneous. Stewart[73] has responded to this by stating that the areas in which PM3 performs better than AM1 (namely hypervalent compounds and nitro compounds) justify the use of PM3. He does, however, concede that the method of parameter optimization reveals that the PM3 parameter set, while an improvement on previous sets, is not the global minimum on the parameter hypersurface. Only continued application of both methods to systems outside of those used in the parameterization will reveal the strengths and weaknesses of each.[74]

Applications of Semi-empirical methods.

The modern semi-empirical methods (PM3, AM1, MNDO, MINDO/3) have each been applied to a wide range of chemical problems, many of which the developers of these methods will not have considered as applications! A 1983 review of MINDO/3[67] lists ca. 180 references to reported MINDO/3 calculations of ground state molecular properties as well as physiochemical and spectroscopic parameters for a wide range of chemical and biochemical systems. Furthermore in the five year period between 1980 and 1985 *Chemical Abstracts* listed 623 papers involving MNDO calculations,[70] and calculations using AM1 have appeared frequently in the literature.

Semi-empirical v. *Ab initio* - to which the future?

In any discussion of semi-empirical methods it is inevitable that comparisons to *ab initio* techniques will be drawn. In fact an objective comparison is probably impossible because the two methods judge their success by slightly different criteria. There is, however, no dispute that a semi-empirical calculation can be performed much more quickly than a corresponding *ab initio* one. As computer time attracts substantial charges per hour a semi-empirical calculation can represent tremendous cost savings, especially on large projects such as the study of potential surfaces. An inaccurate calculation giving misleading results is, however, no substitute for an accurate one regardless of the economic benefits. Dewar has

is, however, no substitute for an accurate one regardless of the economic benefits. Dewar has attempted to compare the accuracy of the major modern semi-empirical methods with *ab initio* methods at three levels of theory.[75] A typical result from that investigation - the average error in calculated heats of formation of ca. 50 small and medium sized molecules - is shown graphically in Figure 14. This indicates that the most recent semi-empirical method

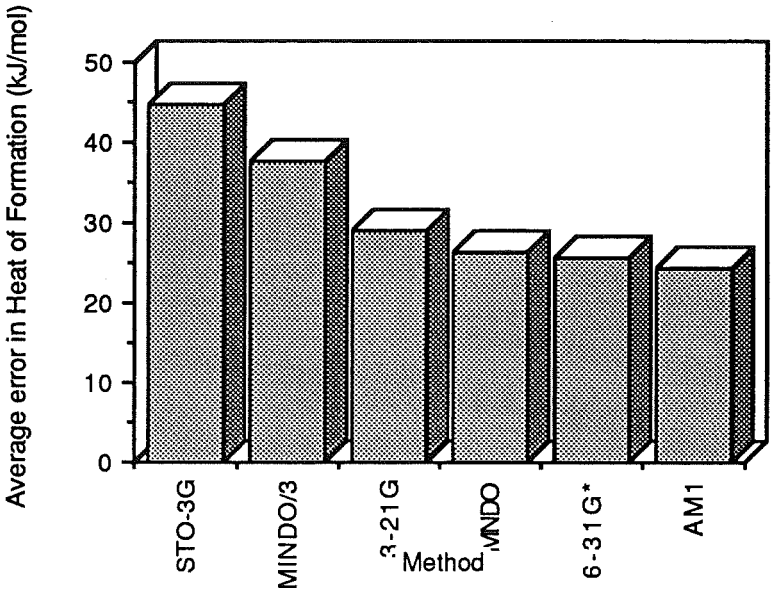

Figure 14. Average errors in heats of formation of 50 molecules calculated by *ab initio* and semi-empirical methods.[75]

performs slightly better than the *ab initio* treatment with a 6-31G* basis set. What is not shown is that it will do the calculations at considerably less cost. An analysis such as this can, however, be misleading. The semi-empirical method is parameterized to reproduce heats of formation, it may not perform as well in the calculation of other properties of interest. Furthermore as Lipscomb[76] has pointed out, everyone desires the achievement of accurate and economical calculations, but it must be considered that semi-empirical methods, with a heavy reliance on parameters "obscure the physical basis of their success". There are two consequences of this. Firstly, without a rigorously understood theoretical basis the reliability of semi-empirical calculations in areas where no comparison with experiment is

* An example[77] is a "complete" search of the potential surface of the benzene molecule. This study using MINDO/3 cost US$5000 dollars in 1975 while Dewar estimated that a 4-31G *ab-initio* study would have cost US$1B. This factor of five orders of magnitude was contested by some leading theoretical chemists (see reference 76).

possible can not be assessed. A good performance in reproducing ground state properties for example does not necessary mean that calculations on the transient species formed during chemical reactions will necessarily be as successful. Secondly if the basis for their success lies heavily on parameterization then the development of semi-empirical methods does not contribute to any effort to produce more rigorous models that aid in the interpretation of molecular structure. An improvement in the performance generally means an improvement in a set of arbitrary parameters which have limited physical interpretation.

Alternatively there is a view that is summed up well by a statement of Dewar :" So far as chemistry is concerned the only criterion is practical success".[64] Semi-empirical methods have certainly been able to achieve a practical success that makesthe arguments against them, which were discussed above, seem to be overstressing the need for rigorous treatments.

The best approach must be that which views the two methods as complementary. *Ab initio* methods can not be satisfactorily applied to all systems of chemical interest, and therefore necessarily some semi-empirical treatment is required and in fact the only alternative. It may be that in the future there will not be a need for semi-empirical methods (at least as we know them today), as *ab initio* methods are being applied with the use of ever faster computers to more and more systems with increasing accuracy and economy. It is also possible that the two methods may begin to converge as new semi-empirical methods with fewer and more meaningful parameters are developed.[78] Lindholm[79] has proposed a radical change, moving away from Hartree-Fock theory with its inability to deal with electron correlation, towards a theory based on density functional theory. Although early attempts at implementing these ideas have not been able to achieve a successful parameterization these ideas have a solid basis in theory.

It is likely that even changes within the the existing MNDO (NDDO) framework may also result in useful improvements in the accuracy of semi-empirical calculations. Theil[80] has proposed several refinements to the MNDO type methods including larger basis sets which include d-orbitals, the use of "effective core potentials" and a change in the reference data for energies from heats of formation at 298 K to binding energies. The existing methods will, however, continue to provide information of use to chemists on a wide range

of chemical and biochemical problems. If these calculations are carried out with a full awareness of their limitations there seems to be little basis for objection.

Chapter 3.

Diastereofacial Selectivity in the Diels-Alder Reaction.

Several theories have been proposed to account for the observed trends in the regio- and stereo- chemistry of Diels-Alder reactions[14] and these can often be applied with predictive success.* When the diene and/or dienophile are facially differentiated or are chiral the situation is more complex and no simple generally applicable theory to enable prediction and control of diastereofacial selectivity has been developed.

In this section the experimental results from the Diels Alder reactions of a number of different classes of diene and dienophile where diastereofacial selection can occur will be reviewed. Emphasis is placed upon investigations which have attempted systematically to develop an understanding of the basis of diastereofacial selection and those which are relevant to the results presented in this thesis. The more important theories which have been proposed to account for the experimental observations will therefore be discussed.

In an early review of the stereochemistry of the Diels-Alder reaction Martin and Hill[81] proposed that dienes and dienophiles will approach each other from the least

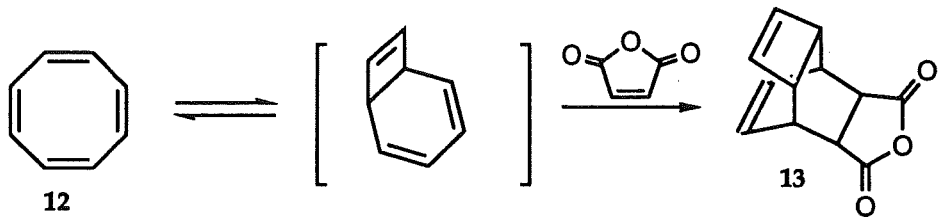

12 13

hindered face on each - the reactions were considered to be under steric control. They discussed several examples consistent with this proposal such as the reaction of cyclooctatetrane[82] **12** with maleic anhydride to give the *anti* product **13**.

* The theoretical soundness of the various treatments remains to be established[17]

5 -Substituted cyclopentadienes.

However at that time one notable exception known to this generalization was a reaction reported by Winstein et al. as part of a study of 7-norbornyl cations.[83] 5-Acetoxy-

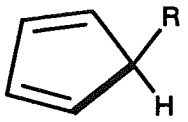

14 **a) R = OAc**
b) R = CH_2OCH_3
c) R = Cl
d) R = Br

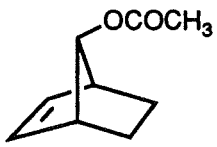

15

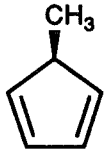

16

1,3-cyclopentadiene **14a**, prepared *in situ* , reacts with ethylene to give an adduct **15** resulting from addition *syn* to the 5-acetate group; namely from the face of the diene offering the greater steric hindrance to an incoming dienophile. 1,3-Cyclopentadienes are reactive dienes because the ring constrains the diene in the cisoid conformation which is necessary for reaction with dienophiles and holds the diene termini in a position which is favourable for orbital overlap with the approaching dienophile. Substitution at the 5-position as in **14** is perhaps of the simplest method of producing a facially dissymetric diene.

The next major observation on the effect of a 5-substituent in a cyclopentadiene was made by Maclean et al.[84] in a study of the reactions of the cyclopentadienide anion. From this anion they prepared the 5-methyl substituted cyclopentadiene **16** which because of its propensity to undergo sigmatropic shifts is a complex mixture of dienes. The methyl group in the unrearranged diene would be expected to exert a steric directing effect favouring attack from the face opposite to the substituent. Reaction with N-phenylmaleimide was however reported to give an unseparated mixture of the four *endo/exo* isomers resulting from equal attack *anti* and *syn* to the methyl group. Only one of the four possible products was fully characterized.*

Corey[85] prepared 5-methoxymethyl-1,3-cyclopentadiene **14b** for a stereocontrolled prostaglandin synthesis. Reaction of this diene with acrylonitrile gave exclusively products where the dienophile approached *anti* to the 5-substituent, consistent with the steric expectations.

*Many early studies suffered from difficulties in unambiguous stereochemical assignment. It was not until the late 1960's that product stereochemistry could be confidently determined.

A study by Williamson et al.,[86] in the same year, of addition to 1,2,3,4,5-pentachlorocyclopentadiene 17 with a variety of dienophiles however pointed to the importance of electronic factors in determining the facial selectivity. Reaction of dimethyl

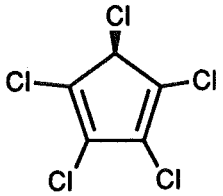

17

fumarate produced a single product arising from the face *anti* to the 5-chloro substituent while reaction with the Z-isomer, dimethyl maleate, was appreciably slower requiring approximately 5 times longer to consume the diene, and gave three products in approximately equal amounts - these were the *endo* and *exo* products resulting from addition *anti* to the 5-chloro substituent and the *endo* product resulting from addition *syn* to the chloro substituent.* Addition *syn-endo* to the 5-chloro substituent was observed with a number of dienophiles; maleic anhydride (90% *syn*), benzoquinone (60%), methyl acrylate (53 %) and acrylonitrile (71.7%). In contrast styrene and propene showed a greater propensity to react *anti -endo* to the chlorine; giving 31.3% and 38% products from *syn* attack respectively . These results are inconsistent with steric considerations alone determining facial selectivity and point to the importance of stereoelectronic effects. Williamson pointed out 'secondary orbital interactions' cannot be invoked to explain the facial selectivity since dienophiles with conjugated π electrons having the potential for such interaction (e.g. acrylonitrile and styrene) gave varying amounts of *anti*-chloro isomers. This however ignores that any such interactions would have different magnitudes for different dienophiles. He noted a relationship between the dipole moment of the dienophile and the extent of *syn* addition and proposed that facial selection is controlled by dipole-dipole, dipole-induced dipole and London dispersion forces. Thus, chlorine, as a more polarizable 5-substituent compared with methyl preferred to be *syn* to those dienophiles that were significantly polar.

* This was in contrast to an earlier study of the reaction where only *syn* products were reported and illustrates something of the experimental difficulties faced by the early researchers into π-facial selectivity. [87]

This idea was extended in a later study[88] which examined the reactions of **17** catalysed by the Lewis acids $AlCl_3$, $TiCl_4$, and BF_3. The effect of the catalyst was not only to increase the rate of reaction and the yield of Diels-Alder product relative to dimerization product, but the catalyst also increased the extent of reaction from the face *syn* to the chlorine. The effect of catalyst on the facial selectivity was rationalized by considering that the Lewis acid-dienophile complex, presumed to be the major reacting species, was more polar than the uncoordinated dienophile and thus the directing effect of the C5-substituted diene was enhanced.

Anh[89] showed that for reactions of **17** there were inconsistencies in the correlation of dipole moment and *syn* addition. For example benzoquinone has no dipole moment but still reacts substantially from the face *syn* to the chlorine. Results of a theoretical study by Anh gave some support to the idea that dipole interactions may be present but considered that orbital interactions were as, if not more, important. He showed the possibility that a stabilizing interaction between the lone pairs of the acetate ether oxygen for **14a**, and the π^* orbital of the approaching alkene dienophile may be important in favouring the *syn* product (Figure 15). This however does not account for the apparent absence of a facial directing effect of a C5-methyl which cannot undergo such a stabilization and therefore a steric

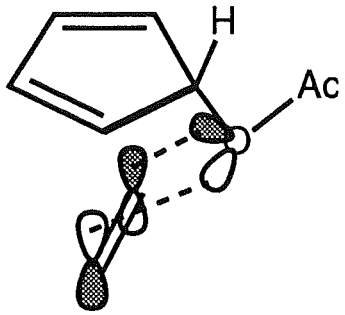

Figure 15. Stabilizing interaction between oxygen lone pair and incoming dienophile proposed for 5-heteroatom substituted cyclopentadienes.

preference would be expected *anti* to the methyl. Any stereoelectronic effect must act in the opposite direction to the steric effect of the methyl and be of comparable magnitude . Anh showed that there is a somewhat better correlation between the calculated (CNDO) LUMO energies for the dienophiles and the observed degree of *syn* face reactivity: dienophiles with the lower LUMO's tend to favour reaction from the face *syn* to the chlorine. Lewis acid coordination to the dienophile would be expected to lower the LUMO and promote *syn*

attack as is observed. This supports the proposition that a stabilizing interaction between the halogen (or heteroatom) and the LUMO of the incoming dienophile may be important.

This theory, proposed by Anh, may be satisfactory for rationalizing the facial selectivity exerted by a 5-chloro substituent on alkene dienophiles. However Breslow et al.[90] showed that the halogens do not all have the same influence on facial selectivity as would be required by this theory. Reaction of a series of dienes **14c** and **14d**, with PTAD were rapid. The bromine and iodine substituted cyclopentadiene gave products resulting exclusively from the addition *anti* to the halogen face, while only the chlorine substituted diene gave a mixture of facial isomers (the ratio of products was not reported). While it could be understood that the large steric bulk of the iodine might override stabilization provided by orbital interactions, the difference between the bromine and chlorine substituted compounds is more difficult to understand.

Anh considered that electron donation from the halogen or heteroatom in the 5-position of cyclopentadienes was important in stabilizing the transition state for the *syn* reaction (i.e. an interaction secondary to the main bond forming one). Instead Fukui[91] drew attention to how the main bond forming or "frontier orbital" interactions may be affected by the presence of a proximate halogen or heteroatom. Fukui's semi-empirical molecular orbital calculations (CNDO/2) showed that the HOMO of 5-chloro and methyl substituted cyclopentadienes was for the chlorodiene "biased" in the region *syn* to the halogen so that there is more electron density on that face in the HOMO orbital. In contrast the methyl group in 5-methylcyclopentadiene caused no detectable differentiation in electron density in the HOMO the two faces. Fukui argued that if there is greater electron density in the HOMO on the face *syn* to the 5-substituent with halogen or heteroatom substituents then a stabilizing charge transfer interaction between the diene HOMO and the dienophile LUMO will favour reaction from that face. He suggested that this explained why poor electron acceptors such as propene favour *anti* addition with 1,2,3,4,5-pentachlorocyclopentadiene. It also explains the increased selectivity observed in the Lewis acid catalysed reactions of this diene as being due to the increased electron accepting ability of the dienophile. The relative importance of the facially unsymmetrical diene HOMO with the activated dienophile LUMO increases with catalysis.

The reaction of the hydroxycyclopentadiene[92] **18** adds support to the 5-substituent "biasing" the HOMO of the diene by electron donation from the oxygen to the diene HOMO. Reactions of diene **18** with N-phenylmaleimide, dimethyl fumarate and styrene show a marked preference for reaction *syn* to the hydroxyl group. The fact that styrene shows a *syn* preference was considered as support that hydrogen bonding was not responsible for the facial selectivity observed with hydroxycyclopentadiene since it could not be operative for styrene. The selectivity was considered a direct result of the HOMO biasing effect of the hydroxyl group. The Fukui theory, however, like all perturbation treatments is based on an examination of reactant orbitals and makes no allowance for changes which may occur during the course of the reaction. More recent experiments cannot be satisfactory explained by any of the three theories of electronic control. These observations and the recent attempts to rationalize them are now discussed.

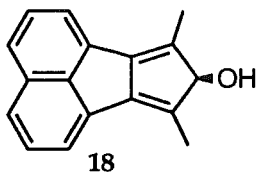

18

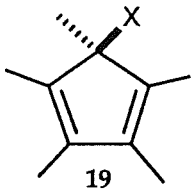

19

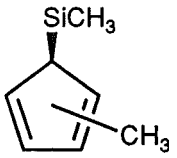

20

Fallis et al.[93] have prepared compounds of pentamethylcyclopentadiene **19** with a variety of X groups and examined reactions with maleic anhydride and N-phenylmaleimide. Variation of the X group allows a measure of the relative directing effect of the X-substituent compared to methyl. When X is an oxygen substituent (X=OH, OCH_3) or nitrogen substituent (X=NHAc, NH_2) there is a strong preference of addition to the face *syn* to the X group. In contrast when the cyclopentadiene has a sulphur substituent at the 5-position (X=SCH_3, $SOCH_3$, SO_2CH_3) reaction occurs almost exclusively *anti* to sulphur. The only exception is when X=SH and 45% of the reaction occurs *anti* to SH. The contrasting facial behaviour exhibited by the OMe/SMe substituted dienes cannot be accounted for by steric effects as SCH_3 group is considered as only slightly larger than a OCH_3. Fallis proposed a number of possible explanations for the variation in selectivity between sulphur and the other heteroatom substituents, oxygen and nitrogen. *Ab inito* calculations for the starting dienes show the electron density is increased on the face *syn* to sulphur, and the sulphur lone pairs interact more strongly with the diene HOMO than

oxygen lone pairs. No detailed explanation was given to account for how this may effect the facial selectivity and it should be noted that the additions occur contrary to that predicted by Fukui based on the electron density of the two faces of the HOMO. There are conformational differences between the oxygen and the sulphur substituents, with oxygen preferring a "distal" conformation thereby leaving the diene more exposed than when the 5-substituent is thiomethyl.

Investigations into the reactions of **19** were extended in later work by Fallis et al.[94] to dienes X = SCH_2Ph and X = SPh. A strong preference for addition *anti* to the sulphur substituents was observed. Fallis et al., however, proposed a new theory to account for these observations and in fact for all the observations of reactions to 5-substituted cyclopentadienes. The explanation was based on the ideas of Cieplak and co-workers[95] which had been focussed towards understanding the directing effects of remote substituents in nucleophilic additions to substituted cyclohexanones. The basis of the "Cieplak effect" is that an incoming nucleophile will add to a carbonyl from the face that allows the greater anti-periplanar hyperconjugative stabilization from an adjacent substituent. By analogy Diels Alder reactions will preferentially occur antiperiplanar to the adjacent σ-bond which is the better hyperconjugative donor because this bond with it's greater electron density will best be able to stabilize the vacant σ* orbital of the incipient electron deficient σ-bond forming at the transition state. This stabilization is shown diagramatically in Figure 16.

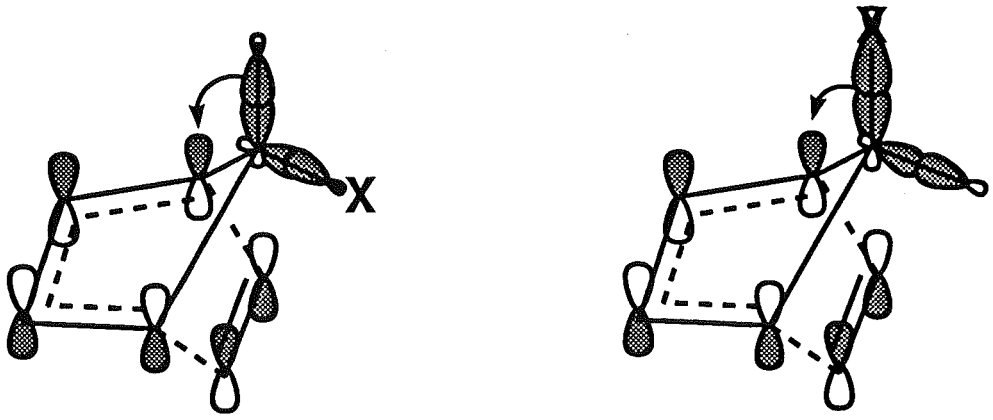

Syn reaction
Stabilization by C-C bond

Anti reaction
Stabilization by C-X bond.

Figure 16. Hyperconjugative stabilization at the transition state in the reactions to the *syn* and *anti* face of a 5-X-substituted cyclopentadiene.

The generally accepted order of increasing σ-donor ability is $\sigma_{CO} < \sigma_{CN} < \sigma_{CCl} < \sigma_{CC} < \sigma_{CH} < \sigma_{CS} < \sigma_{CSi}$ such that oxygen, nitrogen or halogen substituents will favour *syn* addition when the other substituent at the 5-position is a C-C or a C-H bond. Sulphur and silicon containing substituents however, are able to stabilize an *anti* transition state better than an *anti*-periplanar C-C or C-H bond.

While this theory based on conjugative stabilization is simple to apply and accounts well for most of the experimental observations described so far, there are of course situations where steric effects dominate. Fleming et al.[96] examined the reaction of a 5-trimethylsilyl derivative **20** with N-phenylmaleimide. While the C-Si bond is a strong hyperconjugative stabilizer, the complete *anti* attack on the diene is considered to be a result of the bulk of the trimethylsilyl substituent.

Houk[97] has attempted to quantify and separate steric effects by developing an MM2 transition state model for the reactions of **21-23**. The model geometry was based on MNDO calculations of the transition state for the reaction of ethylene and cyclopentadiene.

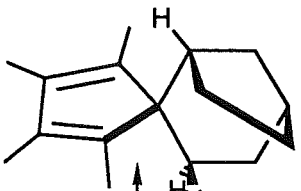

21

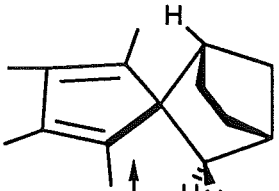

22

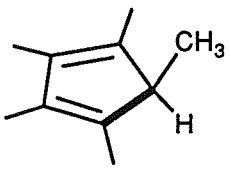

23

Experiments[98] have shown that there is a strong preference (70-100%) for dienophiles to react on the '*anti*' face (i.e *syn* to the methylene bridge for **21** and **22**). Somewhat surprisingly this preference was also observed for the 5-methyl substituted compound **23**. Using the MM2 model Houk was able to predict the observed selectivity for **21-23**. As hyperconjugative effects cannot be reproduced by the MM2 method then the success of a model based on this method in predicting the facial selectivity on steric considerations alone suggests that **21-23** do indeed react under steric control. The advantage of this method is that it is an attempt to consider reaction geometry at the transition state of the reaction and is not based only on considerations of starting materials. For compounds **21-22** the relative σ-donor ability of each of the 5-substituent bonds would be difficult to assess *a priori* in addition to the fact that spiroconjugative effects[99] will result in σ/π mixing in the

the diene. For **23** however the expectation is that the C-H bond would be a better σ-donor that the C-C bond of the methyl group. In fact the complete *anti* preference with cyclic dienophiles calculated by the MM2 model was higher than that observed (80%). The difference between the predicted and the observed ratios for **23** could be due to the influence of hyperconjugative stabilization or stereoelectronic effects at the transition state - an effect which is naturally excluded in the MM2 model. The effect of Lewis acid catalysis in making only a small change in *syn/anti* isomerization but a large change in the *endo/exo* ratio was also rationalized by the use of the steric MM2 model but using longer forming bonds to represent an "earlier" transition state.

So for 5-substituted cyclopentadienes the hyperconjugative stabilizing ability of the 5-substituent can be a useful guide to predicting facial selectivity providing that steric effects at each face of the diene are comparable. It should be noted that in these compounds the 5-substituents are ideally orientated to stabilize the σ* orbital of the forming bond at the transition state and the conclusions drawn from these systems may not be general for other dienes.

1,3-Cyclohexadienes.

1,3-Cyclohexadienes are inherently less reactive towards dienophiles than 1,3-cyclopentadienes since the termini of the diene are not as appropriately placed for optimal overlap with a dienophile. Dienes of this type have, however, been the subject of several important studies into the factors responsible for π-facial selectivity in Diels-Alder reactions. One of the first reported reactions of a facially dissymetric 1,3-cyclohexadiene was the Diels-Alder reactions of the o-quinols **24a**,[100] prepared by the periodate oxidation of the corresponding phenol. When this compound is prepared in the presence of a dienophile such as benzoquinone, a Diels-Alder adduct is isolated. Addition occurs exclusively to the face *syn* to the hydroxy group and with the *endo* stereochemistry expected from normal secondary orbital overlap considerations. The diene also undergoes a dimerization reaction and the dimeric Diels-Alder product is also the product of *syn* face reaction.

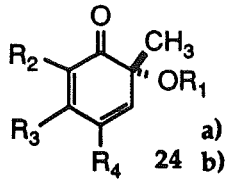

a) R_1 = H; R_3,R_4=H
24 b) R_1 = Ac; R_2= CH_3
R_3 and R_4 = H.

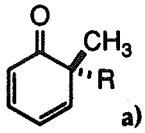

25 a) R=CH_2CH_3
b) R=CH_2Br
c) R=CH_2Cl
d) R=CO_2CH_3

Yates et al.[101] examined the reactions of the acetate derivative **24b**. With maleic anhydride a single adduct resulting from addition *syn* to the acetate and with the carbonyls of the anhydride *syn* to the alkene moiety (*endo*) was reported. Propiolic acid also reacted in the same highly selective manner to give a completely analogous product. Dimerization of the diene also occurs and the dimeric product was the result of reaction on the face *syn* to the acetate. This high *syn* face selectivity has been interpreted as a combination of steric , van der Waals-London and secondary orbital overlap factors in an proposal similar to that made by Williamson for the reactions of 5-substituted cyclopentadienes.[86].

Recently Yates and co-workers have reported reactions between facially dissymmetric 6,6-disubstituted cyclohexadien-1-ones and the acetylenic dienophile, dimethyl acetylenedicarboxylate (DMAD). The reaction of **25a** with DMAD had been reported[102] earlier. However, at that time no attempt was made to assign the stereochemistry of the diastereoisomeric products. Yates determined that the facial course of the reaction varied with the nature of the R-group. With **25b** and **25c**, the reaction gave 8:1 and 6:1 ratios of *anti* to *syn* products respectively. The preference for attack *anti* to the CH_2X groups was considered to arise from steric interactions. With **25d** an *anti* preference was reduced to 3:1 and the facial selectivity was suggested to be the result of unfavourable interaction between the lone pairs on the acetate and orthoganol π-electron density on the approaching acetylenic dienophile or to result from an unfavourable dipole-dipole interaction for reaction on the face *syn* to the ester. A CH_2OAc group was considerably less discriminating and a modest *syn* preference of 0.9:1.0 was reported. It was proposed that a stabilizing interaction between the dienophile at the transition state and the *syn* substituent may occur in parallel with the effect first proposed by Anh to explain the reactions of 5-acetoxycyclopentadiene.[89]

The preference for reaction of a dienophile to the face of a 1,3-cyclohexadiene *syn* to an adjacent heteroatom has also been observed in reactions of natural products. The addition

of nitroethene to N-formylnorthebaine **26** occurs with complete selectivity to give the single product resulting from addition to the face *syn* to the nitrogen.[103] The production of novel

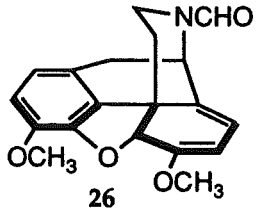

26

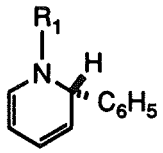

27

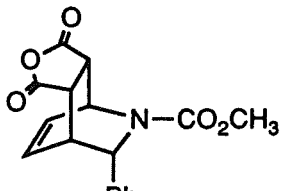

28

compounds with pharmaceutical properties has been the driving force for a study of the Diels-Alder reactions of N-substituted-1,2-dihydropyridines **27**.[104]. Reactions of an extensive series of compounds of type **27** which contain a facially differentiated cyclohexadiene, with PTAD were reported to occur with preference for addition to the face *syn* to the phenyl group. A similar preference was reported in reactions with N-phenyl and N-methyl maleimides. The assignment of product stereochemistry in all these cases was based only on ^{1}H NMR anisotropy effects.

These reactions were later re-examined[105] and the stereochemistry of the products reversed, based on chemical correlations with analogous compounds of known stereochemistry and an X-ray structure of **28**. The reactions in fact proceed from the face *anti* to the phenyl group consistent with the fact that the phenyl group will offer more steric hindrance to attack than the substituent on the nitrogen of the planar amide moiety.

1,3-Cyclohexadienes fused to cage compounds have provided a fertile area for investigating the effect of remote and proximate structure on facial selectivity. A rigid cage structure allows the placement of varying groups about each face of the diene. For example the cage diene **29** presents to an approaching dienophile two carbonyl groups from one face and a cyclobutane group from the other. An early report[106] suggested that benzoquinone

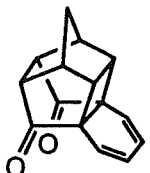

29

added to **29** exclusively from the face *anti* to the carbonyl groups. A later re-examination of this reaction has determined this to be incorrect and alkene dienophiles, including benzoquinone, react with a strong preference for the face of the diene *syn* to the carbonyl groups.[107,108] The dienophiles, DMAD, PTAD and DEAD do not parallel alkenes in their

facial selectivity and show a greater variation in facial selectivity; DMAD (55% *syn*) and azo dienophiles PTAD 64% *syn* , DEAD 100% *anti*. The partitioning to *anti* addition was considered[107] to be the result of destabilizing interactions between the "orthogonal" electron density, the lone pairs on azo and π-system for acetylenes, and the lone pairs on the carbonyl groups. Thus even though the face *syn* to the carbonyl group was apparently the more sterically favoured, as indicated by the strong preference for reaction from this face with alkene dienophiles, with the acetylene and azo dienophiles the destabilizing interaction between the proximate orbitals became important and reaction from the face *anti* to the carbonyl groups becomes competitive. The work described in this thesis extends these studies by an investigation of the diastereofacial selection in the Diels-Alder reactions of a number of derivatives of **29**. These experimental studies are supported by molecular mechanics and molecular orbital calculations on compounds such as **29** and simpler models directed towards elucidating the relative importance of steric and orbital interactions in determining the diastereofacial selectivity observed in the experimental studies.

Prinzbach and co-workers have investigated π-facial selectivity in the *syn-o,o'*-dibenzenes **30**, **31** and **32**.[109] In these compounds the intriguing possibility exits for reaction from the inner faces of the dienes, in a so-called "pincer" reaction, or from the

30

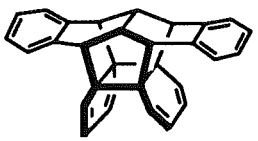

31

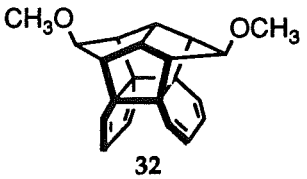

32

outside face of the diene. This latter reaction will result in the formation of an ethylene well placed to react with the remaining diene and as such the process is referred to as a "domino" reaction. In reactions with a variety of dienophiles namely, maleic anhydride, N-phenylmaleimide, benzoquinone, TCNE, singlet oxygen and nitrosobenzene, the "domino" reaction path was favoured and reaction occurred exclusively from the outer face of the diene. No intermediate products could be observed and the second Diels-Alder reaction was considered to occur extremely rapidly following the initial addition. With acetylenic dienophiles however the situation was more complex. In reactions of **30** with acetylenic dienophiles some "pincer" reaction products were observed; 3% for DMAD and 85% for DCA (dicyanoacetylene). Both reactions were effected at high pressure. The difference in

selectivity observed between DMAD and DCA in the reactions with 30 is considered to result from the facet that in DCA both orthoganol π systems are equally activated and complexation can occur to each diene equally, whereas in DMAD only one of the π-faces is activated by conjugation with the ester groups and so the pre-reaction complex with the inner faces of the diene will be less stable.

The domino/pincer selectivity varied only slightly with increasing pressure; for example reaction of 32 with DCA at 1 kbar gave 19:81 domino:pincer while at 14 kbar the ratio was 13:87. Since both processes are almost equally accelerated by an increase in pressure it appears likely that both processes involve two distinct steps involving short lived Diels-Alder intermediates, rather than by a "higher" concerted process involving a "double" $[\pi 4+\pi 2]$ cycloaddition. The differing facial selectivity observed with the different acetylenic dienophiles was considered a result of differential pre-reaction complexation between the π-bonds of the acetylenic dienophiles and the inner faces of the diene. In the case of addition to 31 the pincer reaction, with the two inner face of the diene is less favoured with DCA than the domino reaction since in the latter reaction complexation can also occur between the acetylene and the outer face of the diene and the suitably oriented benzene ring.

The course of π-facial selection in the Diels-Alder reactions of the propellane compounds 33 have been extensively studied by Ginsburg et al.[110] Early observations of Diels-Alder dimerization of **33b** were difficult due to problems in elucidating stereochemistry and the reaction with external dienophiles was therefore examined to

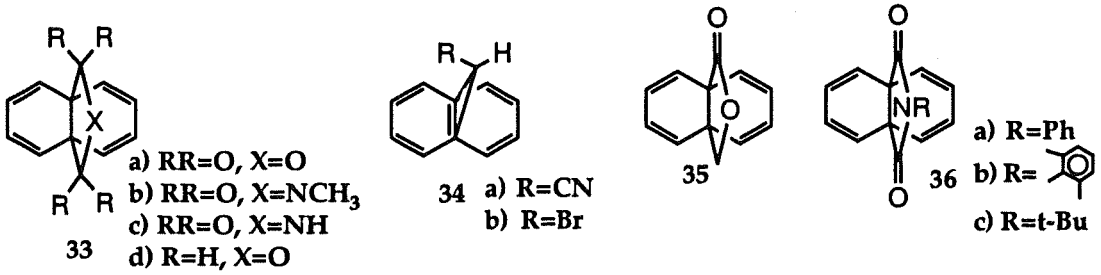

probe facial selectivity.[111] These bis-dienes can add one or two equivalents of a dienophile. Compound 33d reacted with PTAD to give a mono-adduct resulting from reaction *anti* to the ether group. The methylene hydrogen atoms adjacent to the ether oxygen were considered to provide a steric barrier to reaction from that face. The first addition changes the

environment around the remaining diene moeity and so the second equivalent of PTAD reacted from the face *syn* to the ether oxygen. Reaction of **33d** with less reactive dienophiles such as maleic anhydride, benzoquinone and dimethyl fumarate gave only 1:1 adducts which were assumed to be the products of *anti* face reaction, analogous to the reactions of PTAD.

In contrast to this high degree of *anti* selectivity observed in the reactions of **33d** with PTAD, the imide **33b** was reported to give products resulting from exclusive addition *syn* to the heteroatom in both the mono and bis additions and was later reported to undergo a dimerization reaction from the face *syn* to the heteroatom.[112] The report of complete selectivity in the reaction of PTAD with **33b** was also later found to be in error and in fact only 75% of the reaction proceeds *syn* to the heteroatom.[113] For **33b** the steric barriers to the approach of a dienophile from each face of the diene were considered by Ginsburg to be approximately equivalent. This led to the proposition that secondary orbital overlap may be important in determining the facial selectivity of **33b**.[112] The interaction of the carbonyl π^* of **33a-c** and the n_- combination of lone-pair orbitals of triazolinedione dienophiles was proposed to be stabilizing when reaction occurred from the face *syn* to the anhydride or imide bridge.

A substantial number of experiments have been performed to support these assertions. Reaction of PTAD with the diene **34a** and **34b** gave exclusive *anti* face addition products.[114] In reactions of **33a-c** with dienophiles were no secondary orbital overlap was possible such as those of N-phenylmaleimide with exclusive reaction *anti* to the heteroatom bridge was reported.[115] This was confirmed to be the direct result of addition to the *anti* face and the reaction did not proceed via an initial *syn* adduct. A similar result was obtained for the reactions of benzoquinone with **33a-c** and the HC=CH of these dienophiles was presumed to have no greater steric demand than the :N=N: of the triazolinedione PTAD. The former is not able to participate in a stabilizing secondary orbital interaction during *syn* face reaction with **33a-c** thus accounting for the absence of *syn* addition of alkenes.

Reactions of PTAD with **35** [116] give products resulting from *syn* and *anti* addition consistent with a reduced potential for stabilizing secondary orbital overlap and greater steric hindrance from the *syn* face of the diene. Steric effects can override secondary orbital

stabilization: while **36b** and **36c** undergo 50:50 and 60:40 *anti:syn* addition respectively,[117] for the phenyl substituted case **36a**, which provides less steric hindrance to *syn* attack, reaction occurs exclusively *syn* to the heteroatom bridge.

An attempt was made to quantify the secondary orbital stabilizing effect in the reactions of tetraenes **33a-c** with triazolinedione dienophiles in a molecular orbital study by Böhm and Gleiter.[118] The extended Hückel molecular orbital method was used to calculate the potential energy surfaces for the *syn* and *anti* reaction of PTAD and **37**. The latter was regarded as a computationally convenient model for **33a**. They assumed that addition was synchronous and the transition state symmetrical and found that as long as the dienophile remains close and approximately perpendicular to the diene ring the secondary orbital stabilization between the π^* of the anhydride system and the n_- combination of the lone pairs on the approaching dienophile is approximately 17-25 kJ mol^{-1}. This is similar to the stabilizing energy of a hydrogen bond and could account for the exclusive *syn* face reaction of the dienophile. They also investigated whether a σ/π interaction may be important in determining the facial selectivity in the tetraenes **33a-c**. It was calculated that this effect was small and could not explain the unique reactivity of triazolinedione dienophiles as any such interaction is likely to also direct alkene dienophiles. The reaction of singlet oxygen with **33a-c**, where a similar *syn* face selectivity is observed, is the only other dienophile examined with a potential for secondary orbital interaction.[119]

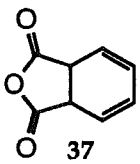

37

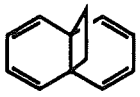
38

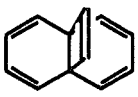
39

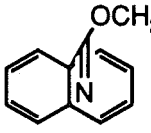

40

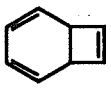
41

There were however several observations in conflict with the secondary orbital overlap hypothesis and theoretical studies have been useful in the resolution of these problems. The observation that PTAD reacted with **38** exclusively from the face *anti* to the ethano bridge was not unexpected. However the similar outcome in the reaction of PTAD with the unsaturated **39** was harder to understand since in **39** there is the possibility for secondary orbital overlap favouring the *syn* face.[120] Reaction of PTAD with **40** similarly

occurs *anti* to the heteroatom despite the possibility of secondary orbital stabilization for *syn* addition.[121] Extended Hückel calculations[118] for the synchronous-symmetrical reaction of PTAD with triene **41**, a model for the reactions of **39**, established that the filled-filled interaction of the two electron π system of the bridging ethylene and the n_+ (considered as a two electron system) combination of lone pairs on the dienophile is closer in energy than the π^* and n_- interaction. This results in a net destabilizing interaction of 21-54 kJ mol^{-1} when reaction occurs from the face *syn to* the ethylene bridge. This interaction was considered to be responsible for the exclusive *anti* face reaction.

A conflict with the secondary orbital hypothesis is that propellanes containing sulphur atoms in the bridging group promote *syn* reaction even though formally no secondary orbital interaction is possible. For example **42** and **43** both react with PTAD exclusively from the face *syn* to the sulphur atom. In order to investigate the reactions of these sulphur containing tetraenes Böhm[118] and Gleiter and calculated the electrostatic potential around

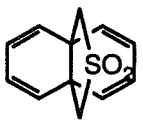

42

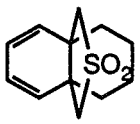

43

the heteroatom using the extended Hückel method and proposed that a stabilizing coulombic interaction between the electron deficient sulphur atom and the electron rich nitrogen atoms on the dienophile favoured *syn* face approach.

Acyclic chiral dienes and chiral dienophiles.

The dienes discussed so far have been cyclic structures, facially differentiated by significantly different structural features proximate to each face. The effects of this differentiation can be clearly observed and quantified without concern for the conformational preferences of the differentiating group at the transition state. In organic synthesis however, the reactions of acyclic dienes are often important and in these situations the conformation of the facially differentiating moeity is often more difficult to define. The most important situations involve either acyclic dienes with a chiral allylic

group or dienophiles with an allylic chiral group in reactions with a cyclic dienes. Recent investigations into both situations will be discussed.

One of the first attempts to develop a model for asymmetric induction in the Diels-Alder reaction was by Trost[122] who synthesized the chiral diene **44** with >95% optical purity.* In this situation the chiral group is not strictly allylic to the diene but is

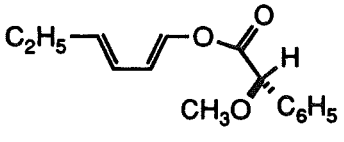

44

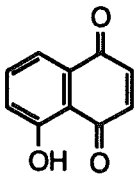

45

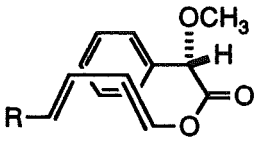

46

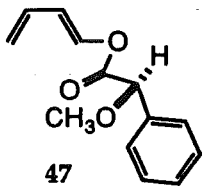

47

nevertheless able to induce selectivity in the reactions of **44** with dienophiles. The reaction of **44** with acrolein gives two diasteroisomers in the ratio 82:18 while the reaction with juglone **45** was reported to occur with complete regio- and facial- selectivity giving only a single product. Trost suggested that the high degree of selectivity observed was the result of the preference of the diene for the conformation **46** stabilized by π-stacking interactions and effectively "blocking" one face of the diene. The greater selectivity in the reaction of the naphthoquinine **45** compared with reaction of acrolein was thought to result from a stronger charge-transfer complex between **44** and **45** that promotes the π-stacked conformation.

Recent experimental and computational investigations into the reactions of dienes of this sort have, however, resulted in a different interpretation for the observed selectivity. The basis of this alternative hypothesis is that the diene **44** prefers a conformation where the methoxy group is perpendicular to the diene moiety as shown in **47** with the dienyl and carbonyl groups essentially coplanar. Stereodifferentiation is a result of the dienophile approaching the diene from the face *anti* to the bulky phenyl group. In order to test this Thornton et al.[123] prepared the related diene **48** which they proposed would have an

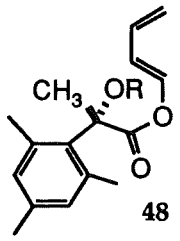

48

a) R=H
b) R=TMS

even greater preference for the "perpendicular" conformation. The methyl groups on the

*The chiral purity was established by studies with chiral shift reagents.

ortho positions of the phenyl groups and at the α-carbon disfavour the linear conformation analogous to **46**. Reaction of **48a** with benzoquinone, N-ethylmaleimide and maleic anhydride gave a high degree of selectivity. The unprotected diene **48a** reacted with the sense of facial selectivity reversed to that of the protected compound **48b**, and this was considered to be the result of a hydrogen bonding interaction between the OH-group on the diene and the approaching diene when reaction occurred from one of the faces only. This was supported by the observed solvent dependence of the facial selectivity: the reaction proceeded with considerably less selectivity in DMF than in toluene, the latter not disrupting the intermolecular hydrogen bond. The geometry of the adduct of N-ethylmalemide was determined by X-ray analysis and hydrogen bonding was also implied in the structure. The phenyl group was determined to be *anti* to the dienophile, further supporting the "perpendicular" model.

Houk et al.[124] have performed MM2 calculations to assess the conformational energy profiles of dienes of this sort. They also considered a fixed MM2 model based on an *ab initio* transition structure for the reactions of butadiene and *s*-trans acrolein. These calculations, while not proving conclusively the validity of the "perpendicular model" when taken in consideration with the experimental study described above, indicate that ground state conformation allows for a reasonable approach to understanding π-facial selectivity in these compounds and a model involving "π-stacking" as a determinant in conformation is not required.

The reactions of dienophiles with allylic chiral groups is of importance in the synthesis of natural products and compounds of pharmacological importance. The unsaturated sugars **49** and **50** were used as chiral dienophiles by Franck et al.[125] in reaction with the *o*-quinone-methide **51**. They considered the face of the diene which reacts

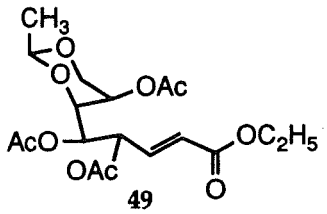

49

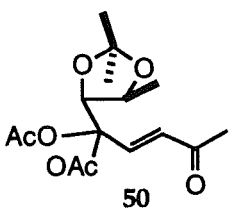

50

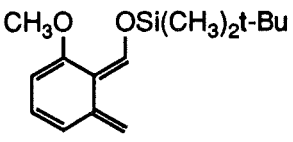

51

would depend on the relative importance of steric and orbital factors as shown in **52**. The reaction with **49** gave a 4:1 selectivity and it was determined by X-ray crystallography that

the major isomer was the result of reaction at the *si* face of the dienophile, thereby avoiding secondary orbital antibonding effects with the allylic oxygen. A similar product ratio was observed in the reaction of **50** with **51** with the major product resulting from reaction *anti* to the allylic oxygen containing substituent.

The addition of dienes *anti* to a heteroatom in a chiral allylic substituent has been reported for a number of different situations and it has been assumed that the oxygen substituent is perpendicular to the plane of the enone as shown in **52**. In a study by Franck[126] aimed at the synthesis of aureolic antibiotics, a Diels-Alder reaction between the facially dissymetric carbohydrate dienophile **53** and the diene **54** played a key role.

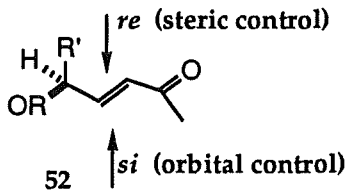

52

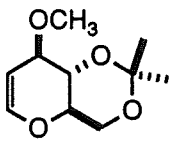

53

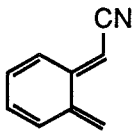

54

The major products were those which resulted from reaction at the face *anti* to the methoxy group so affording the configuration in the product required in the synthesis. The carbohydrate enone **55** prepared by Fraser-Reid et al.[127] was reported to give a single

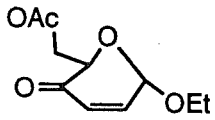

55

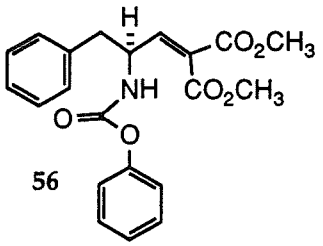

56

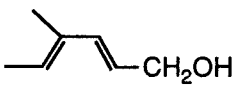

57

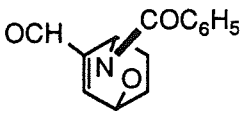

58

product on reaction with butadiene resulting from the addition to the face *anti* to the allylic ethoxy group. Similarly Diels-Alder reaction of **56** with the diene **57** gave only those products which result from addition *anti* to the allylic nitrogen.[128]

One notable exception to this trend has been reported - the addition of butadiene to the cyclic dienophile **58** occurs exclusively from the face of the dienophile *syn* to the N-O bridge.[129] The position of the allylic group is however quite different to the previous examples having the heteroatoms held over the plane of one face of the dienophile. While it has been suggested that the *syn* face of the dienophile is less sterically hindered, this situation corresponds closely to the 5-substituted cyclopentadienes and the hyperconjugative stabilization arguments proposed for those compounds may have relevance in this

situation.[94]

Tolbert and Ali's[130]"demanding test for concertedness" in the Diels-Alder reaction also functions as an investigation of "cooperativity" between two (or more) chiral groups on a dienophile or diene in inducing asymmetry in Diels-Alder reactions. A series of fumarate dienophiles **59** were reacted with the diene **60**. The effect of an *exo* and *endo* bornyl group on the enantioselectivity of the dienophile addition are additive for the

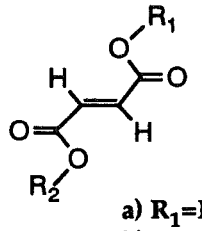

a) $R_1=R_2=CH_3$
59 b) R_1=L-bornyl, $R_2=CH_3$
c) $R_1=R_2$= L-bornyl

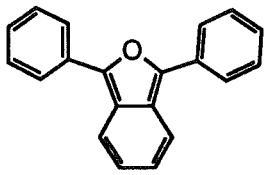

60

dibornyl addition and this shows how separate chiral groups on a dienophile may combine or "cooperate" to increase the selectivity of the reaction which is consistent with the reaction being concerted. The additive effect of the an *endo* and an *exo* chiral bornyl group would not have been expected if the reaction proceeded via the highly unsymmetrical transition state of the non-concerted reaction. "Coopertivity" also exists in chiral substituted dienes. The dienes **61a** and **61b** were prepared by utilization of butadiene-iron tricarbonyl complexes and the Diels-Alder reactions of these dienes with TCNE were investigated.[131] With diene **61a** TCNE gave a 2:1 mixture of diastereoisomers, while with **61b**, the product ratio was 85:15. The increased selectivity for the diene with two identical chiral groups suggests strongly that both groups cooperate in directing the incoming dienophile to one face of the diene.

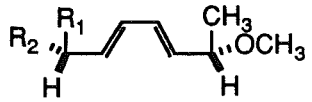

a) $R_1 = CH_3$, $R_2 = OCH_3$
b) $R_1 = R_2 = H$

61

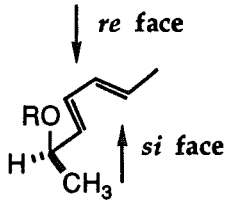

62

The origin of the diastereoselectivity in these acyclic systems is also of interest. Franck and co-workers, who had previously described their observations for a chiral substituted dienophile[127] proposed simple rules for the reaction of chiral allylic substituted

dienes 62 and dienophiles.[132] They observed that the directing effect of allylic substituent is reversed in a diene from that of a dienophile and so developed the following simple rules for predicting facial preference:

Chirality of allylic group	Face Selected dienophile	diene
R	*si*	*re*
S	*re*	*si*

For example reaction of the S chiral diene **63a** with N-phenylmaleimide gave a 5:1 preference and with **63b** a 7.3:1 preference for reaction from the *si* face of the diene. Reaction of **64** with N-phenylmaleimide was reported to give only a single product[133] the

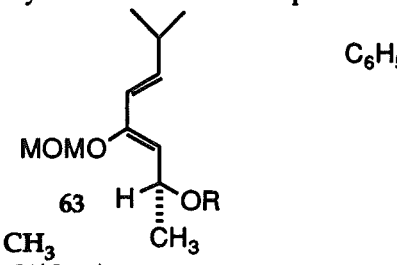

63

a)R = CH_3
b) R = $Si(CH_3)_3$

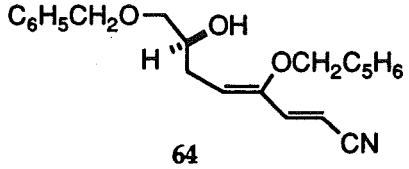

64

MOM = CH_3OCH_2

structure of which was determined by X-ray structural analysis. This reaction was the first where it was demonstrated that complete selectivity could be achieved by a chiral allylic substituent. The facial product conformed to the rules of Franck and the high selectivity was proposed to reflect the steric influence of the Z-alkoxy substituent.

The reactions of the chiral diene **65** have also been studied as part of a synthetic strategy directed towards the development of new antidiabetic drugs.[134] The reaction of N-phenylmaleimide with **65** results in a facial selectivity of 3.2:1, and although the products were not fully characterized, there is some evidence that addition had preferentially occurred from the face expected from application of Franck's rules.

While these simple empirical rules were successful in predicting the facial preference for most reactions of chiral substituted dienes there are some important exceptions. During the total synthesis of the antibiotic actinobolin the intermolecular Diels-Alder reaction of the homochiral diene **66** with an acetylenic dienophile was a key step.[135] Reaction of this diene with methyl propiolate gave a 3:1 mixture of diastereomeric products at 110°C. The major product was determined to be the result of reaction from the face opposite that which would be expected by the application of Franck's rules. This anti

Frank behaviour was also later observed in the reaction of a similar diene **65** with DMAD.[136] These observations prompted Franck to consider exceptions to his

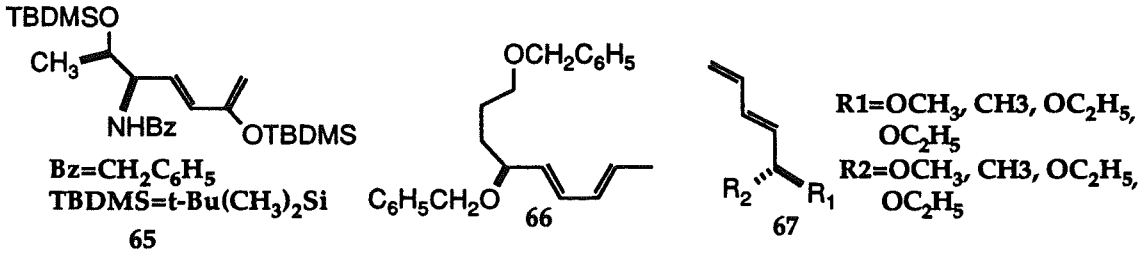

earlier proposal.[137] While his "like" face approach rule holds for the reactions of N-phenylmaleimide, maleic anhydride and acrolein with chiral dienes, TCNE, DMAD and PTAD all favour an "unlike" approach. Franck accepted the earlier proposal made by Reitz[134] and McDougal[133] that the unlike reactivity of DMAD may be the result of unfavourable steric interactions between the substituents on the rigid linear acetylenic dienophile and the alkoxy group on the diene. On this basis methyl propiolate would in these cases presumably react with a different regiochemistry in order to relieve these interactions; however this is not observed. They were also not able satisfactorily to rationalize the reactivity of PTAD and TCNE, except to note that these dienes have often shown atypical behaviour in facially selective reactions.

Franck and Dennenburg have applied molecular orbital theory to the problem of facial selection in chiral dienes such as **67**.[138] Each of the three possible diastereomeric transition states for reaction at each face of the dienes with the conformations shown in Figure 17 were examined using the AM1 semi-empirical method. The dienophiles examined

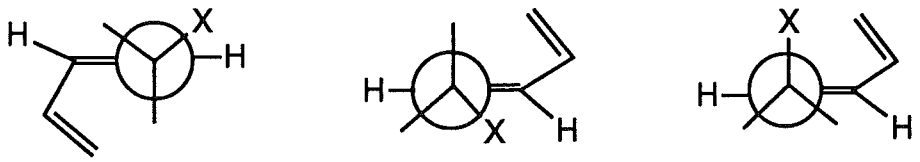

A *anti* **B** *syn* **C** **perpendicular**

Figure 17. Possible conformations for the chiral diene **67** at the transition state. X = heteroatom containing substituent.

were ethylene, acrolein and methyl propiolate. The AM1 method was able to correctly predict the observation of "like" selectivity for the ethylenic dienophiles. More

importantly for the acetylenic dienophiles the "unlike" facial selection was predicted consistent with experiment. In an attempt to understand the origin of the observed facial selection they examined several parameters used to calculate the AM1 transition states. There is no simple correlation between the energy of the transition state and the calculated HOMO-LUMO energy difference at the transition state, the charge on the alkoxy substituent at the transition state or the π-density on the diene at the transition state. Instead they observed that at the transition state the alkoxy group exhibited a preference to lie in a conformation coplanar with the diene as a result of electronic interactions which could not be quantified. Furthermore the alkoxy group appears to favour the *anti* conformation as in A (Figure 17) rather than the *syn* (B). The exception to this is apparently during the reaction of the acetylenic dienophile methyl propiolate where the *syn* arrangement is favoured for steric reasons. They suggested that where a conformational correlation exists between the reactants and the products it is reasonable to predict facial selectivity on the basis of the conformation of the reagent dienes.

These conformational considerations of Franck at al. contrast with an earlier proposal by Hehre and Kahn[139] who stated that electrostatic interactions were the most important and these are "independent of the topological distortions of the participating molecular orbitals". Thus for electron rich dienes and electron deficient dienophiles they formulated the simple rule; "cycloadditions .... should occur preferentially onto the diene face which is the more nucleophilic and onto the face of the dienophile which exhibits the greater electrophilicity". In order to support this assertion they pointed to a number of chiral dienes where addition occurred *syn* to a heteroatom (presumably the face of higher nucleophilicity) and a number of chiral dienophiles where addition occurred on the face *anti* to the heteroatom. This theory was considered to be general for facially dissymmetric dienes and the only exceptions were considered to result from domination of steric effects. If the assignment of the nucleophilic and electrophilic faces of diene and dienophile could be made by inspection and not require calculation, the theory of Kahn and Hehre could be very useful in predicting the course of Diels-Alder reactions of facially dissymmetric dienes and dienophiles. Unfortunately subsequent work has demonstrated that this "rule" is not general enough to be useful. The reversal of selectivity in 5-sulphur substituted

cyclopentadienes[94] for example can not be explained in terms of this theory as the face *syn* to the sulphur atom should remain the more nucleophilic, but a strong preference was observed for reaction to the face *anti* from the sulphur (in contrast to the *syn* preference with an oxygen substituent of approximately the same size). The unusual reactivity of the propellanes discussed above is another example where interactions other than simple electrostatic ones are important.

Experiments have been subsequently performed by Hehre and Overman to test the importance of electrostatic interactions. The dienes they chose for these studies were a class not yet discussed; dienes containing conformationally locked chiral allylic substituents. There have been a number of recent reports of Diels-Alder reactions with such dienes. Such

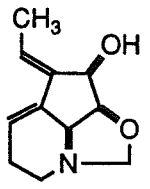

68

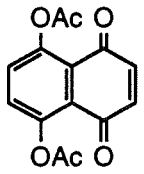

69

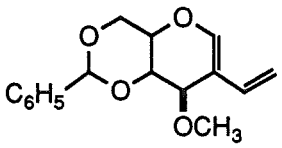

70

dienes are suitable for investigating the influence of allylic substituents on π-facial selection since the position of the directing group is known unambiguously. One example[140] is the reaction of the diene **68** with the quinone dienophile **69** with a 9:1 preference for addition *anti* to the allylic nitrogen and hydroxyl. A similarly strong *anti* face preference occurs for reaction of **70** with maleic anhydride.[141] This effect was less pronounced in reactions with the acetylenic dienophiles DMAD and methyl propiolate indicating that steric influences may also be important.

These reactions favouring the face *anti* to the heteroatom are in direct contrast to expectations based on the electrostatic considerations of Hehre described earlier which would favour *syn* face reaction. Indeed Hehre's own later experiments with dienes of the type **71** and **72** also confirmed a preference for *anti* attack.[142] With the dienophiles TCNE and N-phenylmaleimide a strong (70-90%) preference is similarly observed for

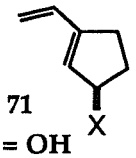

71
a) X = OH

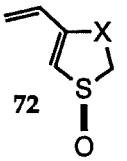

72

reaction *anti* to the allylic heteroatom. One important exception to this trend was the

reaction of **71a** and N-phenylmaleimide in toluene where 64% of the addition occurred on the face *syn* to the hydroxyl group. When the reaction was carried out in methanol however the selectivity is reversed and only 20% of the reaction occurs from the face *syn* to the hydroxyl group. This is strong evidence for the importance if hydrogen bonding if a suitably oriented hydroxyl group is available. The majority of addition reactions to **71** and **72** however occurred on the face *anti* to the allylic substituent consistent with destabilizing electrostatic interactions between the allylic substituent on the diene and the approaching dienophile. The failure of the simple rules proposed by Hehre et al. to account for the now well know *anti* face preference is considered to reinforce the fact that any theory of electrostatic interactions in determining facial selectivity in Diels-Alder reactions must consider all electrostatic interactions, not simply those between the carbons directly involved in bond formation.

Norbornane fused dienes.

The almost exclusive *exo* face attack by a wide variety of reagents on norbornene **73** has prompted research into numerous analogues. A variety of explanations[143] have been proposed over 30 years to account for the facial selectivity in these systems. A recent neutron diffraction study[144] of a derivative **74** of norbornene showed unambiguously that

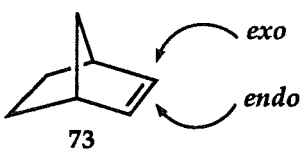

73

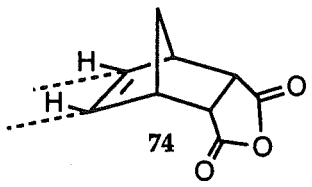

74

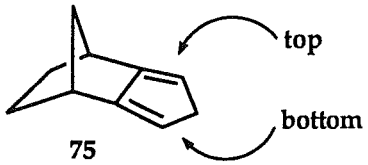

75

the olefinic centres are pyramidalized to the extent of ca. 7.0°. This is greater than previously predicted from *ab initio* calculations (ca. 4.5°) on norbornene itself.[145] The pyramidalization and the related changes in hybridization at the alkene carbons of norbornenes are now widely accepted as a basis for the *exo* reactivity. It is however important to realise that this is a ground state argument and what is important is the relative energy difference in the ground state and the transition for reaction at each face.

The theoretical and experimental interest in the norbornane skeleton led naturally to a large volume of research into the diastereofacial selectivity in the reactions of dienes

fused to a norbornane skeleton such as isodicyclopentadiene **75** where Diels-Alder reaction can occur from either the top or the bottom face of the diene. In direct contrast to the chemistry of norbornenes, **75** undergoes addition reactions under kinetically controlled conditions almost exclusively from the face *syn* to the ethano moiety. The difference in reactivity of the two systems appears at first surprising and accounts for the plethora of papers on this system.

The first reported cycloaddition to this diene was by Alder who reacted it with maleic anhydride and reported a single adduct **76**; the product of exo attack on the diene.[146] There were early reservations expressed about the structural assignment[81] which were strengthened 20 years later when Sugimoto[147] reported that methyl propiolate and methyl acrylate added exclusively from the bottom face of **75**. The issue appeared to be settled when Paquette reported a 1:2 ratio of the bottom face *endo:exo* isomers **77** and **78** in the reaction between maleic anhydride and **75**. The assignment was

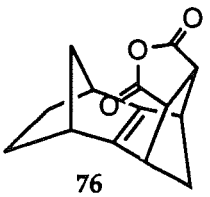

76

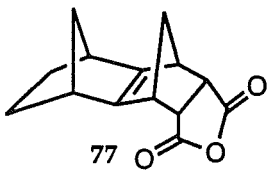

77

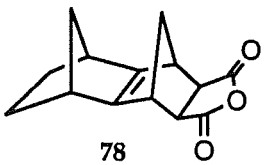

78

made by comparison of the ^1H NMR coupling constants with analogous compounds. An unambiguous proof for the stereochemistry was established by Watson[148] who carried out X-ray structure analyses on the products and determined that they were in fact the top face *endo* product **76** and the bottom face *exo* product **78**. Solvent and temperature have been considered to play some role in facial selectivity with the ratio of products **76:78** and it was later established that the products interconverted under the reaction conditions so that the reaction is at least to some extent under thermodynamic control.[149]

Although most alkene dienophiles appear to favour a kinetic preference from the bottom face in reaction with isodicyclopentadiene there are some notable exceptions.[150] For sterically demanding alkenes reaction is forced to occur from the less hindered top (methano) face. The sterically demanding (E)-1,2-bis(phenylsulfonyl)ethylene[151] was found to react with a strong (ca. 90%) kinetic preference for reaction from the top face of the diene, as was the similarly bulky tetracyanoethylene (TCNE).[152]

Likewise highly reactive dienophiles, such as N-phenyl triazolinedione (PTAD) and N-methyl triazolinedione (MTAD), which were originally reported to react from the bottom face of isodicylcopentadiene[153] were later found to react exclusively from the top face. There was a cross-over in reactivity for highly reactive dienophiles and exclusive bottom face reaction was found with the dehydro derivative **79**.[154]

A number of theories have been proposed[143] to account for the facial selectivity which has been observed in the many cycloadditions to compounds like **75** and these will be now be examined in some detail. One of the first attempts to explain the facial behaviour was by Vogel[155] who proposed that the products resulting from bottom face addition to **75** were the more thermodynamically stable. In order to test this assertion they prepared **80** whose Diels-Alder adducts undergoes equilibration even for products of reactive dienophiles.

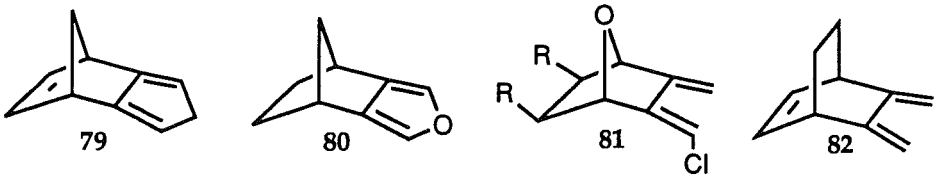

79 **80** **81** **82**

Reactions with maleic anhydride and DMAD which have been shown to be reversible processes, gave exclusively products of bottom face reaction. These products must therefore must be at least 8.4 kJ mol^{-1} more stable than the products which would result from addition of dienophile to the top face of **80**. They proposed a "synergic" effect of the double bond π-anisotropy in the norbornane and 7-oxa-norbornane systems in stabilising the products of bottom face attack. Later studies,[156] however, carried out using 7-oxa substituted substrates such as **81** demonstrated that selectivity in the additions was not necessarily controlled by the stability of the adducts and in these cases top face addition was favoured. These additions and the preference for addition *syn* to the alkene bridge of the bicyclo[2.2.2]octatriene **82**[157] were considered by Vogel to be the result of differential polarizability on each face of the diene. The oxygen in **81** (top face) and the double bond in **82** (bottom face) being the more polarizable were considered better able to stabilize the transition state as reaction from these faces is favoured by the ability of the diene to participate in pre-reaction complexes with the incoming dienophile. The indiscriminate facial reactivity of singlet oxygen in Diels Alder reactions towards these dienes was

considered to arise from the extremely high reactivity of this dienophile.[156]

A detailed examination of the results of semi-empirical (SPINDO, EHT, MINDO) and *ab initio* (STO-3G) calculations on the diene **75** and derivatives led Gleiter and Paquette[158] to suggest that electronic control of selectivity may not be the result of polarizability at each face but rather result from differential secondary orbital overlap with incoming dienophiles at each face. It should be noted that this remains a ground state argument and the validity of the method depends on correlation of this calculated effect with transition state energies. They considered that orbital mixing occurs between the π-orbitals and the high-lying σ-orbitals. The resultant σ/π interaction changes the nature of the π part of the canonical molecular orbitals. This is not a unique result and similar effects were known for cyclohexene[159] and norbornadiene.[160] Their calculations for **83** as a

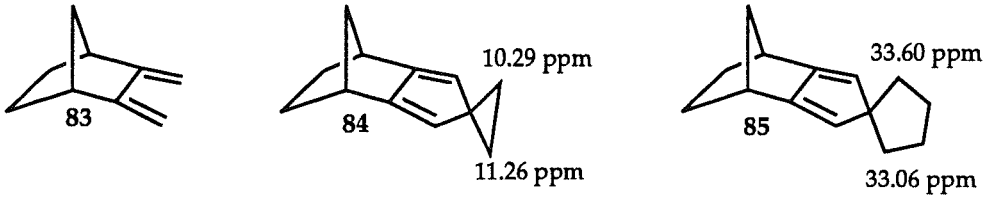

model for **73** indicated that the lowest energy (localized) pre-canonical orbital (π_S) mixed with σ-type orbitals of the proper symmetry located on the norbornane skeleton. The result is that the π-electron density in the π_S orbital is differentiated for each face of the diene, with the top face having greater π_S density. This is in effect a disrotatary motion of the $2p_Z$ lobes on the diene in the way shown in Figure 18. The influence of this differentiation in controlling π-facial selectivity was proposed to be as shown in Figure 18. When reaction occurs from the bottom face of the diene, the antibonding interaction between the HOMO of the incoming dienophile and the π_S of the diene which are of the same symmetry will be smaller than when reaction occurs from the top face of the diene. To support this proposal they applied a quantitative perturbation theory and calculated the difference in 4-electron stabilization energies between the two faces to be 18.7 kJ mol^{-1} for reaction of **83** with ethylene.

In addition to the computational results there is some spectroscopic evidence for σ/π interaction. In compounds such as **84** and **85** the ^{13}C NMR chemical spectra show the most shielded carbon to be *syn* to the face with the highest region of π_S electron density as

predicted by calculation and this is also the face from which dienophiles attack.

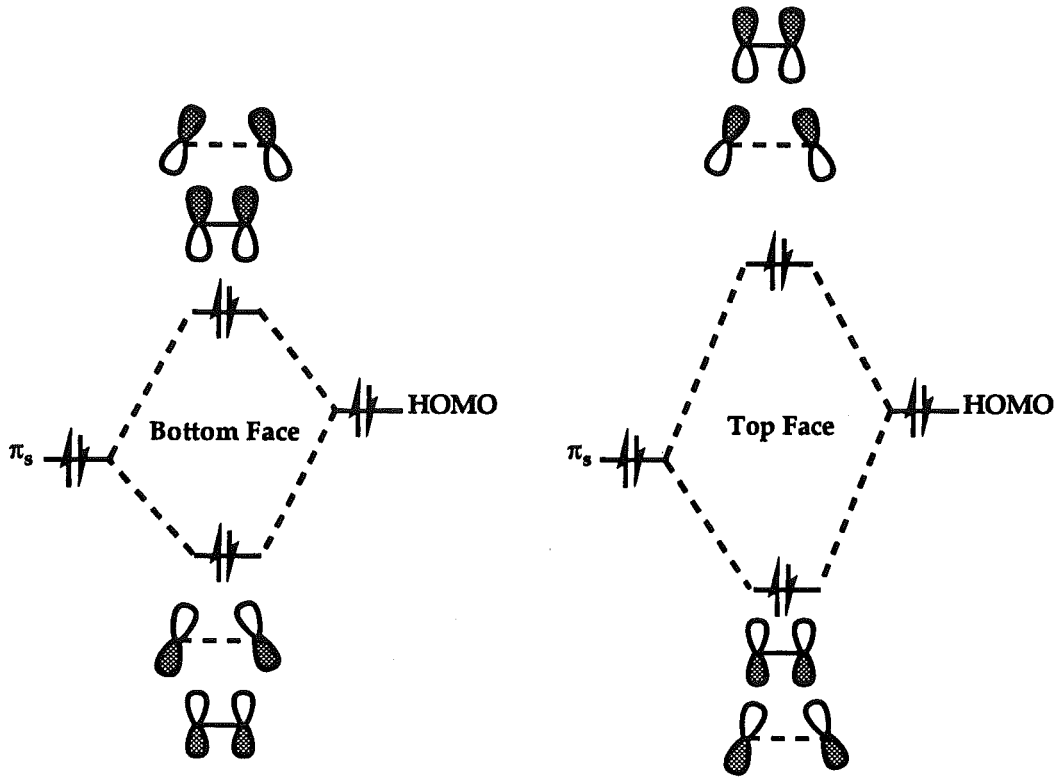

Figure 18. Interaction between the diene π_s and HOMO of the approaching dienophile for reaction at top and bottom face of isodicyclopentadiene.

In a recent extension of these ideas Paquette[161] has examined the derivatives of isodicyclopentadiene to investigate further the influence of σ/π interaction. Reactions of **86** with N-phenyl maleimide, DMAD and benzyne all gave single products which were the result of bottom face attack. It was only with (Z)-1,2-bis(phenylsulfonyl)ethylene that a mixture of facial isomers was obtained and, in particular, a preference for top face reaction.

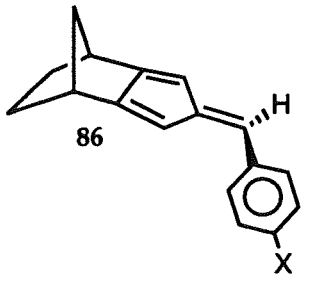

86

X= NMe_2, OCH_3, F, Cl, CH_3, NO_2, CF_3 CN, H.

This is however a result of the steric bulk of the dienophile such that the ethano moiety blocks attack from that face. The ratio of top:bottom face addition to diene **86** is, however, highly dependent on the nature of the para-substituent X. A plot of the Hammet factor σ^+_R for X versus the experimentally observed product ratios was linear with the exception of the CN and NO_2 values. It can be reasonably assumed the the various X-groups do not change

greatly the steric requirements in the reaction at each face. The effect of the para-substituent can be rationalized as follows. Since the largest preference for top face attack was observed with the strongest electron withdrawing groups it may be that electron withdrawal lowers the energy of the σ-orbitals which therefore participate to a lesser extent in the σ/π interaction. Thus, the degree of disrotatary tilting of the $p2_z$ orbitals on the diene is reduced and reaction from the top face will proceed preferentially. These observations reinforce the conclusions from less quantitative studies on the effect of spiro[162] and isopropylidene[163] derivatives of 75 in modulating σ/π interaction and add weight to the proposition that these electronic effects are indeed responsible for the observed facial selectivity.

Paquette has also investigated the addition of N-phenylmaleimide, benzoquinone and 4-cyclopentene-1,3-dione with isodicyclopentadiene derivative 87[162] where the

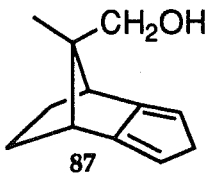

87

possibility exists for hydrogen bonding between the hydroxyl group on the top face of the diene and a dienophile attacking that face. All the dienophiles examined however reacted exclusively from the bottom face consistent with the σ/π interaction hypothesis.

While there is evidence for the σ/π interaction hypothesis, there are however several cases for which it fails satisfactorily to rationalize the observed facial selectivity. Clearly steric factors with a bulky dienophile such as TCNE will overwhelm any secondary orbital effects. The failure of this theory to predict the observed[154] top face preference in the reactions of triazolinediones with 75 is more difficult to explain as these dienophiles should not be any more steric demanding than many of the alkene dienophiles which undergo exclusive bottom face reaction with 75. Finally the σ/π interaction hypothesis is based solely on the calculations of the ground state properties of the reacting species. During the course of the reaction, geometric and electronic rearrangements occur which substantially perturb the molecular orbitals. Until it can be demonstrated that the perturbation theory based on ground state molecules is a satisfactory model for those species at the transition

state then the σ/π interaction hypothesis is weak. Part III of this thesis describes molecular orbital calculations which are directed at determining the significance of σ/π interaction on the diastereofacial selectivity observed in the reactions of the cage diene **29** and related compounds.

In contrast to the stereoelectronic theories described so far, Houk[164] has proposed that torsional and steric considerations may be the most important factors in determination of facial selectivity during the cycloaddition reactions to isodicyclopentadiene and derivatives. He noted that in the STO-3G *ab initio* calculated transition state for the Diels-Alder reaction of ethylene and butadiene[165] the hydrogens at C2 and C3 were bent out of the plane of the diene approximately 14.9° towards the incoming dienophile. This pyramidilization was proposed to be necessary to maintain orbital overlap of the p-orbitals on those carbons with similar orbitals on C1 and C4 as these rotate to achieve the best possible overlap with the dienophile. Houk proposed that, since in isodicyclopentadiene the norbornane skeleton is fused at what is equivalent to C2 and C3 in the diene, this bending may have a significant effect on the facial selectivity in the reactions to this diene. In order to test this hypothesis Houk developed a MM2 model which was based on MNDO calculations for the transition state in the reaction of ethylene at both faces of isodicyclopentadiene. With the positions of the seven carbons in the cyclopentadiene-ethylene and their attached hydrogens, as well as the norbornane bridgehead carbons fixed the positions of all other atoms were optimized and the MM2 energy evaluated at each face. This calculation was carried out using ethylene and maleic anhydride as model dienophiles and a range of isodicyclopentadiene-type compounds as the diene components. The experimental data for maleic anhydride compare well with the calculated ratios of top/bottom face attack except for compounds such as **88** and **89** where 66% top face was

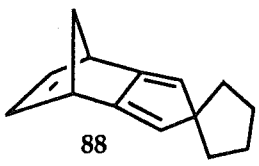

88

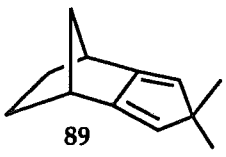

89

predicted but the observed preference for reaction was 96% bottom face. Houk considered that this failure was due to the rigidity of the MM2 model and the resultant inability to relieve steric crowding. Maleic anhydride, however, was in some ways an unfortunate

choice as it's reactions are known to be under thermodynamic control - at least with isodicyclopentadiene **75**.[149]

As there is limited experimental data available for the reactions of ethylene with norbornane fused dienes the calculated predictions for ethylene were compared with the experimental results for the acetylenic dienophile DMAD. Regardless of this there was good agreement between the calculated ratios for ethylene and the observed ratios for the reactions of DMAD. The few exceptions apparently result from the inability of the model to relieve unfavourable steric interactions. After demonstrating that the MM2 model was able to reproduce the experimentally observed facial selectivity, Houk considered the reasons for the bottom face preference. By careful examination of the geometry around the isodicyclopentadiene fragment, he observed that in the top face addition bending occurred in the *endo* direction at the junction between the norbornane and the diene which relieved torsional strain. For the top face attack the torsional interactions were actually increased. This situation is summarized in Figure 19. In addition to these considerations of torsional

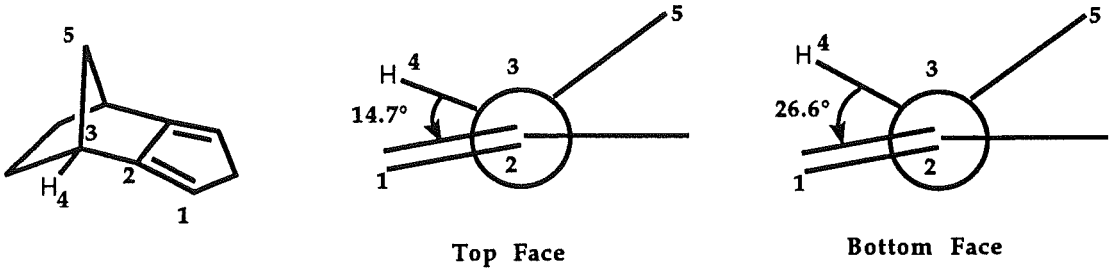

Figure 19. Newman projection looking down C2-C3 of isodicyclopentadiene showing the different torsional interactions at the transition state for top and bottom face reaction with dienophiles.

interactions at the transition state he proposed that with bulky dienophiles or isodicyclopentadiene derivatives such as **88** and **89** steric effects may become important. Thus it was the balance of these two factors which would determine the facial selection observed.

So there is still no definitive explanation for the facial selectivity in isodicyclopentadiene. The two theories discussed both have merit. There is little doubt that σ/π interaction does occur in isodicyclopentadiene and related compounds, however it's significance for determining facial selectivity cannot be easily quantified. In a similar manner, the evidence for bending at the transition state given by Houk is strongly supported by calculation, but the significance of this bending in determining facial selectivity is also

hard to quantify. Certainly the proposition that with highly substituted substrates such as 4,4-dimethylisodicyclopentadiene **89** steric factors may be important in determining π-facial selectivity. It may be, however, that in less sterically biased systems such as **75** itself, the torsional and secondary orbital factors act in concert to promote bottom face addition of dienophiles. Experimental studies into norbornane fused dienes continue with the aim of determining if this is the case. A recent report[166] of the π-facial selectivity in the reactions of the triene **90** has shown a strong preference for reaction from the top face with ethylenic and azo dienophiles, while acetylenic dienophiles and benzyne gave 1:1 mixtures of reaction at each face. This behaviour is difficult to rationalize in the framework of either of the two major theories.

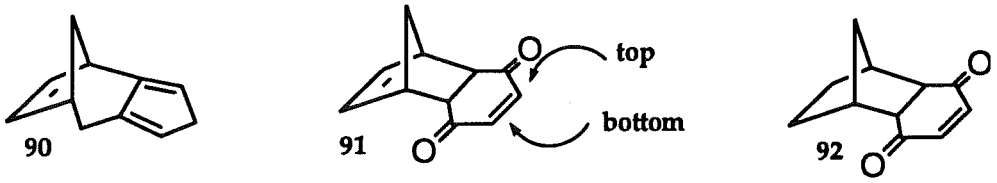

90 **91** **92**

In addition to the studies of norbornane-fused dienes, Mehta[167] has investigated the influence of the norbornane skeleton on facial selectivity in reactions of norbornane fused dienophiles such as **91** and **92**. For simple dienes such as cyclopentadiene, 1,3-cyclohexadiene and cyclooctatetraene, reaction with **92** occurred predominantly from the bottom face of the molecule but the selectivity observed was reversed with additions to the dehydro derivative **91**. Dienes with greater steric demand; 1,3 diphenylisobenzofuran and 1,2,3,4-tetrachloro-5,5-dimethoxycyclopentadiene showed a strong preference for top face addition with **92** which was more marked in **91**. On the basis of these observations and supported by a simple MM2 transition state model similar to that employed by Houk in his investigations into the reactions of isodicyclopentadiene, Mehta concluded that the facial selectivity observed in these cases was the direct result of steric influences at the transition state.

The number and diversity of possible facially dissymmetric dienes and dienophiles which can be persuaded to undergo a Diels-Alder reaction is enormous; the specific examples given above are only a small sample of the many reported in the literature. This very diversity is a severe barrier to the development of a simple theory to account for every example of facial selection in this most useful of carbon-carbon bond forming reactions. There

are simply too many "special cases". The best that can be achieved is to develop an understanding of the important directing influences for each major class of diene and dienophile. Some classes of diene such as the 5-substituted cyclopentadienes have simple, easy to apply theories which apparently account for all the experimental observations which have been made to date. No doubt research is continuing with the aim of uncovering exceptions to these rules, or strengthening them with further examples. For other classes, such as norbornane fused dienes, the origin of the experimentally observed diastereofacial selectivity remains unclear; several theories have been proposed but no one theory can account for all the experimental observations in a simple and elegant manner and is able to make predictions which would be useful to the synthetic organic chemist. Again research will continue as newly developed experimental and theoretical approaches are applied to the remaining problems. The driving force for this is the aim of allowing the synthetic chemist ultimate control over the Diels-Alder reaction and no doubt further developments in understanding the nature of facial selectivity will continue to ensure a place for this procedure in a great many synthetic projects.

Part II.

Diastereofacial Selection in Cage-Fused Dienes. Experimental and Molecular Mechanics Studies.

4. The Application of Molecular Mechanics to Investigate Steric Influences in Determining Facial Selectivity.

A description of the molecular mechanics models used to investigate the role of steric interactions in diastereofacial selection of Diels-Alder reactions to cage-fused dienes.

5. Diastereofacial Selection in Diels-Alder reactions to a Cage Diol.

Experimental and molecular mechanics studies of diastereofacial selection in the Diels-Alder reactions of a diol substituted cage diene.

6. Diastereofacial Selection in Diels-Alder Reactions of Mono and Dimethylidene Substituted Cage Dienes.

Experimental and molecular mechanics studies of diastereofacial selection in the Diels-Alder reactions of mono and dimethylidene substituted cage dienes.

7. Synthetic Studies on Cage Compounds.

Synthetic studies on cage-fused dienes directed towards the production of novel compounds for the study of diastereofacial selection in the Diels-Alder reaction and illustrating the importance of trans-annular interactions in the chemistry of cage compounds.

Chapter 4.

The Application of Molecular Mechanics to Investigate Steric Influences in Determining Facial Selectivity.

The utilization of sophisticated molecular force-fields such as MM2[168] is becoming an important part of computational chemistry. These procedures are able to reproduce accurately a wide range of experimental geometries including those of large organic and bio-organic molecules which cannot be treated with quantum chemical techniques. Because the energies which are determined from the molecular mechanics procedures are only relative, energetic comparisons are restricted to conformers or diastereomeric structures. In the study of facial selectivity, therefore the relative energies calculated for reaction at each face can be used with confidence as a guide to the relative steric influences at each face.

The experiments to investigate facial selectivity in cage compounds which will be described in the next few chapters were also examined with the aid of molecular mechanics calculations. The results of these will be discussed after the relevant experimental results. The modelling method was also applied for additions to diketone **29** where the experimental results have been reported elsewhere.[169] Addition to cage dienes can occur from either the face of the diene *syn* or *anti* to the cyclobutane group and the stereochemistry of the addition products of all the cage dienes discussed here will be described in these terms. The diketone **29** provides a good example to discuss the modelling methods in detail and will be the subject of the remainder of this chapter.

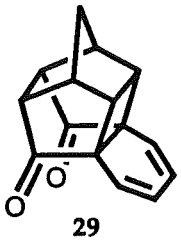

29

Experiments will be described below which demonstrate that Diels-Alder addition reactions to cage compounds such as diketone **29** proceed almost exclusively in a irreversible manner and so the relative product stability of the two facial products is not likely to be

important in determining the observed product distribution. To confirm this the relative facial energies of the two products arising from addition at each face of **29** were evaluated using the MMX force field.[170] This is derived from Allinger's MM2P force-field but has the following important modifications:

• Firstly the electrostatic term in the force field is based on a charge-charge interaction rather than the bond dipole - bond dipole interaction of the original MM2 procedure. This is a more flexible system and allows for electrostatic interactions to take into account the dielectric constant of the immediate environment. The calculations described here were performed with the dielectric constant set to 1.5 D. This is simulating the gas phase or a non-polar solvent environment - the latter being the one which best matches the experimental conditions.

• Secondly, the MMX procedure has an option for performing a Variable Electronegativity Self-Consistent Field (VESCF) calculation including only those atoms comprising a π system. This one-electron treatment gives a better geometry for a conjugated π system than the simpler MM2 procedure where the effects of conjugation in extended π systems are not reproduced. The VESCF calculation is performed several times during the minimization cycle and the bond stretching and torsional parameters are assigned to the π atoms on the basis of the bond order as determined by the SCF calculation.

• Finally, the MMX force-field has one of the largest sets of parameters of any of the MM2 derived methods. This allows meaningful calculations to be carried out over a wide range of bonding situations including acetylenic groups and the MMX procedure also incorporates the steric bulk of lone pairs by considering them as "pseudo-atoms". Hydrogen bonding interactions between acidic hydrogens and other suitable atoms are icorporated in MMX.

The results of the MMX calculations on the products resulting from addition at each face of the diketone **29** with a group of representative dienophiles are given in Table 2. The acetylenic dienophiles DMAD and MP were reported to show a greater variation in facial selectivity than alkene dienophiles. In order to estimate the relative stability of the

Table 2.
Calculated (MMX) energy differences ($\Delta E_{(anti\text{-}syn)}$; kJ mol^{-1}) between adducts resulting from *anti* face and *syn* face reaction and calculated % *anti* face reaction at 80°C of diketone **29** with selected dienophiles.

dienophile	ΔE E_{anti}-E_{syn} (kJ mol^{-1}).	% Reaction at *Anti* Face Calc.	Obs.
maleic anhydride (MA)	+13.6	1.0	>98
benzoquinone (BQ)	+5.6	12.9	>98
acrylonitrile (AN)	+20.3	0.1	>98
tetracyanoethylene (TCNE)	+6.8	9.0	>98
phenyl-triazoline dione (PTAD)[a]	+9.7	2.0	64

[a] Calculated and observed ratios for PTAD correspond to reaction at 0°C.

conformationally flexible products it was necessary to perform a conformational search and so the calculation was carried out using the BAKMDL[171] program with the MM2 force-field. A number of starting geometries were generated by systematic rotations of the conformationally free bonds. For ester bonds a rotation resolution of 180° was used. The structures generated were then minimized in the normal manner. Those which were within 12.6 kJ mol^{-1} of the lowest energy conformer were tabulated and a Boltzmann average energy at the reaction temperature was calculated for each face. The results for DMAD and MP are summarized in Table 3. The results in Table 2 show that for the reactions of diketone **29** with alkene dienophiles the product which is calculated to be more stable was not observed in any of the reactions. This is consistent with these reactions proceeding irreversibility and demonstrates that the observed product ratios result from a facial preference based on kinetic rather than thermodynamic factors. This also militates against an earlier proposal the product stability may be of general importance in influencing facial selectivity.[155,156] For the acetylenic dienophiles the results in Table 3 show that the calculated product ratio for DMAD is close to that observed. This result cannot however be considered to be general

Table 3.
Calculated (MM2) energy differences ($\Delta E_{(anti\text{-}syn)}$; kJ mol^{-1}) between the Boltzmann Average Energies of adducts resulting from *anti* face and *syn* face reaction and calculated *% anti* face reaction at 80°C of diketone **29** with DMAD and MP.

dienophile	ΔE E_{anti}-E_{syn} ; kJ mol^{-1}	% Reaction at *Anti* Face Calc.	Obs.
methyl propiolate (MP)	0.4	47	>98
dimethyl acetylenedicarboxylate (DMAD)	1.9	34	55

because of the experimentally observed irreversibility of this reaction and the contrast with the methyl propiolate result where the product stability does not correlate with the observed product ratio.

Once it was established that product stability does not affect the observed product ratio, it became apparent that a molecular mechanics model which attempts to measure steric interactions at the transition state would be more appropriate. The use of molecular mechanics based models for transition states has largely been developed by Houk and co-workers[172] and although not without criticism[173] it has been successfully applied to problems of stereoselectivity in cycloadditions[97,164] and nucleophilic attack on carbonyl groups[174] as well as in investigations of proximity effects on reactivity in hydroxy acids.[175]

There are two ways in which molecular mechanics can be utilized to model transition states: parameterised methods and fixed (or "rigid") models. The parameterized methods involve the use of parameters which have been developed to reproduce transition structures determined from high level *ab initio* calculations. These parameters are reduced versions of their "ground state" equivalents and are scaled according to the "order" of the partial bonds associated with that parameter. For example, for the Diels-Alder transition state for the reaction of alkenes with dienes the C-C forming sigma bond has a r_0 set to transition state bond distance which was determined by *ab initio* calculations.[40] The stretching constant for the bond is approximately 0.3 times the value for the fully formed bond in the product. This arises because of the "early" Diels-Alder transition state; the order of the forming bond is

judged to be 0.3 or approximately 1/3 formed at the transition state. A similar procedure is followed for all the remaining parameters involved in bonding changes. Two new MMX atom types have been defined to carry transition state modelling of the Diels-Alder reaction and these are used in the transition state as shown in Figure 20. The C#-C# and C*-C* bonds both

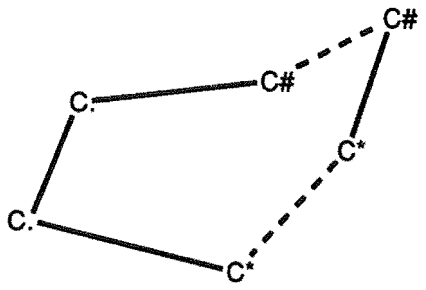

Figure 20. Labelling of transition state atoms in the MMX transition state for the reactions of alkenes with butadiene.

have bond orders approximately 0.3 and may vary independently to allow for perturbations from synchronicity brought about by substitution. When these parameters are used for the prototype reaction of ethylene and butadiene, a geometry is obtained which closely resembles the transition state for the synchronous, concerted pathway calculated by the highest level *ab initio* calculations to date .

To utilize this method for the study of steric interactions at the transition state in the reactions of diketone **29**, the following procedure was followed. First the appropriate atoms of the geometry which was calculated for the product of reaction at each face were substituted with the transition state atom types. A MMX calculation on the resulting structures then gives a MMX steric energy for each face and this should reflect the relative steric interactions at the transition state. The results from this procedure on diketone **29** with representative dieneophiles are shown in Table 4. With the alkene dienophiles shown in Table 4 the calculated energy difference would represent exclusive carbonyl face addition and this is consistent with the experimental observations. The success of this simple parameterised model suggests that the facial selectivity for alkene dienophile addition to diketone **29** is largely determined by steric interactions at the transition state. It is interesting to note that the steric interactions at the transition state predict the opposite facial selectivity to that evaluated at the product geometry. This is a reflection of the distance dependence of the various interactions; in the product geometry the relatively close

Table 4
Calculated (MMX) transition state energy differences ($\Delta E_{(anti\text{-}syn)}$; kJ mol^{-1}) between adducts resulting from *anti* face and *syn* face reaction and calculated % *anti* face reaction at 80°C of diketone **29** with selected dienophiles.

dienophile	ΔE E_{anti}-E_{syn} ; kJ mol^{-1}	% Reaction at *Anti* Face Calc.	Obs.
maleic anhydride (MA)	-15.6	99.5	>98
benzoquinone (BQ)	-18.2	99.8	>98
acrylonitrile (AN)	-17.3	99.7	>98
tetracyanoethylene (TCNE)	-15.2	99.4	>98

carbonyl-dienophile distance for the carbonyl face products seems to disfavour these structures relative to the cyclobutane face.

The reactions of acetylenic dienophiles were also of interest because experiment had shown a much greater variation in facial selectivity and these are thus a more rigorous test for any modelling procedure. Unfortunately, transition state parameters for the Diels-Alder reactions of acetylenic dienophiles are not available for the MMX force-field. An alternative to the parameterized modelling described above is the use of a fixed or rigid model. This methodology has already been utilized in investigations of facial selectivity in the reactions of diisocyclopentadiene, cyclopentadienes[164] and norbornyl-fused *p*-benzoquinones.[167] It should be noted, however, that these studies were all based on a MNDO calculation of the symmetrical transition state for the concerted reaction of ethylene and butadiene and this is not a true transition state on the MNDO potential energy surface, although it is similar to a true transition state on the AM1 potential energy surface.

The fixed model is developed as follows: firstly it is necessary to calculate the geometry of the transition state , usually by using a molecular orbital method, for a prototype case of the reaction of interest. In this study, the AM1 method was used to examine the transition state for the reaction between acetylene and butadiene. The transition state obtained was similar to that obtained by subsequent PM3 as well as high level *ab initio* calculations and so was able to be used with confidence. Once this geometry

was established, the atoms involved in bond formation in the structure to be modelled were fixed at those calculated positions. Then the rest of the structure was added and a molecular mechanics calculation was performed on the resulting geometry. This model is less realistic than the parameterized model described earlier in that it may be somewhat inflexible and some interactions may be over-emphasized. The position of the atoms in the fixed model are however exactly as they were in the original transition state calculation and thus some subtle effects such as bending of the hydrogens on C2 and C3 of the diene at the transition state, are reproduced exactly. These subtle changes have been proposed[40] to be important in determining facial selectivity.

In order to first establish the validity of the fixed model approach, the method was applied to the reactions of alkene dienophiles with diketone **29**. The transition state geometry was based on that reported for the reaction of ethylene and butadiene using the AM1 method. The results are shown in Table 5. A comparison of the results in Table 4

Table 5
Calculated (MM2 - "Fixed Model") transition state energy differences ($\Delta E_{(anti-syn)}$; kJ mol^{-1}) between adducts resulting from *anti* face and *syn* face reaction and calculated % *anti* face reaction at 80°C of diketone **29** with selected dienophiles.

dienophile	ΔE $E_{anti}-E_{syn}$; kJ mol^{-1}	% Reaction at *Anti* face Calc.	Obs.
maleic anhydride (MA)	20.7	100	>98
benzoquinone (BQ)	22.3	100	>98
acrylonitrile (AN)	23.2	100	>98
tetracyanoethylene (TCNE)	18.7	100	>98
MP[a]	12.9	98.8	>98
DMAD[a]	17.0	99.6	45

[a] From differences in Boltzmann average energy between the most significant conformers at the reaction temperature.

with those in Table 5 shows that the MM2 fixed model gives quantitatively the same results as those from the MMX parameterised model, with a high degree of selectivity for reaction from the face of the diketone which is *anti* to the cyclobutane group of diketone **29** predicted

with both models. This close agreement suggests that the fixed model can be applied with confidence to the reactions of alkene dienophiles with diketone **29**.

As noted before the alkyne dienophiles MP and DMAD which have been studied experimentally, are conformationally flexible and so any model must take into account the relative proportions of the possible carboxylate group conformations. To carry this out with the fixed model a systematic conformational search was performed on the structures with the atoms involved in bonding changes restrained to the geometry determined for the reaction of acetylene and butadiene by AM1 calculation. The differences in Boltzmann Average Energy (BAE) for each face should indicate the relative steric interaction at each face. The results of the calculation for diketone **29** with MP and DMAD are shown in Table 5.

While the results for the MP reaction are consistent with experimental observations, those for DMAD predict a greater proportion of the reaction of DMAD with diketone **29** to occur from the carbonyl face than was observed. This may be due to a failure of the model to be able to calculate the small energy differences involved. Alternatively, considering that molecular mechanics is essentially a "steric only" treatment, it is possible that there are orbital interactions involved at the transition state for the reaction of DMAD and diketone **29** which are not present in the prototype reaction of acetylene and butadiene and therefore cannot be incorporated into the model. An example of this would be an anti-bonding interaction between the orthogonal HOMO of the incoming acetylene and filled orbitals on the carbonyl groups for the reaction proceeding from the *anti* face of diketone **29**. This possibility has been investigated by detailed molecular orbital calculations and will be described in a later section.

The reactions of PTAD and nitrosobenzene with the various cage dienes also show a wide variation in selectivity. Unfortunately these reactions cannot yet be investigated by either molecular mechanics methods described above because the required details of the reaction trajectory in each case have not been investigated by molecular orbital calculations.

The application, therefore, of a relatively simple molecular mechanics based method allows a rapid evaluation of at least the steric influences for reaction at each face of a medium sized compound such as diketone **29**. The results obtained by both the models

described are largely consistent with experimental observations: the differences between predictions based on a transition state model and those based on a product geometry model reinforce both the important role of kinetic factors in determining facial selectivity, and the consequent importance of the use of a model which is able to estimate the various interactions at an approximate transition state geometry. The molecular mechanics basis of these models allow calculations to be performed in only a modest amount of computer time, whereas the use of more sophisticated models, such as semi-empirical molecular orbital methods, while giving slightly more insight, would have restricted the number of calculations possible, and so only a fraction of the experimental cases would have been able to be examined by theory. This is especially the case for the conformationally flexible structures. The results described here show that the use of molecular mechanics models of this sort would be useful as part of a pre-synthetic strategy; where facial control is required a simple molecular mechanics calculation may give useful quantitative predictions on facial selectivity and allow decisions to be made on suitable substrates before any experiments are carried out.

Chapter 5.

Diastereofacial Selection in Diels-Alder reactions to a Cage Diol.

The diol **93** was prepared by reduction of the corresponding diketone **29** using lithium aluminium hydride, and this reaction proceeded with complete selectivity to give only the *endo-endo* diol which is consistent with previous reports for similar compounds.[176] Complete *endo-endo* selectivity was also obtained with the use of sodium borohydride in

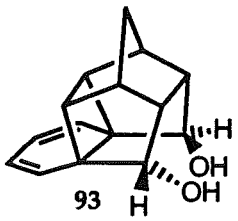

93

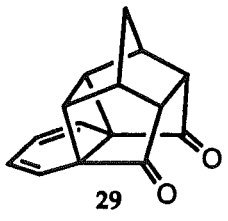

29

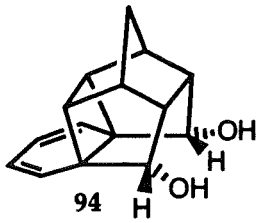

94

ethanol to reduce diketone **29**. The addition of cerium trichloride to the reaction mixture resulted in a *decrease* in the selectivity of the reaction with sodium borohydride and 15% of the *endo-exo* diol **97** was formed as a minor product in the reaction. This is in contrast to the reported effects of the addition of cerium trichloride in the sodium borohydride reduction of the closely related PCUD derived ketone where it was reported to enhance the selectivity of the reaction.[177]

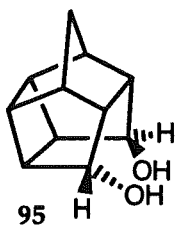

95

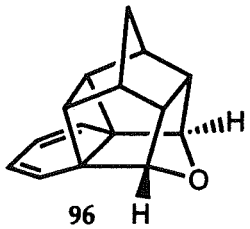

96

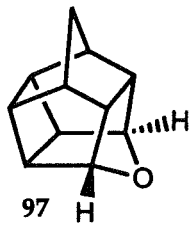

97

Further contrasting behaviour between the reactions of diol **93** and its pentacycloundecane (PCUD) analogue **95** was observed during attempts to dehydrate **93** to form the cyclic ether **96**.

This reaction has been reported to occur easily for **97** and has been used as evidence for the *endo-endo* configuration of the diol.[176] Diol **93**, however was highly resistant to dehydration and the following table summarizes the methods tried and the results obtained:

Reagent/Method	Result
catalytic p-toluene sulphonic acid[177]	No reaction
heating neat to 280°C[176]	Polymerisation
heating in presence of P_2O_5.[178]	Polymerisation
H_2SO_4[179]	Polymerisation

All the above methods were reported to give yields of from 60-90% of the cyclic ether 97 from the diol 95.

There are two possible reasons for the different reactivity towards dehydration of the diol 93 when compared to diol 95. Firstly it is possible that the additional ring in 93 may bring about geometrical changes in the reactive centres- the OH groups. Molecular mechanics calculations for each compound were carried out and the relevant geometrical parameters are summarized below. These calculations show that there are only small

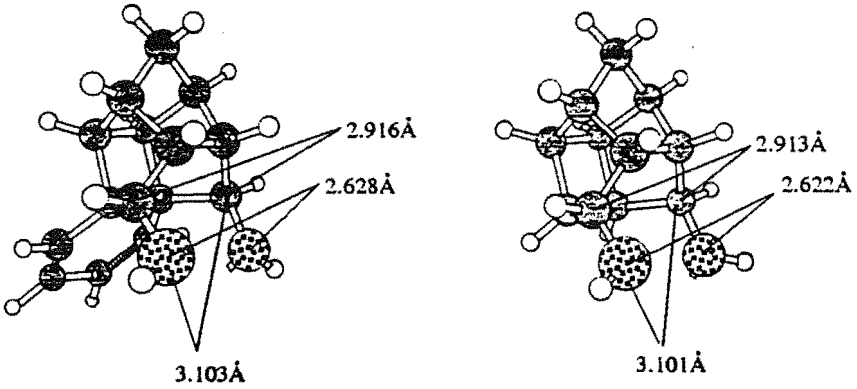

Figure 21. MM2 calculated geometrical parameters for cage diols 93 and 95.

differences in the geometry of the two centres and these are unlikely to be responsible for the differences in reactivity with respect to dehydration. It is more likely that the diene system in 93 provides many alternative pathways leading to aromatic products, once any substantial positive charge builds in the course of loss of the hydroxyl group. This centre is homo-allylic and it would be expected that some positive charge would build up on it during displacement of the hydroxy group, particularly when using strong acid or thermally induced methods. Molecular rearrangements can then lead to a complicated mixture of aromatic products rather than the desired dehydration product. This situation is similar to that observed in the m-chloroperbenzoic acid oxidation of diketone 29 and will be discussed

in greater detail below. The cyclic ether **96** has subsequently been reported as a side product from a reaction where molecular rearrangement has been minimized.[180]

The diol **93** was utilised as a diene component in Diels-Alder addition reactions and was found to undergo these reactions with a high degree of facial selectivity. In all the dienophiles studied the reaction period required was approximately the same as that reported for the corresponding additions to diketone **29**.

The dienophiles, maleic anhydride (MA) and benzoquinone (BQ) reacted with diol **93** with complete selectivity for reaction from the face of the diene *anti* to the cyclobutane group giving **99** and **100**: this was unambiguously established by the use of nOe NMR

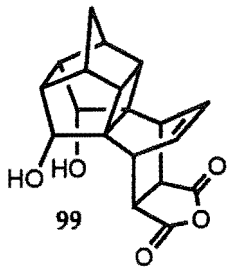

99

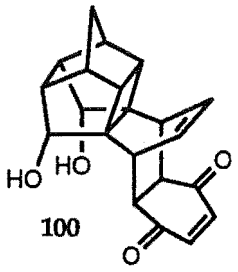

100

experiments as have been described for the reactions of diketone **29**.[107] The tendency for these alkenes to favour reaction exclusively from this face of the diene is the same as observed in the reactions of alkenes with the diketone **29**.

Two representative acetylenic dienophiles, dimethyl acetylenedicarboxylate (DMAD) and methyl propiolate, were reacted with the diol **93** and it was found that with these additions complete selectivity for reaction from the *anti* face of the diene was obtained to give the products **101** and **102** respectively. This is in contrast to the reaction of

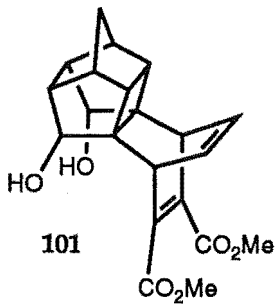

101

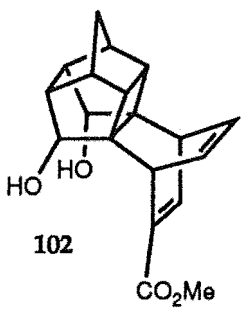

102

DMAD with the diketone**29** where 45% of the reaction took place from the face of the diene *syn* to the cyclobutane group. The azo dienophile phenyl-triazolinedione (PTAD) reacted in a manner similar to the acetylenic and alkene dienophiles to give complete *anti* face selectivity. Again this selectivity was not observed in the reaction of PTAD with

diketone29 where 36% of the reaction took place from the cyclobutane face of the dienophile

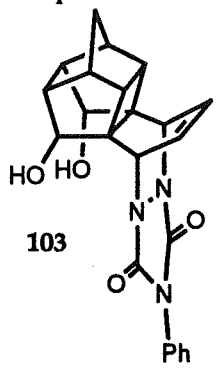

103

to give **103**. The reactive diene benzyne could not be generated in the presence of the diol and therefore its reaction with the diol **93** could not be studied.

The only dienophile which was reacted with the diol **93** to give any degree of cyclobutane face addition was nitrosobenzene. Reaction for one hour at 0°C and immediate recording of a ^{1}H NMR spectrum showed the two products **104** and **105** in the ratio 87:13.

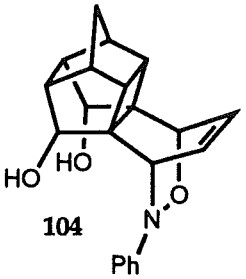

104

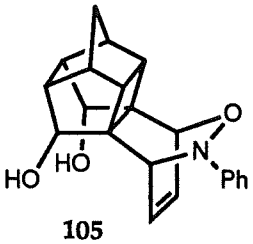

105

This ratio was however determined to be time dependent: when the crude reaction mixture was heated under reflux in benzene solution for three hours, subsequent NMR analysis revealed that the facial isomers **104** and **105** were present in approximately equal amounts. This indicates that the reaction with this dienophile is reversible and the product ratio observed possibly reflects a component of the product stability as well as the kinetic preference for each face. For all other dienophiles there was no evidence of the additions occurring reversibly and so the product ratios will reflect only the kinetic preference for each face. The reversibility of the nitrosobenzene addition to the diol was demonstrated by an experiment in which a mixture of equal amounts of each of the facial isomers **104** and **105** was heated under reflux in a benzene solution in the presence of a 2-fold excess of the reactive diene tetracyclone. After 12 hours' reaction, ^{1}H NMR spectrum revealed that approximately 50% of each of the facial products had returned to the diol **93**. This reversibility of reaction illustrates the possibility of the use of the nitroso-functionality as a protecting group for

dienes in organic synthesis.[181]

In an attempt to understand the high selectivity in the reactions of diol **93** with the various dienophiles studied a series of molecular mechanics calculations were carried out on the products of each reaction and suitable transition state models. The procedure followed was similar to that already described for the reactions of the diketone **29**, with the product stability being first calculated using the MMX force-field and then the MMX force-field transition state model applied fro the reactions of alkene dienophiles and the MM2 fixed model based on AM1 calculations applied to the addition reactions of acetylenic dienophiles.

The results of the MMX calculations on the products resulting from addition of several representative dienophiles are shown in Table 6. For the rotationally flexible

Table 6
Calculated (MMX and MM2) energy differences ($\Delta E_{(anti\text{-}syn)}$; kJ mol^{-1}) between adducts resulting from *anti* face and *syn* face reaction and calculated *% anti* face reaction at 80°C of diol **93** with selected dienophiles.

	ΔE E_{anti}-E_{syn} ; kJ mol^{-1}	% Reaction at *Anti* Face Calc.	Obs.
dienophile			
maleic anhydride[a]	-7.4	92.6	>98
benzoquinone[a]	-8.9	95.4	>98
PTAD[a]	-8.2	94.2	>98
nitrosobenzene[a]	4.4	18.3	variable
MP[b]	-4.9	83.9	>98
DMAD[b]	-10.4	97.0	>98

a MMX force-field.
b BAKMDL (MM2) energy difference between the average Boltzmann energy of significant conformers at 80°C

dienophiles DMAD and MP, the MM2 force-field was used and a systematic conformational search was performed on all the conformationally free bonds in the molecule: the resultant Boltzmann average energy differences are shown in Table 6. The predicted product ratios shown in Table 6 are close to those experimentally observed: this is in contrast to those

calculated by the application of this method to the reactions of the diketone. The product ratio calculated for nitrosobenzene is perhaps the most interesting: the *syn* (cyclobutane) face is predicted to be the more thermodynamically favoured. This is consistent with experimental observations that the reaction of nitrosobenzene with diol **93** occurs reversibly and that the initial reaction mixture at 0° C contains only a small amount of the *syn* face adduct but this mixture equilibrates over time to give a mixture where the product from reaction at the face of the diene *syn* to the cyclobutane group is predominant.

With the exception of the nitrosobenzene reaction, the additions shown in Table 6 have proceeded to give the thermodynamically most stable product. In order to investigate whether the reactions have proceeded under thermodynamic control, or whether the thermodynamic and kinetic pathways are coincident, the transition state models were applied to these reactions and the results are summarized in Table 7. The results in Table 7

Table 7
Calculated (MMX and MM2) transition state energy differences ($\Delta E_{(anti-syn)}$; kJ mol^{-1}) and calculated % *anti* face reaction at 80° C of diol **93** with selected dienophiles.

	ΔE $E_{anti}-E_{syn}$; kJ mol^{-1}	% Reaction at *Anti* Face Calc.	Obs.
dienophile			
maleic anhydride[a]	-11.2	97.8	>98
benzoquinone[a]	-10.1	96.9	>98
methyl propiolate[b]	-23.7	100.0	>98
DMAD[b]	-25.7	100.0	>98

[a] MMX transition state parameters.
[b] MM2 fixed model : difference in BAE of most significant conformers from conformational search at approximate transition state geometry.

show that evaluation of the steric interactions at the transition state geometry for the additions studied indicate that the carbonyl face is also the kinetically favoured and the calculated percentages based on the evaluation of steric interactions at the transition state give a slightly better agreement with the experimental observations. This is in contrast to

the situation in the diketone **29** where the thermodynamically favoured products were not observed.

There are no suitable transition state models for the reactions of nitrosobenzene and PTAD. The former appears to follow the trend shown by the other dienophiles with a kinetic preference for the *anti* face reaction, but because it is reversible it equilibrates at room temperature to a mixture with the *syn* face predominant.

The success of the molecular mechanics transition state model in predicting the observed selectivity for both alkene and alkyne dienophile addition to diol **93** is in contrast to the reactions to the diketone **29** where the molecular mechanics model was only satisfactory for alkene dienophiles. It has been proposed[107] that electron rich dienophiles such as acetylenes may react with the lone pairs on the diketone functionality in an anti-bonding interaction. The diol has lone pairs in a quite different arrangement and any interactions with an incoming dienophile would be considerably different and so the different reactivity observed adds support to the lone-pair repulsion theory.

The relative calculated energy differences between the reaction at each face are larger in the diol **93** than the diketone **29**. As there is little difference in the environment around the face of the diene *syn* to the cyclobutane group between the two compounds the implication is that the diol functionality provides somewhat less steric hindrance to an incoming dienophile from the bottom face of the diene than the diketone and this is also a factor in the high selectivity of reaction to diol **93**. Hydrogen bonding between the diol and an incoming dienophile is also a possible reason for the high bottom face preference. In the transition state and product models however, no evidence was found for this type of intermolecular interaction, with intramolecular hydrogen bonding between the diol groups highly favoured. The experimental observations as well as calculation point therefore to the facial selectivity in reactions to the diol **93** arising from lower steric hindrance to *anti* face attack of the diene. A subsequent section describes additions to cage dienes where the steric hindrance to reaction from the bottom face is increased by substitution of the ketone groups in diketone **29** with methylidene functionality and here the two faces of the diene are less sterically differentiated.

Chapter 6.

Diastereofacial Selection in Diels-Alder Reactions of Mono and Dimethylidene Substituted Cage Dienes.

In order to examine in detail the effect of the carbonyl substituents on the facial selectivity of the Diels-Alder reactions a series of reactions were carried out where the carbonyl oxygens of diene **29** have been selectively replaced by methylidene groups (**106** and **107**) thereby retaining the π electron configuration but replacing the lone pairs of the

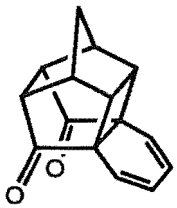

29

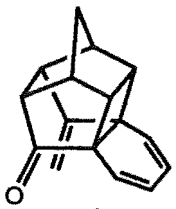

106

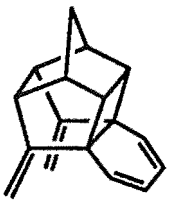

107

carbonyl oxygens with hydrogen atoms in the expectation that this would result in an increase in steric hindrance to carbonyl face addition and encourage reaction from the cyclobutane face of the diene. We also wished to examine whether the selectivity observed in these reactions with alkenes and alkynes could be reproduced by molecular mechanics calculations and have carried out a series of calculations on the adducts of **106** and **107** and modelled the transition state for reactions leading to these adducts in the same manner as has already been described for the reactions of the diketone **29**.

The methylidene derivatives **106** and **107** required for this study were prepared from the diketone **29** using the Wittig procedure which had been successfully applied to the closely related PCUD system.[182] In the presence of 1 equivalent of ylide a 4:1 mixture of (**106** : **107**) was obtained, while with two equivalents of ylide only the dimethylidene product **107** was isolated. In contrast the Peterson reaction, which had also successfully given both the mono and dimethylidene derivatives for the PCUD system[183], gave on reaction with **29** only low yields (ca. 9%) of the mono-methylidene **106**.

Attempts were made to carry out photochemical intramolecular $[\pi 2 + \pi 2]$ cycloadditions by irradiating **106** and **107**. Compound **107** was found to be inert to extensive irradiation in both benzene and acetone. The monomethylidene **106**, however reacted to give

a quantitative yield of **108** which is the product of opening of the cyclobutane ring. A closely

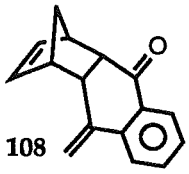

108

related photochemically induced cycloreversion has recently been reported in the literature.[184] In compounds **106** and **107** the methylidene and/or carbonyl groups are held in conformationally rigid 5-membered rings and exhibit π-transannular interactions in a manner similar to that described for other polycyclic bifunctional molecules.[185] The resultant bichromophoric interaction will be reflected in changes in the ^{13}C NMR chemical shifts. The chemical shift of the carbonyl carbon in going from **106** to **107** increases from 210.2 ppm to 215.2 ppm. The quaternary olefin chemical shift in going from **106** to **107** increases from 151.5 ppm to 155.6 ppm but the exocyclic carbon decreases from 105.1 ppm to 102.6 ppm. Similar changes in chemical shift are also observed in the Diels-Alder adducts of **106 and 107** and parallel those reported for the related PCUD series.[185] Photo-electron spectroscopy and theoretical studies[182,186] of **107** confirm that the methylidene groups undergo through-space and through-bond interactions. The ^{1}H NMR spectra for the series of compounds **29, 106,** and **107** also show significant chemical shift variations: the cyclobutane hydrogens in **29** are observed at 3.35ppm; in **106** at 3.23 and 3.01 ppm and in **107** at 2.93 ppm. Thus replacement of the carbonyl oxygens by methylidene groups results in a large (0.42ppm) upfield shift for the spatially distant cyclobutane face protons. This is consistent with a through-space orbital interaction of the σ–anti-bonding orbitals of the carbonyl group(s) with the cyclobutane C-H bonds as shown schematically in Figure 22. This effect has also been observed in the adducts which result from Diel-Alder additions of dienophiles to

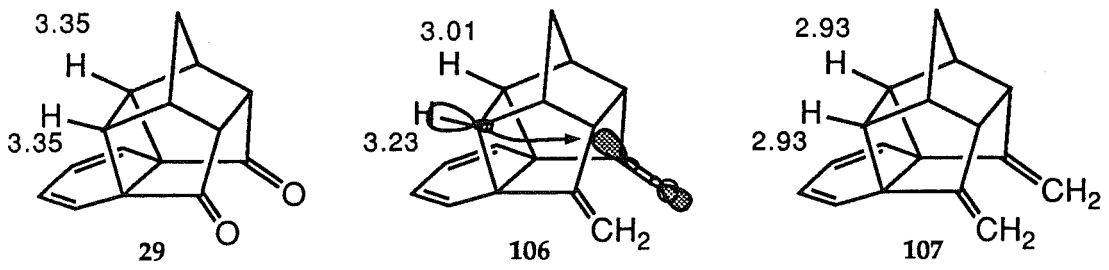

Figure 22. ^{1}H NMR chemical shifts (ppm) of the cyclobutane protons of cage dienes **29, 106** and **107** and proposed orbital interaction shown for **106.**

these dienes and so does not arise from changes in electron density on the diene fragment as a result of orbital σ/π interaction. For the mono-methylidene compound **106** the cyclobutane proton with the smaller upfield shift is assigned to be on the opposite side of the cage from the carbonyl group (Figure 22) on the basis of nOe experiments as shown in Figure 23 for the benzoquinone adduct of **106**.

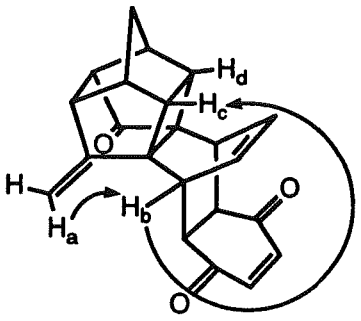

^{1}H NMR Chemical Shifts (ppm)
H_a 4.92
H_b 3.47
H_c 2.56
H_d 2.29
Arrows indicate +ve nOe enhancement.

Figure 23 Selected ^{1}H NMR chemical shifts and observed nOe enhancements for the benzoquinone adduct to **106**.

Diels-Alder Reactions.

Diels-Alder reactions were carried out using the dienes **106** and **107** and dienophiles which the earlier study[107] of **29** had shown to be representative of the larger number originally studied. Compounds **106** and **107** were generally less reactive than **29** and required longer reaction times. A summary of the product ratios of the facial isomers for the reactions of **106** and **107** with maleic anhydride (MA), benzoquinone (BQ), dimethyl acetylenedicarboxylate (DMAD), methyl propiolate (MP) and N-phenyl-triazolinedione (PTAD) is given in Table 8. The stereochemistry of the adducts was determined using Nuclear Overhauser Effect Difference (NOED) spectroscopy; in particular the products resulting from reaction on the face of the dienes *anti* to the cyclobutane face showed mutual NOE enhancements between the olefinic and cyclobutane ring protons as has previously been described[107] for the reactions of **29**. Two dimensional proton-carbon correlation spectroscopy (HETCOR) was used unambiguously to assign the ^{13}C NMR spectra for the adducts. Product ratios were determined by careful 300MHz ^{1}H NMR analysis of the crude reaction mixtures by integration of the olefinic proton signals of the adducts and by careful analysis of other selected signals such as the bridgehead methylenes. In all cases crude recovered material was quantitative and the ^{1}H NMR of the crude reaction mixtures exhibited no evidence for products other than starting material and the facial stereoisomers. No attempts were made

to optimize the isolated yields of the adducts, the primary objective being the measurement of the ratio of facial stereoisomers and the isolation of the individual compounds for characterization. No evidence for interconversion of product stereoisomers was observed. The reaction of diketone **29** with MA and dimethylidene **107** with DMAD, as being

Table 8
Product Ratios[a] for the Diels-Alder Reactions[b] of **29**,**106** and **107**.

dienophile	% reaction at the "*anti* face" **29**	**106**	**107**
maleic anhydride	100	100	85
benzoquinone	100	100	100
dimethylacetylene dicarboxylate (DMAD)	55	25	10
methyl propiolate	100	66	---
phenyl-1,2,4-triazoline dione (PTAD)	64	78	93

[a] Product ratios from 300-MHz ^{1}H NMR of crude reaction mixtures. Estimated error of 2.5%.
[b] All reactions carried out in benzene at 80°C except those involving PTAD (0-5°C in CH_2Cl_2) and DMAD with **107** (110°C in toluene) and MP with **106** (110°C in toluene).

representative reactions, were carefully monitored by NMR and the ratio of facial stereoisomer(s) did not change as the reaction progressed. Reactions with PTAD are such that even at -78^{0}C the reaction was too fast to monitor. Four representative pure products were resubjected to the reaction conditions and found not to undergo isomerization and were recovered unchanged. This is in contrast to the reversibility observed with the reactions of nitrosobenzene and the diol **93**.

The alkene dienophiles, MA and BQ, reacted with the enone **106** with complete selectivity from the face of the diene *anti* to the cyclobutane group giving adducts **109b** and **111b** respectively. This is identical to the selectivity found in reactions of diketone **29**. The introduction of a single methylidene group (**106**) does not provide sufficient steric hindrance to force competitive reaction of these alkene dienophiles from the face of the molecule *syn* to the cyclobutane group. For the reaction with the acetylenic dienophile DMAD, however, the single exocyclic methylidene group had a significant influence on the selectivity; only 25% of the reaction with **106** occurred at the *anti* face to give **115b**, in contrast to the 55% of

115a for **29**. However in the opposite sense the azo dienophile, PTAD, reacts to a greater extent from the *anti* face of **106** to give 78% of **115b** compared with the reaction with **29** giving 64% of **115a**.

While reaction of the ketones **29** and **106** with MA occurred exclusively from the the *anti* face the reaction with the dimethylidene compound **107** is less facially selective with

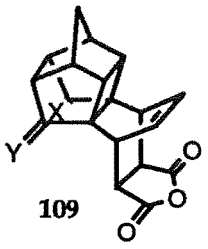

109

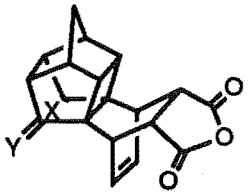

110

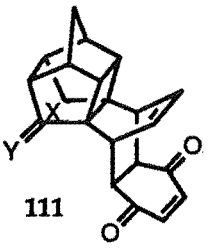

111

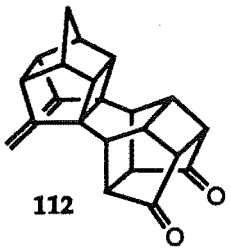

112

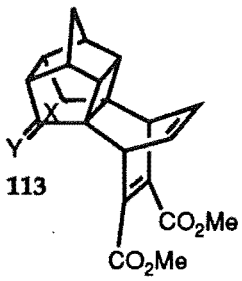

113

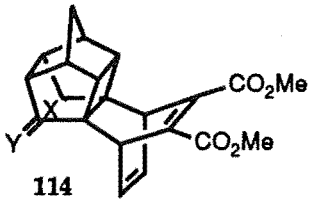

114

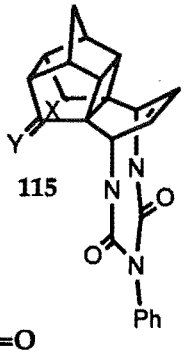

115

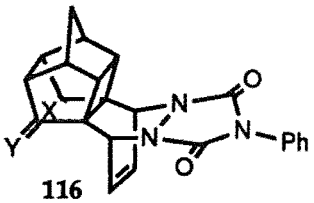

116

a: X=Y=O
b: X=CH_2, Y=O
c: X=Y=CH_2

85% reaction from the *anti* face to give **109c** and 15% of cyclobutane face adduct **110c**. Benzoquinone on the other hand reacts exclusively from the face of the diene *anti* to the cyclobutane for **29**, **106**, and **107**. A solution of the adduct of BQ with **107** on standing in sunlight on a laboratory bench underwent a [π2 + π2] cycloaddition to produce the bis-cage product **112**.

The reaction of **107** with MA is the first example where an alkene dienophile has been observed to react to any extent at all from the face of the diene *syn* to the cyclobutane group and is considered to be a result of the greater steric barrier that the two exocyclic methylidene groups provide to the incoming dienophile. This steric congestion caused by the hydrogens in the reaction of DMAD with **107** is also reflected in the lower reactivity compared with **29** and **106**. This reaction only proceeded in a reasonable time at the higher temperature of 110°C. The facial selectivity for the addition of DMAD to **107** continues the trend established by the reaction with **29** and **106**; only 10% of the reaction now occurs from the *anti* face to give **113c** as the minor product; the *syn* product, **114c**, now dominates (90%).

The facial selectivity for reaction of PTAD with **107** continues the opposite trend to DMAD, in this case 93% of the reaction occurs from the face of the diene *anti* to the cyclobutane group to give **115c** as the major product with **116c** the minor product (7%).

The reaction of the unsymmetrical dienophile methyl propiolate with the unsymmetrical cage diene **106** reached completion only after an extended reaction period (90 days) at 110° C and gave all of the four possible products of this reaction **117,118,119** and **120** in the ratio 45:21:17:17. This corresponds to a ratio for *anti* to *syn* face addition of 66:34.

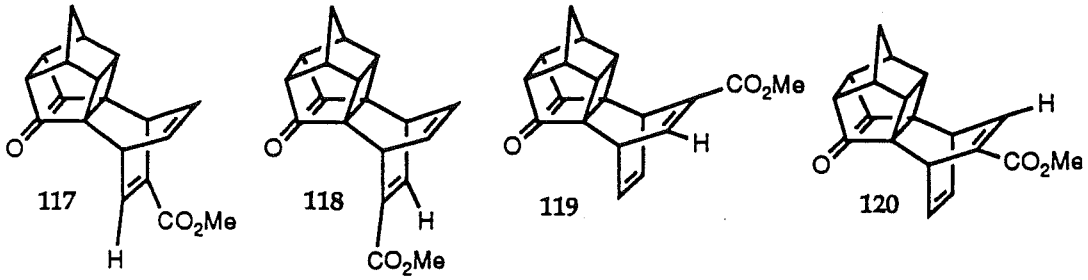

This reaction is less facially selective than the reaction of methyl propiolate with the diketone **29**, which is consistent with the trend observed for the other acetylenic dienophile DMAD. Chromotography on silica resulted in the separation of the product into isomeric pairs **117/118** and **119/112** and recrystallisation of the former gave a pure sample of the major product **117**, the structure and stereochemistry of which were determined by an X-ray structure analysis (Figure 24). This major product **117** is that which corresponds to addition of the methyl propiolate to the face of the diene *anti* to the cyclobutane group and with the

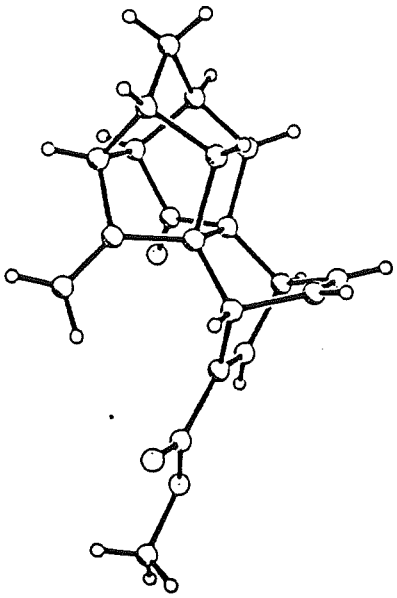

Figure 24. Perspective view of the methyl propiolate adduct **117**.

methoxy-carbonyl group of the diene *syn* to the exocyclic methylene of the cage diene. As might be expected the regioisomeric pair resulting from the addition of methyl propiolate on the face of the diene *syn* to the cyclobutane face were formed in a 1:1 ratio. The other regioisomeric pair however were formed in a ca. 2:1 ratio consistent with the different interactions which will occur between exocyclic methylidene and carbonyl groups on the diene and the methoxy-carbonyl group on the dienophile. No products were observed from reaction of the dimethylidene **107** with methyl propiolate even after an extended reaction period at 110°C.

In summary the results for **106** and **107** shown in Table 8 show the alkene dieneophiles MA and BQ to react from the face of the diene *anti* to the cyclobutane group. While DMAD and MP have a high sensitivity to the introduction of the methylidene groups with the reaction from the *anti* face disfavoured by the introduction of each successive exocyclic methylidene, PTAD shows the opposite trend with an *increasing* selectivity on the face syn to exocyclic methylidene substitution as each carbonyl oxygen is selectively replaced. All the additions to **29, 106** and **107** gave the products of Alder addition, this is consistent with obvious steric constraints and supported undoubtedly by secondary orbital interactions.[110]

In order to investigate any relationship of product stability to the reactions of **106** and **107** the MMX steric energy was calculated for each of the possible products resulting from reaction of **106** and **107** with each of the four dienophiles employed. The procedure followed was that described earlier for the reactions of the diketone **29**. The calculated steric energy differences between the facial isomers as reported in Table 9 shows that product stability does not consistently account for the experimentally observed selectivities. The product stability calculations shown in Table 9 (and earlier in Table 2) show a remarkable sensitivity to the nature of the exocyclic π-system. In particular dipole interactions of the carbonyl group(s) with the dienophile fragment are important in destabilizing the *syn* adduct. In part this is manifested in the difference between the calculated product stability for the adducts of dicarbonyl compound **29** (where the products of reaction with alkene dienophiles from the cyclobutane bearing face of the diene were calculated to be more stable but were not observed) and the calculated facial energy

Table 9.
Calculated (MMX) energy differences ($\Delta E_{(anti\text{-}syn)}$; kJ mol^{-1}) between adducts resulting from *anti* face and *syn* face reaction and calculated % *anti* face reaction at 80°C of **106** and **107** with selected dienophiles.

dienophile	E_{anti}- E_{syn} ; kJ mol^{-1} (Calculated percentage *anti* face reaction at 80°C.)					
	106			**107**		
	calcd.		obs.	calcd.		obs.
MA	-9.5	(97%)	(100%)	-17.6	(100%)	(85%)
BQ	-11.0	(98%)	(100%)	-19.1	(100%)	(100%)
DMAD	0.8	(43%)[a]	(25%)	3.2	(27%)[a]	(10%)
PTAD	-4.0	(83%)	(78%)	-17.1	(100%)	(93%)

[a] BAKMDL (MM2) energy difference between the average Boltzmann energy of significant conformers at 80°C

differences for the products of reaction of alkenes with the mono and di-methylidene derivatives where the observed products were calculated to be the more thermodynamically stable (Table 9). This sensitivity of product stability to substitution makes this system an interesting case to study since such effects should be exhibited in some manner at the various transition state geometries.

As an estimate of the effect of steric and torsional interactions at the transition state MMX calculations were performed of the steric energy at an approximate C_S transition structure for the reactions of **106** and **107** with MA and BQ at each face (Table 10) again following the method described in detail earlier for the reactions of the diketone **29**. With the alkene dienophiles, MA and BQ, this method predicts a strong preference for reaction from the face of the molecule *anti* to the cyclobutane group (Table 10) but this preference falls off somewhat as the carbonyls are replaced with methylidene groups. These calculations are consistent with the experiment (see Table 10). This trend in facial selectivity can be understood in terms of the steric barrier the methylidene hydrogens offer to incoming alkene dienophiles. These calculations do not take account of mixing of reactant orbitals but reflect steric factors associated with the interaction of the polycyclic framework and substituents with the Diels-Alder transition structures and account in broad terms for the facial selectivity observed in the reaction of **106** and **107** with the alkene dienophiles.

Table 10.
Energy differences between transition states (E_{anti}- E_{syn} , kJ mol^{-1}) calculated using MMX transition state parameters and predicted percentage reaction at the *anti* face for the Diels-Alder reactions of **106** and **107**.

dienophile	E_{anti}- E_{syn} : kJ mol^{-1} (Calculated percentage *anti* face reaction at 80°C.)	
	106	**107**
MA		
MMX Parameters	-6.9 (92%)	-3.3 (75%)
Fixed Model[a]	-19.7 (100%)	-13.9 (99%)
Observed.	(100%)	(85%)
BQ		
MMX Parameters	-11.5 (98%)	-3.2 (75%)
Fixed Model[a]	-19.2 (100%)	-14.3 (99%)
Observed.	(100%)	(100%)
DMAD[b]		
Fixed Model[a]	-4.9 (84%)	+7.9 (8%)
Observed.	(25%)	(7%)

[a] Calculated using a fixed model based on AM1 transition state calculations for acetylene or ethylene and cyclohexadiene.
[b] Difference is between average Boltzmann energy of significant conformers at 110°C.

The acetylenic dienophile DMAD however shows a greater sensitivity in selectivity in reactions with **106** and **107** than the reactions of MA and BQ and is therefore an important case for applying the steric MMX transition state model. The 'rigid model' described earlier for the reactions of alkynes with diketone **29** was applied and the relative steric interactions at a geometry approximating the 'transition state' for reaction at each face of **106** and **107** with alkyne dienophiles from the rigid model described above were calculated using the MODEL/BAKMDL program[171] and the results are summarized in Table 10. To allow for the conformationally flexible methoxy-carbonyl groups in the DMAD transition states a conformational search at the fixed transition state geometry was carried out using the BAKMDL program to determine the most significant conformations at the reaction temperature. The energy difference between the two faces is the difference between the average Boltzmann energy of the most significant conformers at the reaction temperature.

In order to assess the validity of the "fixed model" method for determining the steric interactions at a geometry approximating the transition state, a fixed model was developed

based on AM1 calculations of the transition state for the reactions of ethylene and 1,3-cyclohexadiene. The results are shown in Table 10 for the reactions of MA and BQ with the mono-methylidene **106** and di-methylidene **107**. The trends observed were quantitatively the same as those obtained with the transition state parameterized model. In general, however, the calculated energy differences were somewhat larger with the fixed model. This is a reflection of the lesser ability of the fixed model to relieve unfavourable steric interactions between the incoming dienophile and the cage. In this way the "fixed model" is less suitable than the parameterized method, but the overall results appear satisfactory. The rigidity of the model is likely to be of less significance with the less sterically demanding acetylenic dienophiles.

The extent of the DMAD reaction predicted from the carbonyl face (Table 10) is consistent with the experimental results only for the dimethylidene diene **107**. For the carbonyl containing dienes **29** and **106** the carbonyl face addition is greatly overestimated by this fixed "steric only" model. It is not unreasonable that there may be electronic interactions between the incoming acetylene and the π- and σ-orbitals of the carbonyl and methylidene groups and this introduces an electronic interaction not incorporated in molecular mechanics calculations.

There is no similar model available for the reactions of PTAD. A molecular orbital study of the additions of model azo compounds to dienes will be described in a subsequent section and the results from this study, along with experimental evidence[187] indicate that the symmetrical models for acetylene and alkene transition states may be inappropriate for azo dienophiles. The experimentally observed selectivity in the addition reactions of PTAD suggests the importance of filled shell interactions along with steric effects in controlling the facial selectivity.

Chapter 7.

Synthetic Studies on Cage Compounds.

In order to study the effects of remote substitution on the π-facial stereoselection in cage fused diene compounds several attempts were made to prepare novel cage compounds with particular types of terminal substituents. In many cases the use of "standard" methods of functional group interconversion did not give the required compounds. The results of these synthetic studies, which illustrate the importance of transannular interactions in cage compounds, will be discussed in this section.

One of the aims was to introduce terminal halogen substituents into the cage structure as shown in **122**. This would not only result in "soft" electron density *syn* to one face of the

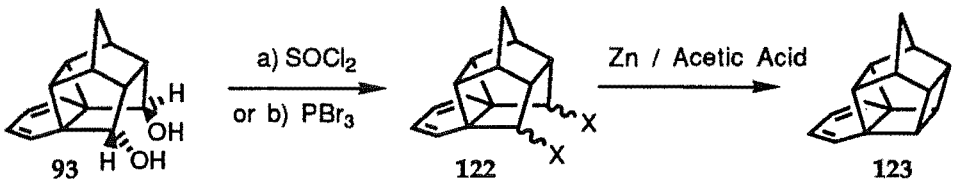

93 **122** **123**

a) X=Cl b) X=Br

diene, but could be an important intermediate in the synthesis of the hydrocarbon **123**. The latter is a particularly interesting diene for the study of facial selectivity as the faces of the diene are only subtly differentiated.

In an attempt to prepare the dibromide compound **122a**, the diol **93** was reacted with PBr_3.[188] The result was not the expected dibromide but a 1:1 mixture of the cyclic phosphite esters **124a** and **124b** which are the products of a transannular attack by the

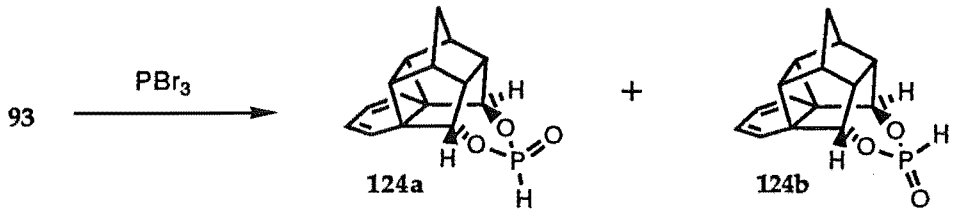

hydroxyl group on the initially formed phosphite ester. The remaining bromine is displaced by a hydroxyl group during the reaction workup and there is a subsequent tautomerism of the H atom across the phosphorus to form the more stable phosphites **124**. These epimeric compounds can be separated and were characterized by ^{1}H and ^{13}C NMR data. A small

quantity of an unidentified unsymmetrical product was produced during the reaction which was thought to be the result of attack on the diene group of **93** by HBr released during the reaction. When the reaction was carried out in the presence of 1 equivalent of pyridine the unsymmetrical product was not detected.

A distinctive feature of the ^{1}H NMR spectra of the phosphite esters is the large ^{31}P to ^{1}H coupling constant of ca. 700 Hz for the proton which is attached directly to the phosphorus. The formation of intermediate phosphite esters is known to occur during the reaction of vicinal diols with PBr_3[189] but in most cases they are displaced by bromide attack. Compounds **124a** and **124b** however, appear to have an unusual resistance to such displacement; no reaction occurred after 8 hours at when the esters were heated under reflux in DMF in the presence of a large excess of LiBr.

In order to prepare the chlorine substituted cage **122b**, the diol **93** was reacted with sulphuryl chloride but this resulted in only a complicated mixture of aromatic products which apparently result from opening of the cage structure. Treatment of diol **93** with thionyl chloride in a similar manner gave not the required dichloride, but the products of trans-annular interaction; the cyclic sulphites **125a** and **125b**. If the reaction is worked up

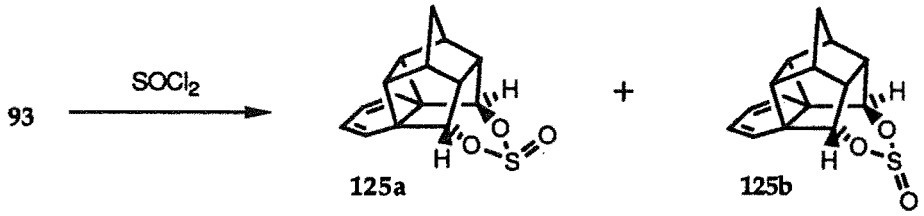

125a 125b

immediately then the product ratio is approximately 1:1, but if left for a prolonged period the two sulphites equilibrate, under catalysis by the HCl formed during the reaction, to give a 87:13 ratio of products. As the equilibrium ratio will reflect the relative thermodynamic stabilities of these isomers, molecular mechanics calculations may be used to assist in the assignment of the sulphite stereochemistry. The MM2 method was used to calculated the steric energy of the two possible conformers for each isomer **125a** and **125b** and the results are shown in Table 11. The results in Table 11 show that the *exo* isomer **125a** is predicted to be the thermodynamically more stable and would dominate when equilibration between the two isomers is possible. The sulphites were separated by chromatography on silica and a

Table 11
MM2 total energies for the two conformers of each isomer 125a and 125b.

Isomer	Conformer	MM2 calculated energy (kJ mol^{-1})	% @25°C
125a	1	382.0	42.3
	2	383.1	23.0
125b	1	384.5	15.6
	2	383.5	19.1

single crystal X-ray structure determination on the major product confirmed that it was the *exo* isomer 125a (Figure 25) consistent with the molecular mechanics calculations and ^1H NMR chemical shift comparisons. The formation of this cyclic sulphite of the diol 93 and the crystal structure analysis is the first unambiguous proof of the *endo-endo* stereochemisty of the diol 93.

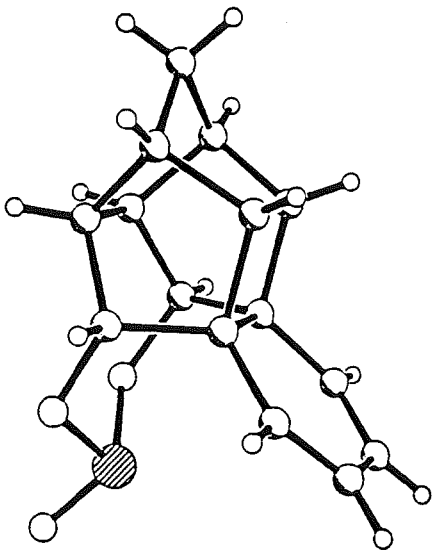

Figure 25. Perspective view of cyclic sulphite 125a.

It has recently been reported that cyclic sulphites resulting from reaction of vicinal diols with thionyl chloride, may be oxidized to cyclic sulphates which are useful intermediates as they are functionally equivalent to epoxides.[190] This suggests that the transformation of 125 to 128 may be feasible to give a newly functionalized alcohol with an effective inversion of stereochemistry. The sulphite 125, however, proved to be resistant to oxidation by a variety of methods. Treatment of the mixture of sulphites with the three-

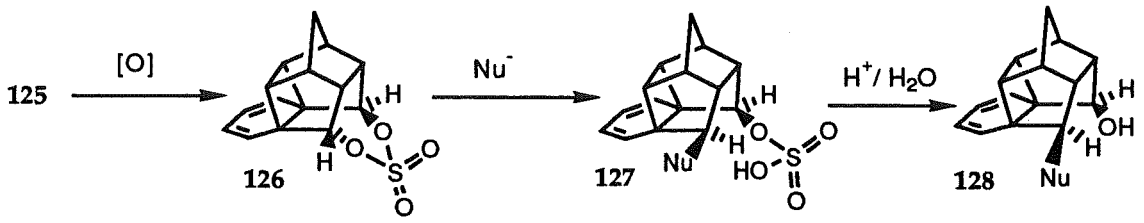

phase system using RuO_4 as the oxidation catalyst, as described by Sharpless[191], resulted only in recovery of unchanged starting material. The activity of the RuO_4 system was demonstrated by the successful oxidation of the cyclic sulphite resulting from the reaction of thionyl chloride and diethyl tartrate. The use of $Ca(MnO_4)_2$ to effect the oxidation[192] of **125** resulted only in a complex mixture of products, while stirring overnight at 0°C with one equivalent of m-chloroperbenzoic acid gave only products where the ^1H NMR spectra indicated that the diene was preferentially oxidized. The apparent difficulty in oxidizing the sulphite **125** to the sulphate **126** may be due to the fact that, unlike the substrates reported in the literature, the parent diol of **125** is not vicinal, and so although the cyclic sulphite can form the ring strain that would result from the introduction of the extra oxygen into the sulphite make oxidation disfavoured.

Because of the unusually high facial selectivity observed in the reactions of diol **93** with all dienophiles studied, the facial selectivity in the reactions of sulphite **125a** with two key dienophiles was examined. The thermodynamically more stable *exo* isomer **125a** was chosen for these studies since the X-ray analysis showed it to have a centrally placed lone pair on the sulphur atom (Figure 25) which may interact with a dienophile approaching from the face of the diene *syn* to the sulphite group.

Reaction of 4-phenyl-1,2,4-triazoline-3,5-dione (PTAD) with **125a** gave two products (**129** and **130**) in the ratio 89:11. These were separated and nOe difference spectroscopy determined that the major product was that resulting from reaction at the face of the diene

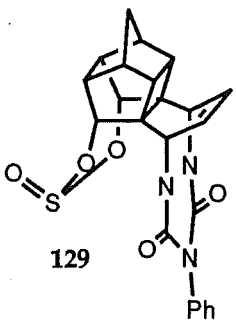

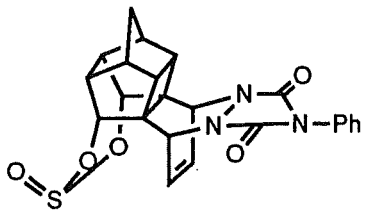

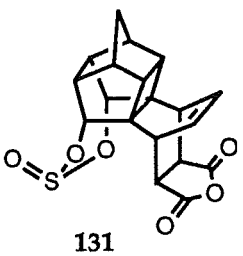

syn to the cyclobutane group (**130**). This is in marked contrast to the 100% *anti* face reaction with diol **93**. The selectivity observed in the reaction of PTAD with the sulphite is characteristic of the reactions of PTAD as it shows a strong preference to react from the face *anti* to a centrally placed lone pair of electrons on a heteroatom - for example in the reactions of the cyclic ether **96**.[193]

Reaction of **125a** with the representative alkene dienophile maleic anhydride, resulted in the formation of only one product **131**, that which arises from reaction *anti* to the cyclobutane group. The contrasting facial selectivity between the azo dienophile PTAD and the alkene dienophiles such as maleic anhydride has been observed in other cage dienes. The preference of the alkene dienophile for reaction from the face of the diene *anti* to the cyclobutane ring is considered to be the result of steric bias as discussed earlier for diketone **29** and the diol **93**. The other dienophile which has been observed to show a variety of facial selectivities in reactions with cage dienes, the acetylene dienophile DMAD, did not react with **125a** after 14 days reflux at 80°C.

The attempts to introduce halogen atoms into the cage diene described above were not successful largely because of the unusual stability of the intermediate sulphites and phosphites during the halogenation procedures. This reinforces the importance of transannular interactions between cage substituents in attempts to modify the cage. Because the halogenation reactions were not successful an alternative route for the synthesis of the diene **123** was explored involving the thiocarbonate **133**. This thiocarbonate was able to be produced cleanly from the reaction of the diol **93** with the thiophosgene equivalent N,N'-thiocarbonyldiimidazole (TCDI)(**132**). Thiocarbonates are known to undergo Corey-Winter

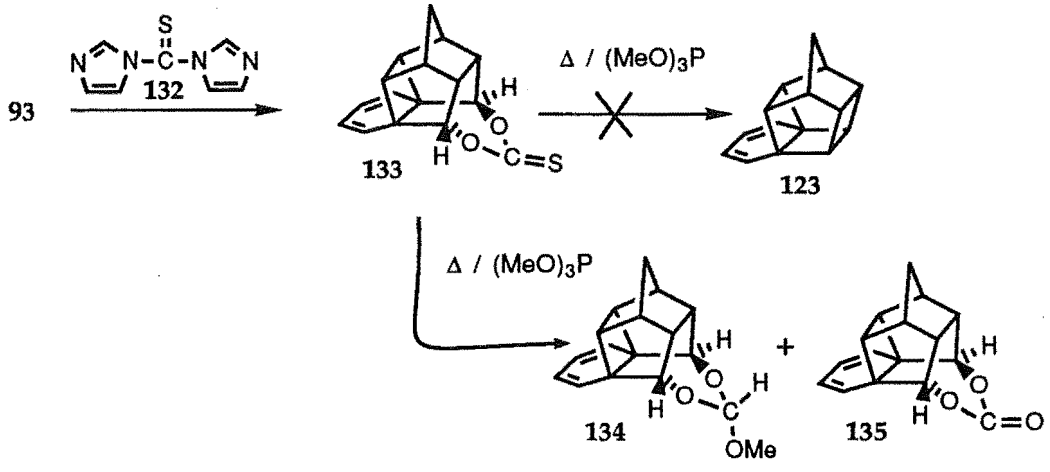

reactions[194] which involve desulphurization of the thiocarbonate by a suitable reagent (usually a phosphite) and subsequent elimination of CO_2. Whereas Corey-Winter reactions of the thiocarbonates formed from vicinal diols give olefins, reaction of the thiocarbonate **133** might be expected to give the required alkane **123**. However, heating of **133** in refluxing trimethyl phosphite ($(CH_3O)_3P$) for an extended period gave largely the methanol adduct **134**. This involves the relief of steric strain in going from the sp^2 hybridised thiocarbonate to the tetrahedral methanol adduct **134**, and apparently occurs in preference to the desulfurization process, which would give the strained diene **123**. The methanol is the result of the small amount of hydrolysis of the phosphite solvent which occurs during the reaction. Also isolated from the reaction was a small amount (ca. 10%) of the carbonate **135**, a product of reaction of water with the carbon of the thiocarbonate after desulfurization.

The exclusive preference for reaction of dienophiles at the face of the diol **93** *anti* to the cyclobutane group, does suggest the possibility that hydrogen bonding between the hydroxyl groups and the approaching dienophile may have a role in directing the facial course of the reaction. Most notable is the 100 % addition of the acetylenic dienophile DMAD and the azo dienophile PTAD to the face of the diene *anti* to the cyclobutane group, even though these dienophiles show a much greater variation in selectivity with all other cage dienes which have been examined. The methylated derivative **136** of the diol **93**,

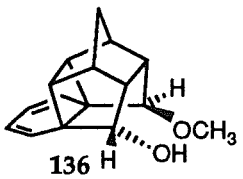

136

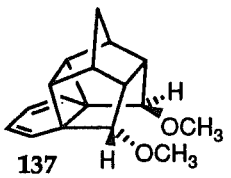

137

would be a suitable substrate for investigating the importance of hydrogen bonding in directing dienophiles as the potential for such hydrogen bonding has been removed without greatly increasing the steric hindrance to reaction from that face. However methylation of the diol **93** with dimethyl sulphate in DMSO/KOH[195], did not result in dimethylation to form **137** even in the presence of a large excess of methylating agent. Instead, only the mono-methylated product **136** could be isolated. This methoxy alcohol can itself be used in reactions with unsymmetrical dienophiles such as methyl propiolate to investigate the importance of hydrogen bonding which would be expected to control the regiochemistry of addition from the face of the diene *syn* to the hydroxyl group. This diene is, however,

surprisingly unreactive towards methyl propiolate with no reaction observed after 25 days reflux at 80°C. Thus no definitive statement can be made about the importance or otherwise of hydrogen bonding in influencing the facial selectivity for compounds like the diol **93**.

There has been a number of recent reports of Baeyer-Villiger oxidations of polycyclic ketones using organic peracids. Surapaneni and Gilardi[196] reported that the oxidation of **138** gave exclusively the Baeyer-Villiger oxidation product **139** and not **140** when treated with m-chloroperbenzoic acid in benzene. In contrast, treatment of the diene **29** with this reagent

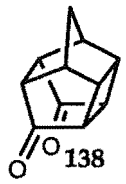

138

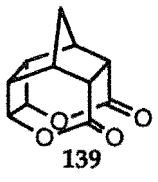

139

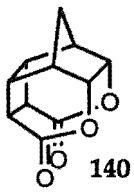

140

has been reported to result in an "inisolable" mixture of products.[197] Treatment of **29** with peracetic acid however, was reported[197] to give the lactone **141**, in 43% yield (no other

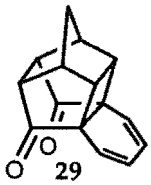

29

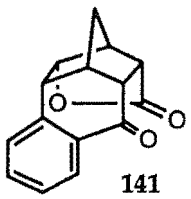

141

products were reported). The relief of steric strain and the gain in aromaticity were considered to provide the driving force for the reaction. The tetrahydro derivative **142** with

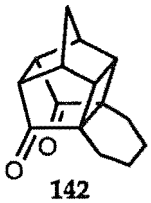

142

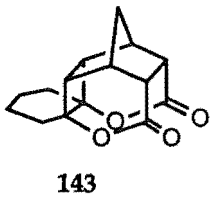

143

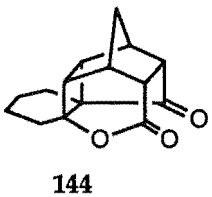

144

MCPBA in benzene was reported by the same workers to give a mixture of the mono-and di-lactones **143** and **144**. Because of the spectroscopic evidence that the diene group in **125** may be epoxidised during the reaction of these cyclic sulphites with oxidizing agents it was decided to investigate the reactions of diketone **29** in detail in order to investigate the competition between Baeyer-Villiger (BV) oxidation of the ketone groups and epoxidation of the diene, as well as the facial selectivity of the epoxidation.

Treatment of **29** with K_2CO_3/H_2O_2 in acetone gave only a complex mixture of products and no attempt at isolation or characterization was made. However, the addition

of MCPBA to a solution of **29** in $CHCl_3$ or CH_2Cl_2, until t.l.c. analysis revealed no starting material, gave a crude product mixture where the ^1H NMR spectrum was considerably cleaner and four products could be identified and were isolated by chromatography. A small amount (ca. 4%) of the product mixture was identified as the anhydride **145**. This compound has identical ^1H and ^{13}C NMR resonances as that reported by Mehta for **145** as formed in the reaction of **29** with cerium ammonium nitrate (CAN).[198] Although it was not isolated in a pure form, there was also spectroscopic evidence for the presence of ca. 11% of the product mixture as the lactone **141**, which was the other product reported by Mehta in the reaction of **29** with CAN and also the only product reported in the peracetic acid oxidation of **29**. The mechanism of formation of these products is shown in Figure 26. Approximately

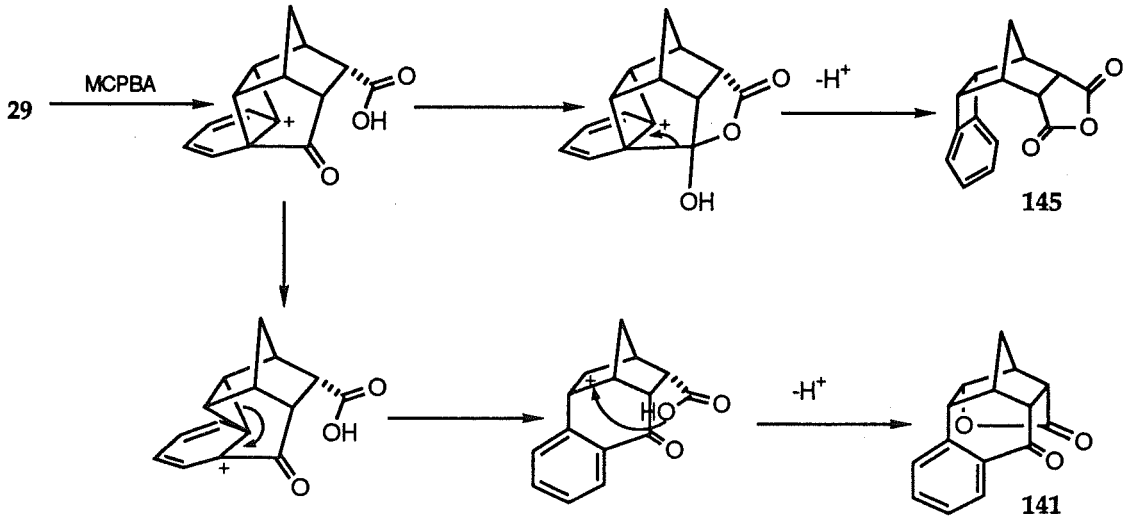

Figure 26. Formation of anhydride **145** and lactone **141** during the m-chloroperbenzoic acid oxidation of diketone **29**.

30% of the product mixture was tentatively identified as two closely related products, where the olefinic signals in the ^1H NMR spectrum were indicative of epoxidation of the diene; **146** and **147**. The remainder of the material was highly insoluble, presumably the products of acid catalysed polymerization.

The epoxide products **146** and **147** were formed in an approximately 2:1 ratio and could not be cleanly separated by chromatography on silica. Recrystallization of the material from ethanol resulted in crystals of the major epoxide which was submitted to X-ray

structure analysis. Although there was some minor disorder in the structure and the crystal was of poor quality, the major epoxide was able to be identified as **146** resulting from first BV oxidation of the diketone and then subsequent (and presumably rapid) mono epoxidation of the diene from the face *syn* to the cyclobutane group (Figure27). The other epoxidation

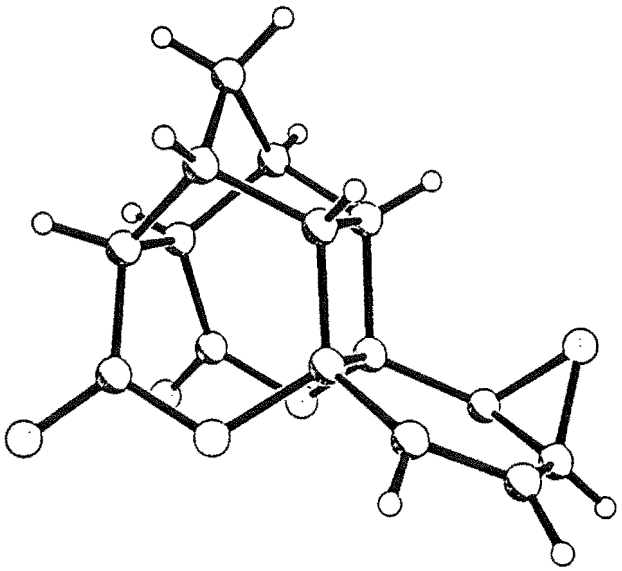

Figure 27. Perspective view of epoxide **146**.

product is apparently less stable as any attempt to recrystallise it results in decomposition to polymeric products. So while the spectroscopic evidence suggests that the minor epoxide product is that resulting from epoxidation of the BV product on the face of the diene *anti* to the cyclobutane group, this cannot be unambiguously established.

It can therefore be concluded that while the diketone does predominantly undergo BV oxidation, subsequent epoxidation of the diene, and cage rearrangement pathways are both competitive. The epoxidation occurs preferentially on the face of the diene *syn* to the cyclobutane group in **29**, a reaction course which is in contrast to the strong preference for reaction from the *anti* face for the Diels-Alder additions to this diene. The facial selectivity in the reactions of electrophilic reagents such as MCPBA to facially dissymmetric dienes like **29** has not been widely studied and further investigations on this area would be valuable.

Part III.

Semi-empirical Molecular Orbital Calculations Directed Towards Investigation of Orbital Control in Addition Reaction.

8. The Application of Semi-empirical Methods to the Study of Reaction Pathways.

A description of the techniques used in applying the AM1 and PM3 molecular orbital methods, as implemented in the MOPAC program, to the study of reaction pathways.

9. AM1 and PM3 Studies of the Diels-Alder Reactions of Acetylene.

Application of the AM1 and PM3 methods to the study of the Diels-Alder reactions of acetylene and several dienes, including a detailed analysis of the significance of orbital changes during the reaction.

10. AM1 Calculations of Acetylene Additions to Cage-fused Dienes.

Application of the AM1 method to the study of the Diels-Alder additions of acetylene to cage-fused dienes as a model for their reactions with substituted acetylenic dienophiles and to examine the significance of orbital interactions for diastereofacial selectivity.

11. Orbital Mixing in Cage-fused Dienes and the Consequences for Diastereofacial Selection in Diels-Alder Reactions.

The AM1 method is used to quantify the degree of s/π interaction in several cage-fused dienes and the significance of these interactions for determining diastereofacial selection in the addition reactions of these compounds is discussed.

12. Cycloaddition Reactions of Diimide.

PM3 calculations for the Diels-Alder reactions of the Z and E forms of diimide (N_2H_2) and butadiene as the prototype for the Diels-Alder reactions of azo dienophiles.

13. The "Cieplak" Effect. Direction of Reaction at Facially Dissymmetric π Systems by Hyperconjugative Interactions.

AM1 and PM3 calculations of substituent effects in the addition of methanol to 2,3-disubstituted 7-norbornanones and the the Diels-Alder reaction of ethylene with 5-substituted cyclopentadienes.

Chapter 8.

The Application of Semi-empirical Methods to the Study of Reaction Pathways.

The detailed study of a reaction pathway by computational methods involves the characterization of the potential energy hypersurface for the species involved. For a N-atom species (a molecule or molecular complex) this is the potential energy with respect to the positions of the atoms; a 3-N dimensional hypersurface is the result. In practice only "chemically interesting" points on the hypersurface need be examined. These are the "minima" which represent the products and reactants and "saddle points" which connect these two. A complete and automatic search of the potential energy hypersurface is not possible at present and would be highly inefficient as many chemically nonsensical local minima and maxima would be located. Chemical knowledge is instead used to investigate in detail those areas which are of interest. Typically one begins by identifying the local minima on the hypersurface which are associated with the "reactants" and "products" in a reaction, as an approximate geometry for these is almost always known. Methods for the subsequent identification of transition states have been described.[199,200]

The investigation of even a simple unimolecular reaction involves a large number of individual calculations in order fully to characterize the reaction pathway, particularly in the location of transition states. For this reason, semi-empirical methods are ideally suited to the study of reaction hypersurfaces and have been applied to a wide variety of reactant systems. The MOPAC program,[201] which originates from the research group of Prof. M.J.S. Dewar, incorporates three currently used semi-empirical methods (MNDO, AM1, PM3) together with a series of routines for the location and characterization of transition states. Most of the calculations reported in this work used the MOPAC program and the appropriate MOPAC options will be discussed in this section.

As described above the first step in the investigation of a reaction pathway is to determine the optimized geometry and energy of the products and reactants in the reaction. Usually a starting geometry can be determined from a preliminary molecular mechanics

calculation or from standard bond lengths and angles. The standard energy minimization routines in the MOPAC program can then be utilized to determine the nearest minimum on the potential energy surface. If the starting geometry was good and there is little conformational flexibility in the molecule this minimum should correspond to a product/reactant geometry. The energy minimization calculation will terminate when a given set of criteria is met; these can be changed by the "PRECISE" or "GNORM=" keywords to give the desired level of precision. Calculation of vibrational frequencies in the harmonic approximation can be performed from the resultant geometry using the FORCE keyword in the MOPAC program. While this is not absolutely necessary, it is a useful check that the structure is indeed a minimum (especially important for conformationally flexible structures) and it can also be used to obtain estimates of thermodynamic parameters with the use of the THERMO option in MOPAC.

Once the minima on the reaction hypersurface have been identified, several strategies can be applied to locate all the possible transition states which may link them. All of these are variations of the basic procedure of generating an approximate structure and then optimizing the geometry of the transition structure by reducing the gradient norm of potential energy with respect to atomic position.

Two "automatic" procedures for transition state location have been described - the SADDLE[200] and the CHAIN[201] procedures. These are similar in that they both take the geometries of the products and reactants and attempt to translate between these two structures in order to obtain a best estimate of the transition state geometry. The CHAIN procedure is guided by a third input geometry representing the approximate transition state geometry. These automatic procedures suffer from a number of difficulties in their use. Firstly the reaction pathway must be a smooth translation between the reactant and product geometries. Special attention must be paid to structure definition; dihedral angle consistency must be maintained. It should be noted in particular that groups such as methyl are "pseudo-chiral" in a structure definition because the atom numbering distinguishes the hydrogen atoms. It is recommended that the SADDLE procedure is used in conjunction with the XYZ option in the MOPAC program since this will run the calculation in cartesian coordinates and thus eliminate some of the problems with geometry definition. However,

the use of XYZ means that full advantage is not able to be taken of any symmetry in the structure under examination. The automatic transition state location procedures work best on relatively simple reactions, but are less effective in the cases where the "reaction coordinate" cannot be easily defined by a single (or possibly two) geometrical parameters. Because of the difficulties in defining the geometry of the "reactant" in intermolecular reactions the CHAIN and SADDLE procedures are easiest to apply to intramolecular reactions such as group migrations.

The most widely used method for approximate transition state location is to perform a number of energy minimization calculations where one (or possibly two) geometrical parameters are varied in a systematic manner. All other geometrical parameters are optimized in this procedure and thus if the geometrical parameters to be varied are chosen carefully an approximate minimum energy reaction path should be described. Monitoring of the energy during this procedure should reveal the approximate locations of saddle points. This reaction surface method has the advantage that it allows a reduction of the 3-N dimensional hypersurface to a 3D representation which can be plotted. In this way if there are multiple pathways linking reactants and products, each can be identified and investigated. Naturally if this reaction path method is to be done in a rigorous manner it will require a large number of calculations and consequently a large amount of computer time. It should be emphasized that a structure corresponding to a maximum in a reaction energy path is, in all but the simplest cases, unlikely to be a true transition state for the reaction pathway. At least one example[202] in the literature exists where this erroneous assumption has been made and this lead to activation barriers which were too high by as much as 80 kJ mol^{-1}.

One of the greatest impediments to the reaction path and reaction surface methods, however, are that some reaction trajectories cannot be described simply in terms of one or two geometrical parameters, i.e. two distances or a distance and an angle. In a bi-molecular reaction the trajectory may involve a rotation or a change of conformation in one or both of the reacting species. In such cases the reaction path methods may give misleading results as false trajectories are found. The three dimensional surface defined by the geometrical parameters which are being varied may be quite different from the "true" potential energy

hypersurface. Here the "automatic" procedures described above may be useful, otherwise it is often possible to apply "chemical common-sense" to derive an appropriate starting geometry; possibly by analogy to a similar but known case.

Once a suitable starting approximate transition state geometry has been identified, the procedure described by McIver and Komornicki[203] can be applied. Essentially this procedure involves minimizing the gradient of potential energy with respect to atomic coordinates. Figure 28 which shows the effect of the different minimization techniques on the geometry using a two dimensional representation of the potential energy hypersurface. In **A** the "normal" energy minimization is illustrated; the energy is reduced until the nearest local minimum is located. Part **B** shows the transition state location using a

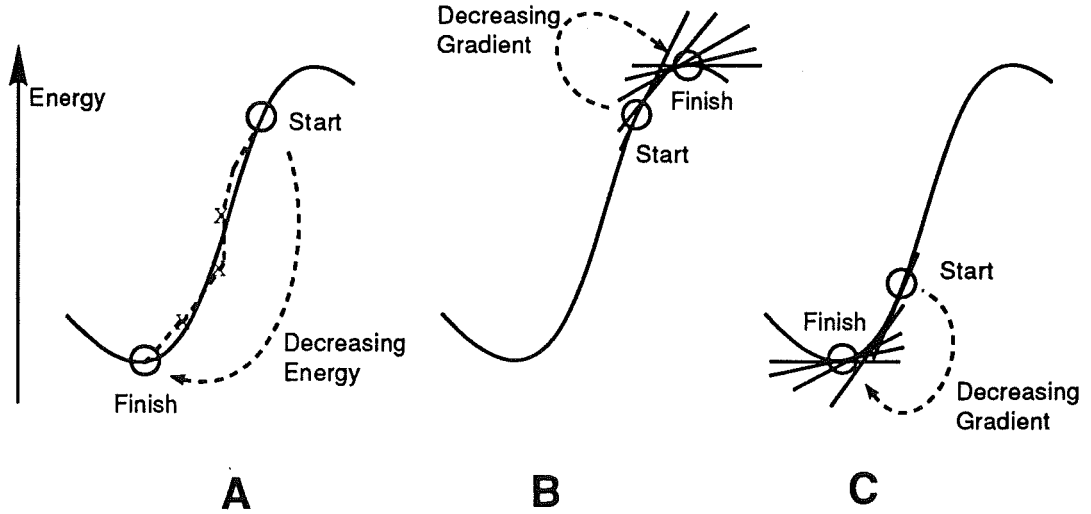

Figure 28. Schematic representation of the effects of energy and gradient minimization techniques.

gradient minimization technique. Here the gradient (represented by the series of tangential lines in Figure 28) is reduced as the starting geometry moves from the starting point to the final point (the transition state). Gradient minimization techniques can, however, converge to minima on the potential energy surface as shown in C. Here the path of lowest gradient leads to a local minimum and this illustrates the importance of a "reasonable" starting geometry being obtained.

On a multidimensional potential energy surface a gradient minimization technique will converge to the nearest region of low gradient. In many cases this may be a point of no chemical interest - one example of this is the multiple minima problem which will be discussed later.

In the MOPAC program there are two routines which may be used to carry out gradient minimization -NLLSQ and SIGMA. In most cases, although slower, the NLLSQ routine is more reliable. Once a structure is identified as a potential transition state and has been refined by a gradient minimization technique, the following conditions which were first discussed by McIver et al[203] must be satisfied before it can be definitely stated that the structure is in fact a true transition state on the potential energy hypersurface:

1) *The structure must represent a stationary point.* This means formally that the gradient of potential energy with respect to atomic coordinates must be zero. In practice reducing the gradient to zero is not possible and an arbitrary criteria is used. In the MOPAC program use of the keyword GNORM=0.0 will attempt to lower the gradient norm to below 0.001 and if it cannot do that the calculation will terminate only after an exhaustive search of the surrounding space. The MOPAC manual[201] notes that this will give the maximum possible refinement.

2) *The matrix of second derivatives of potential energy with respect to atomic coordinates (The Hessian matrix) must have a single and only a single negative eigenvalue.* Because the vibrational frequencies calculated in the harmonic approximation are proportional to the square root of the eigenvalues of the Hessian matrix, then this will result in a "imaginary" vibrational frequency. A physical interpretation of this is that at the transition state there is one vibrational mode that (unlike all the others) results in a lowering of energy as the atoms translate in the direction described by its vectors. The negative eigenvalue should therefore have associated eigenvectors which correspond to the changes in atomic position during the reaction course. In the MOPAC program the FORCE keyword will calculate the Hessian and diagonalize it. It should be noted that imaginary vibrational frequencies are shown as negative in the MOPAC output.

3) *The transition state must be the highest energy point on a continuous line connecting reactants and products.* A detailed reaction path or reaction surface calculation may be able to establish this. Alternatively the IRC/DRC "Intrinsic Reaction Co-ordinate" procedures[204] in the MOPAC program can be used to confirm that a transition state connects two particular minima.

4) *The transition state must be the lowest energy point which will satisfy the above*

three conditions. Again calculation of a detailed reaction surface may help to establish this. As much as possible, chemical reactions should be examined without preconception as to the mechanism and all likely alternatives should be explored with equal vigour.

In many cases, once the gradient has been lowered to a satisfactory level, a frequency calculation will reveal that the Hessian matrix has not one negative eigenvalue but two (and occasionally more) negative eigenvalues and so the condition (3) described above cannot be satisfied. This is the "multiple minima" problem - these so called second-order saddle points are of no chemical interest and indicate that there is a true transition state (a first-order saddle point) nearby on the potential energy hypersurface. Usually the eigenvalue of the largest magnitude will have associated vectors corresponding to the "true" transition state, while the smaller value represents the distortion required to reach the true transition state. One solution therefore, is to carefully examine the vectors corresponding to the spurious (usually smaller magnitude eigenvalue) and to modify the geometry by translating the atomic coordinates along the vectors. Alternatively the IRC method[204] can be used to follow the intrinsic reaction coordinate corresponding to the spurious eigenvalue. As long as the kinetic energy is damped with a sufficiently sort half-life this procedure should lead to the "true" transition state.

The multiple minima problem is common in situations where the reactions of molecules which are conformationally flexible are being studied. Gradient minimization methods will often "drive" conformationally flexible groups to rotational maxima and thus "two transition states" may be found in one search. Another situation which can arise is when there are two closely related pathways. In the Diels-Alder reaction for example with the MNDO semi-empirical method the symmetrical transition structure for the reaction between ethylene and butadiene is a second order saddle point with the "second" negative frequency representing a distortion to a nearby, but lower energy, asymmetrical transition structure.

The following sections describe the application of the techniques described here to a number of investigations which use molecular orbital theory to investigate the role of orbital control in determining reaction stereochemistry.

Chapter 9.

AM1 and PM3 Studies of the Diels-Alder Reactions of Acetylene.

In the application of theory to the study of the Diels-Alder reaction by far the greatest effort has been applied to what is often considered the simplest case; the reaction between ethylene and butadiene.[33,35,40,42,44] There is in fact a computationally simpler reaction, namely the reaction of acetylene and butadiene. This is also the prototype system for the reactions of acetylenic dienophiles which play an important part in the synthetic applications of the Diels-Alder reaction. Surprisingly, however, the reaction of acetylene with butadiene seems to have been largely ignored by investigators and this is true irrespective of the level of theory.

In order to investigate in detail the nature of the reactions of acetylenes with other, more complex dienes and to provide data for the construction of a fixed molecular mechanics model for these reactions, a study was carried out using the AM1[70] and PM3[71] molecular orbital methods for the parent system. Application of the AM1 method to the study of the Diels-Alder reaction has been reported by Dewar.[36] The AM1 results for this reaction suggest a concerted synchronous mechanism which is consistent with high-level *ab initio* studies,[42,44] although Dewar[36] has questioned the generality of this result for the prototype reaction to considerations of more complex dienes. He suggests that the simplest case of a reaction may have an exceptional mechanistic behaviour. In order to examine the validity or otherwise of Dewar's claim we have investigated the reactions of acetylene with a number of dienes: butadiene, 1,3-cyclohexadiene, cyclopentadiene and furan.

The first step in this procedure was to calculate, using AM1 and PM3, the geometries and heats of formation of the the reactants and products for each reaction. This will allow calculation of the enthalpies of reaction and is needed if activation enthalpies are to be calculated. A summary of the main geometrical parameters calculated by the AM1 method for the "reactant" in the forward reaction is shown in Figure 29 with the corresponding AM1 and PM3 calculated and experimental heats of formation in Table 12.

Table 12
Calculated (AM1 and PM3) heats of formation for acetylene and several dienes.

	ΔH_f ;kJ mol^{-1}		
	AM1	PM3	Experimental[a]
acetylene	229.3[b]	212.8[c]	226.7
cisoid-1,3-butadiene	128.4	132.9	-
1,3-cyclohexadiene	73.6[b]	85.3[c]	106.2
cyclopentadiene	155.1[b]	132.9[c]	133.6
furan	12.4[b]	-16.9[c]	-34.8

[a] Cox, J.D; Pilcher, G. , Thermochemistry of Organic and Oganometallic Compounds, Academic Press, 1970.
[b] Consistent with values reported in reference 70
[c] Consistent with values reported in reference 71.

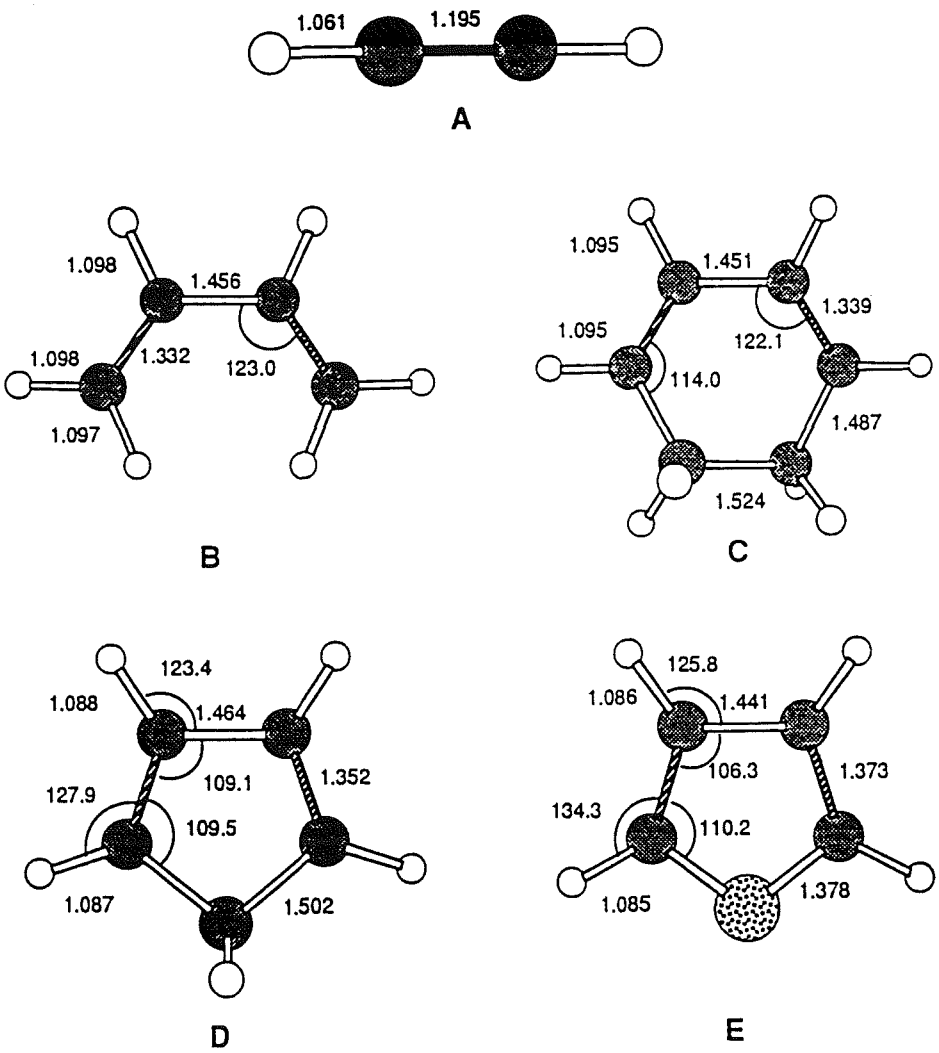

Figure 29. AM1 calculated geometry for (A) acetylene (B) *cisoid* butadiene; (C) 1,3-cyclohexadiene; (D) cyclopentadiene and (E) furan.

The geometries obtained by calculation by AM1 and PM3 are identical but there is variation in the calculated heats of formation. In the sterically crowded 5-membered rings in particular, the AM1 seems to underestimate the stability of cyclopentadiene and furan. The PM3 results are generally closer to the experimental values.

AM1 and PM3 calculations were also performed on the "products" of the "forward" reactions. The main geometrical parameters are shown in Figure 30 and the corresponding calculated heats of formation in Table 13.

Table 13
Calculated (AM1 and PM3) Heats of Formation for the products of Diels-Alder reactions between acetylene and several dienes.

reactants	Calculated Heat of Formation of products ; kJ mol^{-1} AM1	PM3
acetylene/1,3-butadiene	71.1	89.3
acetylene/1,3 cyclohexadiene	132.5	134.4
acetylene/cyclopentadiene	293.7	245.9
acetylene/furan	192.5	148.9

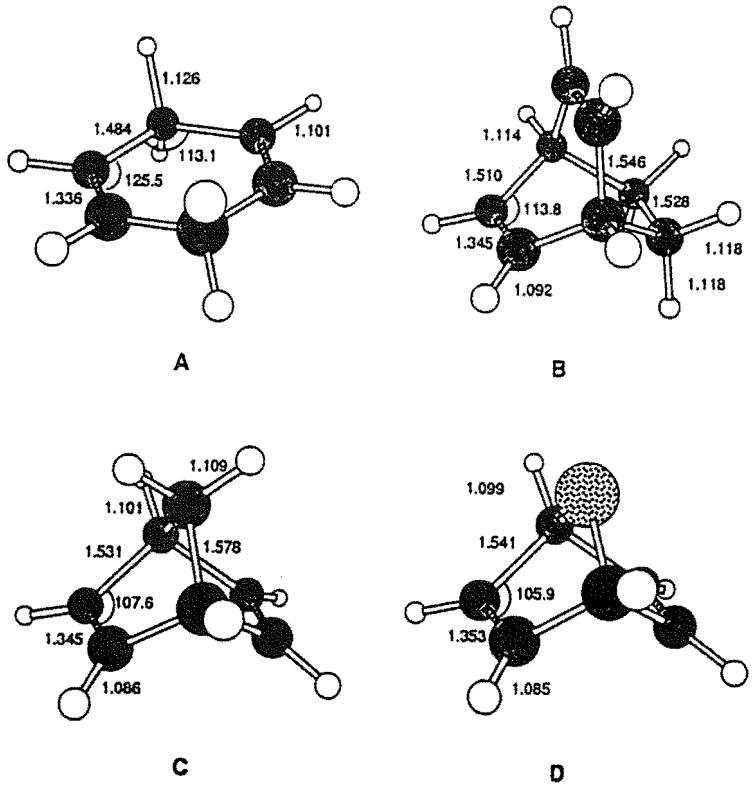

Figure 30. AM1 calculated geometries for the products in the Diels-Alder reactions of acetylene with (A) butadiene; (B) 1,3-cyclohexadiene; (C) cyclopentadiene and (D) furan.

The product of the Diels-Alder reaction of acetylene and butadiene (1,4 cyclohexadiene) was calculated by both methods to have a planar C_S geometry. Although initial experimental data were ambiguous, the planar structure is now considered to be correct.[168]

Having established the calculated heats of formation of the products for these reactions the reaction enthalpy could be evaluated and these are shown in Table 14. The PM3

Table 14
Calculated (AM1 and PM3) reaction enthalpies for the forward reaction of acetylene with various dienes

diene	Calculated Reaction Enthalpy ;kJ mol^{-1} AM1	PM3
1,3-butadiene	-286.6	-286.4
1,3-cyclohexadiene	-170.4	-163.7
cyclopentadiene	-90.7	-99.8
furan	-49.2	-47.0

and AM1 results in Table 14 are in close agreement. All of these cycloaddition reactions are calculated to occur exothermically, but the reactions involving the five-membered ring dienes, cyclopentadiene and furan, are calculated to be considerably less exothermic than the reactions involving butadiene and 1,3-cyclohexadiene.

The exact mechanism of the Diels-Alder reaction has been the subject of much controversy (See Chapter 1). The recently developed semi-empirical method, AM1, and high level *ab initio* calculations,[42,44] predict the reaction of ethylene with butadiene to occur through a symmetrical transition state and to be concerted. This is in contrast to a proposal by Dewar,[35] based on earlier semi-empirical calculations, of a two-step process involving intermediates with some diradical character.

In order to consider both mechanistic possibilities for the reaction of acetylenes a detailed reaction surface was calculated. The distances R1 and R2 defined in Figure 31 were varied systematically in the range 1.5-4.0 Å and all other geometrical parameters were optimized at each point. The results for acetylene and butadiene are shown in Figure 32.

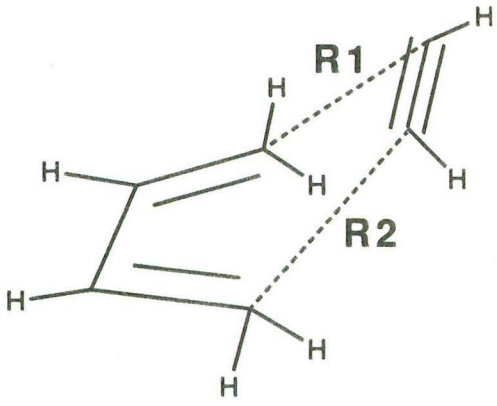

Figure 31. Definition of reaction co-ordinate distances R1 and R2 for the Diels-Alder reaction of acetylene and butadiene.

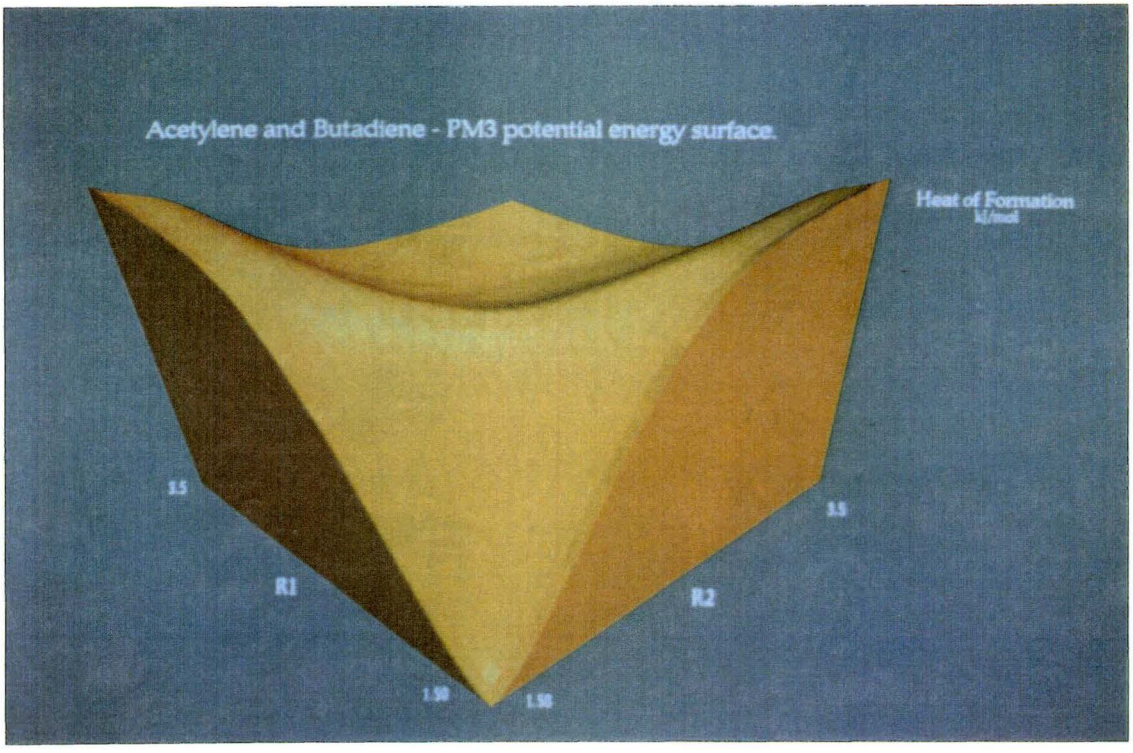

Figure 32. Three dimensional representation of the potential energy surface for the Diels-Alder reaction of acetylene and butadiene.

It can be clearly seen from Figure 32 that the most favourable energy path is along the diagonal pathway corresponding to equal values of the distances R1 and R2 at all times in the reaction profile. A maximum can be seen at values of R1 and R2 of ca. 2.0 Å. The

reaction surface shown in Figure 32 establishes that the reaction of acetylene and butadiene, like that of ethylene and butadiene, follows a concerted and synchronous pathway. The transition state for this reaction was investigated in more detail. A starting geometry was extracted by inspection of Figure 32. AM1 and PM3 gradient minimizations were performed for the reactions of acetylene with the dienes discussed in chapter 8. The starting geometries had values of R1=R2 =2.05 Å and the geometry was restrained to C_S symmetry for computational convenience. The main geometrical parameters for the Cs transition states for each reaction are shown in Figure 33.

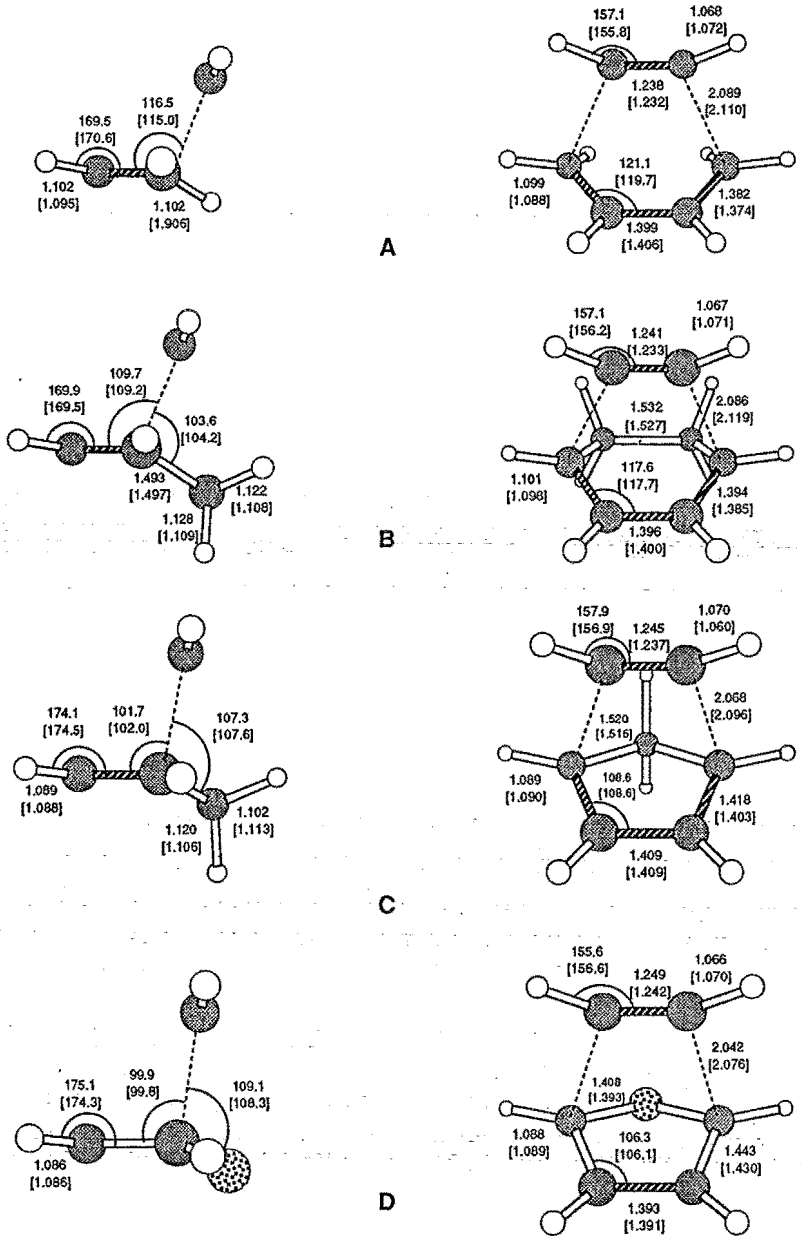

Figure 33. Side and top views of AM1 and PM3 [Square Brackets] calculated geometries for the transition states in the reactions of acetylene with (A) butadiene; (B) 1,3-cyclohexadiene; (C) cyclopentadiene; and (D) furan.

Vibrational frequency calculations were performed on each of the structures shown in Figure 33 and each was found to have one negative eigenvalue in the Hessian matrix. The main vector components of this vibration and the main contributing vectors and imaginary frequencies corresponding to the motion at the transition state along the reaction path are shown in Figure 34 for the AM1 calculations. In all the reactions studied and with both methods (AM1 and PM3) these vectors correspond to a concerted motion of the acetylene towards the diene.

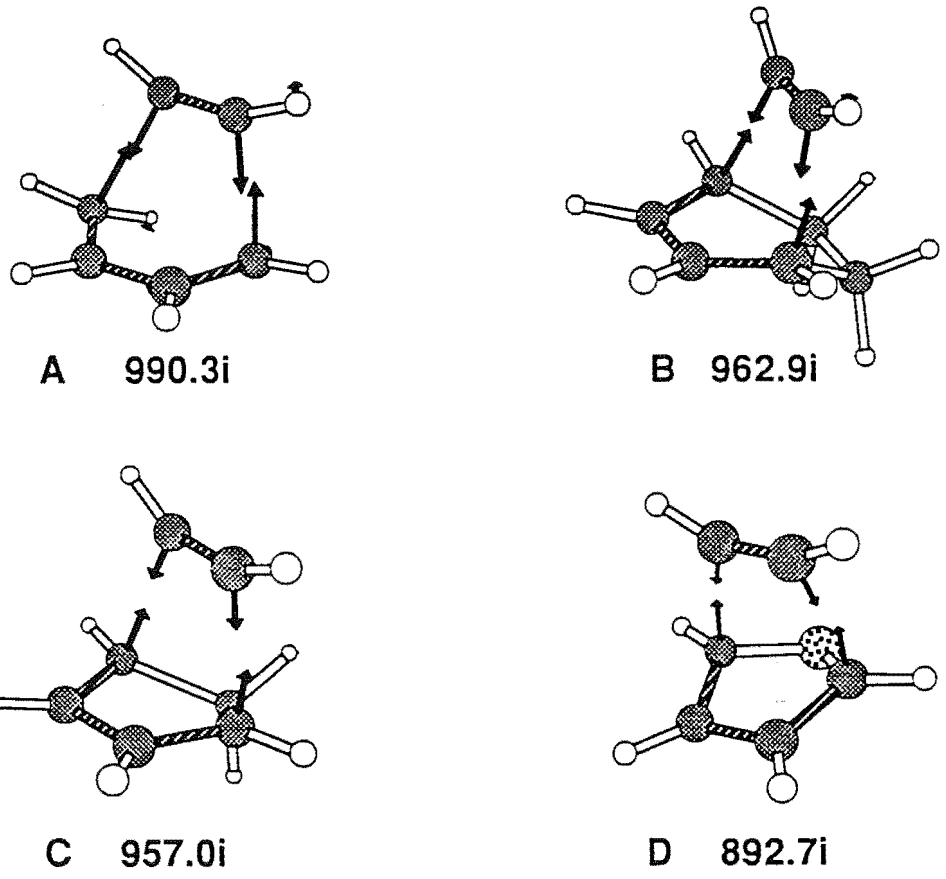

Figure 34 AM1 calculated transition structures for the reactions of acetylene with (A) butadiene; (B) 1,3-cyclohexadiene (C) cyclopentadiene and (D) furan showing the dominating vectors of the symmetric vibrational mode of the single imaginary frequency cm^{-1}.

The geometries shown in Figure 33 all represent an "early" transition state with considerable reactant character remaining at the transition state, consistent with the exothermic nature of this reaction. The PM3 and AM1 geometries are in very close agreement; both predict a forming sigma bond distance (R1 and R2) of approximately 2.1Å for all the model reactions examined. In all cases the hydrogens at C2 and C3 of the diene

are bent out of the plane of the diene and towards the incoming dienophile; this is illustrated in the side views of Figure 33 for the transition structure in the reaction of acetylene and butadiene. This bending was first identified by Houk[40] from a STO-3G calculation of the transition state for the reaction of ethylene and butadiene. The bending was proposed to be the result of the p_z orbitals at C2 and C3 bending to maintain overlap with the distorted termini in the butadiene fragment.

An indication of the amount of reactant character at the transition state is given by the difference between the calculated length of the diene double bonds (C1-C2 and C3-C4) at the transition state and the length of these bonds in the reactant. These differences follow a trend with butadiene having the least lengthening at the transition state (representing the "earliest" transition structure) and furan the most lengthening (the "latest" transition structure). This observation is consistent with the trend in enthalpies of reaction which is shown in Table 14, where the butadiene reaction is calculated to proceed in the forward direction with considerably more energy release than the reaction of furan with acetylene.

AM1 and PM3 calculated heats of formation of the transition structures and calculated activation enthalpies are shown in Table 15. As was the case with the

Table 15
Calculated (AM1 and PM3) transition state heats of formation (kJ mol^{-1}) and calculated activation enthalpies (kJ mol^{-1}) for the forward reaction of acetylene with various dienes.

	Transition State ΔH_f (kJ mol^{-1})		Calculated Activation Enthalpy (kJ mol^{-1})	
Diene	AM1	PM3	AM1	PM3
butadiene	477.5	470.9	119.8[a]	125.3[a]
1,3-cyclohexadiene	452.3	451.8	149.4	154.7
cyclopentadiene	542.0	500.4	157.6	154.7
furan	394.2	352.4	152.5	156.5

[a] Activation enthalpy calculated relative to *cisoid*-1,3 butadiene.

calculated reaction enthalpy, there is a close agreement between the AM1 and the PM3 calculated activation enthalpies shown in Table 15. The calculated activation enthalpy for the reaction of acetylene and butadiene is lower than with the reactions of acetylene with

the other dienes. This is possibly a reflection of the greater steric hindrance that the incoming acetylene dienophile faces when reacting with the cyclic dienes. The angle of attack of the acetylene with respect to the plane of the diene is 116.5° (AM1) in the reaction, but considerably less in the reaction with the cyclic dienes: 109.7° in the 6-membered 1,3-cyclohexadiene and ca. 100° with the 5-membered cyclic dienes, cyclopentadiene and furan.

The calculated geometries of the transition structures as shown in Figure 33 reflect the trend in the calculated reaction enthalpies. The transition structure in the reaction of furan has a calculated (AM1) forming σ-bond distance of 2.042 Å at the transition state compared with the value of 2.089 Å for the transition structure in the reaction with butadiene. This reflects the expectation that the reaction with furan, which is the least exothermic, has the greatest reactant character at the transition state. This trend is consistent for all geometrical parameters.

There has been no experimentally determined activation barrier reported for the reaction of acetylene with these dienes. The best calculated[44] value for the reaction of ethylene and butadiene is 115.1 kJ mol^{-1}. The calculated activation enthalpy for the reaction of acetylene with butadiene is larger than this value and the significance of this will be discussed later. While there are no experimental values for comparison with the AM1 and PM3 results for the reaction of acetylenes, high level *ab initio* calculations for the reaction of acetylene and butadiene have also been reported.[45] Similar calculations have been shown to be able to closely reproduce the experimental activation energies for the reaction of ethylene and butadiene.[44] A transition state for the reaction of acetylene and butadiene with C_S symmetry was determined using both a 4-31G and a 6-31G* basis set[45] and the geometrical parameters are similar to those for the AM1 and PM3 calculated geometries. The primary difference between the *ab initio* and the AM1/PM3 geometries is that the *ab initio* transition states have a forming σ-bond length of 2.198 Å which is about 0.1Å longer than the PM3/AM1 values and the angle of attack of the acetylene with respect to the plane of the diene is 124.8° which is considerably larger than the AM1 value of 116.5°. The calculated activation energy at the MP2/6-31G*//HF/6-31G* level was 60.9 kJ mol^{-1}. This is only half the PM3 calculated value, but the MP2 method is known to underestimate the correlation energy. At the MP4/4-31G*//HF/4-31G the activation energy is calculated to be

119.7 kJ mol^{-1} which is close to the AM1 calculated activation enthalpy of 119.8 kJ mol^{-1}. The good agreement between the high level *ab initio* calculations and the semi-empirical methods in calculations of both transition state geometry and reaction energetics supports the use of the the AM1 and PM3 methods for the study of these cycloadditions.

In a Diels-Alder reaction the total activation enthalpy is made up of contributions from the energy required to distort the reactants to their transition state geometries and the sum of stabilizing charge-transfer and destabilizing exchange interactions. In order to evaluate the magnitude of the enthalpic contribution from distortion of the reactants to the overall activation barrier, the PM3 heat of formation was calculated for each of the reactants at the transition state geometry but at infinite separation from the other reactant. The distortion enthalpy is then the difference between the calculated heat of formation at the transition state geometry and that of the reactants in their starting geometry : these values for the reaction of acetylene with the four dienes are shown in Table 16

Table 16
Calculated (PM3) distortion enthalpy (kJ mol^{-1}) % of calculated activation enthalpies (kJ mol^{-1}) for the forward reaction of acetylene with various dienes.

	Distortion Energy (kJ mol^{-1})		
diene	acetylene	diene	total (% of activation enthalpy)
butadiene	52.0	60.2	112.2 (89.6%)
1,3-cyclohexadiene	51.1	78.2	129.3 (84.1%)
cyclopentadiene	50.1	73.8	123.9 (80.0%)
furan	56.7	80.0	136.7 (87.3%)

There is only a weak correlation between the distortion enthalpies shown in Table 16 and the enthalpies of activation from Table 15 indicating that the relative amount of distortion of the reactants required to reach the transition state geometry is not the sole factor in determining the relative reactivity. In all cases the enthalpic contribution from distortion is 80-90% of the activation enthalpy. This implies the energy required to distort the reactants to their transition state geometries accounts for most of the activation energy

requirement and that the stabilizing electronic charge-transfer and destabilizing exchange repulsions are almost equal, with a slight excess of exchange repulsion. For the trimerization of acetylene Houk et al.[205] have reported the distortion energy for the acetylenes to the 'transition state' geometry at the STO-3G level of calculation as 251 kJ mol^{-1}. The activation barrier for the forward reaction calculated at the same level of theory was 335 kJ mol^{-1} and the 84 kJ mol^{-1} difference in energy was attributed to the excess of exchange repulsion over charge-transfer stabilization. This contrasts with the acetylene butadiene reaction where the repulsive and attractive electronic interactions are approximately balanced at the 'transition state' and the energy required to distort the reactants is slightly lower than the activation barrier for the reaction.

In order to investigate the orbital changes during these cycloaddition reactions an "Extended Frontier Orbital" approach was applied. Conventional Frontier Orbital theory[12,14] considers only the relative orbital energy and symmetry in the reactants, and the mixing of these orbitals in two-electron interactions which are assumed to be stabilizing and the major interactions controlling reactivity. With the availability of detailed molecular orbital calculations the changes in orbital energy can be illustrated in an electron correlation diagram which represents the major bond forming orbitals in the reactants, in the reactants distorted to their transition state geometry (but at infinite separation) and at the transition state. This allows the orbital energy changes to be partitioned into those which are a result of the angle strain and bond deformation which is required to reach the transition state geometry and the orbital energy changes which are a result of intermolecular interactions at the transition state.

The electron correlation diagrams, calculated using the PM3 results, for the Cs 'transition states' for the reaction of acetylene with the four dienes, and including calculated energies of the reaction fragments distorted to the 'transition state' geometry but at infinite separation, are shown in Figure 35. These diagrams are comparable with those which have been prepared by Bach based on *ab initio* calculations for the trimerization of acetylene[206] and the Diels-Alder reaction of ethylene and butadiene. The relative orbital energy levels for the reaction of butadiene and acetylene calculated using the PM3 method are similar to those calculated at the 6-31G* level[45] and so the diagrams prepared

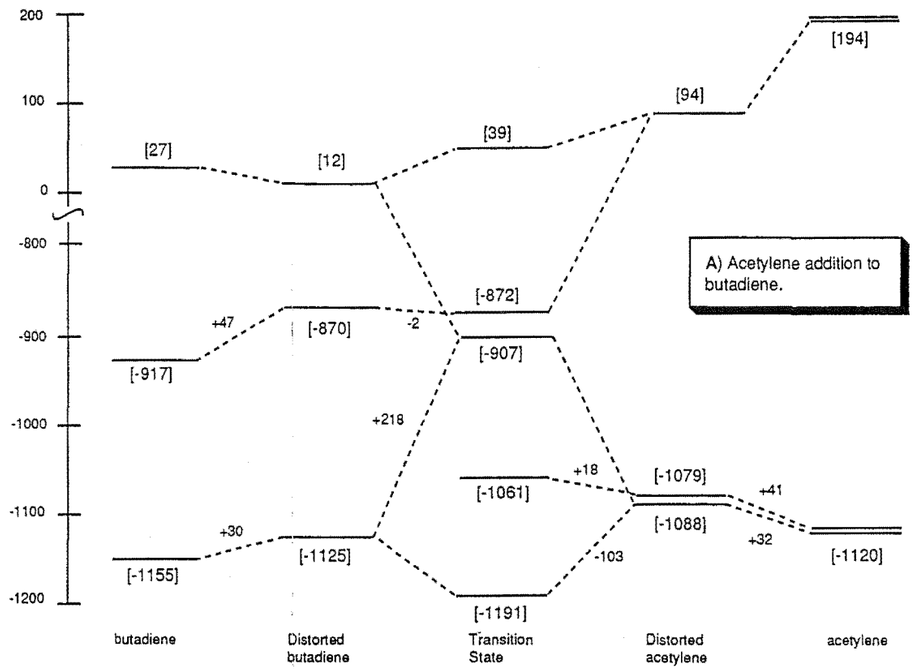

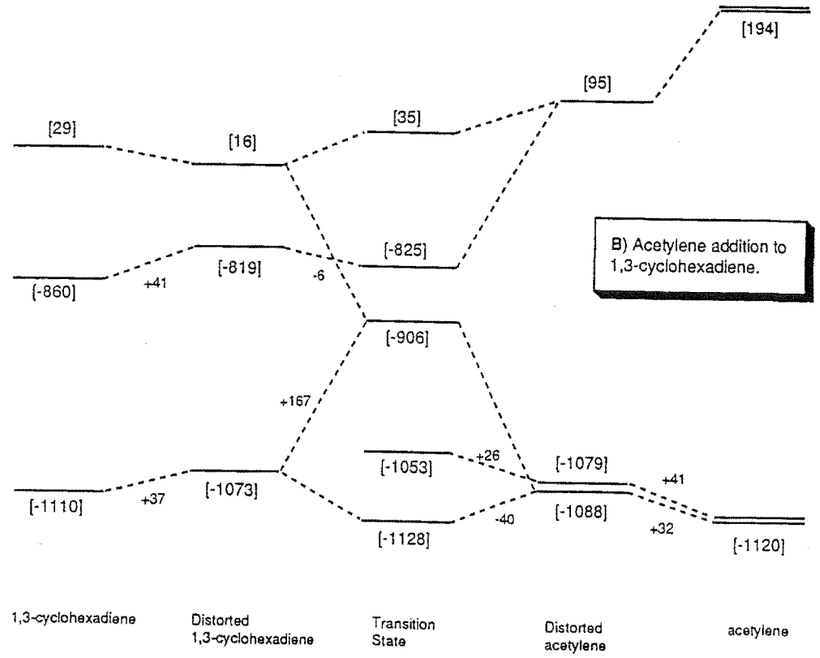

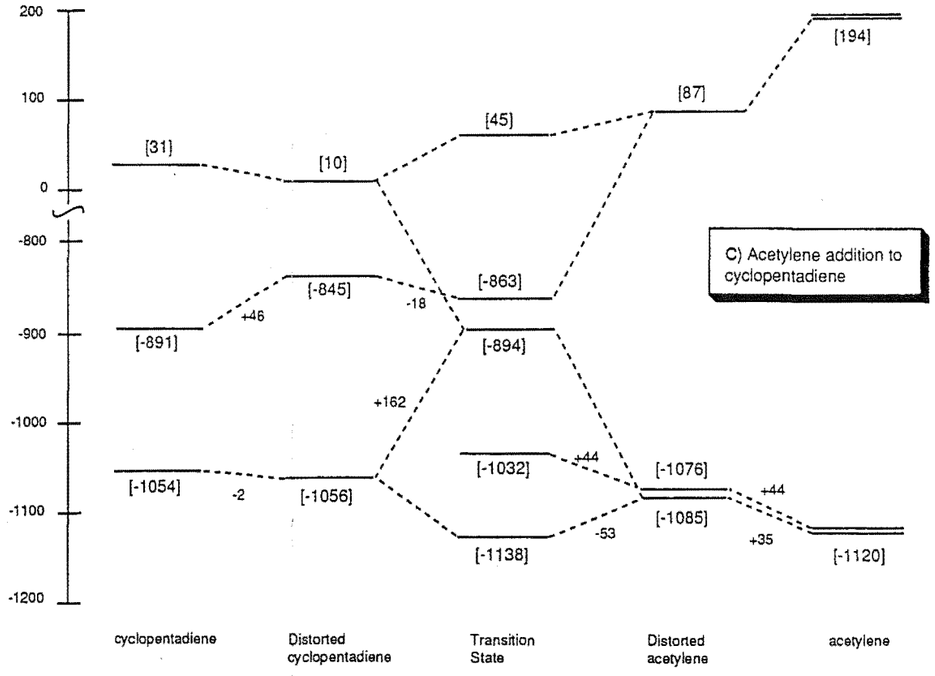

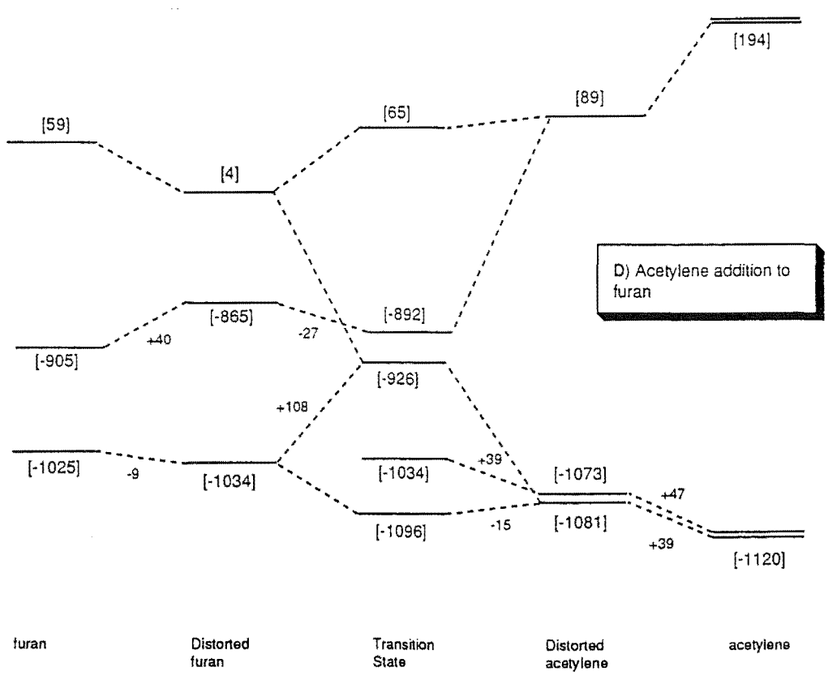

Figure 35. AM1 calculated electron correlation diagrams for the reaction of acetylene with (**A**) butadiene; (**B**) 1,3-cyclohexadiene; (**C**) cyclopentadiene and (**D**) furan. AM1 one-electron energies (kJ mol^{-1}).

from PM3 calculations can be used with some degree of confidence, particularly with respect to changes in orbital energy.

All the diagrams in Figure 35 have the same form and show the major interactions which have been shown to be important from *ab initio* calculations on the Diels-Alder reaction of butadiene with acetylene and ethylene.[42] For the reaction of acetylene with all the dienes studied, the orbital changes due to distortion are essentially the same in both the acetylene and diene fragments. One notable exception to this is that in the five-membered cyclic dienes, furan and cyclopentadiene, the lowest energy molecular orbital of the π-system (Ψ_1) is slightly stabilized by distortion to the transition state geometry whereas in butadiene and 1,3-cyclohexadiene there is a destabilization of 30 and 37 kJ mol^{-1} respectively. The HOMOs in the diene and acetylene fragments are uniformly raised by 35 - 50 kJ mol^{-1} by distortion to the transition state geometry.

There are three main interactions at the transition state which are shown in Figure 35. The first is the diene HOMO - acetylene LUMO interaction which has been the basis of frontier molecular orbital approaches to reactivity. This two electron interaction is in all cases stabilizing with respect to the distorted HOMO of the diene fragment, but not with respect to the HOMO of the undistorted diene; in contrast to expectations based on simple FMO theory. A similar observation has been made for the Diels-Alder reaction of ethylene and butadiene based on *ab initio* calculations. It has been suggested[42] that this apparently erroneous assumption is the reason for the failure of simple FMO theory correctly to predict regiochemistry in Diels-Alder reactions.

The largest destabilizing interaction is, however, the four-electron three-orbital interaction between the Ψ_1 and Ψ_3 orbitals of the dienes and the HOMO of the acetylene. In all cases the net destabilization energy is of the order of 100 kJ mol^{-1}. There is however a third interaction at the transition state which is a unique feature of cycloadditions involving acetylene. In an undistorted acetylene the two HOMO's are degenerate, but during the reaction with a diene, distortion to the transition state geometry removes this degeneracy. Only one of these two orbitals will be oriented such as to be able to undergo a bond-forming interaction with the diene while the other "orthogonal" orbital will undergo compulsory mixing, at least to a small extent, with other filled orbitals of the same

symmetry. The result is a destabilization of this orbital at the transition state. This interaction has been identified as an important contributor to the high activation barrier in the trimerization of acetylene[206] and also in the higher activation barrier for the Diels-Alder reaction of acetylene with butadiene, compared with the calculated barrier for the reaction of ethylene with butadiene.[45] The results from this study indicate that the magnitude of this interaction varies with the nature of the diene, with it being approximately twice the value for reaction with the 5-membered dienes cyclopentadiene and furan, than it is with butadiene and 1,3-cyclohexadiene. Clearly, there are other geometrical factors which will also be important in determining reactivity (the termini of the diene groups are in a favourable position for reaction in the 5-membered dienes for example) and so the relative magnitudes of the orthogonal interaction do not directly relate to the calculated activation energies. However one important point can be made. The dienes with electron density in a position to interact with the incoming acetylene's orthogonal orbital (i.e. the five-membered dienes) showed the largest interaction. Even though this interaction may not be sufficient to determine reactivity in these cases it would be important in situations where there are two faces of the diene available for reaction. Here, most of the electronic interactions should be the same for each face of the diene and only a small perturbation can be important in determining the facial course of the reaction; this perturbation could arise from structure proximate to one face of the diene.

This study utilizing model dienes has exposed an electronic interaction that, while small in absolute terms, may be significant in determining facial selectivity in the addition reactions of acetylenes to facially dissymmetric dienes such as the diketone **29**. In this type of compound, the electronic environment proximate to each face of the diene is quite different and experimental studies described earlier have determined that acetylenic dienophiles show an anomalous facial selectivity which cannot be satisfactory be explained by steric considerations alone. An extension of the analysis reported here for model dienes to cage compounds will be the subject of the next section.

Chapter 10.

AM1 Calculations of Acetylene Additions to Cage-fused Dienes.

Experimental studies involving acetylenic dienophiles as well as force-field calculations of the addition of acetylenic dienophiles to cage compounds have indicated that there may be influences on facial selectivity in the reactions of acetylenic dienophiles which are quite different from those involving alkene dienophiles. In order to investigate this possibility in more detail a number of addition reactions to cage compounds was examined by the AM1 semi-empirical molecular orbital method using acetylene as a model for the acetylenic dienophiles used in experiments; DMAD and MP. The AM1 results for the reactions of acetylene with the model diene systems were consistent with the results of high level *ab initio* calculations and so this method is considered to be suitable for the study of the larger systems, themselves too large to be examined by *ab initio* methods.

The use of acetylene as a model for the larger acetylenic dienophiles was necessitated by the fact that the inclusion of the rotationally flexible methoxy carbonyl groups in the transition state calculations would have made the location and characterization of the transition states in the addition reactions difficult. Not only do rotationally flexible groups cause difficulties in the gradient minimization techniques, but it is likely that there would have been several significant conformers at the transition state for each face and this would have resulted in difficulties in the interpretation of the results. There will be differences between the molecular orbital energy levels in acetylene and those of the substituted acetylenes, and acetylene is a less sterically demanding dienophile, but it is likely that the factors which are operative in determining facial selectivity in these cases should still be apparent with the acetylene model.

As a first step in the investigation of these addition reactions the AM1 method was used to calculate the heats of formation of the products and reacting species. These values are shown Figure 36. In the addition of acetylene to the cage compounds the products resulting from attack at each face of the diene are identical. The AM1 calculated reaction

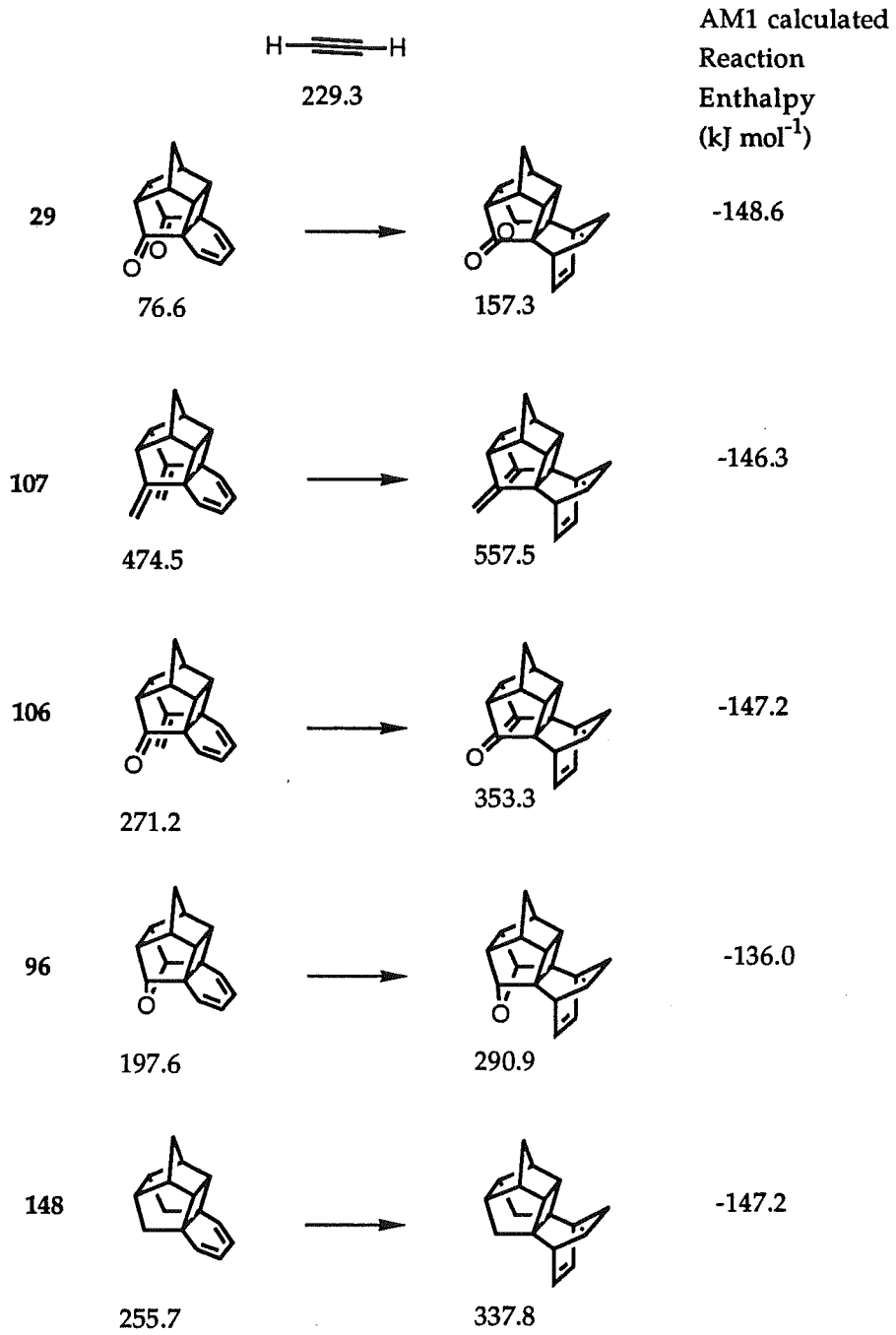

Figure 36. AM1 calculated heats of formation (kJ mol^{-1}) for cage dienes and products of Diels-Alder reactions with acetylene and AM1 enthalpies of reaction (kJ mol^{-1}).

enthalpies shown in Figure 36 are remarkably similar for all the reactions examined. This is most likely a consequence of the similarity in bonding changes which occur during the reaction: the remote substituents have apparently very little influence on the reaction-energy profile of these reactions.

The transition states in the Diels-Alder reaction of acetylene to each face of the cage dienes were located by minimizing the gradient norm of a starting geometry based on the AM1 transition state for the reaction of acetylene and 1,3-cyclohexadiene (Chapter 9). C_S

symmetry was applied for all the reactions except for those to the unsymmetrical enone. The calculated heats of formation of the transition states, the activation enthalpies and the lengths of the forming sigma bonds for the facial transition states are shown in Table 17.

Table 17
AM1 calculated transition state heats of formation (kJ mol^{-1}), activation enthalpies (kJ mol^{-1}) and forming sigma bond distances (Å) in the addition reactions of acetylene to each face of various cage dienes.

Diene	ΔHf (kJ mol^{-1})		Activation Enthalpy (kJ mol^{-1})		σ - bond distance (Å)	
	Syn	*Anti*	*Syn*	*Anti*	*Syn*	*Anti*
29	476.1	462.1	170.2	156.5	2.097	2.087
107	875.6	869.1	171.8	165.3	2.095	2.094
106	671.6	661.6	171.1	161.1	2.094, 2.100	2.089, 2.092
96	599.4	601.0	172.5	174.1	2.093	2.095
148	655.3	643.9	170.3	158.9	2.095	2.088

The calculated geometries of the transition states in each reaction are similar and the transition state in the reaction of acetylene with each face of the diketone **29** are shown in Figure 37. This geometry is highly representative of the others. Diagonalization of the Hessian matrix revealed only one negative eigenvalue for each of the reactions considered. The vectors of this negative value corresponded to a concerted movement of the acetylene and the diene; a representative example for the transition state in the reaction of acetylene with each face of diketone **29** is shown in Figure 37.

The activation enthalpy values given in Table 17 show some interesting trends. Firstly, while the absolute values of the activation enthalpies are high, the predicted reactivity of all the cage compounds towards acetylene is approximately the same with the diketone **29** and the hydrocarbon **148** predicted to be slightly more reactive than the dimethylidene **107** and cyclic ether **96**. This is consistent with the approximate relative reactivity order based on experimental observations of the reactions of DMAD and MP. Secondly, the calculated enthalpies of activation for the reaction from the *syn* face of the diene are all within 2 kJ mol^{-1} of one another while the calculated activation enthalpies for

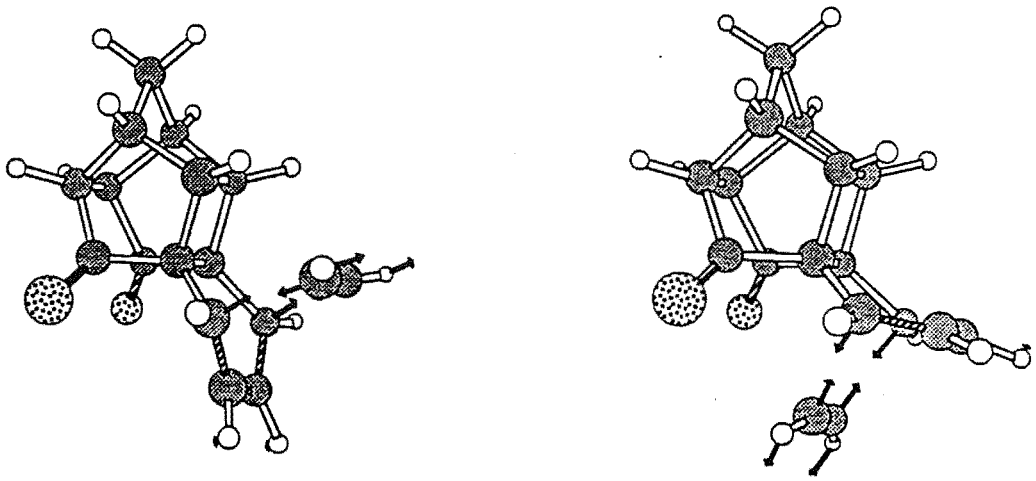

Figure 37. AM1 Transition state geometry for the Diels-Alder reaction of acetylene and diketone **29**. Arrows represent the most significant vectors of the single imaginary frequency.

reaction from the face of the diene *anti* to the cyclobutane group vary to a much greater extent. This implies that interactions between the incoming acetylenic dienophile and the *syn* face of the cage diene are of approximately constant magnitude regardless of the nature of the substituents on the *anti* face. Thus the differences in facial selectivity are apparently the result of direct interactions with the *anti* face substituents.

The addition reactions of acetylene to cage compounds have not been studied by experiment and so no direct comparisons can be made between the calculated results using the acetylene model and the experimental results with the substituted acetylenes. Acetylene itself, being considerably smaller than the substituted compounds, is less sensitive to steric effects from the *anti* face substituents of the cage dienes and thus in most cases more *anti* face reaction is predicted with the model based on acetylene than was observed with the more sterically demanding dienophiles DMAD and MP. However, the trends in facial selectivity are largely consistent with the results of the MM2 based fixed model (Chapter 6). There is however, one notable exception to this; the cyclic ether **96**. This indicates that there may be factors other than relative steric hindrance from each face which are determining the facial selectivity observed in the reactions of the cyclic ether **96**.

In order to further investigate the nature of electronic interactions between the cage dienes and incoming acetylenic dienophiles the extended frontier orbital approach described in the previous chapter for the reactions of acetylenes with model dienes was applied to the reactions of acetylene with the cage dienes. The AM1 heats of formation of the reacting species at their transition state geometries, but at infinite separation, were calculated and the results are summarized in Table 18. The enthalpy of the distorted reactants in all cases

Table 18
AM1 calculated enthalpic contribution from distortion to the activation enthalpy (kJ mol^{-1}) (% of AM1 activation enthalpy) for the reaction of acetylene with several cage dienes.

Diene	*Syn* face Distortion (kJ mol^{-1})			*Anti* Face Distortion (kJ mol^{-1})		
	Acetylene	Cage	Total	Acetylene	Cage	Total
29	60.1	94.8	154.9 (91.0%)	61.1	85.2	146.3 (93.5 %)
107	60.3	95.4	155.7 (90.6%)	61.1	89.2	150.3 (90.9 %)
106	60.1	95.3	155.4 (90.8 %)	60.7	87.7	148.4 (92.1 %)
96	62.3	95.2	157.5 (91.3 %)	61.0	92.2	153.9 (89.9 %)
148	58.6	96.6	155.2 (91.1 %)	61.7	84.0	145.7 (91.7 %)

accounts for approximately 90 % of the calculated activation enthalpy indicating that at the transition state there is a small excess of destabilizing charge - charge interactions over stabilizing charge transfer interactions. While there is some variation in the calculated distortion enthalpy in the reactions from the face of the diene *anti* to the cyclobutane group, the degree of distortion in acetylene is essentially constant for all the reactions examined. In general, no clear trends are apparent in the calculated distortion energies and the degree of distortion required to reach the transition state does not appear to be an important factor in determining facial selectivity.

Analysis of the calculated molecular orbitals in the distorted reactants and the transition state complex is more likely to give insight into the electronic interactions which may be important in the control of facial selectivity. Electron correlation diagrams, similar to those already discussed for the reactions of acetylene with model dienes were prepared for the reaction of acetylene with the cage dienes. A representative example is the reaction of acetylene with diketone **29** which is shown in Figure 38.

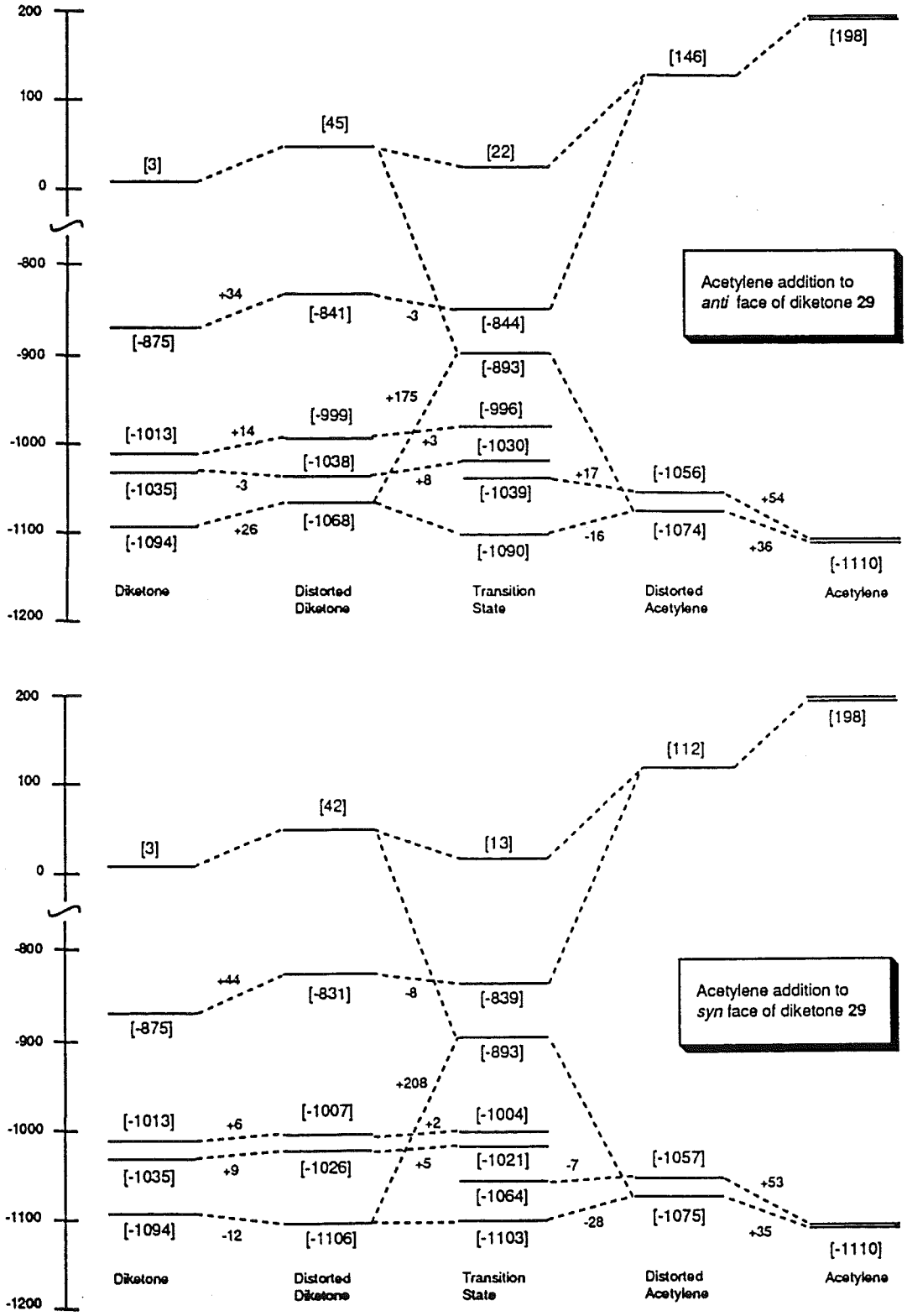

Figure 38. AM1 calculated electron correlation diagrams for the Diels-Alder reactions of acetylene with each face of diketone 29 (AM1 one-electron energies; kJ mol^{-1}).

These electron correlation diagrams show the same major features as those for the model reaction of acetylene with butadiene. Distortion to the transition state geometry generally causes a raising in energy of the filled molecular orbitals, and this occurs to nearly the same extent for all the cage compounds. At the transition state a two-electron stabilizing interaction between the distorted Ψ_1 in the diene and the LUMO in the acetylene and a three-orbital, four-electron destabilization involving the HOMO of the acetylene and the distorted Ψ_1 and Ψ_3 of the diene are the major features. The magnitudes of these interactions are generally similar for reaction at each face and no single bond-forming interaction appears to account for the facial differentiation.

There is however, in all cases a secondary orbital interaction which shows significant variation with the face of reaction; the compulsory mixing of the "orthogonal" π HOMO in the acetylene with filled orbitals of the same symmetry in the cage compound. In order to highlight how this interaction varies with the face of reaction for each of the cage dienes, Figure 39 shows the distorted and transition state calculated AM1 one-electron energy of this orbital for each of the reactions studied. The increase in the orbital energy as a result of distortion to the transition state geometry is constant for all the reactions studied, regardless of the nature of the cage substituents or the face from which reaction occurs. This is consistent with the calculated energy of distortion and the transition state geometries which were also similar for all reactions. For the interactions at the transition state however there are considerable differences in the change in energy of the orthogonal acetylene HOMO. As shown in Figure 39 for the reaction with the diketone **29** and the monomethylidene **106**, the acetylene orthogonal HOMO is destabilized by interactions from the *anti* face of the diene to a much greater extent than in reaction with the *syn* face of the diene; in the case of reaction to the *syn* face of diketone **29**, the HOMO is actually stabilized in its interaction at the *syn* face of the diene. This electronic interaction may account for the over-estimation of the extent to which reaction of DMAD with these dienes would take place by the "steric only" molecular mechanics based model discussed earlier.

It is further interesting to note that for the dimethylidene compound **107** and the hydrocarbon **148**, where the facial selection in the addition of DMAD calculated on the basis of the mechanics based model was close to that experimentally observed, the acetylene

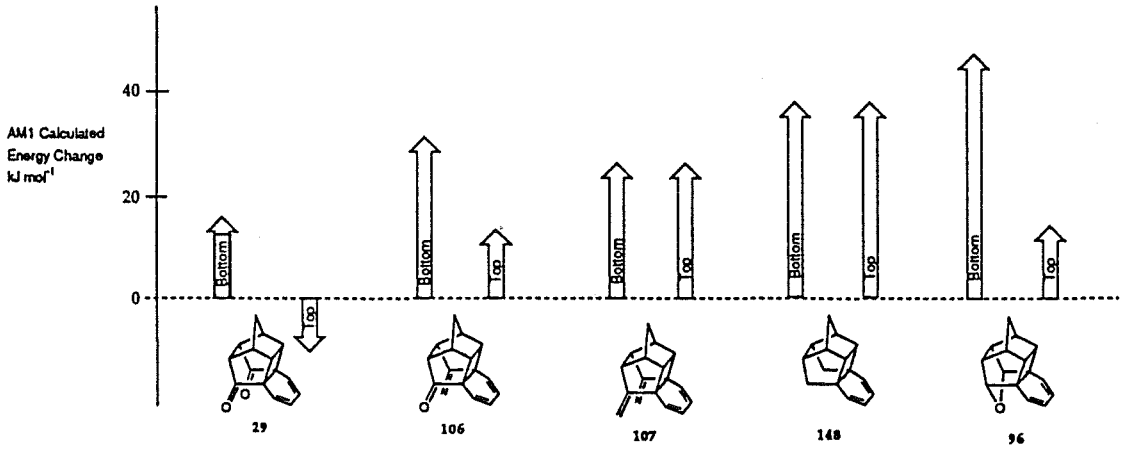

Figure 39. AM1 calculated change in energy for the "orthogonal" HOMO of acetylene as a result of interactions at the transition state in the reaction of acetylene at each face of five cage dienes.

orthogonal HOMO is calculated by the AM1 method to be destabilized at each face by approximately the same amount. In this situation the electronic effects are approximately cancelled and the steric only model was able to reproduce the experimentally observed facial preference.

Finally, the cyclic ether compound **96** has the greatest differentiation in interaction at the transition state, with a very large destabilization of the acetylene orthogonal HOMO upon reaction from the *anti* face of the diene. This can be understood by considering that in this case the geometry at the transition state is such that considerable overlap is possible between the orthogonal HOMO and filled orbitals which are on the ether oxygen. In this way destabilizing interactions are very strong in the reaction from the face of the diene *anti* to the cyclobutane group. In a similar manner to that described for the diketone **29** and the monomethylidene **106**, the steric only model predicts extensive reaction of DMAD to the *anti* face of the cyclic ether **96**. The large destabilization of the orthogonal HOMO in the incoming acetylene from the *anti* face of the diene may explain why most of the reaction with DMAD was observed to occur from the face of the diene *syn* to the cyclobutane group.

The detailed analysis of orbital interaction at the calculated transition state geometry has allowed evaluation of the importance of electronic interactions in determining

facial selectivity. Although no quantitative statements can be made on the basis of this analysis, the trends in the relative magnitudes of interaction of the acetylene orthogonal HOMO appear to rationalize the failure of the molecular mechanics based transition state model to predict the selectivity observed in the additions of DMAD.

While the use of acetylene as a model for DMAD in the AM1 calculations did not allow the prediction of facial selectivity based on total energy differences, it seems to have been successful in highlighting an orbital interaction which is present in acetylenes and not alkenes and therefore provides a simple explanation for the differences in reactivity observed experimentally. Filled-filled orbital interactions of this kind have been identified as contributors to a higher activation barrier in the Diels-Alder reaction of acetylene with butadiene relative to that of ethylene with butadiene,[45] and also as important in the high activation barrier to the trimerization of acetylene.[205,206] It is now clear that for facially dissymmetric dienes, the orthogonal HOMO on an incoming acetylenic dienophile will interact with each face to quite different extents and this may be important in determining the distribution of products observed. Prediction of the extent of this type of secondary orbital interaction is difficult without a detailed description of the orbital interactions at the transition state - semi-empirical molecular orbital calculations using methods such as AM1 provide a good method for doing this with only a modest computational expenditure.

Chapter 11

Orbital Mixing in Cage-fused Dienes and the Consequences for Diastereofacial Selection in Diels-Alder Reactions.

The application of molecular orbital theory to organic molecules has resulted in a convenient and widely accepted description of the electronic structure of such molecules as an underlaying frame-work of σ-bonds "on top" of which lies the π-electron and lone-pair electron systems. Indeed the idea that the σ and π systems are independent of one another is the basis of simple quantitative molecular orbital methods.[30] While this simple picture of the electronic structure of organic compounds has proven to be useful to organic chemists there are some situations where it breaks down. In the simple molecular orbital description of organic compounds two π systems which are not in conjugation or electron-lone pairs on spatially remote atoms would be considered to be localized. These groups may be involved in one or both of two possible interactions. The idea of "through space" interactions within a molecule arises naturally from molecular orbital theory; those groups which are less than about 3.0 Å from one another will have a significant orbital overlap. It was not, however, for some time after the first formulation of molecular orbital theory that the importance of "through bond" interactions was recognized by Hoffmann[207] for "localized" groups at separations greater than 3.0Å. For example he demonstrated the significant splitting in one-electron energy between the lone pairs of *p*-benzyne even though these two lone-pairs are separated by a distance which would preclude orbital overlap. Molecular orbital theory and photoelectron spectroscopy have been used in concert to identify other situations where through bond interactions are important, for example in diazobenzenes, 1,4-cyclohexadiene, 1,4-butadienyl and norbornadiene .[208]

A detailed analysis of interactions of this type within the framework of SCF molecular orbital theory was carried out by Heilbronner and Schmelzer.[209] They proposed the following useful concepts;

Cannonical molecular orbitals (CMO)- These are the set of molecular orbitals which

result from the solution of Hartree-Fock equations and their semi-empirical variants. The effects of orbital mixing and hybridization are naturally included.

Localized molecular orbitals (LMO)- The set of occupied cannonical orbitals can be transformed by a suitable operator into a set of so called "Localized Molecular Orbitals". There is no simple method to determine the transformation which will produce the "most localized" set of molecular orbitals as it is a problem of global optimization. A common method is the intrinsic localization criteria first proposed by Ruedenberg[210] and implemented in the MOPAC program where the best set of N localized molecular orbitals λ_j is obtained upon maximization of the coulombic integral given by:

$$\Sigma [\iint \lambda_j (1) \lambda_j (2) \ e^2/R_{12} \lambda_j (1) \lambda_j (2) \, dv_1 \, dv_2]$$

This is equivalent to considering that the most "localized" set of molecular orbitals represents a maximum of the total inter-orbital electron repulsion. If this localization procedure is applied to ethylene the result would be four degenerate C-H bonds, one C-C bond and a C-C π-bond.

Pre-cannonical molecular orbitals (PCMO). These are combinations of localized orbitals adapted to the symmetry of the molecule. If there is no symmetry then the set of PCMO's is simply the set of LMO's, otherwise those LMO's which are related by symmetry are considered to mix to form a new set. This set is usually referred to by the character symbol of the irreducible representation of that symmetry.

The LMO and PCMO are only convenient representations and have no physical significance. They represent the hypothetical situations where no inter-orbital interactions can occur. "Through bond" interactions of two localized orbital systems were considered by Heilbronner and Schmelzer[209] to be best understood by the involvement of PCMO's as "relay orbitals". For example in norbornadiene **149** the two "localized" π-orbitals can be considered

149

to interact with each other through a sigma framework made up of PCMO's of the correct symmetry. This mixing is known as σ/π interaction and one of the simplest systems where it is important is cyclohexene. The mixing between the localized π-orbital and suitable pre-

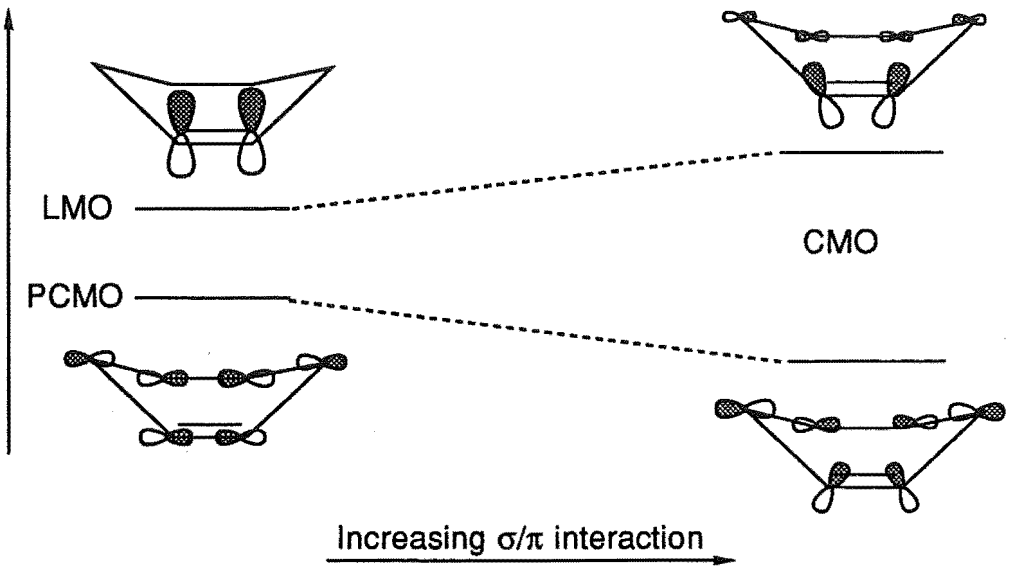

Figure 40. Mixing between the localized π and precanonical σ orbitals in the"tub" conformation of cyclohexene with increasing σ/π interaction.

cannonical σ orbitals is shown in Figure 40 for the "tub" conformation of cyclohexene.[158] Increasing the value of $F_{\mu\upsilon}$ (the matrix element in the Fock matrix for interaction between the two systems) represents an increasing interaction between the hypothetical localized and pre-cannonical molecular orbitals and a tendency towards the cannonical molecular orbitals which are the result of molecular orbital calculations. The consequence of this σ/π interaction can be considered as a disrotatory tilting of the p_z lobes in the atomic orbitals basis set and there will be more contribution to the overall electron density from this molecular orbital on one face of the double bond than on the other. This interaction, it should be emphasized, is a mixing of the localized π-type orbitals and the σ framework and is not the same as the s-p interactions between atomic orbitals which occurs in the process of hybridization.

Interaction between a π system and an adjacent σ framework will also occur in dienes. Gleiter and Paquette have proposed[158] that these interactions and the subsequent facial differentiation in the electron density on the diene may be important in directing the approach of a dienophile to a diene fused to a norbornane skeleton, as is the case for isodicyclopentadiene (see Chapter 3 for a detailed discussion of their hypothesis). This present study is also directed towards understanding the diastereofacial selection of dienes which are fused to cyclic structures and it may be that the σ/π interactions proposed by Gleiter and Paquette, also come into play in the cage fused dienes described here.

The importance of "through bond" interactions in dienes fused to a cyclobutane ring

has been demonstrated by the experimental and theoretical studies of **30** by Gleiter and

30

Prinzbach[211] . Photo-electron spectroscopic measurements and MINDO/3 calculations on this tetraene indicate that the diene rings interact primarily via a "through bond" rather than a "through space" interaction. The 1,4 and 1',4' centres in **30** were shown by an X-ray structure analysis to be separated by an average distance of 3.06Å and so through space interactions would be expected to be weak. The observed interaction between the two π systems was proposed to occur via the Walsh cyclobutane orbitals which act as "relays" in the "through bond" interaction. In a similar manner we may expect cyclobutane mediated "through bond" interactions between the diene π-systems and the exocyclic π systems (carbonyl, methylidene etc) to be important in the cage-fused dienes described here. The resultant changes in π-electron density on the diene faces may have important consequences in determining the course of facial selectivity in the reactions of these dienes with various dienophiles.

AM1 calculations were performed on nine cage dienes in order to examine the orbital interactions between the π and σ systems. For all compounds the PRECISE option in the MOPAC program was employed to extend the default criteria for geometrical and SCF convergence by a factor of 100. Where applicable, C_S was enforced during the calculation. For each structure diagonalization of the Hessian revealed only positive roots demonstrating that each represents an equilibrium geometry on the AM1 potential energy surface. The AM1 calculated heats of formation of each compound are given in Table 19. The geometry of the cage and diene moeity are similar in all the cage dienes shown in Figure 41,

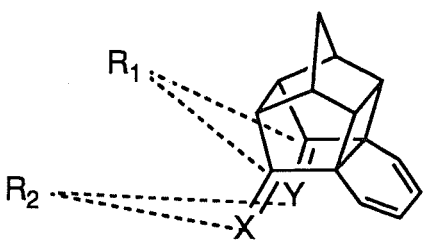

29 X=Y=O
93 X=Y= OH
96 X=Y= -O-
107 X=Y=CH_2
106 X=CH_2 Y=O
148 X = Y = H_2
149 X= -OCH_2CH_2O-
150 X= -SCH_2CH_2O-

Figure 41 Cage dienes for which AM1 calculations were performed and definition of distances R_1 and R_2 as shown in Table 19.

with the greatest variation with different exocyclic substituents represented by the distance R_1 and R_2 and these values are also included in Table 19.

Table 19
AM1 calculated Heats of Formation (kJ mol^{-1}) and distances R_1 and R_2 for cage dienes.

	X	Y	R_1 (Å)	R_2 (Å)	ΔH_f (kJ mol^{-1})
29	=O	=O	2.562	3.932	76.6
93	-OH	-OH	2.731	2.257	-21.4
96	-O-		2.213	-	197.6
106	=O	$=CH_2$	2.549	3.943	271.2
107	$=CH_2$	$=CH_2$	2.559	4.014	474.5
148	H_2	H_2	2.661	2.017	255.7
149	$-OCH_2CH_2O-$	=O	2.623	-	-123.2
150	$-SCH_2CH_2S-$	=O	2.690	-	293.4

The AM1 method is known systematically to underestimate the stability of congested structures such as bicyclobutane where the calculated heat of formation is in error by 110 kJ mol^{-1}, although to a lesser extent than it's predecessor MNDO.[70] As no thermochemical data for these dienes is available direct evaluation of the calculated heats of formation is not possible but it is likely that they are systematically too positive, although relative values are likely to be satisfactory. Examination of the AM1 heats of formation shown in Table 19 shows the destabilizing effect of the successive introduction of a methylidene substituent from **29** to **106** to **107** as revealed by the corresponding increase in heat of formation and an increase in the R_2 distance which represents a movement of the exocyclic substituents further from a parallel arrangement.

A measure of the suitability of the AM1 method for these systems can be obtained by comparing the AM1 calculated geometry for **29** with that which has been determined experimentally by X-ray crystal structure analysis.[212] The overlap of these two geometries is shown in Figure 42. The RMS deviation between the calculated and the experimental structure is 0.027Å. The most significant deviation is represented by the distance between the C-C and O-O distances in the two carbonyl groups. These distances were determined experimentally to be 2.563 and 3.856 Å while the AM1 values are 2.562 and 3.932Å respectively. The close agreement between the experimental and calculated geometries strengthens the use of semi-empirical methods for this study.

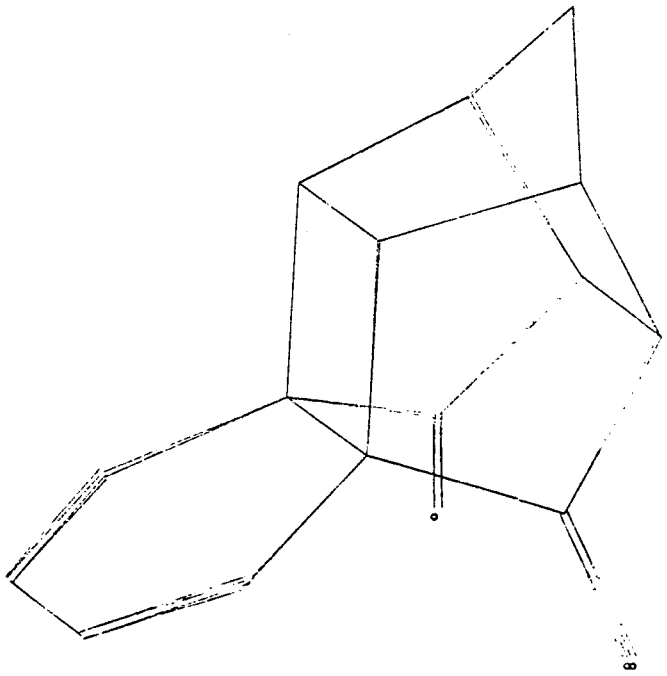

Figure 42 Diagram showing superimposition of AM1 calculated and experimentally determined[212] geometries for the diketone **29**.

Analysis of the AM1 calculated wavefunction for the cage dienes revealed considerable σ/π interaction between the diene π system and the σ framework on the cage fragment. A quantitative analysis of the orbital interactions was not attempted, but by producing a graphical representation of the electron density some qualitative statements can be made about the the nature of the various orbital interactions. Figure 43 shows a stereo-representation of the AM1 calculated orbital electron density for the butadiene-like $\Psi(1)$ orbital in the diketone **29** produced by the CaChe computer system. This diene is a representative example. While as expected the electron density in the $\Psi(1)$ orbital is centred on the diene fragment, there is significant density in the sigma bonds of the cyclobutane groups and the lone pairs on the carbonyl oxygens. This can be considered to result from a "through space" interaction occurring between the lone pairs and the localized diene π system with the strong involvement of the PCMO's of the cyclobutane ring which have the same symmetry as the $\Psi(1)$ orbital.

One important consequence of this orbital mixing is clearly shown in Figure 43. At C1 and C4 and at C2 and C3 the p_z orbital lobes have rotated in a disrotatory manner. The side view shows that the p_z lobes on C1 and C4 are rotated towards the cyclobutane ring and there is consequently a greater amount of electron density in this orbital at C1 and C4 on the

face of the diene *syn* to the cyclobutane group.

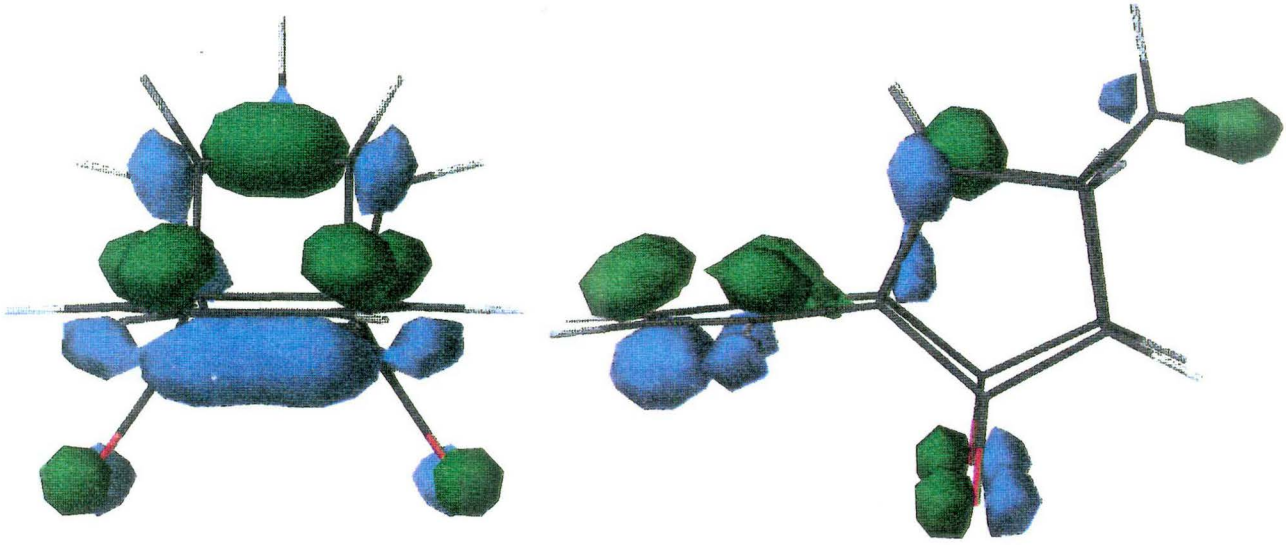

Figure 43. Side and front views of the AM1 calculated butadiene-like Ψ(1) of diketone **29**. Diagram prepared on the CaChe visualisation system with orbital values -0.07 to +0.07.

The experimental studies described earlier for dienes **93, 106 and 107** and the results of others[193] for Diels-Alder reactions of **96** and **148-151** have demonstrated that π-facial selection in these dienes is strongly influenced by the nature of the cage substituents. The selectivity observed for some cases, such as **107** has been successfully rationalized by molecular mechanics calculations (Chapter 6) indicating that steric considerations alone are satisfactory to account for the observed selectivity. For other compounds, however, there is apparently an electronic interaction additional to the steric bias. This is particularly the case in those cages which have substituents with electron lone-pairs such as **29, 96** and **106**. In order to allow assessment of the possible influence of the σ/π interactions on the observed diastereofacial selection in these dienes, it is desirable to be able to quantify how the degree of σ/π interaction varies with the different terminal substituents. In order to do this the cannonical molecular orbitals obtained from the AM1 calculations were analysed as follows: For each diene carbon the coefficients for the p_z atomic orbital contributions to the butadiene-like Ψ(1) and Ψ(2) CMO's were extracted and summed to represent the total electron density resident on the diene for each of Ψ(1) and Ψ(2).

As the AO coefficients are normalized then this sum can easily be considered as a

percentage of the total $\Psi(1)$ or $\Psi(2)$ density. In order to asses the degree of facial differentiation in electron density, the AM1 calculated CMO's were considered for the diene fragment to be a linear combination of p_Z atomic orbitals which were not necessarily perpendicular to the plane of the diene. The extent of rotation of the p_Z was determined and can be described by three angles. The total deviation from a vector perpendicular to the plane of the diene is represented by the angle χ. To projections of this angle, θ and ϕ represent the "sideways" and "forward" components of the orbital lobe tilting respectively, as shown in Figure 44. It should be noted that the angle θ is defined with a different sense for C1 and C2 than for C3 and C4 of the diene in order to allow easier comparison of the extent of this disrotatory motion for unsymmetrical dienes. The numbering of the diene carbons with respect to the substituents X and Y is also shown in Figure 44. The analysis

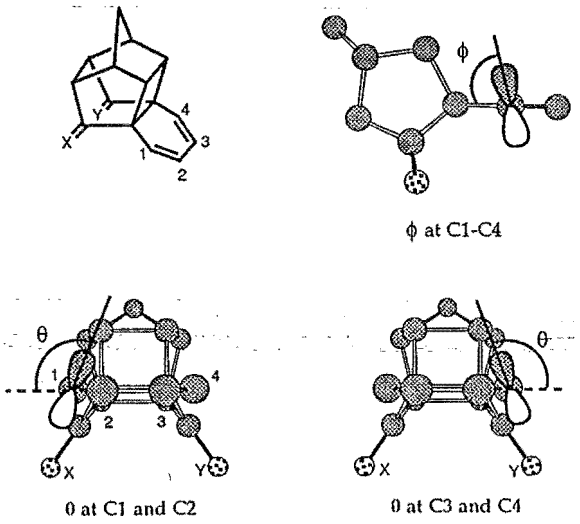

Figure 44. Definition of "orbital tilting" angles and atom numbering for the cage-fused dienes.

described above was carried out for the butadiene-like $\Psi(1)$ and $\Psi(2)$ of the dienes. In order to assess the results, two other dienes were examined. Butadiene represents a system with no σ/π interaction and should have a "pure" diene π-system. The diene **83** was identified by Gleiter and Paquette[158] as one where σ/π interaction was important and the results of an AM1 calculation are included here for comparison with the cage-fused dienes The angles θ, ϕ

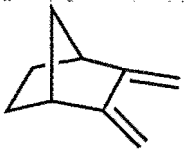

Table 20
AM1 calculated orbital tilting angles, orbital energies and coefficients for the butadiene-like Ψ(1) molecular orbitals cage-fused dienes, **83** and butadiene.

Diene	Ψ(2) orbital energy (eV)	% electron density on diene fragment.	Angles (degrees) and coefficients	C1	C2	C3	C4
butadiene	-12.019	100.0					
			χ	0.8	1.1	1.1	0.8
			θ	90.1	90.1	90.1	90.1
			ϕ	89.2	88.9	88.9	89.2
			coeff.	0.423	0.567	0.567	0.423
83	-10.947	61.9					
			χ	13.3	21.8	21.8	13.3
			θ	101.0	73.2	73.2	101.0
			ϕ	97.4	76.6	76.6	97.4
			coeff.	0.360	0.424	0.424	0.360
29	-11.854	43.8					
			χ	29.7	22.3	22.3	29.6
			θ	112.2	71.9	71.9	112.2
			ϕ	71.4	102.6	102.6	71.4
			coeff.	0.279	0.376	0.376	0.279
93	-11.059	36.6					
			χ	32.7	7.9	7.9	32.7
			θ	118.5	82.1	82.1	118.5
			ϕ	74.7	89.3	89.3	74.7
			coeff.	0.211	0.371	0.371	0.212
96	-11.297	36.7					
			χ	14.3	8.7	8.7	14.3
			θ	97.7	84.3	84.3	97.7
			ϕ	78.2	96.5	96.5	77.6
			coeff.	0.231	0.361	0.361	0.231
106	-11.344	40.4					
			χ	10.9	7.7	7.0	18.3
			θ	98.3	83.5	82.8	107.5
			ϕ	96.9	86.2	90.5	84.8
			coeff.	0.275	0.402	0.358	0.196
107	-11.166	49.0					
			χ	11.9	6.9	6.9	11.9
			θ	101.4	83.6	83.6	101.4
			ϕ	73.5	87.4	87.4	93.5
			coeff.	0.256	0.424	0.424	0.256
148	-11.205	31.7					
			χ	12.5	5.6	5.6	12.5
			θ	97.2	86.4	86.4	97.2
			ϕ	100.2	85.6	85.6	100.2
			coeff.	0.199	0.344	0.344	0.199
149	-11.970	45.7					
			χ	22.5	14.4	16.5	24.9
			θ	106.3	78.7	78.7	104.8
			ϕ	74.9	98.6	102.1	70.4
			coeff.	0.266	0.387	0.395	0.325
150	-11.533	54.5					
			χ	4.3	4.1	12.2	21.5
			θ	94.3	86.4	86.2	96.5
			ϕ	74.9	98.6	102.1	70.4
			coeff.	0.268	0.427	0.442	0.301

Table 21
AM1 calculated orbital tilting angles, orbital energies and coefficients for the butadiene-like Ψ(2) molecular orbitals of cage-fused dienes, **83** and butadiene.

Diene	Ψ(2) orbital energy (eV)	% electron density on diene fragment.	Angles (degrees) and coefficients	C1	C2	C3	C4
butadiene	-9.385	100.0					
			χ	0.2	0.1	0.1	0.2
			θ	90.0	90.0	90.0	90.0
			ϕ	90.2	90.0	90.0	90.2
			coeff.	-0.563	-0.427	0.427	0.563
83	-9.190	92.5					
			χ	0.9	2.9	2.9	0.9
			θ	90.6	90.5	90.5	90.6
			ϕ	89.4	92.9	92.9	89.4
			coeff.	-0.545	-0.402	0.402	0.545
29	-9.068	73.1					
			χ	2.7	0.9	0.9	2.7
			θ	92.0	90.7	90.7	92.0
			ϕ	88.2	90.5	90.5	88.2
			coeff.	-0.472	-0.377	0.377	0.472
96	-8.860	84.2					
			χ	0.6	0.5	0.5	0.6
			θ	89.8	90.0	90.0	89.8
			ϕ	90.6	89.5	89.5	90.6
			coeff.	-0.508	-0.403	0.403	0.508
106	-8.930	76.7					
			χ	1.2	0.8	0.6	1.0
			θ	90.7	89.4	89.6	91.3
			ϕ	89.2	90.5	90.4	90.5
			coeff.	-0.485	-0.400	0.373	0.482
107	-8.812	80.9					
			χ	0.8	0.6	0.6	0.8
			θ	91.2	89.8	89.8	91.2
			ϕ	89.2	90.5	90.5	89.2
			coeff	-0.496	-0.398	0.398	0.496
148	-8.726	80.4					
			χ	0.8	0.3	0.3	0.8
			θ	90.2	89.8	89.8	90.2
			ϕ	90.7	89.8	89.8	90.2
			coeff.	-0.493	-0.398	0.398	0.493
149	-8.784	72.1					
			χ	2.4	0.7	1.7	2.8
			θ	92.9	90.6	90.8	92.9
			ϕ	91.6	89.6	90.7	88.1
			coeff.	-0.465	-0.372	0.384	0.467
150	-8.909	84.4					
			χ	2.1	0.5	1.1	3.1
			θ	92.3	89.6	89.0	91.8
			ϕ	88.6	90.3	89.3	92.0
			coeff.	-0.441	-0.346	0.366	0.422

and χ, AM1 one-electron orbital energies and orbital coefficients and calculated percentage electron density on the diene fragment is shown in Table 20 for the $\Psi(1)$ and in Table 21 for the $\Psi(2)$ molecular orbitals.

Comparison of the data in Table 20 with that in Table 21 confirms that for all the dienes examined the σ/π interaction is considerably more important for the lower lying butadiene-like $\Psi(1)$ orbital than the higher energy $\Psi(2)$ HOMO. Subsequent discussion will therefore be limited to the results for $\Psi(1)$as shown in Table 21.

The results for butadiene shown in Table 21 indicate no significant σ/π interaction as revealed by the fact that the χ angles are all close to zero, while the θ and ϕ angles are essentially 90.0° at each diene carbon. This is as expected and represents a base system of a "pure" π-diene against which the other dienes can be compared. The AM1 calculations for the diene **83** suggest that significant σ/π interaction exists with considerable rotation of the p_Z lobes. The magnitude and sense of rotation is similar to that reported by Gleiter and Paquette[158] based on a series of calculations including minimal basis sets *ab initio* calculations. The ability to reproduce the previously reported σ/π interaction indicates the suitability of the AM1 method for investigating these interactions.

Some variation was observed in the amount of σ/π interaction as revealed by the magnitude of the calculated angles of rotation of the p_Z in the atomic orbital basis for cage-fused dienes. The compounds with the strongest σ/π interaction are the diol **93**, diketone **29** and the acetal **149**. These all have lone pairs on oxygen which can undergo a "through space" interaction with the diene. The carbonyl groups can promote σ/π interaction as the unsymmetrical enone **106**, acetal **149** and thioacetal **150** were all calculated to have the large angles of p_Z lobe rotation on the diene carbons *syn to* the carbonyl group. The least σ/π interaction was observed in the cyclic ether **93** and the hydrocarbon **148**; the latter having a higher energy $\Psi(1)$ orbital thus disfavouring σ/π interaction. The calculated percentage electron density of $\Psi(1)$ which is on the diene carbons does not correlate well with the degree of p_Z rotation.

There is also no clear correlation between the magnitude of the p-orbital rotations shown in Table 21 and the experimentally observed facial selectivity for reactions of these dienes with various dienophiles. The data in Table 21 indicate that all the cage-fused

dienes undergo σ/π interaction to some extent and thus have a greater $\Psi(1)$ electron density at C1 and C4 on the face of the diene *syn* to the cyclobutane. According to the Gleiter and Paquette hypothesis[158] this should direct dienophiles to the face *anti* to the cyclobutane group in order to minimize the antibonding interaction between the $\Psi(1)$ orbital on the diene and the dienophile HOMO. In fact alkene dienophiles do show a strong preference for reaction from the face of the diene *anti* to the cyclobutane group with the cage-fused dienes. This preference, however, can also be rationalized by the molecular mechanics models described earlier, indicating an "inherent" steric preference exists in these dienes for reaction *anti* to the cyclobutane group. The high selectivity in reactions of these dienophiles does not permit evaluation of the relative importance of orbital and steric interactions.

There is, however, a number of dienophiles which react with these cage-fused dienes with a greater variation in selectivity, most notably DMAD and PTAD. For DMAD in reactions with **29**, **106** and **107** molecular mechanics models predict a greater degree of reaction from the face *anti* to the cyclobutane face than was observed indicating that the "inherent" steric preference for reaction from that face is still operative with acetylenic dienophiles. If the differential *anti* bonding interactions of the type proposed by Gleiter and Paquette[158] are important for these dienophiles then this would *reinforce* the *anti* face preference. The experimental results, however, indicate that in fact acetylenic dienophiles such as DMAD react *against* the inherent steric bias of these dienes, particularly for **29**, **106** and the cyclic ether **96**. As described in the previous chapter this is strong evidence that a direct interaction between the dienophile approaching the diene from the face *anti* to the cyclobutane group and the terminal substituent is more important in determining facial selectivity than any orbital interactions between the dienophiles and the distorted orbitals on the diene fragment.

Chapter 12.

Cycloaddition Reactions of Diimide.

Diimide[213] (N_2H_2) **151** is a short lived species which is best known as a reagent for the reduction of double bonds.[214] The *cis* stereospecificity of the hydrogen transfer[215] suggests that the Z-form of diimide is involved in a concerted hydrogen transfer. Experimental[216] and high level theoretical[217] studies have shown that E-diimide is more stable and would be the predominant form at room temperature. A semi-empirical molecular orbital study of the mechanism of hydrogen transfer from diimide during the reduction of a number of systems involving double bonds has recently been reported by Agrafiotis and Rzepa.[218] Reduction can occur as a two step process involving a diradical intermediate where the hydrogens are transferred from the diimide to the double bond sequentially or as a single step process involving transfer of both hydrogens simultaneously

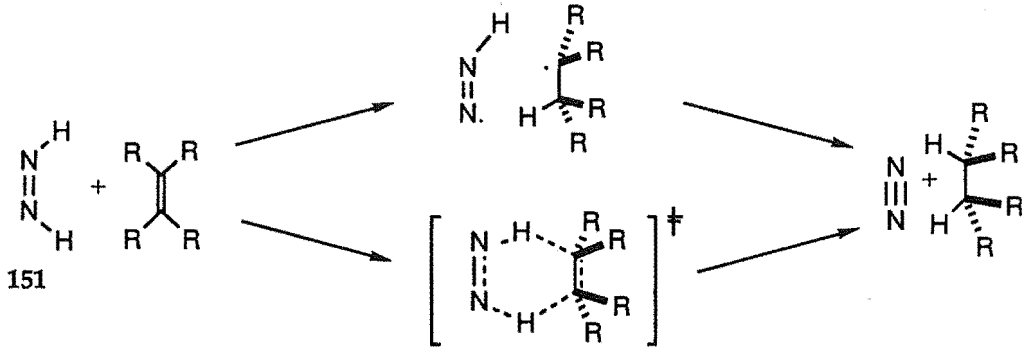

Figure 45. The two possible modes of hydrogen transfer from diimide to a double bond.

(Figure 45).AM1 and MNDO calculations were reported for the reactions of diimide with compounds containing both isolated and conjugated double bonds. The AM1 results predict in general a "concerted and essentially synchronous" transfer of hydrogen from diimide, consistent with the experimentally observed *cis* reduction of alkenes.

Hydrogen transfer from diimide is a rapid process due to the high stability of the resulting nitrogen molecule making the reaction a highly thermodynamically favoured process. Diimide is also an azo compound and as such should be able to act as the 2π component in a Diels-Alder cycloaddition. There is some experimental evidence for this

taking place when hydrogen transfer is disfavoured.[219] For example when a polymer bound diene **152** in a "three phase system" was exposed to diimide the cycloaddition

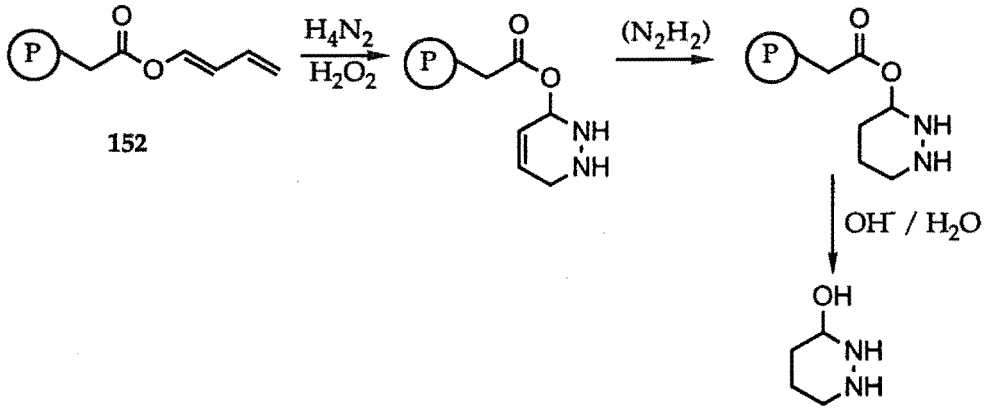

152 **153**

product **153** was isolated. In general, however, conventional experiments attempting to trap diimide as a cycloaddition product with reactive dienes have failed[214] and only products resulting from reduction have been isolated.

Azo compounds are nevertheless important dienophiles in Diels-Alder reactions. They are amongst dienophiles highly reactive and provide a convenient method for introducing two adjacent nitrogen atoms into a six-membered cyclic structure. There is some experimental evidence to suggest that the Diels-Alder reactions of the most important class of azo dienophiles, triazoline diones, may proceed in a non-concerted manner.[187,220] In dichloromethane PTAD reacts with E,Z-2,4-hexadiene **154** to give a Diels-Alder adduct **155** with the stereochemistry expected for a concerted reaction. When the reaction is

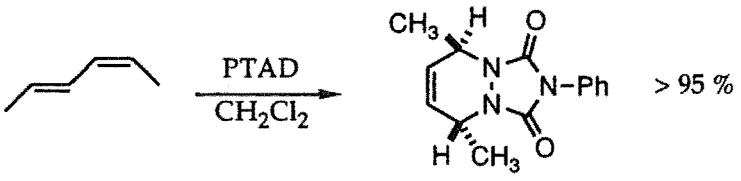

154 **155**

carried out in methanol, however, as well as the Diels-Alder adduct several products **156-158** with methoxy substituents were reported.[187] These results were considered to suggest that an intermediate aziridinium imide of the type **159** may be formed during the reaction

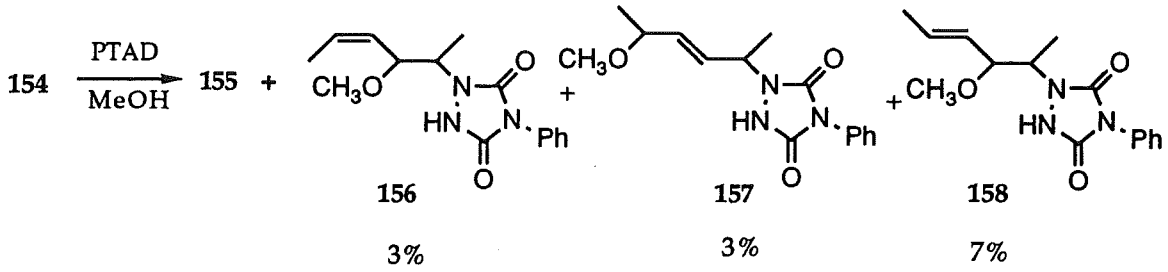

156 157 158

3% 3% 7%

which would be susceptible to attack by methanol. The formation of such an intermediate species implies that, while formally a "Diels-Alder" addition, the reaction of PTAD with dienes may proceed by a reaction pathway that is different from the normal mechanism

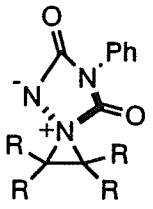

159

of such reactions (See Chapter 1). In order to investigate this possibility semi-empirical molecular orbital calculations were performed to examine the potential energy surface in the region of interaction space important for the cycloaddition of diimide and *cisoid* butadiene.

The results of previous studies,[221] using the AM1 molecular orbital method to examine pericyclic reactions where nitrogen atoms are involved in bonds which are formed or broken during the course of the reaction, led to the suggestion[221] that one of the published parameters for the AM1 method may be incorrect. This is the M_2 parameter in the core-core repulsion function for AM1 (See Chapter 2) which was reported as 2.1Å for nitrogen. The effect of this parameter was proposed to be an over-estimation of the internuclear repulsion between nitrogen and other atoms when separated by distances >1.9Å , similar to the bond distances found in the transition species of pericyclic reactions. This would have the effect of favouring asynchronous reaction pathways where the internuclear interactions can be minimized relative to those of synchronous ones. Agrafiotis and Rzepa[218] have suggested that reducing the value of the M_2 parameter to ca. 1.6Å will result in the AM1 method producing results which are more consistent with *ab initio* calculations. In the AM1 method the parameters should be treated as a self consistent set and such an arbitrary change to a single parameter should be avoided. In the latest parameterization of the NDDO method,

PM3[71] the equivalent parameter to the AM1 M_2 (known as c_2 in the PM3 formulation) has a value of 1.716Å and the results in terms of reported average errors in calculated heats of formation for nitrogen containing compounds (especially nitro compounds) show a significant improvement over those for AM1. For this reason the calculations which will be discussed here will be largely from PM3 studies although some AM1 calculations will be reported for purposes of comparison of the two methods.

As the first step in examining the cycloaddition reactions of diimide and butadiene PM3 calculations were performed for the reactants and products in the reaction. PM3 calculations for butadiene have already been discussed in the section on the Diels-Alder reactions of acetylenes (Chapter 9). PM3 calculations were performed for both the Z- and E-forms of diimide as well as the transition state for the interconversion between the two isomers. The calculated geometrical parameters for these species are shown in Figure 46, and calculated heats of formation in Table 22. The E-diimide form is predicted by the PM3

Table 22
PM3 calculated heats of formation (kJ mol^{-1}) for E-diimide, Z-diimide and the transition state for E-Z interconversion.

	Heat of formation (kJ mol^{-1})	Enthalpic barrier to E-Z interconversion.
E-diimide	158.0	151.3
Z-diimide	179.4	129.9
E-Z transition state	309.3	-

calculations to be 21.4 kJ mol^{-1} more stable than the Z-form consistent with experiment[216] and high level *ab initio*[217] calculations. The barrier to interconversion from the E to the Z isomer was calculated by the PM3 method as 151.0 kJ mol^{-1} which would suggest that diimide should isomerize only slowly under laboratory conditions. Diimide can be generated in the Z-form from the decomposition of hydrazine and this is the usual method used to prepare diimide. The cycloadditions of both forms of diimide with butadiene were examined by the PM3 method. Z-Diimide is a model for cyclic azo compounds such as PTAD, the reactions of which have been extensively studied.

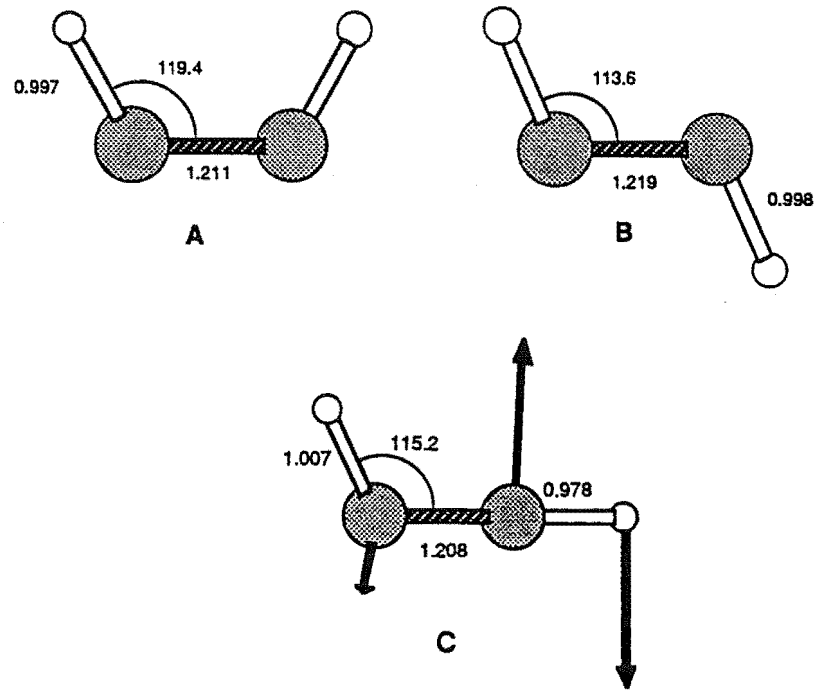

Figure 46. PM3 calculated geometries for; A) Z-diimide;B) E-diimide; C) transition structure for E-Z interconversion showing major contributing vectors to single imaginary frequency.

The product of Diels-Alder reaction of diimide and butadiene is 1,2,3,6-tetrahydropyridazine **160**. Molecular mechanics calculations established that the twist chair conformation of **160**, analogous to that expected for cyclohexene, is approximately 40

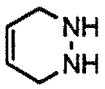

160

kJ mol^{-1} more stable than the boat conformation. There are three possible arrangements of the hydrogens on the tetrahedral nitrogens in such a twist chair conformation - the hydrogens can be diaxial (**A**), diequatorial (**C**) or in an arrangement with one in an equatorial position and the other axial (**B**). PM3 calculations were carried out for all three possibilities and the calculated geometries are shown in Figure 47. Vibrational frequencies were calculated for these species and in each case it was established that they are minima on the PM3 potential energy surface. A transition state for interconversion between these forms via an inversion of the stereochemistry at one nitrogen was also located and the geometry for this species is also shown in Figure 47. The most significant contributing vectors

of the single imaginary vibrational frequency are also shown. Calculated heats of formation and enthalpic barriers to interconversion are given in Table 23. The PM3 calculations

Table 23
PM3 calculated heats of formation and enthalpic barriers to interconversion for the H-diaxial; H-diequatorial and H-axial/equatorial conformers of **160** and calculated heat of formation for the transition state for nitrogen inversion in **160**.

Conformer	Heat of Formation ($kJ\ mol^{-1}$)	Enthalpic Barrier to Interconversion.
di-axial	148.5	44.2
di-equatorial	155.1	37.6
axial-equatorial	162.5	30.2
Nitrogen Inversion TS	192.7	-

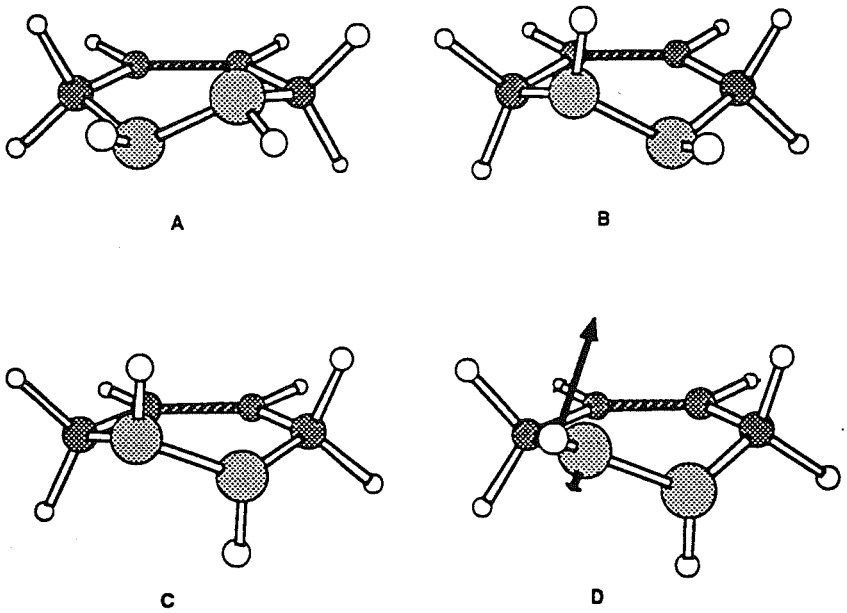

Figure 47 PM3 calculated geometries for 1,2,4,6-tetrahydropyridazine. A) di-equatorial; B) equatorial-axial; C) di-axial; D) transition state for nitrogen inversion.

indicate that the H-diaxial form of 60 is the preferred conformation as it is 6.6 $kJ\ mol^{-1}$ more stable than the H-diequatorial form, but the low barriers to interconversions suggest that this process would be highly facile. So while the diequatorial form of **160** may be the initially formed product from the Diels-Alder addition of Z-diimide and butadiene, the relative PM3 energetic ordering of the conformers suggests that inversion will occur rapidly

to give predominantly the H-diaxial form of **160**.

In order to investigate the transitional species in the reaction of E-diimide with *cisoid* butadiene, the geometrical arrangement of the two reactants shown in Figure 48 was utilized. Calculations were performed using the AM1 and PM3 methods and systematically

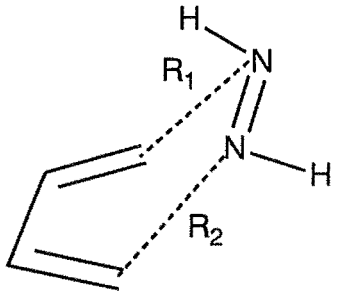

Figure 48 Definition of distances R_1 and R_2 used in the AM1 and PM3 calculations of the Diels-Alder additions of E-diimide and butadiene.

varying the distances R_1 and R_2 shown in the figure over the range 1.5-3.5 Å with full optimization of all the remaining geometrical variables. The results obtained with the AM1 method are shown represented as a 3-dimensional surface in Figure 49. The high energy in the transition state region and resulting deep ridges are almost certainly artifacts of the imperfect AM1 core-core repulsion expression for nitrogen containing atoms as discussed earlier and no attempt was made to characterize any stationary points on this potential energy surface. The PM3 potential energy surface for the same region of R_1, R_2 space is shown in Figure 50 as a 3-dimensional representation. This figure shows that the PM3 surface is considerably more continuous than that obtained with the AM1 method for this geometry definition. The surface obtained with the PM3 method has the same "ridge" which separates the reactants from the products as has been identified in the PM3 and AM1 calculations for the Diels-Alder reaction of acetylene and butadiene. In the case of the reaction of acetylene however, there was a single "valley" which connected the reactants with the products corresponding to a concerted and synchronous approach of the dienophile to the diene. For diimide this "valley" is considerably less pronounced and examination of Figure 50 suggests that there is in fact a number of smaller "valleys" where stationary points may be located. Gradient minimization techniques were applied to the geometries corresponding to "valleys" in Figure 50 and three unique stationary points were obtained; the main geometrical parameters and calculated heats of formation are shown in Figure 51 and Table 24.

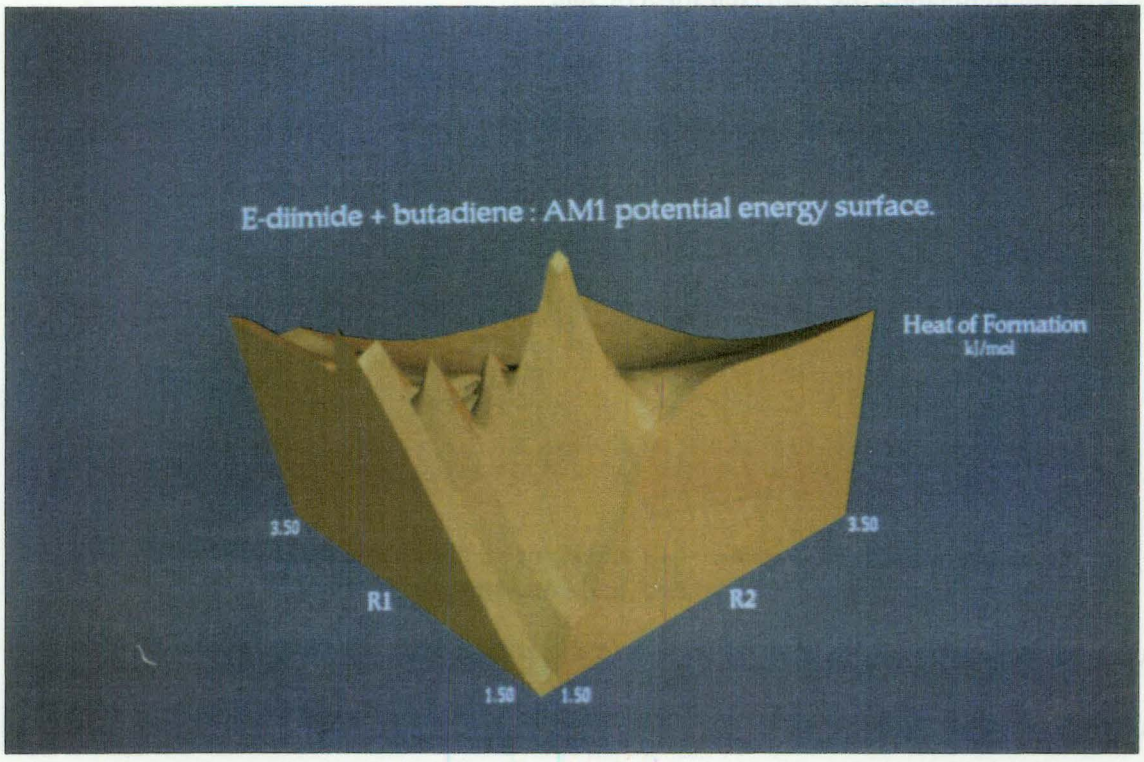

Figure 49 AM1 calculated potential energy surface for the Diels-Alder reaction of E-diimide and butadiene.

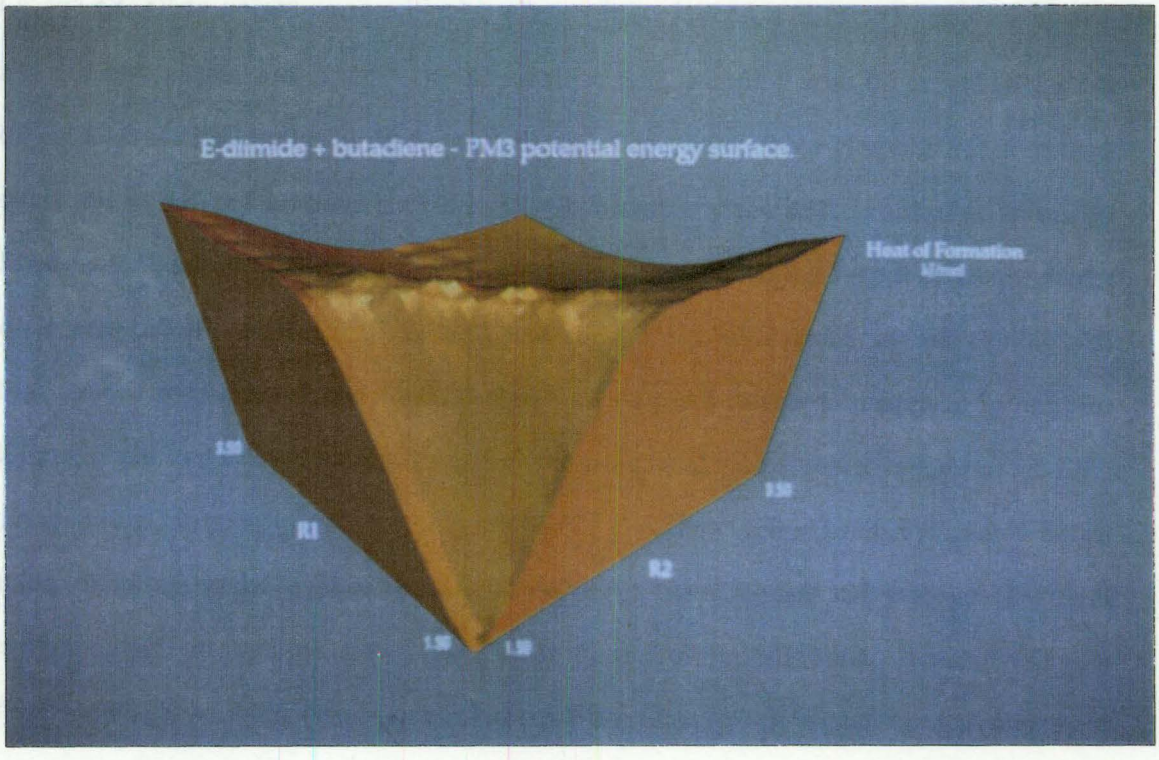

Figure 50. PM3 calculated potential energy surface for the Diels-Alder reaction of E-diimide and butadiene.

Table 24
PM3 calculated heats of formation and activation enthalpies for stationary points located for the reaction of E-diimide and butadiene.

	R_1 (Å)	R_2	Heat of Formation (kJ mol^{-1})	Enthalpy of Activation (kJ mol^{-1})
A	2.002	2.106	442.2	151.3
B	2.422	2.167	453.1	162.2
C	1.666	2.432	444.8	153.9

Vibrational frequencies were calculated for the species A-C shown in Figure 51 and each was determined to have one imaginary vibrational frequency. Somewhat surprisingly all the three stationary points on the potential energy surface are calculated by the PM3 method to be genuine "transition states". The lowest energy species, A, corresponds to the near

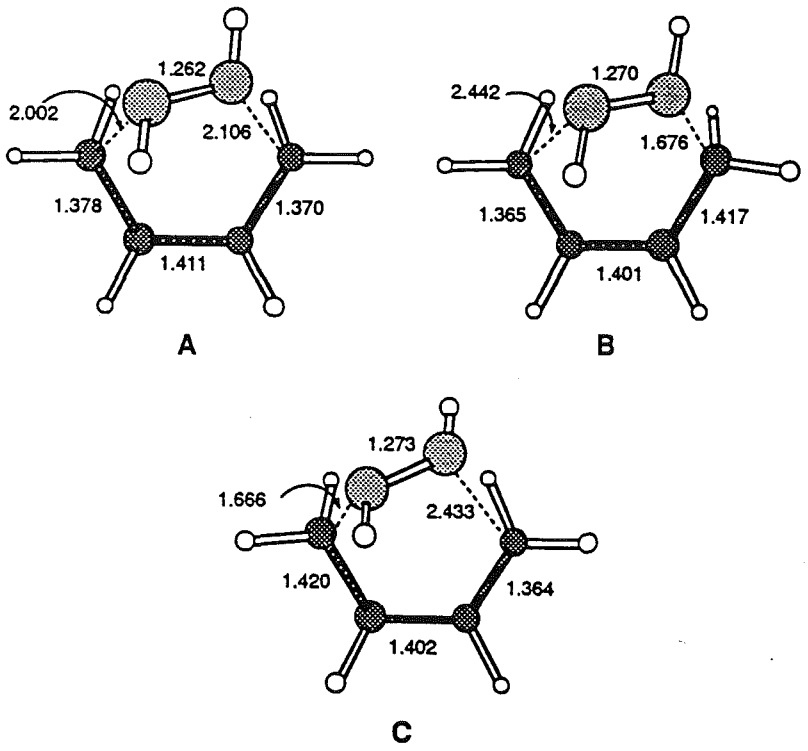

Figure 51. Transition state geometries obtained for the Diels-Alder reaction of E-diimide and butadiene.

symmetrical approach of the the E-diimide to the butadiene in a reaction which is almost certainly synchronous. The other two species B and C are higher energy points but close

enough to **A** in energy for some small proportion of the reaction to be considered as occurring via them. The lower energy point, **B**, has the *endo* hydrogen attached to the nitrogen with the shorter forming bond length at the transition state and this is clearly a favoured arrangement. The existence of the **B** and **C** points indicates the possibility for an asynchronous pathway for this reaction which is of comparable energy with the synchronous one via point **A**. This is a feature unique to the diimide system and no analogous stationary points have been identified from the many previously reported MO calculations of the Diels-Alder reactions for a number of carbon based dienophiles (See Chapter 1).

The Diels-Alder reaction of the Z-form of diimide was investigated by the PM3 method using the procedure described above for E-diimide. The Z-diimide can be considered to approach the diene in either an *endo* or an *exo* mode* and the potential energy surface for both of these possibilities was examined by systematic variation of the geometrical parameters R_1 and R_2 as shown in Figure 52. The resultant potential energy surfaces are

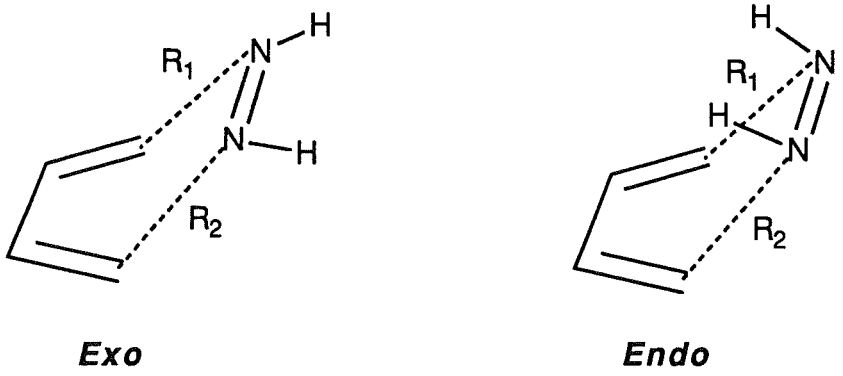

Figure 52. Definition of R_1 and R_2 for the PM3 calculations of the Diels-Alder reactions of butadiene with Z-diimide in both *exo* and *endo* modes.

shown as contour representations in Figure 53 for the *endo* mode and Figure 54 for the *exo* mode. These figures show the same significant features as other Diels-Alder reactions with a ridge separating products and reactants. The surface obtained for the *exo* approach is similar to that obtained for the PM3 calculation of the Diels-Alder reaction of acetylene and butadiene with a single "valley" connecting the reactants with the products. This corresponds to a synchronous approach of the dienophile to the diene. In contrast examination of the surface obtained for the *endo* mode of addition reveals that the valley

* The two modes of addition would in practice give identical products

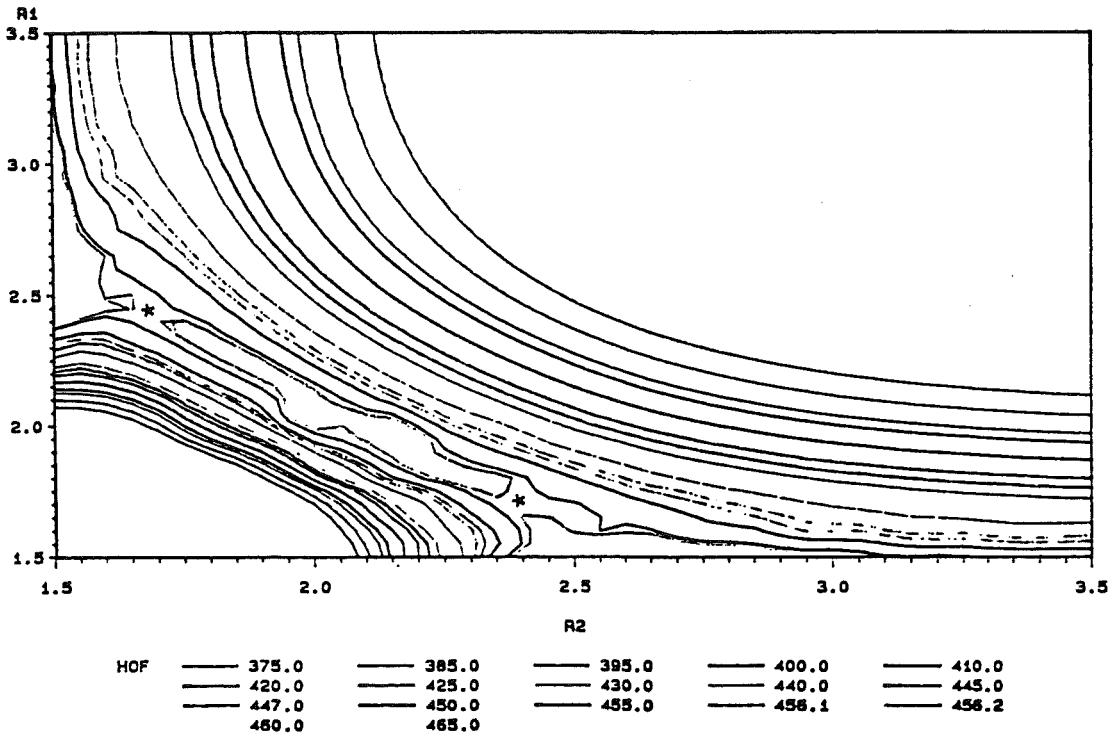

Figure 53. Contour plot of the PM3 potential energy surface for the Diels-Alder reaction of Z-diimide (*endo*) and butadiene.

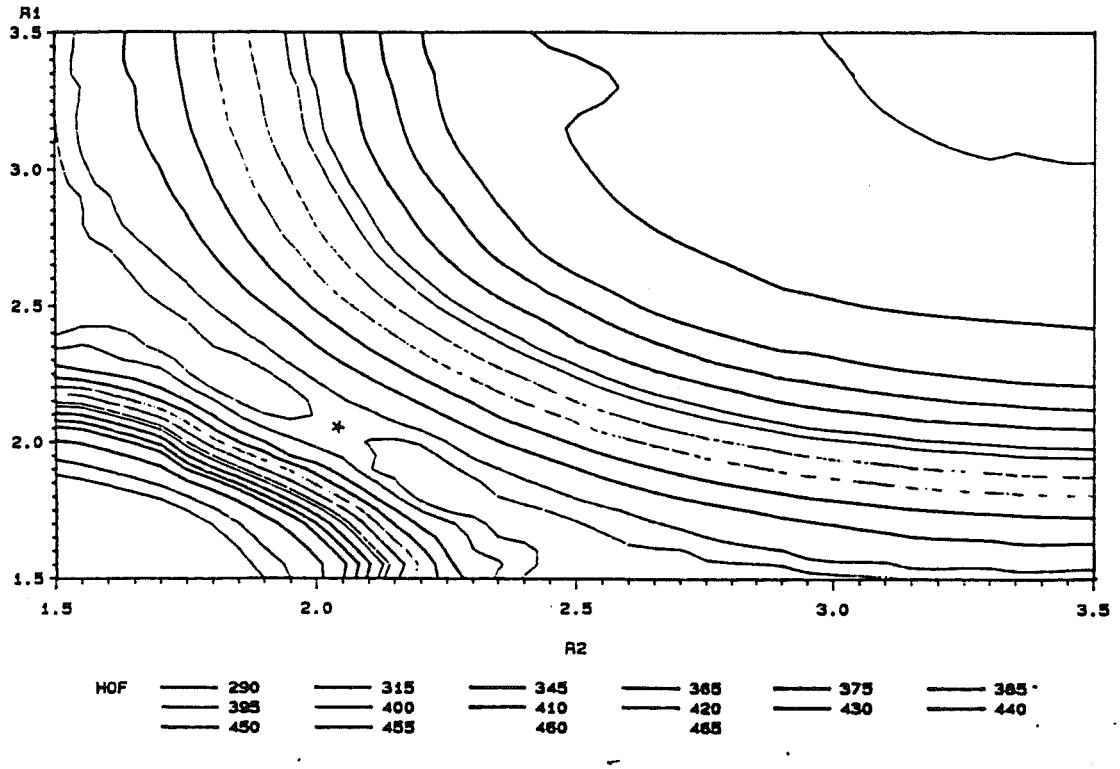

Figure 54. Contour plot of the PM3 potential energy surface for the Diels-Alder reaction of Z-diimide (*exo*) and butadiene.

which connects the products and the reactants does not correspond to simultaneous formation of both the new C-N bonds. Instead there are two symmetry-equivalent unsymmetrical approaches of the Z-diimide to the diene. The likely location of the stationary points for both these modes of addition was obtained by inspection of the contour maps (the points marked with asterisks). The main geometrical parameters of the stationary points obtained by the gradient minimization procedures are shown in Figure 55. Frequency calculations were performed using the PM3 method for these points and each was confirmed to have the single imaginary vibrational frequency required for a transition state. The major contributing vectors of each imaginary frequency are also shown in Figure 55. Heats of formation and calculated enthalpies of activation for these species are given in Table 24.

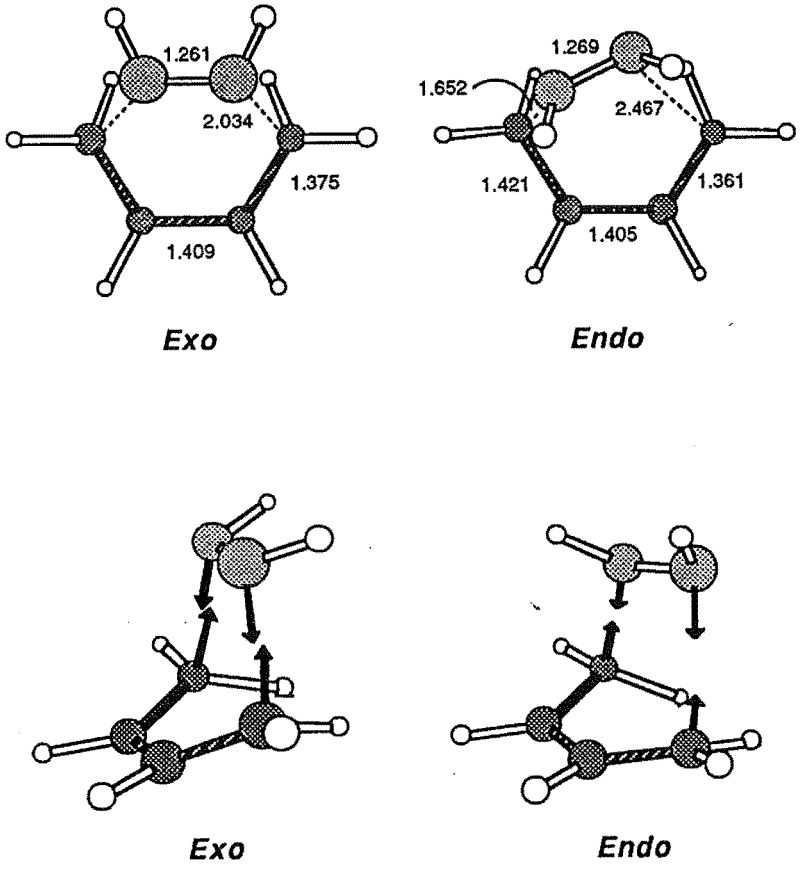

Figure 55 PM3 calculated stationary points for the Diels-Alder reaction of Z-diimide and butadiene in the *endo* and *exo* modes.

Table 25
PM3 calculated heats of formation for stationary points for the *endo* and *exo* addition modes of Z-diimide to butadiene.

	R_1 (Å)	R_2	Heat of Formation (kJ mol^{-1})	Enthalpy of Activation (kJ mol^{-1})
endo	1.652	2.467	456.2	158.5
exo	2.033	2.033	471.0	143.9

The potential energy surface for the interaction of diimide and butadiene examined so far have been confined to regions of space in which transient species for the Diels-Alder reactions of ethylenic and acetylenic dienophile have been identified. As discussed at the beginning of this section there is experimental evidence to suggest that, at least for triazoline dione dienophiles, intermediate species may be formed during the reaction which have geometrical arrangements which would not have been included in the potential energy surfaces examined so far. In order to investigate this possibility for the reaction of diimide and butadiene, PM3 calculations were performed for the likely intermediates if the reaction were to proceed via an aziridinium imide intermediate. Two conformationally related stationary points were located whose geometries and heats of formation are shown in

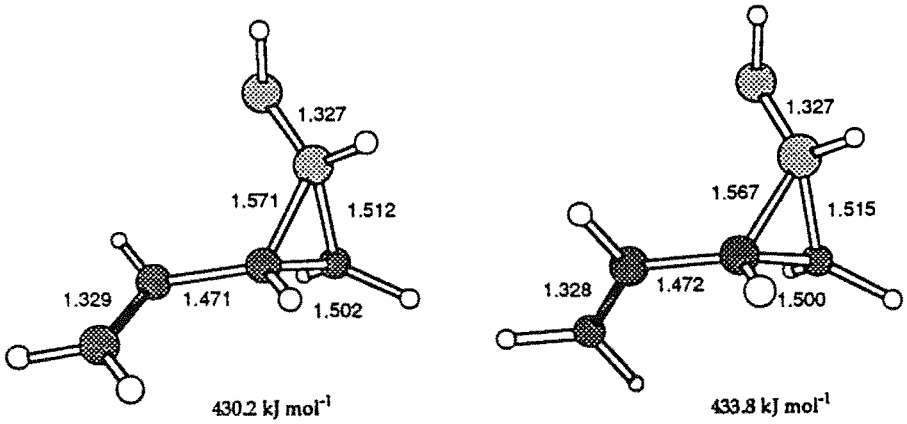

Figure 56. PM3 geometries and heats of formation for aziridinium imide intermediates in the reaction of butadiene and diimide.

Figure 56. Frequency calculations for the species shown in Figure 56 revealed that all the vibrational frequencies for these species are positive which confirms them to be minima on the PM3 potential energy surface. The calculated charge separation on the nitrogen is as expected for such species. The calculated atomic charges for the nitrogens are +0.8619 and -

0.7301. The most significant factor, however, is that the calculated heats of formation as shown in Figure 56 for these *intermediate* species are only slightly less than those calculated for the various *transition states* for the concerted (synchronous and asynchronous) Diels-Alder reactions of diimide and butadiene. Unless the aziridinium imide species are formed with essentially no energy of activation, any reaction pathway involving the formation of these species will not be energetically competitive with the concerted process. For this reason no further work was carried out to identify transition states linking these intermediates with the reactants or products.

The PM3 calculations reported above for the reaction of diimide and butadiene suggest that the Diels-Alder addition of azo compounds may follow a significantly different reaction path from those which have been proposed for the Diels-Alder addition of ethylenic and acetylenic dienophiles. The PM3 calculations predict that the most energetically favoured mode of addition for diimide and butadiene is the reaction of the Z-diimide in an *endo* configuration and although this reaction is predicted to occur with a single kinetic step, the new C-N bonds are not formed simultaneously. This will have important consequences for understanding and modelling the reactions of azo compounds. Experiments described in this work and elsewhere[193] have shown that azo dienophiles frequently react with facially dissymmetric dienophiles with strikingly different facial selectivities to those of alkene and acetylenic dienophiles. On the basis of these PM3 calculations for the reactions of diimide, this may be considered to be the result of the asynchronous reaction of azo dienophiles with the consequence that steric and electronic interactions between azo dienophiles and facially dissymmetric dienes at the transition state will be considerably different from those with alkene and acetylenic dienophiles. Furthermore, while the heats of formation from the PM3 calculations of the possible aziridinium intermediate in the reactions of diimide and butadiene suggest that these species are not important for this reaction, such intermediates may be substantially stabilized by substitution on the nitrogen and for cyclic azo compounds such as PTAD. Highly asynchronous pathways involving such intermediates may be important. This must be considered as a factor in the unique facial reactivity of azo dienophiles. Further calculations involving substituted azo compounds are required in order to evaluate the

relative importance of each of the possible reaction pathways which have been proposed here on the basis of PM3 calculations. This would be most useful for reactions involving dienophiles for which experimental data are available, since this allows direct comparison of theory and experiment. The application of *ab initio* molecular orbital theory to the study of the prototype reaction of diimide and butadiene would also be useful in order to allow assessment of the semi-empirical PM3 method for investigating the potential energy surfaces for the cycloadditions of azo compounds.

Chapter 13.

The "Cieplak" Effect. Direction of Reaction at Facially Dissymmetric π Systems by Hyperconjugative Interactions.

Recent publications by Cieplak et al.[95] have drawn attention to the possibility that hyperconjugative stabilization at the transition state may be important in determining the π-facial diastereoselection for addition reactions to facially dissymmetric π-systems. Cieplak's conclusions are based on considerations of the importance of electron donation from suitably oriented σ-bonds to the σ* orbital which is forming at the reaction centre. His theory can be summarized in the statement that "addition will occur antiperiplanar to the most electron-rich bond". With this theory Cieplak has been able to rationalize the effect

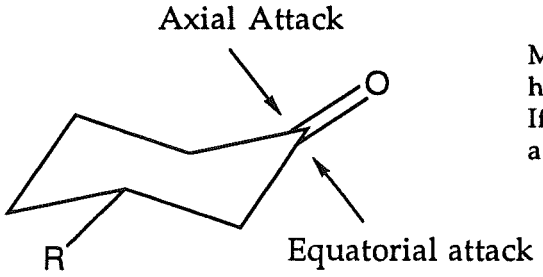

Most nucleophiles attack from the least hindered equatorial face.
If R is electron releasing then axial attack is promoted.

Figure 57. The effect of remote substitution on the stereochemistry of nucleophilic attack on cyclohexanone.

of remote substitution on the reaction of nucleophiles with cyclohexanone (Figure 57). No previous hypothesis has been able to successfully account for all the large number of experimental observations for this system.

Since Cieplak's original report other workers[222,223] have prepared compounds with facially dissymmetric carbonyl groups which allow the testing of the Cieplak hypothesis without the inherent steric preference or conformational uncertainty found in the reactions of cyclohexanones. Mehta et al.[222] have prepared a series of 2-*endo*-3-*endo*-disubstituted 7-norbornanones **161** and investigated the effect of remote substitution on the facial course of reduction of the ketone group. Some of the results obtained by Mehta for the $NaBH_4$ reduction of **161** are shown in Figure 58. As shown in Figure 58, electron withdrawing

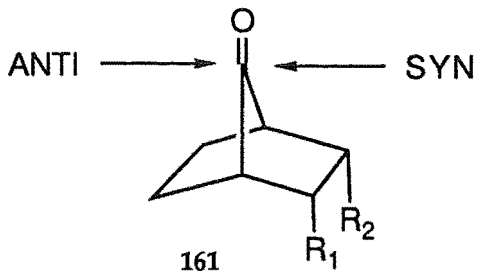

Reduction with $NaBH_4$
Syn:Anti Ratios.

R_1=R_2 = $C(O)OCH_3$	84:16
R_1=R_2 = CH_2OCH_3	40:60
R_1=R_2 = vinyl	36:64
R_1=vinyl; R_2 = ethyl	25:75
R_1 = R_2 = ethyl.	20:80

Figure 58. Facial selection observed for the reduction of 2-*endo*-,3-*endo* -disubstituted 7-norbornanones.

substituents in the 2 and 3 positions of **161** promote addition of hydride on the face of the ketone *syn* to the substituents, while electron releasing groups promote addition to the face of the ketone *anti* to the substituents. The 2,3 substituents will have only a minimal direct steric effect on the course of the reaction. The π-facial selectivity observed was rationalized by Mehta by considering the possible participation of σ-bonds which are antiperiplanar to the direction of nucleophile attack. Figure 59 illustrates schematically the orbital interactions which are proposed to be important at the transition state for this reaction. As

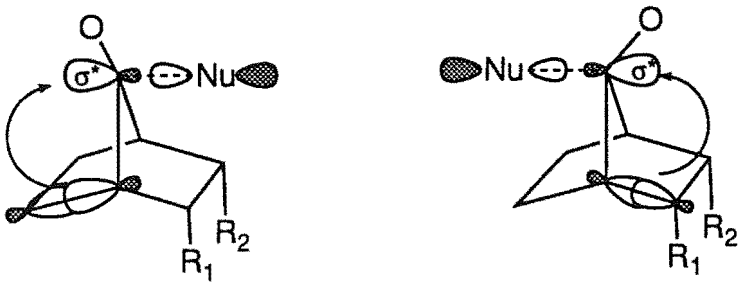

Figure 59. Proposed hyperconjugative interactions at the transition state for *syn* and *anti* reaction of nucleophiles with 7-norboranones.

the nucleophile is forming a new bond with the carbonyl system, a σ* orbital is also developing on the face of the ketone opposite to that of attack by the nucleophile. This incipient orbital is considered to be electron deficient and so donation of electron density can occur from suitably arranged σ-bonds as shown in Figure 59. Thus it was proposed that if the substituents at the 2 and 3 positions are electron withdrawing then this will *reduce* the electron donating ability of the bonds which are antiperiplanar to the nucleophile. Attack therefore occurs from the face of the ketone *syn* to the electron withdrawing substituents. Conversely if the substituents at the 2 and 3 positions are electron releasing then *anti* addition occurs. The substituents increase the electron donating ability of the adjacent bonds which lie antiperiplanar when nucleophile attacks from the *anti* face.

While this qualitative theory is able successfully to rationalise the experimental observations for these norbornanone systems, molecular orbital calculations on the diastereotopic transition states would be useful in order to quantify the nature of the electronic interactions at the transition state. This section will describe AM1 and PM3 semi-empirical molecular orbital calculations directed towards investigating the importance of hyperconjugative stabilization at the transition state for nucleophilic addition to facially dissymmetric 9-norbornanones.

Experimental studies of nucleophilic addition to carbonyl groups in the gas phase[224] have shown that many reactions of anionic species and other strong nucleophiles with carbonyl compounds proceed without activation. Dewar[225] has suggested that all reactions of anions with neutral species will proceed without activation in the gas phase and that in solution phases, desolvation of the anion accounts for a significant proportion of the barrier to reaction. The semi-empirical PM3 and AM1 methods in common with most *ab initio* and semi-empirical procedures are only suitable for modelling gas phase phenonoma unless solvent molecules are explicitly included.[226] No allowance is made in semi-empirical or *ab initio* molecular orbital calculations for the interactions of the species of interest with solvent. For these reasons the "transition states" for reactions such as hydride addition to carbonyl compounds cannot be modelled by the gas phase AM1 and PM3 procedures as these methods will predict reaction without activation barriers. Preliminary AM1 calculations were performed for the hydride transfer from BH_4^- to

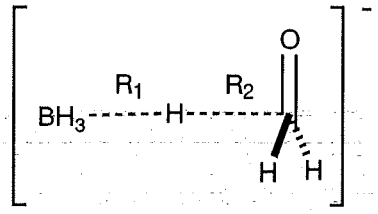

Figure 60. Distances R1 and R2 used in AM1 calculations of potential energy surface for hydride transfer from BH_4 to formaldehyde.

formaldehyde to confirm that this is the case. The R_1 and R_2 distances (Figure 60) were varied systematically over the range 1.1 to 2.1 Å and the potential energy surface obtained is shown in Figure 61 in a 3-dimensional representation. Examination of Figure 61 shows that the hydride transfer will occur in a linear transfer mode without activation as there is

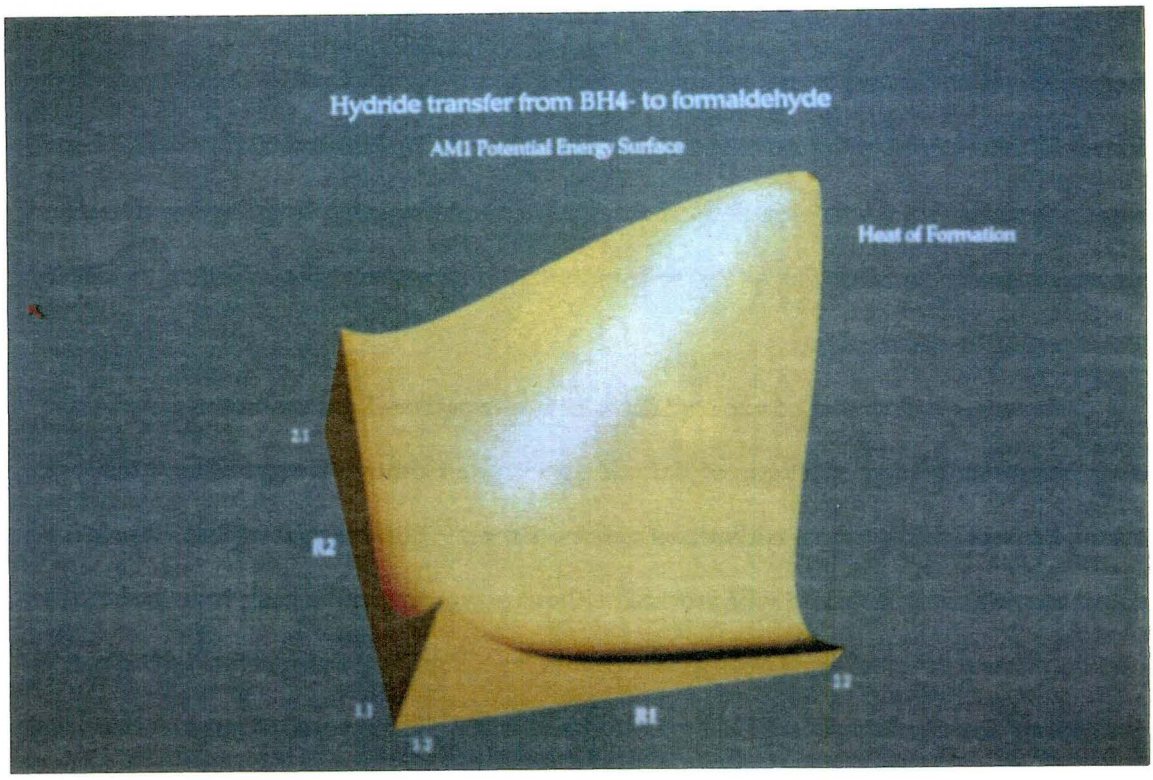

Figure 61. AM1 calculated potential energy surface for the linear transfer of hydride from BH_4^- to formaldehyde.

a reaction channel from the point R_1=1.2, R_2=2.1 (BH_4^- + CH_2O) to the point R_1=2.1, R_2 = 1.1 (BH_3 + CH_3O^-) without an intervening maximum in energy. Similar pathways not involving a transition state were obtained for calculations of hydride transfer in other than a linear mode.

Although the reactions of charged species with carbonyl containing compounds may occur without activation in the gas phase, this is not necessarily the case for neutral species. One such reaction of neutral species which has been studied by *ab initio* [227] and semi-empirical[228] molecular orbital methods is the hydration of formaldeyhde which was predicted to occur with a significant activation even in the gas phase. For this reason it was decided to perform AM1 and PM3 calculations for the the analogous reaction of methanol with formaldehyde to give the hemiacetal as a model for examining the importance or otherwise of hyperconjugative interactions at the transition state for nucleophilic addition. The PM3 and AM1 results for this system are summarized in the reaction-energy profile shown in Figure 62. These calculations predict the course of the reaction to occur via the

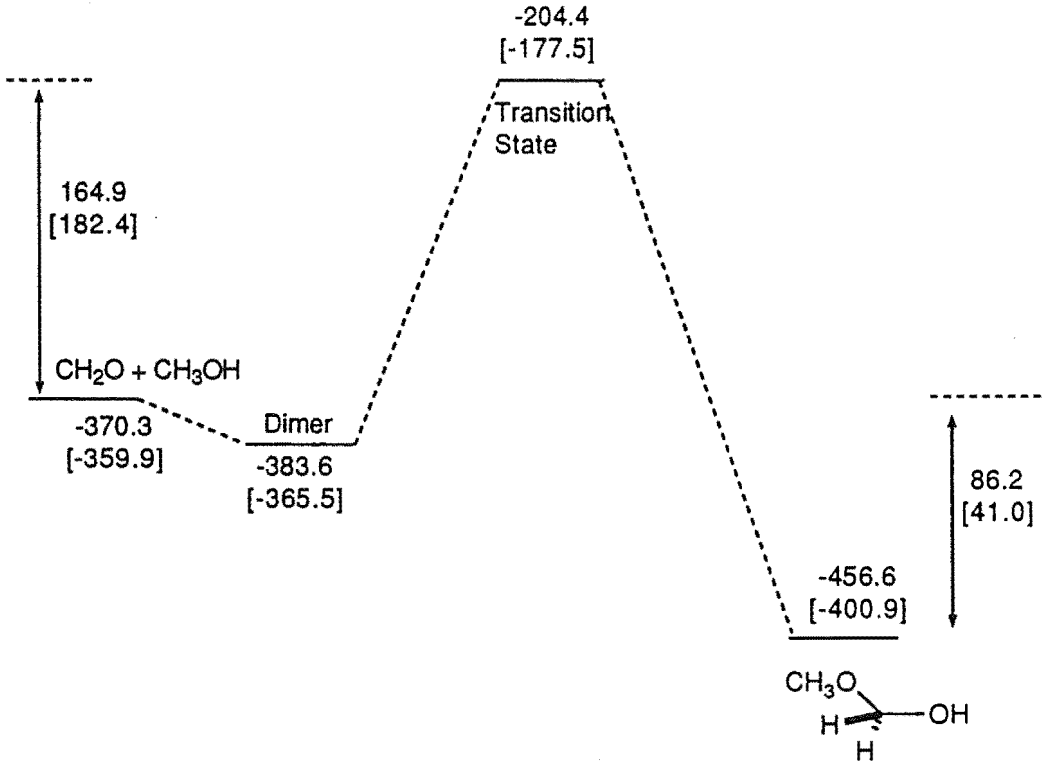

Figure 62. AM1 and PM3 [square brackets] calculated reaction energy profile for the reaction of methanol and formaldehyde. Heats of formation in kJ mol-1.

involvement of a hydrogen bonded dimer. This is followed by addition of methanol, with a transition state involving the transfer of the hydroxyl proton (of the methanol) to the oxygen of the carbonyl in concert with the attack by the methanol oxygen on the carbonyl carbon of formaldehyde. The major AM1 calculated geometrical parameters for the transition state in this reaction are shown in Figure 63. A frequency calculation was performed for this transition state using the AM1 and PM3 methods and both gave a single

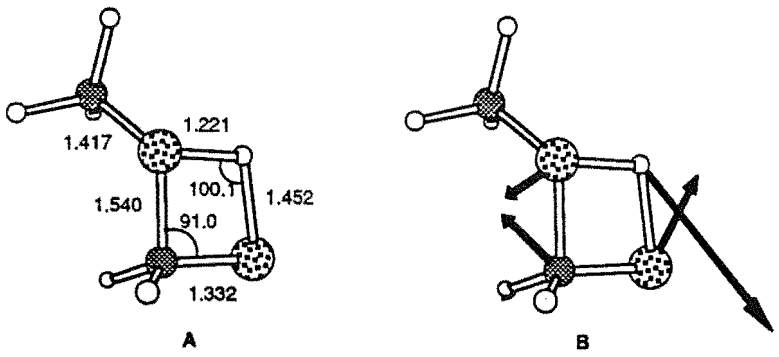

Figure 63. A) AM1 calculated geometry for the transition state in the reaction of methanol and formaldehyde. B)Major contributing vectors of the single imaginary frequency of the transition state.

imaginary vibrational frequency, the major contributing vectors of which are shown in Figure 63b. The vectors shown in Figure 63b confirm the concerted nature of proton transfer with addition of the alcohol oxygen to the carbonyl group. These results parallel those obtained from *ab initio* and semi-empirical calculations for the hydration of formaldehyde. One of these studies[228] compared the semi-empirical and *ab initio* results and concluded that the AM1 method was better able to treat these types of reactions and so only the AM1 method was used to investigate the addition of methanol to 2,3-disubstituted 7-norbornanones **161**.

With the AM1 transition state geometry for the addition of methanol to formaldehyde as a starting geometry, transition states were located for the addition of methanol to a number of 2,3-disubtituted-7-norbornanones for both *anti* and *syn* addition. Full gradient optimization procedures were applied to all geometrical parameters and frequency calculations on each of the resulting stationary points confirmed them to be transition structures. For conformationally flexible substituents, ($R=CO_2CH_3$ and $R=CH_2CH_3$) molecular mechanics calculations using the MM2 force-field were performed for the parent ketone with a procedure involving the systematic rotation of each rotatable bond at 60° intervals. In both cases a single conformation was identified which would account for ca. 70% of the conformer population at room temperature and this substituent geometry was used as a starting geometry for the AM1 transition state calculations. The AM1 calculated enthalpies of activation for the diastereotopic transition states and the calculated percentage *syn* reaction at 25° is shown in Figure 64. The predicted *syn* to *anti*

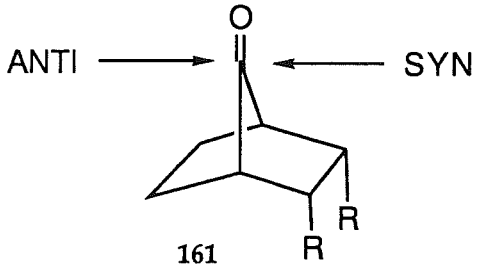

161

AM1 calculated activation enthalpies.

	SYN	ANTI	%*Syn* at 25°C
a) R= CH_2CH_3	217.2	215.5	33.4 %
b) R=CO_2CH_3	213.8	207.2	6.9 %
c) R=F	213.4	206.9	7.3 %

Figure 64. AM1 calculated enthalpies of activation (kJ mol^{-1}) for the reaction of methanol and 2,3-disubstituted 7-norbornanones **161a-c**.

ratio of 33:67 for **161a** is consistent with the experimental results obtained by Mehta for the reduction of **161a** (Figure 58), where this electron releasing substituent was found to promote reaction *anti* to the substitution. The AM1 results for the electron withdrawing substituents in **161b** and **161c** are at variance with the experimental observations as the AM1 calculations

continue to predict predominantly *anti* reaction, whereas in the experimental studies the electron withdrawing groups were shown to promote reaction at the *syn* face.

The failure of these AM1 calculations to reproduce the experimentally observed facial selectivities for the nucleophilic addition to **161** could arise by a combination of factors. The AM1 method has been shown to be satisfactory for investigating a variety of ground state phenonoma, and gives results which are quantitatively in agreement with *ab initio* calculations and experiment for a number of reaction pathways. Reproducing the small energy differences observed for the diastereotopic transition states is a demanding test for any molecular orbital procedure. Addition of methanol to carbonyl containing compounds, although it proceeds with a calculable activation in the gas phase, may not be a satisfactory model for comparing the importance of hyperconjugative stabilization in the additions of charged nucleophiles such as hydride ion. Examination of the transition state geometry for the addition of methanol, as shown in Figure 63, reveals that the bond between the oxygen of the methanol and the carbon of the aldehyde is substantially formed at the transition state with a bond length of ca. 1.5 Å. One of the requirements for hyperconjugative stabilization to be important is that this bond be partially formed at the transition state and therefore highly electron deficient in nature. As this is not the case for the addition of methanol, then electron donation from antiperiplanar bonds will be of lesser importance than when a reaction involves an "earlier" transition state. Thus stabilization which is important in determining facial selectivity for the "early" transition state reaction will be less important relative to steric and electrostatic interactions. It is the latter situation which applies for the addition of methanol to these carbonyl compounds.

Hyperconjugative stabilization by antiperiplanar σ-bonds has recently been proposed to account for the facial selectivity observed in the Diels-Alder reactions of 5-substituted cyclopentadienes.[95] The major experimental results for this system have already been discussed in detail in Chapter 3. In order to be able further to investigate the suitability of AM1 calculations for reproducing such two-electron stabilization at the transition state of cycloaddition reactions, a series of AM1 calculations were performed on each of the diastereotopic transition states for the Diels-Alder reactions of **162a-d** as a model for the reactions of **19** which have been the subject of experimental studies.[94]

The AM1 method predicts a concerted reaction pathway, involving a symmetrical transition structure for the reaction of ethylene and butadiene[5] consistent with the experimental evidence and high level calculations (See Chapter 1). Using this published transition state geometry as a starting point, AM1 gradient minimization procedures were used to locate transition structures for the addition of ethylene to each face of **162a-d**. Each structure was found to have a single imaginary vibrational frequency as required for a genuine transition state. The most important geometrical parameters for the AM1 calculated transition state for reaction of ethylene and **162a** are shown in Figure 65 and this geometry is representative of transition states for the reactions of ethylene and **162b-d**. The most

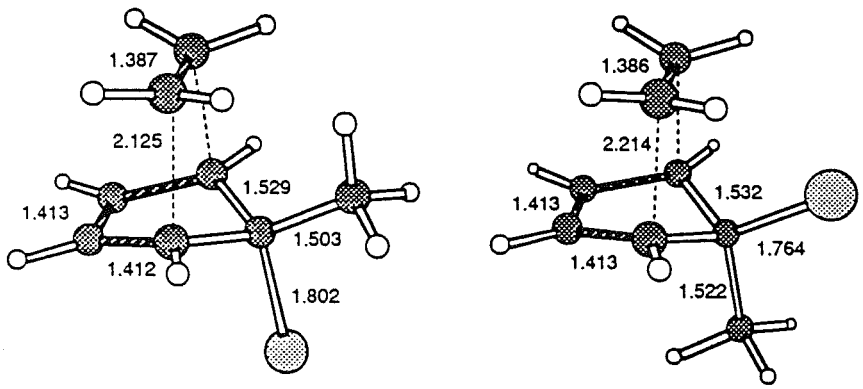

Figure 65 AM1 calculated geometry for the transition state in the Diels-Alder reaction of ethylene at both faces of 5-methyl-5-chloro-cyclopentadiene (**162a**).

notable feature of the transition state geometry for the reaction of ethylene at each face of the diene (Figure 65) is that the diene C-X bond length for the *anti* addition of the dienophile is considerably longer than the comparable bond length when the X-substituent is *syn* to the approaching dienophile. For example when the ethylene is reacting *syn* to the chlorine in **162a** then the chlorine bond length is calculated as 1.764Å, while for the reaction *anti* to the chlorine this distance lengthens to 1.802Å. Such a lengthening of the C-X bond is consistent with the donation of electron density from the σ-bond of the *anti* substituent to the forming σ* orbital as proposed by Cieplak and discussed above (Figure 59). The AM1 calculated enthalpies of activation for the reaction of ethylene and **162a-d** are shown in Table 26 together with the calculated *syn:anti* ratios. The results in Table 26 show that for

Table 26
AM1 calculated enthalpies of activation (kJ mol^{-1}) for the Diels-Alder reaction of ethylene at each face of **162a-d** and calculated *syn* to *anti* ratios.

	X	Enthalpy of Activation (kJ mol^{-1})		*Syn:Anti* Ratio	
		Syn	*Anti*	Calcd. for **162.**	Expt. for **19.**
162a	Cl	131.9	134.6	66:34	100:0
162b	OH	116.9	135.9	100:0	100:0
162c	OCH_3	123.8	141.0	100:0	100:0
162d	SCH_3	139.1	141.0	76:24	10:90

X=Cl, OH and OCH_3 AM1 calculations are in quantitative agreement with the experimental observations obtained for the additions of N-phenylmaleimide and maleic anhydride to **19a-c**. For the sulphur substituted case, however, the AM1 reaction continues to predict that reaction will occur predominantly from the face of the diene *syn* to the X-group (in this case SCH_3) whereas the experimental results showed a dramatic reversal of selectivity with only 10% of the addition occuring *syn* to the sulphur substituent in the reaction of **19d**.

It should be noted that the difference in AM1 calculated enthalpy of activation for reaction at each face is considerably less for the sulphur containing group than for **162a-c**. This implies that, while the AM1 method cannot fully reproduce the experimental observations, the trend for reduced *syn* face reaction with sulphur containing substituents is reproduced by these calculations.

Current semi-empirical methods, such as AM1, in general appear to be somewhat limited for quantitative investigations into the role of hyperconjugative stabilization at the transition state for addition reactions to π systems. This is a result of a general limitation of all molecular orbital methods which only reproduce gas phase phenomena. In the gas phase, reactions for which hyperconjugative stabilization has been proposed to be important in determining facial selectivity, proceed without activation. The AM1 method is not able to satisfactorily reproduce experimentally observed substituent effects in the Diels-Alder reactions of 5-substituted cyclopentadienes where hyperconjugative stabilization effects

have been proposed to be important in determining facial selection. The failure of AM1 to reproduce substituent effects in Diels-Alder reactions has also be noted by Houk[47] where it was determined that only high level *ab initio* calculations could reproduce the observed effects of substitution on reactivity and it may be that such procedures are required to reliably investigate the "Cieplak effect". However to parallel the semi-empirical calculations reported here with high level *ab initio* methods would be a major undertaking at the present time and require considerable computing resources.

Experimental.

General.

NMR spectra were recorded on a Varian XL300 spectrometer equipped with a 5 mm probe operating at 299.930 and 75.426 MHz for ^{1}H and ^{13}C, respectively. Chemical shifts are listed in p.p.m. relative to tetramethylsilane. Difference nOe spectra were obtained in an arrayed experiment with the decoupler offset 10,000 Hz and then cycled with low power over the multiplet peaks of the desired proton for irradiation, a procedure based on that of Kinns and Sanders.[229] Heteronucler proton-carbon correlated spectra were recorded using a sequence that ensures full ^{1}H-^{1}H decoupling.[230] All dienophiles were obtained commercially. Melting points are uncorrected.

The general procedure for the addition reactions of the dienophiles to the cage dienes was as follows: the diol (*ca.* 0.44 mmol) was dissolved in benzene. To this, a slight excess of the dienophile was added and the reaction was heated under reflux. The reaction progress was followed by t.l.c. (silica gel with a 7:3 mixture of ether and petroleum ether as elutant). When no starting material could be detected (15 min to 9 days) the solvent was removed and ^{1}H and ^{13}C NMR spectra of the crude product were recorded. The crude addition products were then separated either by recrystallization, or by radial chromotgraphy on silica gel.

Hexacyclo[10,2,1,$0^{2,11}$,$0^{4,9}$,$0^{4,14}$,$0^{9,13}$]pentadeca-5,7-diene-3,10-dione (29).

The Diels-Alder adduct of cyclopentadiene and 1,4-napthoquinone in benzene (8.0g, 1% w/v) in a quartz vessel submerged in an ice-water bath was irradiated with a low-pressure 450W mercury lamp (Hanovia) with a Pyrex filter for 8 h. The solvent was removed under reduced pressure to leave a crude product which was recrystallized from dichloromethane/petroleum ether to give a colourless solid mp: 111-112 °C (lit.[231] 111-112°); IR (KBr) 3250, 2980, 1790 cm^{-1}. ^{1}H NMR ($CDCl_3$) δ 1.76 (d, J = 11.2 Hz, H15b); 1.98 (d, J = 11.2 Hz, H15a); 2.80 (br s, H2,H11); 2.99 (br s, H1,H12); 3.35 (br s, H13,H14); 5.39 (m,

H5,H8); 5.98 (m, H6,H7); ^{13}C NMR ($CDCl_3$) δ 38.9 (C15); 44.2 (C1,C2); 50.1 (C4,C9); 51.6 (C13,C14); 54.6 (C2,C11); 119.8 (C5,C8); 124.7 (C6,C7); 210.2 (C3,C10).

Hexacyclo[10,2,1,$0^{2,11}$,$0^{4,9}$,$0^{4,14}$,$0^{9,13}$]pentadeca-5,7-diene-3-*endo*-10-*endo*-diol (93).

(i) By reduction of **29** with lithium aluminium hydride.

To a stirred solution of **29** (4.0 g) in dry ether (80 mL) at 0-5 °C in an ice bath was added a suspension of lithium aluminium hydride (1.5 g) in ether (100 mL). The reaction mixture was allowed to warm to room temperature and stirring was continued overnight. The mixture was heated under reflux for one hour and, after cooling, water (60 mL) was cautiously added. The aqueous layer was treated with dilute hydrochloric acid (20 mL, 7%) and extracted with chloroform (6 x 15 mL). The combined organic extracts were dried with anhydrous sodium sulphate and after removal of the solvent gave an orange oil which solidified on standing to form crude product. Recrystallization from dichloromethane/ petroleum ether gave **93** as off-white prisms (3.06 g, 75%): mp 147-149 °C; IR (KBr) 3350, 3250, 2980 cm^{-1}; ^{1}H NMR ($CDCl_3$) δ 0.91 (d, J = 10.6 Hz, H15b); 1.53 (d, J = 10.6 Hz, H15a); 2.38 (m, H1,H12); 2.42 (m, H2,H11); 2.76 (m, H13,H14); 3.53 (s, H3,H10); 5.10 (br, (exchangable with D_2O), OH); 5.37 (m, H5,H8); 5.85 (m, H6,H7); ^{13}C NMR ($CDCl_3$) δ 32.4 (C15); 42.5 (C1,C12); 45.8 (C14,C13); 47.4 (C4,C9); 54.1 (C2,C11); 75.9 (C3,C10); 124.0 (C5,C8); 128.0 (C6,C7); HRMS required for $C_{15}H_{16}O_2$: 228.1150, found 228.1147.

(ii) By reduction of **29** with sodium borohydride.

To a stirred solution of **29** (3.6 g) in ethanol (200 mL), cooled to 0-5 °C in an icebath, was added $NaBH_4$ (1.26 g), portionwise over 3 h. The reaction mixture was allowed to warm to room temperature and stirred for a further 3h, then a solution of hydrochloric acid (50 mL; 10%) was added. The aqueous layer was extracted with dichloromethane (6 x 50 mL), washed with water (6 x 50 mL), dried ($MgSO_4$) and the solvent removed to give a crude material (2.69 g) which was purified by recrystallization from dichloromethane/ petroleum ether to give diol **93** with physical and spectroscopic properties identical with that obtained from the $LiAlH_4$ reduction. A repeat of this procedure with the addition of 12.6 g $CeCl_3.6H_2O$ gave a mixture of the diol **93** (85%) and another compound (15%) which was identified by ^{1}H and ^{13}C NMR data as the *endo-exo* diol **94**.

Attempted Dehydration of the diol 93.

(i) Catalysed by *p*-toluene sulphonic acid.

The diol **93** (100 mg) was dissolved in 10 mL dichloromethane and 5 mg of *p*-toluene sulphonic acid was added. The reaction mixture was stirred at room temperature for 72 h. T.l.c. analysis revealed no change in the composition of the reaction mixture. The solvent was removed under reduced pressure and ^{1}H NMR analysis revealed only the starting diol.

(ii) Heating to 280 °C.

The diol **93** (100 mg) was placed in a 5 mL flask and heated in an oil bath at 280 °C for 5 minutes. The flask was then cooled and the black material extracted with dichloromethane. Removal of the solvent under reduced pressure and ^{1}H NMR analysis of the crude material revealed a complex mixture of products.

(ii) Heating in the presence of P_2O_5.

The diol **93** (100 mg) was finely ground with 20 mg of P_2O_5. The solid mixture was placed in a flask without solvent and heated in an oil bath at 180 °C for 10 minutes. The resulting black residue was then heated under reflux with 20 mL of dichloromethane for 20 minutes. A further 40 mL of dichloromethane was added and the solution was washed with a saturated solution of $NaHCO_3$ (2 x 40 ml), dried ($MgSO_4$) and the solvent removed to give a dark orange residue (32 mg). ^{1}H NMR analysis of the crude material revealed a complex mixture of products.

(iii) Dehydration with H_2SO_4.

The diol **93** (50 mg) was added to 5 mL concentrated H_2SO_4 and stirred at room temperature for 4h. The reaction mixture was carefully poured into 25 mL ice-water and solid K_2CO_3 added until the evolution of gas ceased. The mixture was extracted with 50 mL dichloromethane, washed with water (2 x 40mL), dried ($MgSO_4$) and the solvent removed to give 35 mg of an orange gum. ^{1}H NMR analysis of the crude material revealed a complex mixture of products.

Acetylation of diol 93 with acetic acid/acetic anhydride and H_2SO_4.

To a stirred solution of diol **93** (200 mg) in 6 mL acetic acid and 2 mL acetic anhydride was added a 1% (v/v) solution of sulphuric acid in acetic acid.[232] Stirring was

continued at room temperature for 120 seconds after which time the reaction was quenched by pouring into a mixture of 50 mL ether and 50 mL saturated sodium bicarbonate solution. Solid sodium bicarbonate was added until effervesence ceased. The ether layer was washed with 50 mL of water and dried over magnesium sulphate. Removal of the solvent gave a white solid (225mg). Recystallization from petroleum ether/dichloromethane gave hexacyclo-[10,2,1,$0^{2,11}$,$0^{4,9}$, $0^{9,13}$]-pentadeca-5,7-diene-3-*endo*-10-*endo*-diacetate (**98**) as white prisms: mp 142-143 °C; ^{1}H NMR ($CDCl_3$) δ 0.97 (d, J = 11.0 Hz, H15b); 1.59 (d, J=11.0 Hz, H15a); 2.11 (s, 6H, CH_3); 2.53 (m, H2,H11); 2.55 (m, H1,H12); 2.81 (m, H13,H14); 4.65 (s, H3,H10); 5.41 (m, H5,H8); 5.84 (m, H6,H7); ^{13}C NMR ($CDCl_3$) δ 21.6 (CH_3); 31.9 (C15); 42.6 (C1, C12); 43.0 (C2, C11); 45.8 (C4, C9); 53.4 (C13, C14); 74.8 (C3, C10); 123.3 (C5, C8); 127.0 (C6, C7); 171.3 (C=O); HRMS required for $C_{19}H_{20}O_4$: 312.1361, found 312.1366.

Hydrolysis of the diacetate 98.

To a solution of diacetate **98** (400 mg) in methanol (50 mL) was added a solution of sodium hydroxide (400 mg) in water (3 mL). The reaction was followed by t.l.c. on silica gel using chloroform as the elutant. After 24 h no starting material remained. The solvent was removed under reduced pressure to leave a white solid with identical ^{1}H and ^{13}C NMR spectra to the diol.

Addition reactions to the diol 93.

(i) Maleic anhydride (45mg) was heated under reflux with diol **93** (100 mg) in 10 mL benzene for 4h during which time a white solid precipitated from the reaction mixture. Recrystallization from chloroform/benzene gave 15-oxa-octacyclo-[10,5,2,$1^{5,8}$,$0^{2,6}$,$0^{2,11}$, $0^{4,9}$, $0^{7,11}$,$0^{13,17}$]eicos-18-ene-14,16-dione-3-*endo*-10-*endo*-diol (**99**) as white needles: mp 290-292 °C (dec); IR (KBr) 3590,3000,1890 cm^{-1}; ^{1}H NMR ($CDCl_3$) δ 1.02 (d, J = 10.8 Hz, H20b); 1.56 (d, J = 10.8 Hz, H20a); 2.04 (m, H6,H7); 2.28 (m, H5,H8); 2.49 (m, H4,H9); 2.25 (br s, $W_{h/2}$ = 90 Hz, OH); 3.20 (m H1,H12); 3.99 (s, H3,H10); 4.03 (m, H13,H17); 6.46 (dd, J=3.2, 4.5 Hz, H19,H20); ^{13}C NMR ($CDCl_3$) δ 34.5 (C20); 37.9 (C5,C8); 40.6 (C1,C12); 41.0 (C6,C7); 43.32 (C13,C17); 46.6 (C2,C11); 47.2 (C4,C9); 75.0 (C3,C10); 133.5 (C18,C19); 173.1 (C14,C16); HRMS required for $C_{19}H_{18}O_5$: 326.1151, found: 326.1151. Anal. Calcd for

$C_{19}H_{18}O_5$: C, 69.91; H, 5.56. Found: C, 69.80; H, 5.68.

(ii) Reaction of diol **93** (100 mg) with benzoquinone (50 mg) for 24 h in refluxing benzene gave, on removal of the solvent, octacyclo[10,6,2,$1^{5,8}$,$0^{2,6}$,$0^{4,9}$,$0^{7,11}$,$0^{8,13}$] heneicosa-15,19-diene-14,17-dione-3-*endo*-10-*endo*-diol (**100**) which was recrystallized from petroleum ether/dichloromethane as yellow prisms: mp 235-237 °C; IR (KBr) 3400,3000,1680 cm^{-1}; ^1H NMR ($CDCl_3$) δ 0.97 (d, J = 10.5 Hz, H21b); 1.53 (d, J = 10.6 Hz, H21a); 1.98 (m, H6,H7); 2.23 (m, H5,H8); 2.41 (m, H4,H9); 3.26 (m, H1,H12); 3.91 (m, 4H, H3,H10,H13,H18); 4.29 (br s, $W_{h/2}$=30Hz, OH); 6.37 (dd, J = 3.3, 4.5 Hz, H19,H20); 6.65 (s, H15,H16); ^{13}C NMR ($CDCl_3$) δ 34.3 (C21); 40.4 (C5,C8); 40.9 (C1,C12); 43.5 (C6,C7); 44.7 (C13,C18); 47.4 (C4,C9); 47.6 (C2,C11); 74.9 (C3,C10); 134.3 (C19,C20); 141.8 (C15,C16); 200.4 (C14,C17); HRMS required for $C_{21}H_{20}O_4$: 336.1361, found: 336.1354. Anal. Calcd for $C_{21}H_{20}O_4$: C, 74.97; H, 6.0. Found: C, 74.68; H, 6.40.

(iii) Reaction of diol **93** (100 mg) with dimethyl acetylenedicarboxylate (DMAD) (62 mg) for 7 days in refluxing benzene and removal of the solvent gave dimethyl heptacyclo-[10,2, 2,$1^{5,8}$,$0^{2,6}$,$0^{2,11}$,$0^{4,9}$,$0^{7,11}$]heptadeca-13,15-diene-3-*endo*-10-*endo*-diol-13,14-dicarboxylate (**101**) which was recrystallized as white prisms from petroleum ether/dichloromethane: mp 142-145 °C; IR (KBr) 3350,3000,1730,1700,1640 cm^{-1}; ^1H NMR ($CDCl_3$) δ 1.05 (d, J = 10.8 Hz, H17b); 1.57 (d, J = 10.6 Hz, H17a); 1.98 (m, H6,H7); 2.26 (m, H5,H8); 2.38 (m, H4,H9); 3.80 (s, 6H, CH_3); 3.85 (m, H3,H10); 3.88 (m, H1,H12); 6.57, (m, H15,H16); ^{13}C NMR ($CDCl_3$) δ 33.5 (C21); 41.0 (C5,C8); 41.9 (C6,C7); 44.6 (C1,C12); 45.4 (C4,C9); 52.8 (CH_3); 56.7 (C2,C11); 73.7 (C3,C10); 128.3 (C15,C16); 142.5 (C13,C14); 168.5 (C=O); HRMS required for $C_{21}H_{22}O_6$: 370.1416, found: 370.1419; Anal. Calcd for $C_{21}H_{22}O_6$: C, 67.08; H, 5.91. Found: C, 66.78; H, 5.62.

(iv) Reaction of diol **93** (100 mg) with methyl propiolate (37 mg) in benzene for 9 days gave methyl heptacyclo[10,2,2,$1^{5,8}$,$0^{2,6}$,$0^{2,11}$,$0^{4,9}$,$0^{7,11}$]heptadeca-13,15-diene-3-*endo*-10-*endo*-diol-13-carboxylate (**102**) which was recrystallized from petroleum ether/ dichloromethane as white crystals: mp 161-163 °C; IR (KBr) 3350,3000,1740,1720 cm^{-1}, ^1H NMR ($CDCl_3$) δ 1.05 (d, J = 10.7 Hz, H17b); 1.57 (d, J = 10.7 Hz, H17a); 1.97 (m, H6,H7); 2.28 (m, H5,H8); 2.33 (m, H4,H9); 3.58 (m, H12); 3.60 (d, J = 1.6 Hz, H10); 3.75 (s, 3H, CH_3); 3.89 (m, H1); 3.98 (m, H3); 6.52 (m, H16); 6.59 (m, H16); 7.42 (m, H14); ^{13}C NMR ($CDCl_3$) δ

35.5 (C17); 41.0,41.3 (C5,C8); 41.6,42.0 (C6,C7); 42.7 (C1); 43.7 (C12); 45.2,45.9 (C4,C9); 52.0 (CH_3); 55.7,57.2 (C2,C11); 73.9 (C10); 74.1 (C3); 134.4 (C15), 135.7 (C16); 137.1 (C13); 146.8 (C14); 168.9 (C=O); HRMS required for $C_{19}H_{20}O_4$: 312.1361, found: 312.1366; Anal. Calcd for $C_{19}H_{20}O_4$: C, 73.05; H, 6.46. Found: C, 73.29; H, 6.61.

(v) Reaction with 4-phenyl-1,2,4-triazoline-3,5-dione (PTAD)

To a stirred solution of diol **93** (100 mg) in dichloromethane (10mL), cooled to 0-5 °C in an ice bath, a solution of PTAD (78 mg) in dichloromethane (15 mL) was added dropwise until a faint red colour persisted in the reaction mixture. Removal of the solvent gave a light brown crude product (170 mg) which was adsorbed onto a radial chromatograph plate. Elution with 80% ether/petroleum ether gave 15-phenyl-13,15,17-triazaoctacyclo[10,5,2,$1^{5,8}$,$0^{2,6}$, $0^{2,11}$,$0^{4,9}$,$0^{7,11}$,$0^{13,17}$]eicos-18-ene-14,16-dione-3-*endo*-10-*endo*-diol (**103**) which when recystallised from petroleum ether/dichloromethane gave light brown crystals (125mg): mp 283-285 °C (dec); IR (KBr) 3400,3000,1790,1730,1500 cm^{-1}; ^1H NMR ($CDCl_3$) δ 1.06 (d, J = 10.7 Hz, H20b); 1.63 (d, J = 10.7 Hz, H20a); 2.14 (m, H6,H7); 2.36 (m, H5,H8); 2.56 (m, H4,H9); 4.06 (s, H3,H10); 5.00 (m, 4H, OH,H1,H12); 6.65 (m, H18,H19); 7.43 (m, phenyl); ^{13}C NMR ($CDCl_3$) δ 34.5 (C20); 40.9 (C5,C8); 41.6 (C6,C7); 46.4 (C4,C9); 55.1 (C1,C12,C2, C11); 73.8 (C3,C10); 125.7, 128.2, 129.0, 130.3, 131.4 (C18,C19 and phenyl); 155.6 (C14,C16); HRMS required for $C_{23}H_{21}O_4N_3$: 403.1530, found: 403.1570. Anal. Calcd for $C_{23}H_{21}O_4N_3$: C, 68.46; H, 5.25. Found: C, 68.46; H, 5.25. Further elution with ether gave unreacted diol **93** (25mg).

10-Methylidenehexacyclo[10,2,1,$0^{2,11}$,$0^{4,9}$,$0^{4,14}$,$0^{9,13}$]pentadeca-5,7-diene-3-one (106).

A solution of trimethylsilylmethylmagnesium chloride[183] in THF was prepared by reacting 0.11g (0.45mmol) of magnesium turnings with trimethylsilylmethyl chloride (0.55g, 0.44mmol) in 20 mL dry THF. With ice-cooling a solution of diketone **29** (1.0g, 0.44 mmol) in THF (10 mL) was slowly added and the reaction mixture was heated under reflux for seven hours. The mixture was then cooled in an ice-bath and thionyl chloride (0.53g, 0.45mmol) was added slowly. The mixture was strirred at room temperature overnight then hydrolysed by the careful additon of saturated ammonium chloride solution (20 mL). The layers were separated and the aqueous layer was extracted with ether (2 x 20mL). The

organic layers were combined, dried with magnesium sulphate and the solvent removed to leave 1.05 g of a brown solid residue. The solid material was adsorbed onto a silica gel radial chromatograph plate. Elution with dichloromethane gave hexacyclo[10,2,1,$0^{2,11}$, $0^{4,9}$,$0^{4,14}$,$0^{9,13}$]pentadeca-3,5,7-triene-10-one (**106**) (90mg) which was recrystallized from pentane/dichloromethane as white prisms: m.p. 59-61 °C; IR (KBr) 3010, 1730 cm^{-1}; ^1H NMR ($CDCl_3$) δ 1.51 (d, J = 11.0 Hz, H15b); 1.84 (d, J = 11.0 Hz, H15a); 2.61 (m, H2); 2.74 (m, H1,H12); 3.03 (m, H14); 3.13 (m, H11); 3.23 (m, H13); 4.60 (d, J = 1.3 Hz, C=CH_2, *anti*); 4.86 (s, C=CH_2, *syn*); 5.41 (m, H5,H8); 5.93 (m, H6,H7); ^{13}C NMR ($CDCl_3$) δ 37.3 (C15); 43.1 (C12); 48.0 (C1); 49.6 (C9); 50.1 (C14); 52.0 (C4); 53.8 (C11); 54.7 (C2); 56.9 (C13); 105.1 (C=$\underline{C}H_2$); 120.6 (C8); 123.4 (C6); 123.9 (C5); 124.5 (C7); 151.5 (C10); 215.2 (C3); HRMS required for $C_{16}H_{14}O$: 222.1044, found: 222.1039. Anal. Calcd for $C_{16}H_{14}O$: C, 86.45; H, 6.35. Found: C, 86.84; H, 6.45. Further elution with methanol gave diketone **29** (125mg).

3,10-Dimethylidene hexacyclo[10,2,1,$0^{2,11}$,$0^{4,9}$,$0^{4,14}$,$0^{9,13}$]pentadeca-5,7-diene (107).

To 50 mL of dry dimethyl sulfoxide was added under nitrogen 136 mg (4.54 mmol) of an 80% suspension of NaH in mineral oil. The mixture was stirred at 60 °C for 2h. The resulting solution was cooled to room temperature and 1.62 g (4.54 mmol) of methyltriphenylphosphonium bromide was added. A dark yellow solution formed immediately and the mixture was stirred at room temperature for 2h after which time 1.0 g (4.45 mmol) of the diketone **29** was added. The reaction mixture was stirred and kept for three days in an oil bath at 60 °C. The solution was then cooled and poured into 50 mL of water. The combined DMSO/water layer was extracted with 100, 75 and 50 mL portions of pentane. The extracts were combined, washed with a 1:1 water/DMSO mixture (2 x 50 mL) and with water (2 x 50 mL), dried ($MgSO_4$) and evaporated to yield 510 mg of a white solid. The crude solid was adsorbed onto a column of 30 g of alumina and elution with petroleum ether gave **107** (101 mg, 10.3%) which was recrystallized from ethanol to give waxy white needles, m.p. 85-86 °C; IR (KBr) 3000, 1700, 1100, 980 cm^{-1}; ^1H NMR ($CDCl_3$) δ 1.25 (d, J = 10.7 Hz, H15b); 1.67 (d, J = 10.7 Hz, H15a); 2.50 (m, H1,H12); 2.85 (m, H2,H11); 2.93 (m, H13,H14); 4.46 (d, J = 1.3 Hz, C=CH_2, *syn*); 4.71 (d, J = 1.3 Hz, C=CH_2, *anti*); 5.44 (m, H5,H8); 5.88 (m, H6,H7); ^{13}C NMR ($CDCl_3$) δ 35.0 (C15); 46.7 (C1,C12); 50.4 (C4,C9);

52.9 (C2,C11); 55.8 (C13,C14); 102.6 (C=$\underline{C}H_2$); 123.0 (C6,C7); 125.1 (C5,C8); 155.6 (C3,C10); HRMS - CI required for $C_{17}H_{17}$ (M^++1): 221.1330, found: 221.1327. Further elution with a 3:20 mixture of ether/petroleum ether gave **107** (398 mg, 40.2%). A repeat of this procedure but with two equivalents of base and phosphonium salt on 3.0 g of diketone gave 1.55 g of a crude waxy material. Chromatrography on alumina (60 g) gave, on elution with petroleum ether, 1.2 g (40.7%) of **107** , which was identical in all respects to the material obtained above.

Diels Alder Addition Reactions to the Monomethylidene Diene 106.

(i) A solution of **106** (200 mg) and maleic anhydride (89 mg) in benzene (20 mL) was heated under reflux for 2 days. The solvent was removed under reduced pressure to give 10-methylidene-15-oxaoctacyclo[10,5,2,$1^{5,8}$,$0^{2,6}$, $0^{2,11}$, $0^{4,9}$, $0^{7,11}$, $0^{13,17}$]eicos-18-ene-3,14,16-trione (**109b**) which was recrystallized from ethanol as white needles (230 mg): mp 240-241 °C; IR (KBr) 2970, 1840, 1810, 1720 cm^{-1}; ^1H NMR ($CDCl_3$) δ 1.58 (d, J = 11.3 Hz, H20b); 1.86 (d, J = 11.3 Hz, H20a); 2.34 (m, H7); 2.56 (m, H4); 2.63 (m, H5,H6); 2.71 (m, H8); 3.10 (m, H9); 3.28 (m, H1); 3.41 (m, H12); 3.46 (dd, J = 3.1, 8.9 Hz, H13); 3.85 (dd, J = 3.3, 8.9 Hz, H17); 4.87 (s, C=CH_2, *syn*); 4.94 (s, C=CH_2, *anti*); 6.51 (m, H18,H19); ^{13}C NMR ($CDCl_3$) δ 32.2 (C1); 34.9 (C12); 39.0 (C20); 39.4 (C17); 39.9 (C7); 40.9 (C13); 42.6 (C8); 46.7 (C5); 47.6 (C6); 52.5,53.1 (C11,C2); 54.8 (C4); 55.3 (C9); 105.0 (C=CH_2); 132.9,133.4 (C18, C19); 155.7 (C10); 172.4,172.6 (C14,C16); (C3 was not observed); HRMS required for $C_{20}H_{16}O_4$: 320.1049, found 320.1046. Anal. Calcd for $C_{20}H_{16}O_4$: C, 74.98; H, 5.04. Found: C, 74.94; H, 4.98.

(ii) A solution of **106** (200 mg) and benzoquinone (98 mg) in benzene (20 mL) was heated under reflux for 2 days. Removal of the solvent gave 10-methylideneoctacyclo [10,6,2,$1^{5,8}$,$0^{2,6}$,$0^{2,11}$,$0^{4,9}$,$0^{7,11}$,$0^{13,18}$]heneicosa-15-19-diene-3,14,17-trione (**110b**) which was recrystallized from ethanol as yellow needles (211 mg): mp 313-316 °C (dec.); IR (KBr) 2950, 1680 cm^{-1}; ^1H NMR ($CDCl_3$) δ 1.54 (d, J = 11.0 Hz, H21b); 1.83 (d, J = 11.0 Hz, H21a); 2.29 (m, H6); 2.51 (m, H4); 2.56 (m, H7); 2.61 (m, H8); 2.85 (m, H5); 3.08 (m, H9); 3.35 (m, H13); 3.39 (m, H1); 3.47 (m, H12); 3.69 (m, H18); 4.92 (s, C=CH_2, *syn*); 4.94 (s, C=CH_2, *anti*);

6.41 (m, H19,H20); 6.66 (m, H15,H16); ^{13}C NMR ($CDCl_3$) δ 34.5 (C1); 37.7 (C12); 38.9 (C21); 40.0 (C6); 42.6 (C5); 43.5 (C18); 44.6 (C13); 46.5 (C8); 47.8 (C8); 53.0,53.9 (C11,C2); 55.1 (C4); 55.4 (C9); 104.8 (C=$\underline{C}H_2$); 134.2, 133.7 (C19,C20); 141.2, 142.0 (C15,C16); 155.7 (C22); 198.5, 198.7 (C14,C17); 217.3 (C3); HRMS required for $C_{22}H_{18}O_3$: 330.1256, found: 330.1253. Anal. Calcd for $C_{22}H_{18}O_3$: C, 79.97; H, 5.50. Found: C, 80.27; H, 5.90.

(iii) To an ice-cooled solution of **106** (300 mg) in dichloromethane (15 mL) was slowly added dropwise a solution of 4-phenyl-1,2,4-triazoline-3,5-dione (236 mg) in dichloromethane (15 mL). The solution was stirred at 0-5 °C for 1 hour after which time a faint red colour was persistent and analysis by t.l.c. showed no starting material remained. The solvent was removed at room temperature under reduced pressure to give a solid residue which was adsorbed onto silica gel on a radial chromatograph. Elution with a 1:1 mixture of ether/petroleum ether gave 10-methylidene-15-phenyl-13,15,17-triazaoctacyclo-[10,5,2, $1^{5,8},0^{2,6},0^{2,11},0^{4,9},0^{7,11},0^{3,17}$]eicos-18-ene-3,14,16-trione (**116b**) which was recrystallized from ethanol as colourless prisms (85 mg): mp 243-244 °C; IR (KBr) 3020, 1790, 1720 cm^{-1}; ^1H NMR ($CDCl_3$) δ 1.84 (d, J = 11.2 Hz, H20b); 1.99 (d, J = 11.2 Hz, H20a); 2.57 (m, H4); 2.82 (m, H8); 2.87 (m, H5); 3.11 (m, H9,H7); 3.34 (m, H6); 4.53 (s, C=CH_2, *syn*); 4.85 (s, C=CH_2, *anti*): 5.01 (dd, J = 2.2, 5.0 Hz, H1); 5.10 (dd, J = 2.2, 4.8 Hz, H12); 6.57 (m, H18,H19); 7.37 (m, phenyl); ^{13}C NMR ($CDCl_3$) δ 38.1 (C7); 40.4 (C20); 43.3 (C5); 45.1 (C6); 47.7 (C8); 50.7 (C1); 53.2 (C12); 54.0 (C4); 54.5 (C9); 55.6, 55.8 (C2,C11); 105.7 (C=$\underline{C}H_2$); 118.6,125.5,128.4, 129.1,131.3 (C18, C19 and phenyl); 146.8 (C10); 211.6 (C3); HRMS required for $C_{24}H_{19}N_3O_3$: 397.1426, found: 397.1431; Anal. Calcd for $C_{24}H_{19}N_3O_3$: C, 72.52; H, 4.82, N, 10.55. Found: C, 72.58; H, 4.83; N, 10.72. Further elution with ether gave 10-methylidene-15-phenyl-13,15,17-triazaoctacyclo[10,5,2,$1^{5,8},0^{2,6},0^{2,11},0^{4,9},0^{7,11},0^{3,17}$]eicos-18-ene-3,14, 16-trione (**115b**) which was recrystallized from ethanol as white cubes (210 mg): mp 296-298 °C; IR (KBr) 3000,1760,1720,1640 cm^{-1}; ^1H NMR ($CDCl_3$) δ 1.62, (d, J = 11.2 Hz, H20b); 1.91 (d, J = 11.2Hz, H20a); 2.42 (m, H6); 2.66 (m, H7,H8); 2.73 (m, H4,H5); 3.19 (m,H9); 5.00 (s, C=CH_2, *anti*); 5.13 (dd, J = 2.2, 5.1 Hz, H1); 5.17 (s, C=CH_2, *syn*); 5.23 (dd, J = 2.2, 5.1 Hz, H12); 6.68 (m, H18,H19); 7.39 (m, phenyl); ^{13}C NMR ($CDCl_3$) δ 38.2 (C7); 40.0 (C20); 42.5 (C5); 44.7 (C6); 47.3 (C8); 49.8 (C1); 50.2,51.3 (C2,C11); 52.4 (C12); 54.3 (C4); 105.0 (C=$\underline{C}H_2$);

118.6,125.5,128.1,129.7,129.9,131.4 (C18, C19 and phenyl); 146.7 (C10); 155.6,155.7 (C14,C16); 211.1 (C3); HRMS required for $C_{24}H_{19}N_3O_3$: 397.1426, found: 397.1429; Anal. Calcd for $C_{24}H_{19}N_3O_3$: C, 72.52; H, 4.82; N, 10.55. Found: C, 72.53; H, 4.84; N, 10.60.

(iv) A solution of **106** (200 mg) and dimethyl acetylenedicarboxylate (128 mg) in benzene was heated under reflux for 8 days after which time the solvent was removed under reduced pressure to leave an oily residue which was adsorbed onto silica gel on a radial chromatograph. Elution with a 1:5 mixture of ether/petroleum ether gave dimethyl 10-methylidene-3-oxoheptacyclo[10,2,2,$1^{5,8}$,$0^{2,6}$,$0^{2,11}$,$0^{4,9}$,$0^{7,11}$]heptadeca-13,15-diene-13,14-dicarboxylate (**114b**) which was recrystallized from ethanol as white prisms (98 mg): mp 147-148 °C, IR (KBr) 2860, 1750, 1715, 1640 cm^{-1}; ^1H NMR ($CDCl_3$) δ 1.65 (d, J = 10.9 Hz, H17b); 1.77 (d, J = 10.9 Hz, H17a); 2.42 (m, H4,H6); 2.64 (m, H7,H8); 2.71 (m, H5); 2.99 (m, H9); 3.81 (6H, s, OCH_3); 3.95 (dd, J = 1.9, 3.3 Hz, H1); 4.05 (dd, J = 1.9, 4.0 Hz, H12); 4.58 (s, C=CH_2, *syn*); 4.75 (s, C=CH_2, *anti*); 6.53 (m, H15,H16); ^{13}C NMR ($CDCl_3$) δ 38.6 (C6); 39.2 (C1); 40.2 (C17); 41.8 (C12); 43.2 (C5); 45.3 (C7); 47.7 (C8); 52.4 (OCH_3); 53.2 (C5); 53.8 (C9); 59.1,60.1 (C2,C11); 104.5 (C=$\underline{C}H_2$); 132.7,133.1 (C15,C16); 142.6,143.4 (C13,C14); 149.6 (C10); 166.2,166.5 (C=O); 214.6 (C3); HRMS required for $C_{22}H_{20}O_5$: 364.1311, found 364.1307; Anal. Calcd for $C_{22}H_{20}O_5$: C, 72.50; H, 5.54. Found: C, 72.41; H, 5.42. Further elution with a 2:5 mixture of ether/petroleum ether gave dimethyl 10-methylidene-3-oxoheptacyclo [10,2,2,$1^{5,8}$,$0^{2,6}$,$0^{2,11}$,$0^{4,9}$,$0^{7,11}$]heptadeca-13,15-diene-13-14-dicarboxylate (**113b**) which was recrystallized from ethanol as colourless plates (32 mg): mp 180-182 °C, IR (KBr) 2860, 1740, 1710, 1640 cm^{-1}; ^1H NMR ($CDCl_3$) δ 1.55 (d, J = 11.0Hz, H17b); 1.77 (d, J = 11.0Hz, H17a); 2.19 (m, H6); 2.36 (m, H4); 2.47 (m, H7); 2.55 (m, H5); 2.60 (m, H8); 2.92 (m, H9); 3.67,3.74 (s, 6H, OCH_3); 3.88 (m, H1); 4.08 (m, H12); 4.70 (s, C=CH_2, *syn*); 5.05 (s, C=CH_2, *anti*); 6.62 (m, H15,H16); ^{13}C NMR ($CDCl_3$) δ 38.5 (C6); 39.7 (C1); 40.0 (C17); 42.0 (C12); 42.9 (C5); 45.7 (C7); 47.4 (C8); 52.5 (OCH_3); 52.9 (C4); 54.3 (C9); 59.3,59.7 (C2,C11); 105.9 (C=$\underline{C}H_2$); 134.9,135.0 (C15,C16); 141.9,144.8, (C13,C14); 148.9 (C10); 166.2,166.4 (C=O); (C3 not observed); HRMS required for $C_{22}H_{20}O_5$: 364.1311, found 364.1310; Anal. Calcd for $C_{22}H_{20}O_5$: C, 72.50; H, 5.54. Found: C, 72.51; H, 5.37.

(v) A solution of **106** (200 mg) and methyl propiolate (76 mg) in toluene was heated under reflux for 90 days after which time the solvent was removed under reduced pressure to leave an oily residue which was adsorbed onto silica gel on a radial chromatograph. Elution with a 1:4 mixture of ether/petroleum ether gave two fractions each of which was determined to contain 2 closely related products. Recrystallization of the earlier eluted fraction from ethanol gave the major product from the reaction: methyl 10-methylidene-3-oxoheptacyclo[10,2,2,$1^{5,8}$,$0^{2,6}$,$0^{2,11}$,$0^{4,9}$,$0^{7,11}$]heptadeca-13,15-diene-13-carboxylate (**117**) as colourless prisms: mp 147-148 °C, IR (KBr) 2860, 1750, 1715, 1640 cm^{-1}; ^1H NMR ($CDCl_3$) δ 1.62 (d, J = 11.0 Hz, H17b); 1.83 (d, J = 11.0 Hz, H17a); 2.26 (m, H6); 2.39 (m, H4); 2.53 (m, H7); 2.61 (m, H5); 2.67 (m, H8); 2.96 (m, H9); 3.70 (m, H1); 3.71 (s, 3H, OCH_3); 4.25 (m, H12); 4.65 (s, C=CH_2, *syn*); 4.73 (s, C=CH_2, *anti*); 6.50 (m, H15); 6.68 (m, H16); ^{13}C NMR ($CDCl_3$) δ 38.0 (C6); 38.6 (C1); 39.6 (C12); 40.2 (C17); 43.1 (C5); 45.3 (C7); 47.6 (C8); 51.3 (C5); 51.6 (C9); 52.4 (OCH_3); 53.0,54.4 (C2,C11); 104.5 (C=$\underline{C}H_2$); 133.8,134.5 (C15,C16,C14); 146.3 (C13); 149.6 (C10); 163.1 (C=O); (C3 not observed); HRMS required for $C_{20}H_{18}O_3$: 306.1256, found 306.1237; Anal. Calcd for $C_{20}H_{18}O_3$: C, 78.40; H, 5.90. Found: C, 78.17; H, 6.30. The other products were not obtained pure by recrystallization.

Diels-Alder Additions to the Dimethylidene Diene 107

(i) A solution of 200 mg of **107** and maleic anhydride (89 mg) in 20 mL of benzene was heated under reflux for 3 days. Removal of the solvent under reduced pressure gave a solid residue which was adsorbed onto silica gel on a radial chromatograph. Elution with a 1:10 mixture of ether/petroleum ether gave 3,10-dimethylidene-15-oxaoctacyclo[10,5,2,$1^{5,8}$, $0^{2,6}$,$0^{2,11}$,$0^{4,9}$,$0^{7,11}$,$0^{13,17}$]eicos-18-ene-14,16-dione (**109c**) which was recrystallized from ethanol as white needles (210 mg): mp 253-255 °C; IR (KBr) 3020, 1880, 1790 cm^{-1}; ^1H NMR ($CDCl_3$) δ 1.31 (d, J = 1.0 Hz, H20b); 1.69 (d, J = 11.0 Hz, H20a); 2.35 (m, H6,H7); 2.39 (m, H5,H8); 2.80 (m, H4,H9); 3.32 (m, H1,H12); 3.48 (m, H13,H17); 4.69 (s, C=CH_2, *syn*); 4.79 (s, C=CH_2, *anti*); 6.52 (m, H18,H19); ^{13}C NMR ($CDCl_3$) δ 34.7 (C1,C12); 36.9 (C20); 40.8 (C13,C17); 45.2 (C6,C7); 46.5 (C5,C8); 52.0 (C2,C11); 53.0 (C4,C9); 102.5 (C=$\underline{C}H_2$); 133.5 (C18,C19); 152.3 (C3,C10); 173.0 (C14,C16); HRMS required for $C_{21}H_{18}O_3$: 318.1260, found: 318.1253; Anal. Calcd for $C_{21}H_{18}O_3$: C, 79.21; H, 5.70. Found: C, 79.49; H, 5.50. Further

elution with a 3:20 mixture of ether/petroleum ether gave 3,10-dimethylidene-15-oxaoctacyclo[10,5,2,$1^{5,8}$,$0^{2,6}$,$0^{2,11}$,$0^{4,9}$, $0^{7,11}$,$0^{13,17}$]eicos-18-ene-14,16-dione (**110c**) which was recrystallized from ethanol as colourless prisms (23 mg): mp 285-287 °C; IR (KBr) 3020, 1890, 1790 cm^{-1}; ^1H NMR ($CDCl_3$) δ 1.52 (d, J = 11.0 Hz, H20b); 1.69 (d, J = 11.0 Hz,H20a); 2.50 (m, H5,H8); 2.65 (m, H7,H8); 2.76 (m, H4,H9); 3.33 (m, H1,H12); 3.69 (d, J = 1.6 Hz, H13,H17); 4.42 (s, C=CH_2, *syn*); 4.65 (s, C=CH_2, *anti*); 6.36 (m, H18,H19); ^{13}C NMR ($CDCl_3$) δ 35.4 (C1,C12); 38.5 (C20); 43.0 (C13,C17); 43.3 (C6,C7); 46.6 (C5,C8); 51.9 (C4,C9); 55.0 (C2,C11); 102.7 (C=$\underline{C}H_2$); 131.4 (C18,C19); 152.2 (C3,C10); 172.8 (C14,C16); HRMS required for $C_{21}H_{18}O_3$: 318.1260, found: 318.1262.

(ii) A solution of **107** (200 mg) and benzoquinone (105 mg) in benzene was heated under reflux for 3 days. Removal of the solvent under reduced pressure gave 3,10-dimethylideneoctacyclo[10,6,2,$1^{5,8}$,$0^{2,6}$,$0^{4,9}$,$0^{7,11}$,$0^{13,18}$]heneicosa-15,19-diene,14,17-dione (**111c**) which was recrystallized from ethanol to give yellow prisms (188 mg): mp 256-257 °C; IR (KBr) 2950,1680 cm^{-1}; ^1H NMR ($CDCl_3$) δ 1.27 (d, J = 10.6 Hz, H21b); 1.66 (d, J = 10.6 Hz, H21a); 2.20 (m, H6,H7); 2.37 (m, H5,H8); 2.78 (m,H4,H9); 3.36 (m, H1,H12, H13,H18); 4.78 (s, C=CH_2); 6.42 (m, H19,H20); 6.66 (s, H15,H16); ^{13}C NMR ($CDCl_3$) δ 36.9 (C21); 38.0 (C1,C12); 44.7 (C13,C18); 45.2 (C6,C7); 46.6 (C5,C8); 53.2 (C4,C9); 102.2 (C=$\underline{C}H_2$); 134.1 (C19,C20); 141.8 (C15,C16); 153.2 (C3,C10); 199.4 (C14,C17); HRMS required for $C_{23}H_{20}O_2$: 328.1463, found: 328.1457; Anal. Calcd for $C_{23}H_{20}O_2$: C, 84.11; H, 6.14. Found: C, 84.51; H, 6.19. A solution of **111c** (100 mg) in chloroform (5 mL) was exposed to sunlight for 12 days. Removal of the solvent gave a quantitative yield of 3,16-dimethylidene decacyclo[16,2,1,$0^{2,17}$,$0^{4,15}$,$0^{4,20}$,$0^{5,9}$,$0^{6,13}$,$0^{7,12}$, $0^{10,14}$,$0^{15,19}$]heneicosa-8,11-dione (**112**) which was recrystallized from ethanol as white prisms (85 mg): mp >260 °C (dec); IR (KBr) 2985, 1670 cm^{-1}; ^1H NMR ($CDCl_3$) δ 1.43 (d, J = 10.8 Hz, H21b); 1.78 (d, J = 10.8 Hz, H21a); 2.27 (m, H5,H14); 2.48 (m, H1,H18); 2.73 (m, H9,H10,H19,H20); 2.84 (m, H2,H17); 3.00 (m,H7,H12); 3.48 (m, H6,H13); 4.55 (s, C=CH_2, *syn*); 4.71 (s, C=CH_2, *anti*); ^{13}C NMR ($CDCl_3$) δ 34.5 (C6,C13); 34.8 (C5,C14); 36.8 (C21); 44.3 (C9,C10); 45.2 (C19,C20); 45.5 (C7,C12); 45.9 (C4,C15); 46.3 (C1,C18); 52.8 (C2,C17); 102.0 (C=$\underline{C}H_2$); 153.6 (C3,C16); 211.2 (C8,C11); HRMS required for $C_{23}H_{20}O_2$: 328.1463, found: 328.1458; Anal. Calcd for $C_{23}H_{20}O_2.C_2H_5OH$: C, 80.17; H, 7.00. Found: C, 80.07; H, 6.77.

(iii) To an ice-cooled solution of **107** (400 mg) in dichloromethane (15 mL) was slowly added dropwise a solution of 4-phenyl-1,2,4-triazoline-3,5-dione (315 mg) in dichloromethane (15 mL). The solution was stirred at 0-5 °C for 1 h after which time a faint red color was persistent. The solvent was removed at room temperature under reduced pressure to give a solid residue which was adsorbed onto silica on a radial chromatograph. Elution with a 1:5 mixture of ether/petroleum ether gave 3,10-dimethylidene-15-phenyl-13,15,17-triazaoctacyclo[10,5,2,$1^{5,8}$,$0^{2,6}$,$0^{2,11}$,$0^{4,9}$,$0^{7,11}$,$0^{13,17}$]eicos-18-ene-14,16-dione (**115c**) which was recrystallized from ethanol as colourless needles (585 mg): mp 203-204 °C; IR (KBr) 2990, 1780, 1710 cm^{-1}; ^1H NMR ($CDCl_3$) δ 1.38 (d, J = 10.9 Hz, H20b); 1.76 (d, J = 10.9 Hz, H20a); 2.34 (m, H6,H7); 2.50 (m, H5,H8); 2.91 (m, H4,H9); 4.89 (s, C=CH_2, *syn*); 5.00 (s, C=CH_2, *anti*); 5.11 (m, H1,H12); 6.69 (m, H18,H19); 7.40 (m, 5H, phenyl); ^{13}C NMR ($CDCl_3$) δ 36.9 (C20); 43.4 (C6,C7); 46.2 (C5,C8), 50.5 (C2,C11); 52.6 (C1,C12); 52.9 (C4,C9); 103.7 (C=$\underline{C}H_2$); 125.5 (C18,C19); 128.1,129.0,130.0,132.5 (phenyl); 150.4 (C3,C10); 155.6 (C14,C16); HRMS required for $C_{25}H_{21}O_2N_3$: 395.1634, found: 395.1635; Anal. Calcd for $C_{25}H_{21}O_2N_3$: C, 75.72; H, 5.36; N, 10.63. Found: C, 75.72; H, 5.36; N, 10.63. Further elution with a 3:10 mixture of ether/petroleum ether gave 3,10-dimethylidene-15-phenyl-13,15,17-triazaoctacyclo[10,5,2,$1^{5,8}$,$0^{2,6}$,$0^{2,11}$,$0^{4,9}$,$0^{7,11}$,$0^{13,17}$]eicos-18-ene-14,16-dione (**116c**) which was recrystallized from ethanol to give colourless prisms (23 mg): mp 237-239 °C; IR (KBr) 2980, 1740, 1710 cm^{-1}; ^1H NMR ($CDCl_3$) δ 1.59 (d, J = 10.9 Hz, H20b); 1.83 (d, J = 10.9 Hz, H20a); 2.57 (m, H5,H8); 2.83 (m, H4,H9); 3.02 (m, H6,H7); 3.02 (m, H6,H7); 4.38 (s, C=CH_2, *syn*); 4.73 (s, C=CH_2, *anti*); 5.06 (m, H1,H12); 6.53 (m, H18,H19); 7.47 (m, 5H, phenyl); ^{13}C NMR ($CDCl_3$) δ 38.6 (C20); 43.7 (C6,C7); 46.5 (C5,C8); 52.5 (C1,C12); 53.3 (C4,C9); 53.6 (C2,C11); 103.4 (C=$\underline{C}H_2$); 125.5 (C18,C19); 128.2,128.9,129.0,129.1 (phenyl); 150.7 (C3,C10); 155.6 (C14,C16); HRMS required for $C_{25}H_{21}O_2N_3$: 395.1643, found: 395.1625.

(iv) A solution of **107** (500 mg) and dimethyl acetylenedicarboxylate (325 mg) in toluene (30 mL) was heated under reflux for 14 days. The solvent was removed under reduced pressure and the residue was adsorbed onto silica gel on a radial chromatograph. Elution with a 1:5 mixture of ether/petroleum ether gave 3,10-dimethylidene heptacyclo[10,2,2,$1^{5,8}$,$0^{2,6}$,$0^{2,11}$,$0^{4,9}$,$0^{7,11}$]heptadeca-13,15-diene-13,14-dicarboxylate

(**114c**) which was recrystallized from ethanol as colourless plates (398 mg): mp 154-155 °C; IR (KBr) 2990, 1730, 1715, 1670, 1640; ^{1}H NMR ($CDCl_3$) δ 1.42 (d, J = 10.7 Hz, H17b); 1.69 (d, J = 10.7 Hz, H17a); 2.33 (m, H6,H7); 2.42 (m, H5,H8); 2.70 (m, H4,H9); 3.81 (s, 6H, OCH_3); 4.01 (dd, J = 2.9, 4.2 Hz, H1,H12); 4.44 (s, C=CH_2, *syn*); 4.65 (s, C=CH_2, *anti*); 6.48 (m, H15,H16); ^{13}C NMR ($CDCl_3$) δ 38.5 (C17); 42.1 (C1,C12); 44.1 (C6,C7); 46.7 (C5,C8); 51.8 (C4,C9); 52.3 (OCH_3); 57.8 (C2,C11); 102.2 (C=$\underline{C}H_2$); 132.6 (C15,C16); 143.5 (C13,C14); 153.7 (C3,C10); 166.7 (C=O); HRMS required for $C_{23}H_{22}O_4$: 362.1518, found: 362.1510; Anal. Calcd for $C_{23}H_{22}O_4$: C, 76.21; H, 6.12. Found C, 76.09; H, 6.07. Further elution with a 1:5 mixture of ether/petroleum ether gave a 5:1 mixture of (**114c**) and 3,10-dimethylidene heptacyclo[10,2,2,$1^{5,8}$,$0^{2,6}$,$0^{2,11}$,$0^{4,9}$,$0^{7,11}$]heptadeca-13,15-diene-13,14-dicarboxylate (**113c**) which was not obtained in a pure form. Repeated recrystallization of this mixture from ethanol gave samples enriched in **113c** (2:5 mixture of (**114c**):(**113c**)) which has the following spectral parameters: ^{1}H NMR ($CDCl_3$) δ 1.39 (d, J = 10.8 Hz, H17b); 1.69 (d, J = 10.8 Hz, H17a); 2.19 (m, H6,H7); 2.37 (m, H5,H8); 2.70 (m, H4,H9); 3.76 (s, 6H, OCH_3); 4.22 (m, H1,H12); 4.65 (s, 4H, C=CH_2); 6.48 (m, H15,H16); ^{13}C NMR ($CDCl_3$) δ 38.1 (C17); 42.4 (C1,C12); 44.2 (C6,C7); 46.1 (C5,C8); 52.1 (C4,C9); 52.2 (OCH_3); 57.8 (C2,C11); 102.7 (C=$\underline{C}H_2$); 135.4 (C15,C16); 143.5 (C13,C14); 153.2 (C3,C10); 166.7 (C=O).

Reaction of PBr_3 with the diol 93.

A solution of diol **93** (200 mg, 0.89 mmol) in 10 mL of benzene was cooled in an ice bath with stirring. PBr_3 (200 mg, 0.92 mmol) was added over 2h and the reaction was followed by t.l.c. The reaction mixture was washed with water (2 x 10mL), dried ($MgSO_4$) and the solvent removed to yield 205 mg of a yellow oil. The crude product was adsorbed onto silica gel on a radial chromatograph and elution with a 2:3 mixture of ethyl acetate/petroleum ether gave **124b** (50 mg): ^{1}H NMR ($CDCl_3$) δ 1.06 (d, J = 11.0 Hz, H15b); 1.68 (d, J = 11.0 Hz, H15a); 2.49 (m, H1,H12); 2.81 (m, H2,H12); 2.94 (m, H13,H14); 4.10 (d, J=26 Hz, H3,H10); 5.42 (m, H5,H8); 5.94 (m, H6,H7); 6.95 (d, J=701.1 Hz, PH), ^{13}C NMR ($CDCl_3$) δ 32.9 (C15); 41.3 (C1,C12); 45.9 (C13,C14); 47.0 (C4,C9); 54.2 (C2,C11); 79.7 (C3,C10); 124.3 (C5,C8); 125.6 (C6,C7). Further elution with ethyl acetate gave **124a** (45 mg): ^{1}H NMR ($CDCl_3$) δ 1.11 (d, J = 11.1 Hz, H15b); 1.25 (d, J = 11.1 Hz, H15a); 2.57 (m,

H1,H12); 2.75 (m, H2,H11); 2.84, (m, H13,H14); 4.05 (d, J = 27.4 Hz, H3,H10); 5.43 (m, H5,H8); 5.93 (m, H6,H7); 6.75 (d, J = 879.1 Hz, PH). Further elution with ethyl acetate gave an unidentified unsymmetrical compound (20 mg) and unreacted diol **93** (30 mg).

Attempted displacement of the phosphite ester 124 by bromide ion.

A sample of the 1:1 mixture of phosphites **124a** and **124b** (144 mg) was dissolved in 10 mL DMF. LiBr (130 mg) was added and the mixture was heated under reflux for 8h. The solvent was then removed under high vacuum, and ^{1}H and ^{13}C NMR analysis of the residue revealed only the starting phosphite esters in a 1:1 ratio.

Reaction of diol 93 with sulphuryl chloride.

The diol **93** (500 mg) was dissolved in 30 mL ethyl acetate containing 1.12 g of triethylamine. The solution was cooled in an ice bath and 600 mg of sulfuryl chloride was added slowly. When t.l.c. analysis indicated that all the starting material had been reacted, the mixture was extracted with ethyl acetate, washed with water (4 x 100mL) and dried ($MgSO_4$). Removal of the solvent under reduced pressure gave 556 mg of a yellow oil. ^{1}H NMR analysis of the crude material revealed a complex mixture of products with no olefinic signals corresponding to the diene group.

Reaction of diol 93 with thionyl chloride.

The diol **93** (300 mg) was dissolved in 25 mL CCl_4 and 179 mg of thionyl chloride (freshly distilled from quinoline) was added dropwise with strirring over 10 minutes. The solution was heated under reflux for 30 minutes in order to drive off the HCl formed, then cooled, and extracted with ethyl acetate (50 mL). The organic layer was washed with water (2 x 40 mL), 10% $NaHCO_3$ solution (2 x 40 mL), and again with water (2 x 40 mL). The solvent was removed under reduced pressure to give 240 mg of an orange gum. This residue was adsorbed onto silica gel on a radial chromatograph and elution with a 3:7 mixture of ether/petroleum ether gave **125a**, which was recrystallized from ethanol as colourless prisms: mp 195-199 °C; IR (KBr) 3010, 1610; ^{1}H NMR ($CDCl_3$) δ 1.11 (d, J = 11.0 Hz, H15b); 1.72 (d, J = 11.0Hz, H15a); 2.46 (m, H1,H12); 2.89 (m, H13,H14); 2.96 (m, H2,H11); 4.13 (s,

H3,H10); 5.48 (m, H5,H8); 5.92 (H6,H7), ^{13}C NMR ($CDCl_3$) δ 33.5 (C15); 41.8 (C1,C12); 46.0 (C2,C11); 47.7 (C4,C9); 52.8 (C14,C14); 82.0 (C3,C10); 124.4 (C5,C8); 125.4 (C6,C7). HRMS required for $C_{15}H_{14}O_3S$: 274.0664, found: 274.0644. Anal. Calcd for $C_{15}H_{14}O_3S$: C, 65.68; H, 5.15; S, 11.67. Found: C, 65.69; H, 5.18; S, 11.92. Further elution with ether gave **125b**, which was recrystallized from ethanol as white needles: mp 198-199 °C; IR (KBr) 3010, 1590; ^1H NMR ($CDCl_3$) δ 1.14 (d, J = 11.1 Hz, H15b); 1.73 (d, J = 11.1 Hz, H15a); 2.62 (m, H1,H12); 2.81 (m, H2,H11); 2.86 (m, H13,H14); 4.09 (s, H3,H10); 5.41 (m, H5,H8); 5.90 (m, H6,H7), ^{13}C NMR ($CDCl_3$) δ 33.5 (C15); 44.1 (C1,C12); 45.2 (C2,C11); 47.1 (C4,C9); 52.2 (C13,C14); 78.8 (C3,C10); 124.4 (C5,C8); 125.6 (C6,C7). HRMS required for $C_{15}H_{14}O_3S$: 274.0664, found: 274.0670. Anal. Calcd for $C_{15}H_{14}O_3S$: C, 65.68; H, 5.15; S, 11.67. Found C, 65.65; H, 5.11; S, 11.67.

RuO_4 catalysed oxidation of cyclic sulphites 125a and 125b.

The diol **93** (1.0 g, 4.5 mmol) was dissolved in 25 mL CCl_4 and 595 mg (0.5 mmol) of thionyl chloride was added. The solution was heated under reflux for 30 minutes then cooled in an ice-bath and 20 mL CH_3CN, 0.5 mg $RuCl_3.3H_2O$ and 1.44 g (6.75 mmol) of $NaIO_4$ were added. Finally, 30 mL of water was added and the mixture was stirred vigorously so as to ensure homogeneity of the phases for 12 h. The reaction mixture was then extracted with ether (100 mL) and the ether washed with water (2 x 40 mL), saturated $NaHCO_3$ (2 x 40 mL), dried ($MgSO_4$) and the solvent removed under reduced pressure. A ^1H NMR analysis of the crude product revealed only the formation of the sulphites **125a** and **125b** in a 65:35 ratio with spectroscopic data identical to those obtained for the pure samples. A repeat of the above procedure using diethyl tartrate as the diol gave a single product with the following spectroscopic data consistent with the formation of a cyclic sulphite: ^1H NMR ($CDCl_3$) δ 1.48 (t, J = 11.3 Hz, 6H, CH_3); 4.38 (m, 4H, CH_2); 5.48 (s, 2H); ^{13}C NMR ($CDCl_3$) δ 14.0 (CH_3); 62.7 (CH_2); 79.4 (O-C-CO_2); 171.5 (C=O).

Reaction of cyclic sulphite 125a with PTAD.

The cyclic sulphite **125a** (250 mg, (0.9 mmol)) was dissolved in 10 mL of dichloromethane and cooled in an ice-bath to 0-5 °C. A solution of PTAD (175 mg, 1.0 mmol)

in 10 mL dichloromethane was added dropwise over one hour. The solvent was removed to leave 340 mg of an orange solid which was adsorbed onto silica gel on a radial chromatograph. Elution with a 3:7 mixture of ethyl acetate/petroleum ether gave **129** which was recrystallized from ethyl acetate/petroleum ether as white needles : mp 278-279 °C; ^{1}H NMR ($CDCl_3$) δ 1.44 (d, J = 11.0 Hz, H20b); 1.93 (d, J = 11.0 Hz, H20a); 2.51 (m, H5,H8); 2.84 (m, H4,H9); 3.35 (m, H6,H7); 4.40 (s, H3,H10); 5.00 (m, H1,H12); 6.56 (m, H18,H19); 7.37 (m, 5H, phenyl); ^{13}C NMR ($CDCl_3$) δ 37.3 (C4,C9); 37.4 (C20); 42.1 (C5,C8); 46.4 (C6,C7); 53.4 (C2,C11); 54.6 (C1,C12); 82.3 (C3,C10); 125.5,128.3,128.4,129.2 (Phenyl); 128.8 (C18,C19); 156.2 (C=O). HRMS required for $C_{23}H_{19}N_3O_5S$: 449.1045, found: 449.1044. Anal. Calcd for $C_{23}H_{19}N_3O_5S$: C, 61.46; H, 4.26; N, 8.35. Found: C, 61.47; H, 4.53; N, 8.37. The other isomer was not able to be obtained free of the major product after repeated recrystallization from ethanol and petroleum ether/ethyl acetate mixtures. The following spectroscopic data were extracted from a mixture enriched in **130**: ^{1}H NMR ($CDCl_3$) δ 1.25 (d, J = 11.0Hz, H21b); 1.85 (d, J = 11.0 Hz, H21a); 2.15 (m, H4,H9); 2.92 (m, H5,H8); 3.42 (m, H6,H7); 4.61 (H3,H10); 5.11 (m, H1,H12); 5.70 (m, H18,H19); 7.45 (m, phenyl).

Addition of maleic anhydride to sulphite 125a.

The sulphite **125a** (70 mg) was dissolved in 20 mL benzene and 27.5 mg of maleic anhydride was added. The mixture was heated under reflux for 6 days, then cooled and the solvent removed under reduced pressure to leave a white solid. ^{1}H NMR analysis of the crude material showed the reaction was 90% complete and only one product was detected. This was recrystallized from ethanol to give **131** as colourless prisms: mp 293-294 °C; ^{1}H NMR ($CDCl_3$) δ 1.13 (d, J = 11.0 Hz, H20b); 1.79 (d, J = 11.0 Hz, H20a); 2.05 (m, H4,H9); 2.34 (m, H5,H8); 3.32 (m, H6,H7,H13,H17); 3.62 (m, H3,H10); 4.51 (m, H1,H12); 6.51 (m, H18,H19); ^{13}C NMR ($CDCl_3$) δ 36.2 (C20); 37.1 (C4,C9); 39.6 (C5,C8); 40.8,41.4 (C1,C12,C13,C17); 46.7 (C6,C7); 51.0 (C2,C11); 85.8 (C3,C10); 133.7 (C18,C19); 172.8 (C14,C16). HRMS required for $C_{19}H_{16}O_3S$: 372.0668, found 372.0667.

Preparation of thiocarbonate 133 from diol 93.

The diol **93** (800 mg, 3.5 mmol) was dissolved in 25 mL benzene and 750 mg (4.2 mmol) N,N'-thiocarbonyldiimidazole **132** (TCDI) was added. The mixture was heated at reflux under a nitrogen atmosphere for 6 h, then cooled and the insoluble material filtered off. The reaction mixture was extracted with ether (100 mL) which was then washed with water (2 x 40 mL) and brine (2 x 40 mL), dried ($MgSO_4$) and the solvent removed to yield 856 mg of a yellow residue. The crude material was recrystallized from ethyl acetate to give **133** as white needles: mp 265-267 °C; ^{1}H NMR ($CDCl_3$) δ 1.16 (d, J = 11.2 Hz, H15b); 1.75 (d, J = 11.2 Hz, H15a); 2.56 (m, H1,H12); 2.95 (m, H13,H14); 3.05 (m, H2,H11); 4.23 (m, H3,H10); 5.43 (m, H5,H8); 5.96 (H6,H7), ^{13}C NMR ($CDCl_3$) δ 34.1 (C15); 42.6 (C1,C12); 46.0 (C2,C11); 46.7 (C4,C9); 53.2 (C13,C14); 87.4 (C3,C10); 124.3 (C5,C8); 125.0 (C6,C7). HRMS required for $C_{16}H_{14}O_2S$: 270.0714, found 270.0714. Anal. Calcd for $C_{16}H_{14}O_2S$: C, 71.09; H, 5.22; S, 11.84. Found: C, 70.96; H, 5.34; S, 11.68.

Attempted desulphurization of thiocarbonate 133.

A sample of the thiocarbonate **133** (400 mg, 0.37 mmol) was added to 4 mL of trimethyl phoshite and the mixture was heated to reflux for 3 days under a nitrogen atmosphere. The mixture was then cooled and poured into 50 mL 1M NaOH solution and extracted with dichloromethane (2 x 25 mL). The organic phase was dried ($MgSO_4$), filtered, and the solvent removed under vacuum to give 214 mg of a white solid. This was adsorbed onto silica gel on a radial chromatograph and elution with a 1:5 mixture of ethyl acetate and petroleum ether gave **134** which was recrystallized from ethanol as colourless needles: mp 115-116 °C; ^{1}H NMR ($CDCl_3$) δ 1.05 (d, J = 10.6 Hz, H15b); 1.63 (d, J = 10.6 Hz, H15a); 2.37 (m, H1,H12); 2.65 (m, H2,H11); 2.87 (m, H13,H14); 3.41 (s, 3H, OCH_3); 3.83 (m, H3,H10); 5.45 (s, 1H, $OCHO_2$); 5.49 (m, H5,H8); 5.87 (m, H6,H7). ^{13}C NMR ($CDCl_3$) δ 34.0 (C15); 41.1 (C2,C12); 47.1 (C2,C11); 53.0 (C4,C9); 54.8 (C13,C14); 77.4 (OCH_3); 79.0 (C3,C10); 109.4 (OCO_2); 123.2 (C5,C8); 127.3 (C6,C7). HRMS required for $C_{17}H_{18}O_3$: 270.1256, found 270.1254. Further elution with a 2:3 mixture of ethyl acetate/petroleum ether gave **135**, which was recrystallized from ethanol as colourless needles: mp 138-140 °C; ^{1}H NMR ($CDCl_3$) δ 1.12 (d, J = 11.1 Hz, H15b); 1.70 (d, J = 11.1 Hz, H15a); 2.56 (m,

H1,H12); 2.93 (m, H2, H11,H13,H14); 4.02 (m, H3,H10); 5.41 (m, H5,H8); 5.93 (m, H6,H7). ^{13}C NMR ($CDCl_3$) δ 33.7 (C15); 42.2 (C1,C12); 45.4 (C2,C11); 46.4 (C4,C9); 53.5 (C13,C14); 82.5 (C3,C10); 124.8 (C5,C6,C7,C8); (C3 was not observed). HRMS required for $C_{16}H_{14}O_3$: 254.0943, found: 254.0948.

Methylation of diol 93.

The diol **93** (1.0 g, 4.4 mmol) was added to 50 mL of DMSO containing 490 mg (8.8 mmol) of KOH. The mixture was stirred at room temperature and 1.26 g (1.0 mmol) of dimethyl sulphate was added over three hours. The mixture was heated at 60 °C for 3 h and then quenched by pouring into 800 mL of ice-water. The aqueous mixture was extracted with ethyl acetate (4 x 250 mL), dried ($MgSO_4$) and the solvent removed to give 519 mg of a brown oil which was adsorbed onto silica gel on a radial chromatograph. Elution with a 1:1 mixture of ethyl acetate/petroleum ether gave **136**: mp 80-81 °C; ^1H NMR ($CDCl_3$) δ 0.88 (d, J = 10.9 Hz; H15b); 1.50 (d, J = 10.9 Hz, H15a); 2.35 (m, H1,H12,H2); 2.53 (m, H11); 2.71 (m, H13,H14); 3.20, 3.26 (s, H3,H10); 3.40 (s, 3H, OCH_3); 5.36 (m, H5,H8); 5.55 (d, J = 12.1, OH); 5.80 (m, H6,H7). ^{13}C NMR ($CDCl_3$) δ 32.5 (C15); 42.2,42.4,42.5 (C1,C2,C12); 46.1 (C11); 46.5,47.5 (C4, C9); 53.8,54.1 (C13,C14); 56.0 (OCH_3); 76.1 (C3); 85.0 (C10); 123.3,123.4 (C5,C8); 127.4,128.9 (C6,C7). HRMS required for $C_{16}H_{15}O_2$: 242.1307, found: 242.1310.

Reaction of diketone 29 with *m*-chloroperbenzoic acid.

The diketone **29** (400 mg, 1.8 mmol) was dissolved in 30 mL of dichloromethane and 382 mg (2.2 mmol) of *m*-chloroperbenzoic acid was added. The reaction mixture was stirred at 0 °C for 4h and then allowed to warm to room temperature and the stirring was continued overnight. The reaction mixture was extracted with 100 mL of chloroform, washed with a saturated solution of $NaHCO_3$ (2 x 100mL), water (2 x 100 mL), dried (Na_2SO_4) and the solvent removed to give 485 mg of an orange gum. The crude material was adsorbed onto silica gel on a radial chromatograph and elution with a 3:7 mixture of ethyl acetate/petroleum ether gave **145**: mp 190-192 °C, ^1H NMR ($CDCl_3$) δ 2.12 (m, 2H, H16a,H16b); 3.15 (m, H1,H10); 3.34 (t, J = 2.8 Hz, H11,H15); 3.90 (m, H2,H9); 7.08 (dd, 2H, J = 3.0,5.2, H4,H7); 7.25 (dd, 2H, J = 3.0, 5.1, H5,H6). ^{13}C NMR ($CDCl_3$) δ 41.8 (C2,C9); 48.7

(C1,C10); 49.6 (C1,C15); 49.6 (C2,C9,C16) 126.7,128.2,145.1 (C3-C8). Further elution with a 2:1 mixture of ethyl acetate/petroleum ether gave a mixture of two products with similar spectroscopic characteristics in a 2:1 ratio. The minor product was unstable and could not be purified by recrystallization, but the major **146** was recrystallized from dichloromethane/petroleum ether as colourless plates: mp 265-266 °C (dec); ^{1}H NMR ($CDCl_3$) δ 1.18 (m, 2H,H18a,H18b); 2.52 (m, 1H,H16); 2.88,2.92 (m, H1,H15); 3.14 (m, 1H,H17); 3.40 (m, 2H, H2,H14); 3.53 (m, 2H, H6,H8); 5.96 (d, J = 10.5 Hz, H10); 6.40 (dd, J =3.7, J = 10.5, H9); ^{13}C NMR ($CDCl_3$) δ 37.9,38.7,39.5,40.3,41.0 (C1,C2,C15,C16,C17); 44.2,44.4 (C2, C14); 47.2 (C18) 51.7 (C8); 52.9 (C11); 55.9 (C5); 125.8 (C10); 130.7 (C9); 168.6 (C3,C10). Elution with ethyl acetate gave a mixture of **146** and a compound with the following spectroscopic data consistent with that reported for **142**: ^{1}H NMR ($CDCl_3$) δ 3.49 (m, 1H); 4.92 (m, 1H); 7.18-7.55 (m, 4H). The remaining fractions contained material which was highly insoluble.

Crystallography

Table 27 lists the crystal data and X-ray experimental details for the structure determinations. Intensity data were collected with a Nicolet R3m four-circle diffractometer by using monochromatized Mo Kα radiation. Cell parameters were determined by least squares refinement, the setting angles of at least 20 accurately centred reflections ($2\theta > 17°$) being used. Throughout data collections (ω scans; ±h, +k, +l) the intensities of three standard reflections were monitored at regular intervals and in all cases this indicated no significant crystal decomposition. The intensities were corrected for Lorentz and polarization effects but no corrections for absorption were deemed necessary. The space groups followed from systematic absences.

The structures were solved by conventional direct methods, and refined on |F| by blocked cascade least-squares procedures. In the structure of the epoxide **146** the position of the epoxide oxygen was disordered over two chemically equivalent positions in the ring. All non-hydrogen atoms were refined with anisotropic thermal parameters, except for the lower occupancy disordered epoxide oxygen of **146**. Hydrogen atoms were included in calculated positions with isotropic thermal parameters equal to the isotropic equivalent of their carrier carbon atoms. The functions minimized were $\Sigma w(|F_o| - |F_c|)^2$, with $w = [\sigma^2(F_o) + gF_o^2]^{-1}$. All calculations were performed on a Nova 4X computer using SHELXTL (Version 4.1, 1983).

Final atom coordinates and bonding geometries are listed in Tables 28-33. Perspective views and atom labelling are shown in Figures 66-68.

Table 27. Crystal data and X-ray experimental details.

	117	**125a**	**146**
Formula	$C_{20}H_{18}O_3$	$C_{15}H_{14}O_3S$	$C_{15}H_{12}O_5$
Molecular Weight	306.4	274.3	272.3
Crystal System	monoclinic	monoclinic	monoclinic
Space Group	$P2_1/n$	$P2_1/c$	$P2_1/n$
a (Å)	8.852(4)	6.866(3)	6.625(6)
b (Å)	7.564(4)	12.914(5)	14.197(15)
c (Å)	22.195(7)	13.435(5)	12.235(10)
β(°)	96.92(3)	97.41(3)	90.46(7)
V (Å^3)	1477(1)	1181(1)	1151(2)
Dc (g cm^{-3})	1.38	1.54	1.57
Z	4	4	4
F (000)	648	576	568
μ (cm^{-1})	0.86	2.62	1.10
Diffractometer	Nicolet R3m	Nicolet R3m	Nicolet R3m
Radiation	Mo Kα	Mo Kα	Mo Kα
Wavelength (Å)	0.71069	0.71069	0.71069
Temperature (°C)	-120	-120	-120
Crystal dimensions (mm)	0.38 x 0.22 x 0.05	0.35 x 0.21 x 0.12	0.55 x 0.30 x 0.03
Scan mode	ω	ω	ω
2θ range (°)	3-50	3-56	3-50
Solution method	Direct methods	Direct methods	Direct methods
Unique data	2588	2843	2025
Observed data (I > 3σ(I))	1461	2043	562
Observed criterion	I > 3σ(I)	I > 3σ(I)	I > 2.5σ(I)
Number of parameters	208	172	185
Function refined	$\Sigma w(\|F_o\| - \|F_c\|)^2$	$\Sigma w(\|F_o\| - \|F_c\|)^2$	$\Sigma w(\|F_o\| - \|F_c\|)^2$
Weighting	$[\sigma^2(F_o)+gF_o^2]^{-1}$	$[\sigma^2(F_o)+gF_o^2]^{-1}$	$[\sigma^2(F_o)]^{-1}$
g	0.00147	0.00063	0
Residual features (e.Å^{-3})	< 0.23	< 0.37	< 0.36
R	0.042	0.038	0.068
wR	0.053	0.050	0.035

Table 28. Atomic coordinates (x 10^4) and equivalent isotropic displacement coefficients ($Å^2$ x 10^3) for **117** with e.s.d.'s in parentheses.

atom	x	y	z	U_{eq}[a]
C(1)	7728(3)	-684(4)	9464(1)	22(1)
C(2)	6257(3)	-60(4)	9084(1)	19(1)
C(3)	5251(3)	1249(4)	9359(1)	21(1)
O(3)	5532(2)	2101(3)	9825(1)	26(1)
C(4)	3814(3)	1282(4)	8920(1)	22(1)
C(5)	3496(3)	-691(4)	8785(1)	27(1)
C(6)	5130(3)	-1402(4)	8747(1)	23(1)
C(7)	5516(3)	-694(4)	8122(1)	24(1)
C(8)	4057(3)	336(4)	7883(1)	25(1)
C(9)	4216(3)	2022(4)	8283(1)	24(1)
C(10)	5888(3)	2454(4)	8307(1)	20(1)
C(10a)	6491(4)	3992(4)	8177(1)	27(1)
C(11)	6654(3)	697(4)	8449(1)	19(1)
C(12)	8406(3)	529(4)	8436(1)	23(1)
C(13)	9119(3)	1549(4)	8987(1)	22(1)
C(13a)	10134(3)	3070(4)	8925(1)	24(1)
O(13a)	10458(2)	3651(3)	8444(1)	36(1)
O(13b)	10726(2)	3737(3)	9465(1)	28(1)
C(13b)	11803(4)	5184(4)	9446(2)	36(1)
C(14)	8752(3)	925(4)	9517(1)	22(1)
C(15)	8430(3)	-2044(4)	9072(1)	26(1)
C(16)	8779(3)	-1423(4)	8543(1)	25(1)
C(17)	2782(3)	-729(5)	8125(1)	31(1)

[a] Equivalent isotropic U defined as one third of the trace of the orthogonalized U_{ij} tensor.

Table 29. Bond lengths (Å) and angles (°) for **117** with e.s.d.'s in parentheses.

C(1)-C(2)	1.545(4)	C(1)-C(14)	1.515(4)	C(1)-C(15)	1.524(4)
C(2)-C(3)	1.504(4)	C(2)-C(6)	1.556(4)	C(2)-C(11)	1.596(4)
C(3)-O(3)	1.221(3)	C(3)-C(4)	1.516(4)	C(4)-C(5)	1.542(4)
C(4)-C(9)	1.596(4)	C(5)-C(6)	1.554(4)	C(5)-C(17)	1.530(4)
C(6)-C(7)	1.559(4)	C(7)-C(8)	1.551(4)	C(7)-C(11)	1.579(4)
C(8)-C(9)	1.552(4)	C(8)-C(17)	1.531(4)	C(9)-C(10)	1.511(4)
C(10)-C(10a)	1.325(4)	C(10)-C(11)	1.510(4)	C(11)-C(12)	1.559(4)
C(12)-C(13)	1.523(4)	C(12)-C(16)	1.526(4)	C(13)-C(13a)	1.476(4)
C(13)-C(14)	1.340(4)	C(13a)-O(13a)	1.218(4)	C(13a)-O(13b)	1.353(3)
O(13b)-C(13b)	1.455(4)	C(15)-C(16)	1.331(4)		

C(2)-C(1)-C(14)	105.0(2)	C(2)-C(1)-C(15)	105.5(2)
C(14)-C(1)-C(15)	108.0(2)	C(1)-C(2)-C(3)	118.7(2)
C(1)-C(2)-C(6)	121.4(2)	C(3)-C(2)-C(6)	104.3(2)
C(1)-C(2)-C(11)	109.7(2)	C(3)-C(2)-C(11)	108.6(2)
C(6)-C(2)-C(11)	90.0(2)	C(2)-C(3)-O(3)	128.0(2)
C(2)-C(3)-C(4)	104.1(2)	O(3)-C(3)-C(4)	127.9(3)
C(3)-C(4)-C(5)	103.4(2)	C(3)-C(4)-C(9)	108.8(2)
C(5)-C(4)-C(9)	102.8(2)	C(4)-C(5)-C(6)	101.2(2)
C(4)-C(5)-C(17)	104.6(2)	C(6)-C(5)-C(17)	103.4(2)
C(2)-C(6)-C(5)	107.4(2)	C(2)-C(6)-C(7)	90.8(2)
C(5)-C(6)-C(7)	103.0(2)	C(6)-C(7)-C(8)	102.8(2)
C(6)-C(7)-C(11)	90.6(2)	C(8)-C(7)-C(11)	106.7(2)
C(7)-C(8)-C(9)	101.4(2)	C(7)-C(8)-C(17)	103.5(2)
C(9)-C(8)-C(17)	104.8(2)	C(4)-C(9)-C(8)	101.8(2)
C(4)-C(9)-C(10)	111.0(2)	C(8)-C(9)-C(10)	103.0(2)
C(9)-C(10)-C(10a)	126.8(3)	C(9)-C(10)-C(11)	103.5(2)
C(10a)-C(10)-C(11)	129.5(3)	C(2)-C(11)-C(7)	88.6(2)
C(2)-C(11)-C(10)	111.3(2)	C(7)-C(11)-C(10)	103.9(2)
C(2)-C(11)-C(12)	107.6(2)	C(7)-C(11)-C(12)	121.5(2)
C(10)-C(11)-C(12)	119.5(2)	C(11)-C(12)-C(13)	105.6(2)
C(11)-C(12)-C(16)	105.9(2)	C(13)-C(12)-C(16)	107.5(2)
C(12)-C(13)-C(13a)	121.5(3)	C(12)-C(13)-C(14)	114.1(3)
C(13a)-C(13)-C(14)	124.4(3)	C(13)-C(13a)-O(13a)	124.6(3)
C(13)-C(13a)-O(13b)	112.9(2)	O(13a)-C(13a)-O(13b)	122.5(3)
C(13a)-O(13b)-C(13b)	116.5(2)	C(1)-C(14)-C(13)	114.5(2)
C(1)-C(15)-C(16)	114.4(3)	C(12)-C(16)-C(15)	114.3(3)
C(5)-C(17)-C(8)	94.7(2)		

Table 30. Atomic coordinates (x 10^4) and equivalent isotropic displacement coefficients (Å^2 x 10^3) for **125a** with e.s.d.'s in parentheses.

atom	x	y	z	U_{eq}[a]
C(1)	2725(3)	3941(2)	-2464(2)	19(1)
C(2)	2087(3)	2807(2)	-2279(2)	16(1)
C(3)	3592(3)	2337(2)	-1419(1)	13(1)
C(4)	4308(3)	1257(2)	-1541(2)	17(1)
C(5)	3629(3)	453(2)	-1057(2)	20(1)
C(6)	2197(3)	584(2)	-348(2)	19(1)
C(7)	1461(3)	1512(2)	-154(2)	16(1)
C(8)	2025(3)	2478(2)	-660(1)	14(1)
C(9)	546(3)	2944(2)	-1531(2)	16(1)
C(10)	478(3)	4140(2)	-1388(2)	19(1)
C(11)	2452(3)	4318(2)	-706(2)	17(1)
C(12)	2430(3)	3424(2)	35(2)	16(1)
O(13)	4164(2)	3369(1)	789(1)	19(1)
S(14)	5872(1)	2562(1)	572(1)	19(1)
O(14)	7445(2)	2770(1)	1375(1)	30(1)
O(15)	6600(2)	3139(1)	-386(1)	19(1)
C(16)	5197(3)	3177(2)	-1304(2)	16(1)
C(17)	4017(3)	4177(2)	-1461(2)	17(1)
C(18)	841(3)	4564(2)	-2412(2)	23(1)

[a] Equivalent isotropic U defined as one third of the trace of the orthogonalized U_{ij} tensor.

Table 31. Bond lengths (Å) and angles (°) for **125a** with e.s.d.'s in parentheses.

C(1)-C(2)	1.558(3)	C(1)-C(17)	1.545(3)	C(1)-C(18)	1.533(3)
C(2)-C(3)	1.570(3)	C(2)-C(9)	1.559(3)	C(3)-C(4)	1.494(3)
C(3)-C(8)	1.585(3)	C(3)-C(16)	1.540(3)	C(4)-C(5)	1.340(3)
C(5)-C(6)	1.465(3)	C(6)-C(7)	1.339(3)	C(7)-C(8)	1.495(3)
C(8)-C(9)	1.567(3)	C(8)-C(12)	1.540(3)	C(9)-C(10)	1.558(3)
C(10)-C(11)	1.552(3)	C(10)-C(18)	1.532(3)	C(11)-C(12)	1.527(3)
C(11)-C(17)	1.580(3)	C(12)-O(13)	1.462(2)	O(13)-S(14)	1.624(2)
S(14)-O(14)	1.450(2)	S(14)-O(15)	1.622(2)	O(15)-C(16)	1.464(2)
C(16)-C(17)	1.526(3)				

C(2)-C(1)-C(17)	100.8(2)	C(2)-C(1)-C(18)	103.3(2)
C(17)-C(1)-C(18)	104.5(2)	C(1)-C(2)-C(3)	108.0(2)
C(1)-C(2)-C(9)	103.0(2)	C(3)-C(2)-C(9)	90.4(1)
C(2)-C(3)-C(4)	118.3(2)	C(2)-C(3)-C(8)	89.5(1)
C(4)-C(3)-C(8)	116.0(2)	C(2)-C(3)-C(16)	101.3(2)
C(4)-C(3)-C(16)	115.3(2)	C(8)-C(3)-C(16)	113.0(2)
C(3)-C(4)-C(5)	122.0(2)	C(4)-C(5)-C(6)	122.0(2)
C(5)-C(6)-C(7)	122.1(2)	C(6)-C(7)-C(8)	122.1(2)
C(3)-C(8)-C(7)	115.7(2)	C(3)-C(8)-C(9)	89.5(1)
C(7)-C(8)-C(9)	118.6(2)	C(3)-C(8)-C(12)	113.3(2)
C(7)-C(8)-C(12)	115.0(2)	C(9)-C(8)-C(12)	101.4(2)
C(2)-C(9)-C(8)	90.6(1)	C(2)-C(9)-C(10)	103.0(2)
C(8)-C(9)-C(10)	108.3(2)	C(9)-C(10)-C(11)	100.5(2)
C(9)-C(10)-C(18)	103.4(2)	C(11)-C(10)-C(18)	104.2(2)
C(10)-C(11)-C(12)	101.0(2)	C(10)-C(11)-C(17)	102.6(2)
C(12)-C(11)-C(17)	113.3(2)	C(8)-C(12)-C(11)	102.8(2)
C(8)-C(12)-O(13)	116.7(2)	C(11)-C(12)-O(13)	114.4(2)
C(12)-O(13)-S(14)	116.6(1)	O(13)-S(14)-O(14)	103.5(1)
O(13)-S(14)-O(15)	98.7(1)	O(14)-S(14)-O(15)	103.3(1)
S(14)-O(15)-C(16)	116.6(1)	C(3)-C(16)-O(15)	116.5(2)
C(3)-C(16)-C(17)	102.8(2)	O(15)-C(16)-C(17)	115.1(2)
C(1)-C(17)-C(11)	102.8(2)	C(1)-C(17)-C(16)	100.9(2)
C(11)-C(17)-C(16)	113.7(2)	C(1)-C(18)-C(10)	95.1(2)

Table 32. Atomic coordinates (x 10^4) and equivalent isotropic displacement coefficients ($Å^2$ x 10^3) for **146** with e.s.d.'s in parentheses.

atom	x	y	z	U_{eq}[a]
C(1)	6547(11)	4232(6)	7669(6)	43(4)
C(2)	6047(13)	4776(7)	6630(7)	41(4)
C(3)	4838(15)	5637(8)	6823(7)	47(5)
O(3)	3420(9)	5922(5)	6242(4)	54(3)
O(4)	5157(8)	6193(5)	7721(4)	41(3)
C(5)	6796(12)	5961(7)	8449(6)	38(4)
C(6)	6238(12)	6438(6)	9524(6)	39(4)
O(7)[b]	7219(11)	6088(7)	10472(6)	55(4)
O(7')[c]	11019(33)	6515(18)	9630(18)	68(9)
C(8)	7575(14)	7003(7)	10084(7)	49(4)
C(9)	9632(14)	7207(7)	9648(7)	39(4)
C(10)	10240(13)	6843(7)	8685(7)	45(4)
C(11)	8969(11)	6163(8)	8015(6)	35(4)
O(12)	8943(8)	6624(4)	6908(4)	51(3)
C(13)	8566(13)	6049(7)	6036(7)	33(4)
O(13)	8587(9)	6476(5)	5177(5)	66(3)
C(14)	8266(12)	5033(7)	6193(7)	36(4)
C(15)	9661(13)	4584(7)	7029(7)	43(4)
C(16)	9563(12)	5141(6)	8076(7)	31(4)
C(17)	7425(12)	4899(7)	8531(7)	36(4)
C(18)	8453(13)	3727(7)	7323(7)	48(4)

[a] Equivalent isotropic U defined as one third of the trace of the orthogonalized U_{ij} tensor.
[b] Disordered; occupancy 75%. [c] Disordered; occupancy 25%.

Table 33. Bond lengths (Å) and angles (°) for **146** with e.s.d.'s in parentheses.

C(1)-C(2)	1.522(12)	C(1)-C(17)	1.529(12)	C(1)-C(18)	1.515(12)
C(2)-C(3)	1.482(15)	C(2)-C(14)	1.611(12)	C(3)-O(3)	1.241(11)
C(3)-O(4)	1.367(11)	O(4)-C(5)	1.437(9)	C(5)-C(6)	1.528(11)
C(5)-C(11)	1.565(11)	C(5)-C(17)	1.567(14)	C(6)-O(7)	1.415(11)
C(6)-C(8)	1.374(12)	O(7)-C(8)	1.404(14)	O(7')-C(9)	1.346(26)
O(7')-C(10)	1.345(24)	C(8)-C(9)	1.496(13)	C(9)-C(10)	1.351(13)
C(10)-C(11)	1.517(13)	C(11)-O(12)	1.505(10)	C(11)-C(16)	1.505(14)
O(12)-C(13)	1.365(11)	C(13)-O(13)	1.214(11)	C(13)-C(14)	1.469(15)
C(14)-C(15)	1.514(12)	C(15)-C(16)	1.507(12)	C(15)-C(18)	1.501(13)
C(16)-C(17)	1.564(12)				

C(2)-C(1)-C(17)	109.9(8)	C(2)-C(1)-C(18)	100.5(6)
C(17)-C(1)-C(18)	99.9(6)	C(1)-C(2)-C(3)	113.6(7)
C(1)-C(2)-C(14)	101.5(7)	C(3)-C(2)-C(14)	111.2(8)
C(2)-C(3)-O(3)	125.8(9)	C(2)-C(3)-O(4)	121.6(8)
O(3)-C(3)-O(4)	112.6(9)	C(3)-O(4)-C(5)	118.5(7)
O(4)-C(5)-C(6)	104.2(7)	O(4)-C(5)-C(11)	116.1(6)
C(6)-C(5)-C(11)	116.1(7)	O(4)-C(5)-C(17)	117.3(7)
C(6)-C(5)-C(17)	116.0(7)	C(11)-C(5)-C(17)	87.3(7)
C(5)-C(6)-O(7)	115.9(7)	C(5)-C(6)-C(8)	121.9(7)
O(7)-C(6)-C(8)	60.4(6)	C(6)-O(7)-C(8)	58.3(6)
C(9)-O(7')-C(10)	60.3(11)	C(6)-C(8)-O(7)	61.2(6)
C(6)-C(8)-C(9)	121.4(8)	O(7)-C(8)-C(9)	117.1(8)
O(7')-C(9)-C(8)	119.3(13)	O(7')-C(9)-C(10)	59.8(11)
C(8)-C(9)-C(10)	121.1(8)	O(7')-C(10)-C(9)	59.9(11)
O(7')-C(10)-C(11)	116.8(13)	C(9)-C(10)-C(11)	123.1(8)
C(5)-C(11)-C(10)	116.2(7)	C(5)-C(11)-O(12)	112.4(6)
C(10)-C(11)-O(12)	102.2(7)	C(5)-C(11)-C(16)	92.7(7)
C(10)-C(11)-C(16)	116.3(7)	O(12)-C(11)-C(16)	117.7(7)
C(11)-O(12)-C(13)	116.4(7)	O(12)-C(13)-O(13)	112.0(9)
O(12)-C(13)-C(14)	120.7(7)	O(13)-C(13)-C(14)	127.3(8)
C(2)-C(14)-C(13)	113.0(8)	C(2)-C(14)-C(15)	103.5(7)
C(13)-C(14)-C(15)	114.8(7)	C(14)-C(15)-C(16)	108.8(7)
C(14)-C(15)-C(18)	100.4(7)	C(16)-C(15)-C(18)	101.2(7)
C(11)-C(16)-C(15)	118.5(7)	C(11)-C(16)-C(17)	89.5(7)
C(15)-C(16)-C(17)	103.5(7)	C(1)-C(17)-C(5)	116.9(7)
C(1)-C(17)-C(16)	103.4(6)	C(5)-C(17)-C(16)	90.4(7)
C(1)-C(18)-C(15)	97.5(7)		

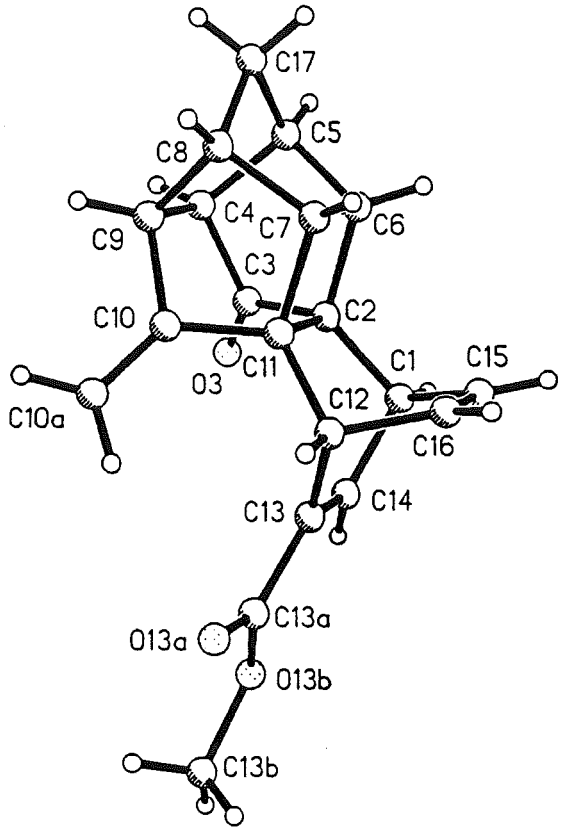

Figure 66. Perspective view and atom labelling of **117**.

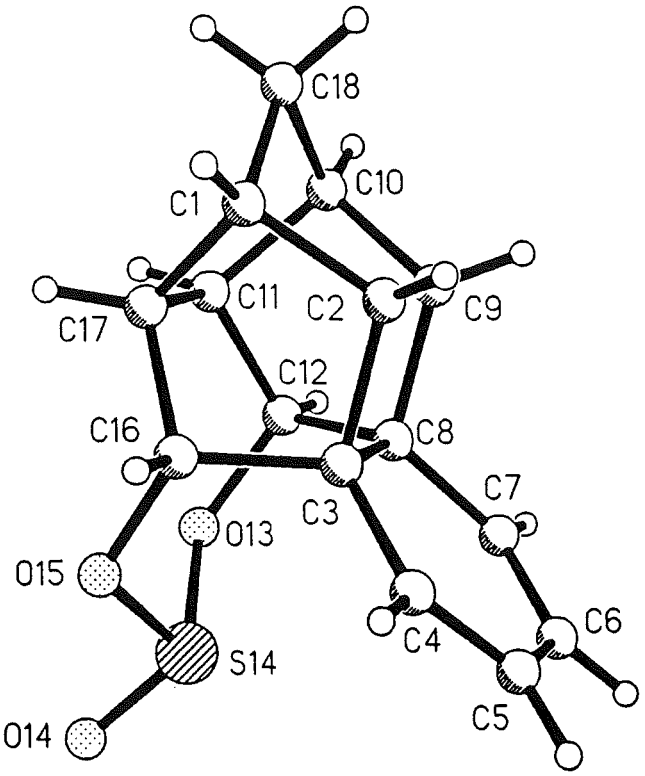

Figure 67. Perspective view and atom labelling of cyclic sulphite **125a**.

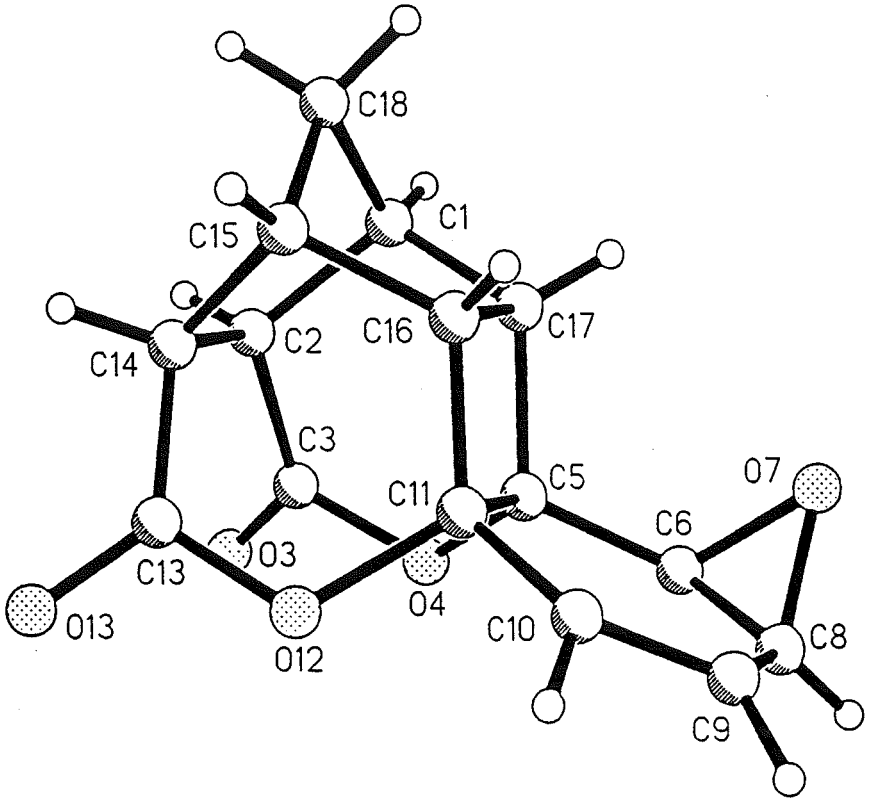

Figure 68. Perspective view and atom labelling of epoxide **146**.

Computer Software Tools.

Macintosh programs: ModelView and Molvib.

During the course of this work two Macintosh programs were developed to assist in the graphical analysis of computational results and these will be described in this section. All the "ball and stick" structures shown in this thesis were produced using Molvib or ModelView. As far as possible these programs have been designed to conform to the Macintosh human interface guidelines and thus be as easy to use as possible and allow for transfer of data with other Macintosh programs such as Word or Chemdraw. ModelView and Molvib have many similar features particularly in the basic manipulations of structures etc. and so much of the following discussion applies to both programs. The features which are specific to each are clearly indicated.

Program description and overview.

ModelView is a Macintosh program for the viewing of files produced by the molecular mechanics programs MODEL and BAKMDL. In particular the program allows for easy viewing of multiple structures such as may be generated from a conformational search in BAKMDL. The Boltzmann distribution and average Boltzmann energy can be calculated. Distances, angles and dihedral angles can be queried for any individual structures as well as for all the structure in a file. So for example it is possible to determine the Boltzmann average distance between any two atoms in a structure based on the Boltzmann distribution of the energies of the structures in the file. Polar maps can be generated in order to provide a "fingerprint" for the conformation and allow ready identification of cyclic structures and in a similar way a linear graph" may be generated for a chain conformation. Conversion of all the structures in a Model file to separate Chem3D™ files is possible and the display and manipulation of Chem3D™ files is also supported. ModelView can also be used to view files created by the Macromodel program and the MOPAC/AMPAC programs.

Molvib is a Macintosh program for the graphical analysis of the normal vectors of vibration as calculated by the MOPAC program. It reads the the MOPAC output from a

calculation with the FORCE keyword and displays the normal vectors for any of the 3N frequencies as arrows in a Ball and Stick or wireframe representation of the structure. The movement of the atoms in any frequency can be viewed in an animated display. This is useful as an aid for solving the "multiple minima" problem in reaction studies and for confirming the vectors of an "imaginary" frequency (for a transition state) correspond to movement along the reaction co-ordinate. Measurements of calculated distances, angles and dihedral angles can be made for any atoms in the structure. Multiple windows are possible so that several structures can be viewed at once. Molvib can create files which have all the frequency information in them. These files are considerably smaller than the original text output and so are convenient for the archiving of the the results of a MOPAC FORCE calculation. The essential text output can be re-constructed and a Chem-3D file of the structure can be generated.

System Requirements.

Molvib and ModelView only work on a Macintosh with a floating-point accelerator and have been tested on an SE/30 and a MacIIci. It is recommended that System 6.0 or a more recent system is used. Output has been tested on Apple LaserWriter and Hewlett Packard DeskWriter printers. No conflicts with INIT's or other system configurations have yet been identified.

The File Menu.

The standard Macintosh functions are found in the File menu:

• **New** has no function in Molvib or Modelview.

• **Open...** allows the opening of files which have been saved from Molvib or text files for ModelView. To open MOPAC output files see "View the Structures" below.

• **Close** This command will first prompt the user to save any changes to the file and will then close the currently active window.

• **Save and Save As...** These commands function only in Molvib and will save the current structure in the Molvib file format. These files are 1/4 to 1/2 the size of the original MOPAC output and are suitable for archiving the results of a MOPAC Force calculation.

Files in the Molvib format are much quicker to open than converting from the MOPAC output file every time you wish to view a structure. If you save a file the view orientation, view mode, vector displayed etc will be saved.

• **Revert to saved...** has no function in Molvib or ModelView.

• **Page Setup...** presents the standard Macintosh page-setup box for the printer driver which is current - i.e that set through the chooser.

• **Print...** presents the standard print dialog box for the standard printer. Wireframe graphics are converted to "black on white" before being printed.

• **Preferences** allows several user adjustable options to be set. These are as follows:

Font: The font used in the measurements window can be set by the use of this pop-up menu.

Size: The size of the font used in the measurements window can be set from this pop-up menu. Note that only "real" font sizes (i.e non-scaled) are a available for any given font.

Default File Type: (ModelView only) If you are constantly opening one type of input file then it will be convenient to set the default file type to that file type.

Boltzmann Measurements Enabled at Startup: (ModelView only) The normal situation will be that Boltzmann measurements will be enabled at startup and so all queries on any structure in the file will produce a Boltzmann distribution for that parameter. If you don't wish this to be the case then switch this option off and the Boltzmann measurements option will have to be explicitly turned on (from the Info menu) when you wish to make Boltzmann measurements.

Polar maps and Chain Graphs: (Model View Only).

Include Scale: This option when switched on will include the dihedral scale on all subsequently generated polar maps and chain graphs.

Report data to Measurements: If you wish to have a record of the numerical values used to produce a polar map or chain graph then this option should be switched on. The data will then be echoed to the measurements window

and can be printed or saved from there. Note that if the measurements window is not visible then this option will not show the window in the same way that queries do.

Like the view options described below the preferences can be made **Permanent, Temporary** (i.e for this session only) or **Cancelled** depending on which button is used to dismiss the preferences dialog box.

• **Quit** is used to leave the Molvib or ModelView programs and return to the finder.

The Edit Menu.

In the Edit menu only the Copy and Show Clipboard are ever active. The others are simply for the use of the desk accessories under the Apple menu - in particular Paste has no function in Molvib or Modelview.

• **Copy** takes a copy of the current image in the active window and places it in the clipboard. This can then be pasted into an application such as ChemDraw™ for further labelling or a document in a word processing program such as Word.

• **Show Clipboard** displays the current contents of the clipboard.

Opening files.

a) Molvib.

The files to be read by Molvib must be in a text file format and present on the Macintosh. We have found the Kermit file transfer system convenient to transfer text files from a VAX to our Macintoshes, but any method of transferring text files is suitable.

In order to view the results of a FORCE calculation from MOPAC the following procedure should be followed:

• Transfer the *.out output file from MOPAC to the Macintosh where the Molvib program is to be run. If desired the file can be edited to contain only the sections "Orientation of Molecule in Force Calculation" and "Mass -Weighted Co-ordinate analysis" and several lines on either side of each section.

• Start up Molvib by double clicking on the program icon

• Choose **From Mopac *.out** from the **Convert** menu. Choose the file you wish to view, click **OK** and the program will begin reading the structure in the file. For a large number of vectors this may take some time. If the input file does not match the file format required file format then the read will be aborted. If you wish to cancel the read then Press ⌘-'.'.

• Once the read is completed then the structure will be visible in it's own window.

b) ModelView.

The files to be read by Model View must be in a text file format and present on the Macintosh. In order to view the results of a conformational search in BAKMDL the following procedure should be used:

• Transfer the *.dat output file from BAKMDL to the Macintosh where the Model View program is to be run.

• The format of these files must not be changed from that produced by BAKMDL.

• Start up ModelView by double clicking on the program icon

• Choose **Open** from the **File** menu. Ensure that the appropriate file type (BAKMDL in this case) is visible in the pop-up menu at the bottom of the dialog box. Choose the file you wish to view, click **OK** and the program will begin reading the structures in the file. For a large number of structures this may take some time. If the input file does not match the file format in the pop-up menu then the program will almost certainly crash. In order to cancel the file read it is possible to press ⌘-'.' on the keyboard. This will interrupt the file read at the current structure.

Note for reading Chem3D™ files. Chem3D files should be saved as Cartesian files with bonding referenced by position. Chem3D parameters and not MM2 parameters should be in place when preparing files for transfer to Model View.

• When all the structures have been read the **Structures** menu will become enabled and this will contain a list of the structures in the file. Choosing any of

these items will bring up a window containing a graphic representation of that structure. As many windows can be open at once as memory will allow - about 16 on a 1mB machine. If the window is already open for a structure the name in the structures menu will be marked with a tick mark. If you choose an item from the structures menu which already has a tick mark then the window containing that structure will be brought to the front.

The Tools Window.

The tools window will open with the first structure window that is opened and will be closed with the last structure window closed. It can also be made visible or hidden at any time by choosing the **Show Tools** item from the **View** menu (or by hitting ⌘-T). The tools window is a so-called floating window and as such will always cover the structure windows. The tools window allows the structure(s) visible on the screen to be rotated in real time to any orientation.

The major part of the tools window is the rotate box. When the mouse is clicked in this box and the mouse button is held down, the cursor disappears and cross-hairs appear. As long as the mouse is held down the position of the mouse will be tracked and some action will be taken. The values of the current mouse position are shown in the X,Y and Z boxes under the rotate box. The maximum dimension of the rotate box can be changed by holding down the shift or option keys before and while tracking in the rotate box. If no keys are down then the default values for the axes are ± 30°, if the option key is down it is ± 45°, if the shift key is down the maximum values are ± 60°. What action the rotate box performs is determined by the settings which have been chosen. These are determined by the buttons above and below the rotate box:

• **Rot. or Trans.** If the Rot. radio button is active then the rotate box will rotate the structure(s). This is the default and the most common use for the tools window. The amount and orientation of the rotation is determined by the position of the mouse in the rotate box. It may take some practice before the user become familiar with rotate box, there is a tendency to "over-shoot" for small structures in the wireframe representation because the rotation ability is quite fast. Rotation is initially about the X and Y axes but the Y- axis can

be changed for the Z - axis by clicking on the button on the right hand side of the box. This will toggle between the Y and the Z-axes. The rotation sign convention is illustrated in the following diagram:

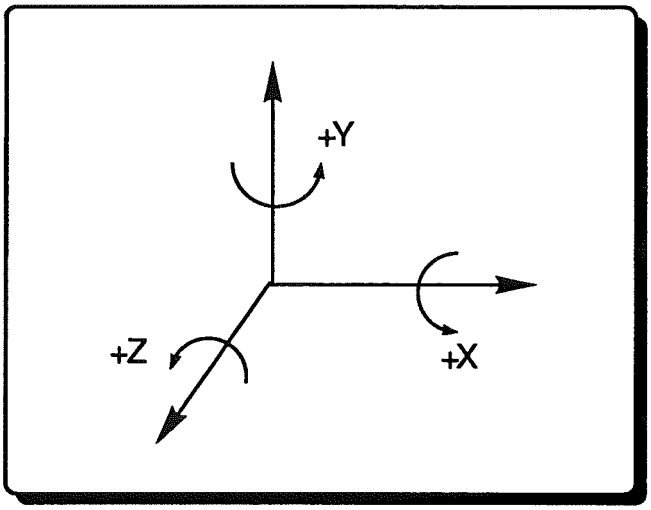

Small changes in the view are best achieved by placing the crosshairs near the centre of the box and clicking the mouse button several times.

If the Trans. button is selected then the rotate box will function to translate the structure on the screen. For example clicking in the top right quadrant of the rotate box will move the structure up and to the right on the screen. This is useful for examining large structures. If the Y/Z axis button is toggled to the Z-axis then movement in the +/- X direction (up or down) will have no effect and movement in the other direction (side-to-side) will expand or reduce the display in the current window. Again this is useful for examining a small part of a larger structure particularly when querying various parameters in the Ball and Stick mode. You should note that this expansion/reduction of the image does not actually change the coordinates of the structure which is displayed. So the molecule is not being brought closer to the observer but in fact it remains at a fixed distance and is simply "stretched" (or reduced) in the X and Y dimensions. The structure will return to it's original size whenever the window is resized or closed and reopened.

Note: *The translation mode can have a special function if viewing in the stereo mode - see Stereo Views below.*

- **Follow mouse.** If this option is on then the program will track the position of the

mouse in the rotate box and attempt to redraw the structure to reflect the changes in position within the rotate box. This is of course most useful with the wireframe representations where it allows "real-time" rotation.

• **All windows.** If this option is on then the rotations/translations specified through the rotate box will affect all the windows that are open on the screen. This allows say, two structures in their windows side by side to be rotated together. Once several windows are rotated at once performance will begin to deteriorate especially for large structures.

The View Modes.

In Molvib and ModelView there are two modes available for displaying structures on the screen : "WireFrame" and "Ball and Stick". The modes are accessed from the **View** menu. The one current has a check mark against it. Changing the view mode only applies to the structure which is currently displayed in the front-most window.

The Key-command equivalents ⌘-**W** and ⌘-**B** give wireframe and Ball and Stick modes respectively.

• **Wireframe.** This is the default mode when a file is converted and is useful for manipulating the structure into a desired orientation for viewing because even quite large structures can be rotated in real time. While rotating the structures can give a sense of depth, the disadvantage of the wire frame representation is that it does not present a unambiguous perspective of a structure or allow easy identification of functionality. Furthermore, it is not possible to query the atomic parameters from the wire frame mode. The width of the wire-frame and the background (black or white) can be set from the View Options -see below.

• **Ball and stick.** While the Ball and Stick mode is slower to rotate it does allow for a better perspective view and the atoms are easily identified. Furthermore atoms can be selected by Shift-Clicking (i.e clicking on them while holding down the shift key on the keyboard). This allows various geometrical parameters such as dihedral angles as well as coupling constants to be queried. The patterns displayed for the various atom types are totally arbitrary and cannot be changed by the user. The relative atomic sizes are chosen to roughly represent the standard relative covalent radii.[233] These cannot be changed by

the user (the absolute atom size can however - see View Options below).

•**Rotate by...** Choosing the **Rotate by** command in the **View** menu allows the user a second method of re-orientating the molecule. It presents a dialog box with three fields where values may be entered in for rotation about the X,Y and Z axes. This is most useful for rotations of 90 or 180 degrees where one wishes to "flip" a structure etc. When the dialog box appears the insertion point is in the "X" box. Pressing the "Tab" key will move to the other boxes sequentially. Clicking on the **OK** button will execute the rotations as you have entered them.

• **View down bond.** This option is only enabled when two atoms have been selected by Shift-Clicking on them. Once this option is selected then the molecule will be reorientated viewing down the selected bond.

• **Center of Mass.** After a executing a view down bond operation the "center of the rotation" is changed to the first atom which was selected. In order to enable the rotation to be returned to around the centre of mass this command is enabled after a **View Down Bond** operation.

• **Show/Hide H's.** For some large structures it is more efficient to view them with the hydrogens removed - this command simply toggles the display of the hydrogens on and off. Note that in the absence of hydrogens the rotation speed is increased: although the hydrogen positions are still calculated after every rotation the drawing of the structure is speeded up.

•**Show/Hide Serial Numbers.** Choosing this option from the view menu will toggle the display of the atom serial numbers. These are useful as all measurements will reference these numbers. These numbers are sequential for the position of the atoms in the input file and reflect the atom numbers as included in the input file (i.e. from MOPAC for Molvib; from MODEL,BAKMDL,MacroModel, Chem3D or MOPAC for ModelView.

•**Stereo View.** Choosing this command will toggle the current window in/out of the stereo mode. When in the stereo mode the structure displayed in the window will be shown as a stereo diagram and can be viewed with the aid of a suitable viewer to give a three dimensional representation of the structure. The stereo diagrams are best viewed from a printed copy and represent one structure drawn with a rotation of 5° relative to the other.

When in the stereo mode, the translation function of the rotate box has an added function to that in the mono mode. If the control key is held down then movement in the Y-direction of the rotate box controls the separation between the two images. The other X/Y/Z translation functions will operate as normal in the stereo mode if the control key is not held down. While selecting atoms (i.e for geometry queries) in the stereo mode use the right hand structure - the selections however will be reflected in both structures.

• **Show Vectors.** (Molvib only) This command is used to display the vectors which have been read from the MOPAC file. A dialog box will be presented with a scrollable list of frequencies (in cm^{-1}). Choose the desired frequency and then click on the Display button and the vectors corresponding to that frequency will be displayed. In the wireframe mode the vectors are shown as dark grey lines. In the Ball and Stick mode they are represented by black arrows. The vectors can be removed by choosing the Show Vectors command again and clicking on the Remove button. The Reverse Signs check box can be activated to display the inverse of the vectors : due to microscopic reversibility this is an equally valid interpretation. With the display of vectors for each new frequency, the structure will be redrawn in the original orientation from the MOPAC file. This is because the vector information for all the frequencies cannot be rotated to match the geometry - this would take far too long and impair the performance. Vibrational modes which have a negative force constant are indicated by imaginary frequencies in Molvib - i.e. 912.3i - the "i" indicating an imaginary number. The last six frequencies for any structure are the "trivial" ones and represent the rotational and vibrational modes. This can be easily confirmed by showing the vectors of these frequencies.

•**Animate Vibration.** (Molvib only) This command only becomes active once the vectors are being displayed for a particular vibrational frequency. Choosing this command will present an animated display of the atomic displacement for that particular vibrational mode. Five frames are prepared and are played back at rate proportional to the frequency. For large structures there may be a delay while the frames are prepared and this is indicated by the cursor changing to the number of the frame which is currently being prepared. All other view functions (rotation, resizing etc) are possible during the animation, but will function more slowly due to the time required to set up the animation.

Choosing a different frequency will continue the animation for that frequency. The magnitude of the atomic displacement is determined by the value of the vector scaling factor - see View Options below and the direction of the vibration can be reversed by choosing Reverse Signs from the Show Vectors box.

•**View Options.** The view options allow the user to adjust some of the parameters for the Ball and Stick representation to suit their individual preference. These options are controlled by scroll bars, the current setting is shown on the left of the scroll bar. There are five bars as follows:

• **Atom sizes:** This controls the radii of all the spheres used to represent the atoms in the Ball and Stick mode. The relative sizes for the different atom types cannot be changed.

• **Bond sizes:** The width of the bonds drawn between the spheres in the Ball and Stick mode can be adjusted by the use of this parameter. At the smallest value the bonds are not much wider than two line widths.

• **Perspective factor.** In order to give a perception of depth the size of the spheres in the Ball and Stick mode are scaled by a factor which is determined by the value of their z-co-ordinate. The co-ordinate values are scaled to be in the range -1 to 1 and the following relationship is used to determine the scaling factor:

Warp:= d/(d-1-z) where d is the perspective factor and z is the z co-ordinate. The value of d can be changed by using the perspective factor scroll bar. Larger values of d give a "flatter" perspective with less scaling for a given distribution of z- values while smaller values will give a "deeper" perspective with atoms in the "Front" (i.e the largest z) being scaled considerably more the those in the rear.

• **Wireframe width:** The width of the lines drawn in the wireframe representation may be changed as required. For very large structures it may be necessary to reduce the width of the lines from the default values.

• **Vector width:** (Molvib Only) The width of the vectors drawn in the Ball and Stick representation can be varied by setting this bar.

• **Vectors Scaling:** (Molvib Only) The vectors can be scaled to allow an optimum viewing position. This will also affect the atom displacement in the animation.

In addition to the scroll bars described above there are also two check boxes which can be used to change the way the structures are viewed.

• **Resize window to page.** When this option is checked the current structure window will be resized to be the size of the page which has been defined in the "Page Setup" dialog box, i.e. A4 letter etc. This function is only useful when running the program on large monitors where the windows may be larger than a page. If this is the case the window must be resized to at least the size of the page or else printing the window will not print the whole structure.

• **Black on white.** If this button is checked then the wire-frame representation will be drawn as a "black on white" representation which is suitable for printing or cutting and pasting into another program such as ChemDraw™. If this button is unchecked then the wire-frame representation will be as white on a black background which will almost certainly be unsuitable for printing, but some people will find the illusion of depth is greatly enhanced in this mode.

Once the values have been set there are three buttons which can be used to dismiss the "View options" dialog box. The effect of the clicking on each of the three buttons is as follows:

Cancel: No changes are made to the "View Option" values.

Temporary: The changes made will take effect immediately but will be reset one the program is reset.

Permanent: The changes made will take place immediately and will become the default values for the program - every time the program is used subsequently these values will be set for the "View Options".

The view options are global and effect every structure which is drawn *after* new settings are made.

Measurements

Molvib and ModelView have the facility to allow measurement of certain geometrical parameters by the use of the commands in the **Info** menu.

The measurements window.

Like the tools window this is "floating" window and will always be in front of other document windows. The measurements window is a text window where all the results of measurements and other calculations will be displayed. The font and size of the text in the measurements window can be set from the **Preferences** in the **File** menu - see "Preferences" below. The **Info** menu has a series of commands has a set of commands which relate to the measurements window:

• **Show/Hide Measurements.** This command allows the user to display or hide the measurements window. This command can also be activated by pressing ⌘-M on the keyboard. Furthermore the measurements window, like most other Macintosh windows can be dismissed by clicking in the box on the top left corner.

• **Clear Measurements.** (⌘ -L) The text in the measurements window is cumulative - i.e. as measurements are made they are appended to the text. If you wish to clear the measurements in the window choose this command. Naturally this command is only enabled when there is text in the window.

• **Save Measurements ..** The text in the measurements window can be saved as a text file suitable for reading by a word-processor such as Word or MacWrite. The file created in this way has its file type set to a Word text file type so double clicking on it will also start up Word and open the file for view.

• **Print Measurements** Because the measurements window is a "floating window" it is not possible to print the contents by using the Print command in the File menu as the Measurements window is always active. Therefore to print the contents of the window it is necessary to choose the Print Measurements command from the Info menu. This prints the contents of the window in the font and size displayed using the usual print interface for the printer which has currently been specified from the Chooser desk accessory.

• **Querying the geometry.** Most of the commands in the **Info** menu are involved in

allowing the user to query certain geometrical parameters of the structure which is currently displayed.

The query commands are:

• **Distance:** [Two atoms selected; ⌘-D]

This will report the distance between the two selected atoms in Angstrom units.

• **Angle:** [Three atoms selected, ⌘-A]

The angle command will report the angle in degrees made between the three selected atoms in the order First-Second-Third atom selected.

• **Dihedral:**[Four atoms selected, ⌘-E]

When four atoms are selected then the **Dihedral** command becomes active. The dihedral angle reported is the one First-Second-Third-Fourth atom selected. The usual sign convention is followed:- if looking down the bond Second-Third then if the angle from First-Fourth involves a clockwise movement then the sign is positive, otherwise the sign of the dihedral angle is negative. All query commands report to the Measurements window and as such if this is not currently visible then it will be shown after a query command is executed.

• **Coupling Constant.** (ModelView only) [Four atoms selected, First and fourth are Hydrogens, Second and third are carbons, First bound to second, second bound to third and third bound to fourth; ⌘-J]. If four atoms selected are H-C-C-H this command will enable a vicinal coupling constant to be calculated using the empirical relationship described by Haasnoot et. al.[234] . Users should be aware of the reported shortcomings in this method - most notable are the fact that no norbornanes were used in the data set used to derive the relationship and so the performance of this method for calculating vicinal coupling constants in these types of compounds is poor. Further-more no rotationally flexible compounds were used in the data-set and only a limited range of couplings in the region 6-8 Hz were included in the set used to derive the relationship. For H-sp^2-sp^3-H coupling arrangements, the simpler relationship of Garbisch[235] is used. When the "Boltzmann Measurements" option is on, the average Boltzmann coupling constant and the coupling constant distribution is calculated. This is useful for relating measured to calculated coupling for rotationally flexible compounds.

All query commands report to the Measurements window and as such if this is not

currently visible then it will be shown after a query command is executed.

• **Use Boltzmann Measure.** (Model View only) This command toggles on and off the Boltzmann measurements option. If the the Boltzmann measurements option is on then there will be a tick mark beside the command in the Info menu. The Boltzmann measurements mode means that all measurements on the structure currently displayed will be performed on all the structures which have been read in and a Boltzmann distribution of that parameter will be calculated at the current temperature. The Boltzmann average value of that parameter will also be calculated and displayed in the measurements window. If the Boltzmann Measurements option is not on (i.e. no tick mark beside the command) measurement will apply only to the structure which is queried. Currently the Boltzmann mode can only be entered for structures read in from BAKMDL generated files as only these have the required energy information to build the distribution. In the preferences the Boltzmann Measurements mode can be set to be enabled or disabled at startup - see the Preferences section below for more information.

• **Change Temperature.** (ModelView only) The default temperature for the Boltzmann distribution calculations is 23° C, but this can be changed by choosing the Change temperature command from the info menu. It is up to the user to ensure that the value entered in the box is a valid number and not a character as no error checking is done and the results could be unpredictable.

• **Show Boltz. Energies.** (ModelView only) If this command is selected from the Info menu, a report of the Average Boltzmann Energy and the Boltzmann population distribution (at the current temperature -see above) will be generated in the measurements window.

• **Polar Maps.** (ModelView only).

Polar Maps are a useful method for providing a graphical representation of the the conformation of medium and large cyclic systems. An example of a polar map is shown in the Figure 69. There are two steps to building a polar map for a structure. Firstly to enter the polar map definition mode choose **Define Polar Map** from the **Info** menu. The cursor will change to indicate that you are in this mode. While defining polar maps all commands work as expected, except that for obvious reasons you cannot query the geometry. To define a polar map click on the atoms in the ring you wish to build the polar map for (it is not

necessary to hold down the shift key). Click around the ring and to complete the definition

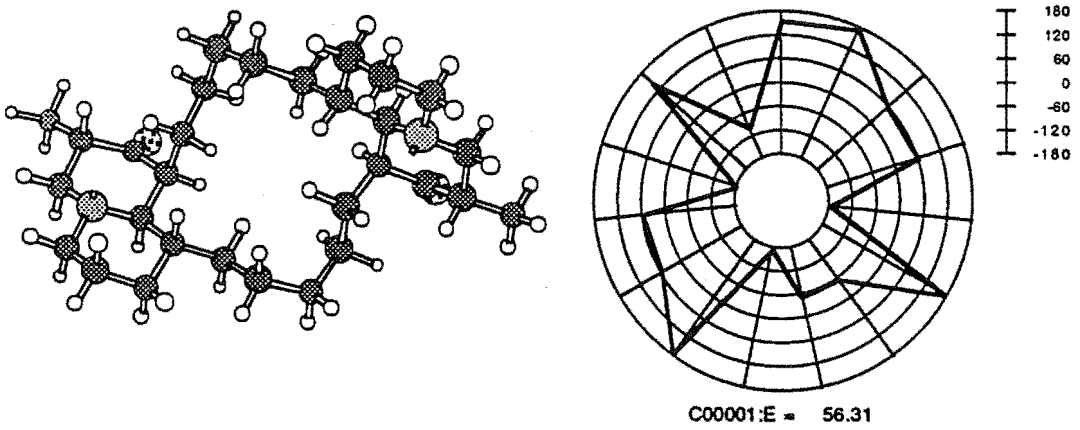

Figure 69. Low energy conformer from conformational search for the marine natural product Petrosin and polar map of this conformation.

click on the first atom in the ring again completing the ring. If you click outside of any atom during the definition a warning beep will sound and the atoms which have already been selected are not effected. It is the user's responsibility to ensure that the same atom is not selected twice during the Polar Map definition: there is no error checking done.

If you wish to abandon the definition you can choose **Define Polar Map** from the **Info** menu to halt the definition. During the definition process the **Structures** menu will be disabled as it is not possible to change structures during the definition process. The rotation and translation commands do, however, function normally and the structure can be rotated during the polar map definition without effecting those atoms which have been selected.

Once the definition is completed by clicking on the first atom to complete the cycle, there will be a beep and all the selected atoms will be deselected. The polar map can now be displayed with the **Show Polar Map** command from the **Info** menu. This will produce the polar map in its own window. If the "Report data to Measurements" option is enabled in the preferences (see above) then the dihedral angles used to build the polar map will be echoed to the measurements window. The polar map can be printed when its window is active and can also be copied to the Clipboard (and then to programs such as ChemDraw™ for further labelling, scaling etc) by using the **Copy** command in the **Edit** menu. The polar map window can be resized, but the polar map itself is fixed and cannot be scaled or moved within the

window. One of the useful things about generation of polar maps for a file of BAKMDL structures is that once a polar map is defined for one structure then the polar map for any other conformation can be viewed without redefinition. If the structures are not conformers, (i.e. a MODEL file of different structures) then the polar map should be redefined for each structure, otherwise the results will have no meaning. For a complete description of the use of polar maps in conformational analysis see Weiler et al.[236]

• **Chain Graphs.** (ModelView only)

While polar maps are useful for the analysis of cyclic structures they cannot be sensibly applied to the analysis of the conformations of chains. A chain graph displays graphically the N-3 dihedral angles formed by N atoms in a chain. An example of the chain graph is shown in the Figure 70. The procedure for generating a chain graph is similar

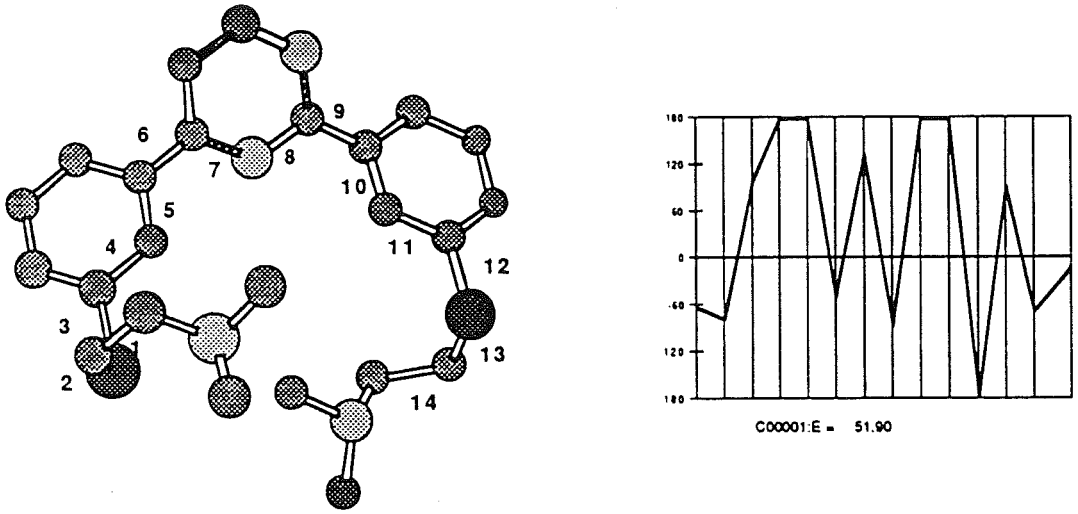

Figure 70. Low energy conformer of a bio-active cation and the chain graph for this conformer.

to that for a polar map. First choose **Define Chain Graph** from the **Info menu**. Then click on the atoms which make up the chain to select them. To complete the definition click again on the first atom which made up the chain. There must of course be at least four atoms selected for the definition to be complete. Like with the polar map definition, clicking outside of any atom produces a warning beep. There is no checking that atoms are not multiply selected. Once the definition is complete the **Show Chain Graph** command will be enabled in the **Info** menu. Choosing this will display the chain graph in its own window, and like the polar map it can be printed or copied to the clipboard.

File Conversions.

a) Molvib.

At present Molvib can only read files generated from the MOPAC program (using the **From Mopac *.out** command from the **Convert** menu) but it is likely that it will be extended to also read the output of the Gaussian series of programs. At present, however, that option in the **Convert** menu is permanently disabled. As well as it's own file format Molvib can also prepare two sorts of text files:

• **To Chem3D™** For further graphic processing a Chem3D™ file of the geometry can be prepared. This file can be read by Chem3D™ to show the geometry only with no vibrational information.

• **To Text** Occasionally it may be necessary to recreate the MOPAC output file. Choosing this command will allow the preparation of a Text file which has the cartesian co-ordinates of the molecule and the Mass-Weighted Co-ordinate Analysis presented just as they where in the original MOPAC file. The text file can be edited with a word-processor such as Word or Macwrite.

b) ModelView.

For further graphical manipulation it may be required to convert the structures which have been read into Model View from a BAKMDL or MODEL file to a series of CHEM3D™ files. This is done from the sole command in the Convert menu : To Chem3D™ . A list of structures will first be presented to the user to allow them to choose the structures to be converted. If all the structures which have been read in are to be converted then select all the structures by dragging down from the first one to the last. If there are more structures than can be displayed in the window then the list can be scrolled by either using the scroll bar on the left or by "dragging" below the window and the list will autoscroll. Note that it is not necessary to hold down the shift key while making multiple selections in this window. When the appropriate selections have been made then click on the OK button (or on the Cancel button if you don't wish to continue with the conversion). If you clicked the OK button the standard Macintosh file box will appear for you to choose the base filename for the converted files. If you choose "Transfer" as the filename and there are 5 structures

selected for conversion then the files will become "Transfer_001" to "Transfer_005". The converted files can be created in any folder and do not need to be located in the same folder as the application. The converted files have the Chem3D™ text file type and therefore have the appropriate icon and will start up Chem3D™ and read in the file when double-clicked on.

Technical notes.

Molvib and ModelView were developed using THINK Pascal v3.0 and the Think Class Library (Symantec Ltd) and the resource editor ResEdit (Apple Computer). The program design is object-oriented and each was the result of approximately 5000 lines of Pascal code to define the class behaviour on top of that defined in the class library.

Pi_Tilt.

Program description and overview.

Pi_Tilt is a program for the analysis of the degree of σ/π interaction in dienes based on the results of semi-empirical molecular orbital calculations such as those from the MOPAC program. The input is the calculated orbital co-efficients in each of the four π-type molecular orbitals for the diene carbons and the output is the degree of tilting, expressed in terms of three angles (see below), and the percentage electron density of each orbital which is centred on the diene carbons.

Theory and program function.

The atomic orbital co-efficients that are calculated by the MOPAC program are normalized so that the sum of the squares of all the co-efficients for a molecular orbital will be 1. In this manner the percentage electron density for any molecular orbital on any set of atoms can be assessed by adding the squares of the atomic orbital co-efficients and multiplying by 100. In Pi_Tilt the contribution from the s-atomic orbitals is assumed to be negligible and is not considered.

The main function of Pi_Tilt is to determine the degree of σ/π interaction for a diene system as represented by the degree of "tilting" of the p_z lobes of the diene. The diene is first considered to lie in the X-Y plane with a sole contribution to the π-molecular orbital arising from the p_z atomic orbital lobes of the diene; that is the situation in a "pure" diene system such as butadiene. Pi_Tilt then determines the direction and magnitude of this "p_z" lobe based on the contributions from the input atomic orbital orbital coefficients. This situation is shown in the figure:

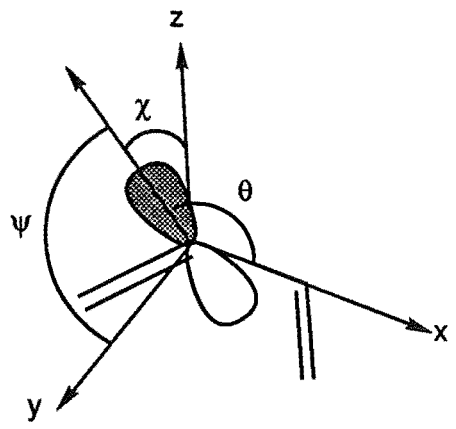

In Pi_Tilt the degree of tilting is represented as the combination of three angles χ, θ and ψ as shown in the figure. These angles are determined by considering the p_z lobe at each diene carbon as a vector, which is the vector sum of the input coefficients, with its origin at each of those carbons. The angle χ is then the angle which this vector makes with the z-axis and represents the total amount of tilting from perpendicular. For a "pure" diene system such as butadiene this value should be close to zero as the p_z lobes should be approximately perpendicular to the plane of the diene. The angles θ and ψ represent the amount of tilting projected on the X and Y axes respectively. In a "pure" diene system these values should be approximately 90°.

Program input and operation.

The program input file format is as follows:

Line1: 80 characters max. A title for the calculation.

Then for each of the four π-type molecular orbitals the following 5-lines:

The one-electron energy of the orbital (Not used in calculation but useful for identification etc.)

The atomic orbital co-efficients P_x, P_y, P_z for C1.

The atomic orbital co-efficients P_x, P_y, P_z for C2.

The atomic orbital co-efficients P_x, P_y, P_z for C3.

The atomic orbital co-efficients P_x, P_y, P_z for C4.

where C1,C2,C3 and C4 are the four carbons of the diene fragment.

Then four lines of the cartesian co-ordinates for the atoms C1-C4

x,y,z for C1

x,y,z for C2

x,y,z for C3

x,y,z for C4.

This data should be in a file with a ".dat" suffix. When the program is run (i.e. by typing RUN PI_TILT) it will prompt the user for the name of the the data file. The output is written to a file with a ".out" suffix.

Program source.

Pi_Tilt is written in Vax Pascal and the source is included below. The code should be able to be compiled on other computers, with the only Vax/VMS specific feature being the inclusion of the external function Mth$acosd as Vax pascal has no built-in inverse cosine function. To compile this program under VAX/VMX the following commands should be issued: PASCAL Pi_Tilt.pas

LINK/EXE=Pi_Tilt.exe Pi_Tilt.obj

```
program Pi_Tilt (Input, Output);
    { A Program for the analysis of Pi-orbital tilting in dienes          }
    { Uses the results of semi-empirical calculations (e.g. MOPAC)        }
    { Will request name of input filename (.DAT)                          }
    {       D.Q. McDonald          1989                                   }

    const
        MAXATOMS = 4;       {Maximun number of carbon atoms}
    type
        Atomstype = record
                        x, y, z: real;
                    end;
        Vectype = record
                        i, j, k: real;
                    end;
        Phitype = record
                        energy: real;
                        porb: array[1..maxatoms] of vectype;
                    end;
        anglestype = array[1..maxatoms, 1..maxatoms] of real;
        coeftype = array[1..maxatoms, 1..maxatoms] of real;
    var
        Phi: array [1..maxatoms] of phitype;
        atoms: array [1..maxatoms] of atomstype;
        xvec, vec: array [1..maxatoms] of vectype; {perpendicular and x-vector}
        Vec1to4, Vec1to2, Vec2to3, Vec3to4: vectype;
                                            {molecular co-ordinate vectors}
        Title: packed array [ 1..80] of char;
        chi: anglestype;
        theta, psi: anglestype;             {The angles to the bonds}
        i, j: integer;
        coeff: coeftype;
        perc: array [1..maxatoms] of real;

    function Mth$acosd(COSINE : REAL): REAL;EXTERNAL;

    function Posvec (v1: vectype): vectype;
                {reverses the sign of a vector}
    var
                temp: vectype;
    begin
        Temp.i := -(V1.i);
```

```
        Temp.j := -(V1.j);
        Temp.k := -(V1.k);
        Posvec := temp;
end;            {posvec}

procedure Cross_Prod (v1, v2: vectype; var v3: vectype);
        {Calculates the cross Product of V1 and V2 and returns in V3}
begin {Cross_Prod}
        v3.i := v1.j * v2.k - v1.k * v2.j;
        v3.j := v1.k * v2.i - v1.i * v2.k;
        v3.k := v1.i * v2.j - v1.j * v2.i;
end;    {Cross_Prod

function Dot_Prod (var V1, V2: vectype): real;
        {Calculates the vector dot product}
begin    {Dot_Prod}
        Dot_prod := V1.I * V2.I + V1.J * V2.J + V1.K * V2.K;
end;    {Dot_prod}

function Distance (V1: vectype): real;
        {Calculates the scaler length of a vector}
begin {Function Distance}
        Distance := SQRT(V1.I * V1.I + V1.J * V1.J + V1.K * V1.K);
end;    {Function Distance}


function Percent (PHI: phitype): real;
        {calculates the percentage of electron density on C1-C4}
var
                i, j: integer;
                temp: real;
begin {percent}
        temp := 0.0;
        for i := 1 to maxatoms do
                begin
                        with phi.porb[i] do
                                begin
                                        temp := temp + i * i + j * j + k * k;
                                end;            {with phi}
                end;    {for i}
        Percent := temp * 100.0;
end;    {Percent}

function Sub (a1, a2: atomstype): vectype;
        {subtracts a2 from a1 and returns the difference as a vector}
var
                tempvec: vectype;
begin {Sub}
        tempvec.i := a1.x - a2.x;
        tempvec.j := a1.y - a2.y;
        tempvec.k := a1.z - a2.z;
        sub := tempvec;
end;    {Sub}


function Coefficent (p1: vectype): real;
        {calculates the coefficents in the z direction}
var
                temp1, temp2: real;
begin {coefficent}
```

```
        temp1 := distance(p1);
        temp2 := p1.i + p1.j + p1.k;   {Add up the vectors to get the sign}
        if temp2 < 0.0 then
                coefficent := -temp1
        else
                coefficent := temp1;
end;    {Coefficent}

procedure Readit;    {Opens and reads the data file}
var
                i, j: integer;
                filename: packed array[1..80] of char;
                thefile: text;
begin   { Procedure Readit}
        Writeln('');
        Writeln('Enter the data (.dat) filename -with extensions');
        Writeln('');
        Readln(filename);
        Open ( thefile , filename , HISTORY := OLD );
        Reset(thefile);                         {Prepare for read}
        Readln(thefile, title);
        for i := 1 to maxatoms do
                begin
                        Readln(thefile, Phi[i].energy);
                        for j := 1 to maxatoms do
                                begin
                                        with phi[i] do
                                                begin
                                Readln(thefile, porb[j].i, porb[j].j, porb[j].k);
                                                end;   {with}
                                end;   {for j}

                end; {for i}

        for i := 1 to maxatoms do
                begin
                        with atoms[i] do
                                begin
                                Readln(thefile, x, y, z);
                                end;   {with}
                end;   {for i}
        Close(thefile);
end;    {Procedure Readit}

function angle (v1, v2: vectype): real;
{Calculates the angle between V1 AND V2 }
var
                DOT, DIST1, DIST2, ANG, TEMP: REAL;
begin           {Function Angle}
        DIST1 := DISTANCE(V1);
        DIST2 := DISTANCE(V2);
        DOT := DOT_PROD(V1, V2);
        TEMP := (-DOT / (DIST1 * DIST2));
        ANGle := MTH$ACOSD(TEMP);
end;    {Function Angle}

procedure WriteIt;              {Writes the output file}
var
                thefile: text;
                i, j: Integer;
```

```
            filename: packed array [1..80] of char;
begin
        Writeln('Enter the output filename');
        readln(filename);
        open ( thefile , filename , history := new );
        rewrite(thefile);
        Writeln(thefile, '');
        Writeln(thefile, '');
        Writeln(thefile, '                    Program Pi_Tilt     ');
        Writeln(thefile, '                              ***************       ');
        writeln(thefile, '');
        writeln(thefile, '          An Analysis of Pi orbital tilting in Dienes');
        writeln(thefile, '');
        writeln(thefile, '       ', title);
        writeln(thefile, '');
        writeln(thefile, '');
        for i := 1 to maxatoms do
                begin
                        writeln(thefile, '');
                        writeln(thefile, '  Phi:', i : 1);
                        write(thefile, '  Energy = ', phi[i].energy : 9 : 5);
                        case i of
                                1 :
                                        writeln(thefile, ' eV');
                                2 :
                                        writeln(thefile, ' eV  (HOMO)');
                                3 :
                                        writeln(thefile, ' eV  (LUMO)');
                                4 :
                                        writeln(thefile, ' eV');
                        end;   {case}
                        writeln(thefile, '');
                writeln(thefile, '   Percentage Electron density = ', perc[i] : 5 : 1);
                        writeln(thefile, '');
                        writeln(thefile, '');
                        write(thefile, '              ', '      C1');
                        write(thefile, '     ', '          C2');
                        write(thefile, '     ', '          C3');
                        writeln(thefile, '     ', '          C4');
                        writeln(thefile);
                        write(thefile, 'Chi:     ');
                        for j := 1 to 4 do
                                begin
                                        write(thefile, '           ', chi[i, j] : 7 : 3);
                                end;   {for  j}
                        writeln(thefile, '');
                        writeln(thefile);
                        write(thefile, 'Theta:  ');
                        for j := 1 to 4 do
                                write(thefile, '           ', theta[i, j] : 7 : 3);
                        writeln(thefile, '');
                        writeln(thefile);
                        write(thefile, 'Psi:     ');
                        for j := 1 to 4 do
                                write(thefile, '           ', psi[i, j] : 7 : 3);
                        writeln(thefile);
                        writeln(thefile);
                        writeln(thefile);
                        write(thefile, 'Coeff.     ');
                        for j := 1 to 4 do
```

```
                                    begin
                                        write(thefile, '          ', coeff[i, j] : 8 : 5);
                                    end; {for j}
                                writeln(thefile, '');
                                writeln(thefile, '');
                                writeln(thefile);
                                writeln(thefile, '');
                            end;  {for i}
        end;  {Procedure Writit}

begin       {The main program begins here }
        Readit;                 {Read the data file}
        VEC1TO4 := sub(atoms[1], atoms[4]);
        Vec1to2 := sub(atoms[1], atoms[2]);
        Vec2to3 := sub(atoms[2], atoms[3]);
        vec3to4 := sub(atoms[3], atoms[4]);  {Find Plane Vectors}
{Now find vectors perp. to the plane}
        cross_prod(VEC1TO2, VEC1TO4, VEC[1]);
        cross_prod(VEC1TO2, VEC2TO3, VEC[2]);
        cross_prod(Vec2to3, vec3to4, VEC[3]);
        cross_prod(Vec1to4, vec3to4, VEC[4]);
{And also find the Xvector - perp. to VEc[i] and vec1to4 or vec2to3}
        cross_prod(VEC[1], VEC1TO4, XVEC[1]);
        cross_prod(VEC[2], VEC2TO3, XVEC[2]);
        cross_prod(VEC[3], VEC2TO3, XVEC[3]);
        cross_prod(VEC[4], VEC1TO4, XVEC[4]);
        for i := 1 to maxatoms do
            begin
                for j := 1 to maxatoms do
                    begin
                        coeff[i, j] := coefficent(phi[i].porb[j]);
                        if coeff[i, j] < 0 then {make vector positive if neg.}
                        chi[i, j] := angle(vec[j], posvec(phi[i].porb[j]))
                        else
                            chi[i, j] := angle(vec[j], phi[i].porb[j]);

                        if (i = 1) or (i = 4) then
                            theta[i, j] := angle(VEC1TO4, phi[i].porb[j])
                        else
                            theta[i, j] := angle(VEC2TO3, phi[i].porb[j]);
                        psi[i, j] := angle(xvec[j], phi[i].porb[j]);
                    end;  {for j}
                perc[i] := percent(phi[i]);
            end;  {for i}
        WriteIt;        {write out the result}
end.  {Program Pi_tilt}
```

XSurface

Program description and overview.

XSurface is a program for the visualization of data such as potential energy surfaces; that is where there is one variable (i.e. Energy) which may depend on the value of two other variables (these may be geometrical variables for a potential energy surface). The data for XSurface must be complete (no interpolation will be done) and equally spaced. The data for the independent variables must be regularly spaced and quite dense; at least a 20x20 grid would be required for a smooth appearance. XSurface allows the data to be plotted as a three dimensional surface. This will work best for functions which vary smoothly, and this includes most potential energy surface. The surfaces produced by XSurface are highly "realistic" and by changing the reflective and emission properties of the material which the surface is displayed in, and by placement of up to four independent light sources around the model, the data can be displayed in a way which best shows subtle features which may not be seen in other representations such as contouring. The surface model may be rotated to any angle and expanded as required. XSurface runs on an IBM RS/6000 workstation and requires the High Performance 3D graphics card and the Z-buffering option. The program is written in the C language (approximately 2000 lines) and uses the AIX windows toolkit to support a graphical user-interface.

Program operation and input.

The input file for the program is a text file with the following format:

First line - NPOINTS an integer which specifies the number of points along each side of the grid of data.

Then the next (3 x NPOINTS x NPOINTS) lines should be the following data (one per line)

X a real number representing the first independent variable for the first observation

Y a real number representing the second independent variable for the first observation.

Z a real number representing the dependant variable for the first observation.

The scale of Z relative to X and Y is not important as it will be scaled by the program before

being displayed. The text file should have a ".sur" suffix.

XSurface is run by first ensuring that you have a path to the executable (i.e. the program is in the directory you invoke it from or in a directory listed in the PATH variable) and the by the XSurface "filename" command. The filename is optional but if it is not included XSurface will open only an empty display. XSurface consists of two windows. The larger is a GL window where the surface is displayed, the other is a standard X-window which has the controls for the viewing of the model. The XSurface controls are as follows:

The File menu contains the **Open** and **Quit** commands. Clicking on **Quit** will leave the program. The **Open** button is used to open a new file for display. The files displayed in the File selection box are filtered to show only those which have the "*.sur" suffix. Clicking on one of these files and then on the OK button will open the file for display. There will be a short delay between the opening of the file and the display of the surface as the file is read from the disk and the file selection box will remain visible during this time.

The surface model can be rotated and translated by the use of the arrow buttons. For example clicking on the upward facing arrow rotates the structure in a +X direction. The amount of the rotation in controlled by the value which is set in the **Rotate by:** menu. This can be 1, 5, 10 or 20 degrees for every click in the appropriate arrow key. Rotation about the Z-axis is accomplished by the use of the **+Z** and **-Z** buttons. The surface model can be brought closer to the viewing point (i.e effectively expanded) by clicking the **In** button and moved away from the viewing point by clicking on the **Out** button.

The surface model can be displayed with or without "sides" on the surface by the use of the "**Show Sides**" toggle button. In a similar way the axes can be displayed by clicking on the "**Show Axes**" toggle button. An approximate first derivative surface (calculated by finite differences) can be displayed by choosing the "**First Derivative**" button from the "**Derivatives**" menu. The display is returned to the original function by choosing the "**Normal**" button from the "Derivatives" menu.

Finally the surface properties and lighting of the model can be modified. A number of standard material types; Neutral, Silver, Gold and Green have been defined and these are applied by choosing the appropriate button from the "**Material**" menu. The **Custom** button allows the use of a custom material for which the specular, diffuse and ambient

reflections as well as the emission and shininess properties can be determined by the user. Up to four lights can also be placed by the user around the model. The colour and position of the light (X,Y,Z -which define the direction of a light at infinite distance) can be set. Any of the lights may be turned off by setting their colour to black (i.e. Red,Green Blue value of 0,0,0). The default lighting for XSurface is a single white light (Light1) placed on the X axis. The interactions of the lights and surface materials as well as the specification of material properties is quite complex and some experimentation may be required to get the desired lighting and shading effects. For more information users are refered to the sections on "Lighting Models and Material Properties" in the "Graphics Programming Concepts" section of the AIX Info-Explorer (CD-ROM).

References

1. Diels, O.; Alder, K., *Justus Liebigs Ann. Chem.*, **1928**, *460*, 98.
2. Sauer, J.; Huisgen, R.; Grashey, R., in "*The Chemistry of the Alkanes*"; Patai, S. ed.; Wiley-Interscience, New York, **1964**.
3. Wassermann, A., "*Diels-Alder Reactions*", Elsevier Publishing Co., Amsterdam, **1965**.
4. Woodward, R. B.; Katz, T.J., *Tetrahedron*, **1959**, *5*, 70, and references contained therein.
5. Dewar, M. J. S.; Olivella, S.; Stewart, J. J. P., *J. Am. Chem. Soc.*, **1986**, *108*, 5771.
6. Levine, I., "*Quantum Chemistry*", 2nd. Ed, Allyn and Bacon, Boston, **1974**.
7. Wheland, G. W.; Pauling, L., *J. Am. Chem. Soc.*, **1935**, *57*, 2086.
8. Coulson, C. A.; Longuet-Higgins, H. C., *Proc. Roy. Soc.*, **1947**, *192A*, 16.
9. Pople, J. A., *Proc. Roy. Soc.*, **1955**, *233A*, 233.
10. Pople, J. A., *Proc. Roy. Soc.*, **1955**, *233A*, 241.
11. McWeeny, R., *Phys. Rev.*, **1962**, *126*, 1028. Diercksen, G.; McWeeny, R., *J. Chem. Phys.*, **1966**, *44*, 3554.
12. Fukui, K., *Bull. Chem. Soc. Japan.*, **1966**, *39*, 498.
13. Hoffmann, R.; Woodward, R. B., *J. Am. Chem. Soc.*, **1965**, *87*, 4388. Hoffmann, R.; Woodward, R. B., *Angew. Chem., Int. Ed. Engl.*, **1969** , *8*, 781.
14. Houk, K. N., *Acc. Chem. Res.*, **1975**, *8*, 361. Fleming, I., "*Frontier Orbitals and Organic Reactions*", Wiley, New York, **1976**.
15. Houk, K. N., *J. Am. Chem. Soc.* , **1973**, *95*, 4092.
16. Eisenstein, O.; Lefour, J-M.; Anh, N. T., *J. Chem. Soc., Chem. Commun.*, **1971**, 969. Eisenstein, O.; Anh, N. T., *Tetrahedron Lett.*, **1971**, 1191.
17. Dewar, M. J. S., *J. Mol. Struct. (Theochem).*, **1989**, *200*, 301.
18. Dewar, M. J. S.; Dougherty, R. C., "*The PMO Theory of Organic Chemistry*", Plenum Press, New York, **1975**.
19. Herndon, W. C.; Hall, L. C., *Theoret. Chim. Acta*, **1967**, *7*, 4. Herndon, W. C.; Feuer, J.; Hall, L. C., *Tetrahdron*, **1968** , *24*, 2575.

20. Herndon, W. C.; Feuer, J., *J. Org. Chem.*, **1968**, 33, 417.

21. Sustmann, R.; Binsch, G., *Mol. Phys.*, **1971**, *20*, 1.

22. Sustmann, R.; Binsch, G.; *Mol. Phys.*, **1971**, *20*, 9.

23. Salem, L., *J. Am. Chem. Soc.*, **1968**, *90*, 543. Salem, L., *J. Am. Chem. Soc.*, **1968**, *90*, 553.

24. Klopman, G., *J. Am. Chem. Soc.*, **1968**, *90*, 223.

25. Sustmann, R.; Sicking, W., *Chem. Ber.*, **1987**, *120*, 1315. Sustmann, R.; Sicking, W., *Chem. Ber.*, **1987**, *120*, 1323.

26. Sustmann, R.; Daute, P.; Sauer, R.; Sicking, W., *Tetrahedron Lett.*, **1988**, *29*, 4699.

27. Brown, R. D., *J. Chem. Soc.*, **1950**, 691.

28. Brown, R. D., *J. Chem. Soc.*, **1951**, 1955.

29. Hopff, H.; Schweizer, H. R., *Helv. Chim. Acta*, **1959**, *42*, 2315.

30. Streitwieser, A. Jr, *"Molecular Orbital Theory for Organic Chemists"*, John Wiley and Sons, New York, **1961**.

31. Kikuchi, O., *Tetrahedron*, **1971**, *27*, 2791.

32. Burke, L. A.; Leroy, G.; Sana, M., *Theoret. Chim. Acta*, **1975** , *40*, 313.

33. Townshend, R. E.; Ramunni, G., Segal. G; Hehre, W.J.; Salem, L., *J. Am. Chem. Soc.*, **1976**, *98*, 2190.

34. McIver, J. W. Jr, *J. Am. Chem. Soc.*, **1972**, *94*, 4782.

35. Dewar, M. J. S.; Griffin, A. C.; Kirschner, S., *J. Am. Chem. Soc.*, **1974**, *96*, 6225.

36. Dewar, M. J. S., Olivella, S., Rzepa, H. S., *J. Am. Chem. Soc.*, **1978**, *100*, 5650.

37. Dewar, M. J. S., *J. Am. Chem. Soc.*, **1984**, *106*, 209.

38. Caramella, P.; Houk, K. N.; Domelsmith, L. N., *J. Am. Chem. Soc.*, **1977**, *99*, 4511.

39. Ortega, M; Oliva, A.; Lluch, J. M.; Bertrán, J., *Chem. Phys. Lett.*, **1983**, *102*, 317.

40. Houk, K. N.; Brown, F. K., *Tetrahedron Lett.*, **1984**, *25*, 4609.

41. Houk, K. N.; Lin, Y-T; Brown, F. K., *J. Am. Chem. Soc.*, **1986**, *108*, 554.

42. Bernardi, F.; Bottoni, A.; Robb, M. A.; Field, M. J.; Hillier, I. H.; Guest, M. F., *J. Chem. Soc., Chem. Commun.*, **1985**, 1051. Bernardi, F.; Bottoni, A.; Robb, M. A.; Field, M. J.; Hillier, I. H.; Guest, M. F.; Venturini, A., *J. Am. Chem. Soc.*, **1988**, *110*, 3050.

43. Bernardi, F.; Bottoni, A.; Olivucci, M.; McDouall, J. J. W.; Robb, M. A.; Tonachini, G., *J. Mol. Struct. (Theochem).*, **1988** , *165*, 341.

44. Bach, R. D.; McDouall, J. J. W.; Schlegel, H. B.; Wolber, G., *J. Org. Chem.*, **1989**, *54*, 2931.

45. Coxon, J. M.; Grice, S. T.; Maclagan, R. G. A. R.; McDonald, D. Q., *J. Org. Chem.*, **1990**, *55*, 3804.

46. Choi, J. Y.; Lee, I., *J. Chem. Soc., Faraday Trans. II*, **1989**, *85*, 867.

47. Houk, K. N.; Loncharich, R. J.; Blake, J. F.; Jorgensen, W. L., *J. Am. Chem. Soc.*, **1989**, *111*, 9172.

48. Birney, D.; Houk, K. N., *J. Am. Chem. Soc.*, **1990**, *112*, 4127.

49. Gajewski, J.; Peterson, K. B.; Kagel, J. R.; Huang, Y. C. J., *J. Am. Chem. Soc.*, **1989**, *111*, 9078.

50 Roothaan, C. C. J. , *Rev.Mod. Phys.*, **1951**, *69*, 23.

51. Hall, G. G., *Proc. Roy. Soc. London, Ser. A.*, **1951**, *541*, 205.

52. Parr R. G., *"The Quantum Theory of Molecular Electronic Structure."*, W. A. Benjamin, New York, **1963**.

53. McGlynn, S.P.; Vanquickenborne, L.G.; Kinoshita, M.; Carroll, D.G., *"Introduction to Applied Quantum Chemistry"*, Holt, Reinhart and Wilson, New York, **1972**.

54. Hoffmann, R., *J. Chem. Phys.*, **1963**, 39, 1397.

55. Allen, L. C.; Russell, J. D., *J. Chem. Phys.*, **1967** , *46*, 1029.

56. Pople, J. A.; Santry, D. P.; Segal, G. A., *J. Chem Phys.*, **1965**, *43*, S129.

57. Pople, J. A., *Trans. Faraday Soc.*, **1953**, *49*, 1375. Pariser, R.; Parr, R.G., *J. Chem Phys.*, **1953**, 21, 767.

58. Pariser, R., *J. Chem. Phys.*, **1956**, *24*, 250.

59. Pople, J. A.; Segal, G. A., *J. Chem. Phys.*, **1965**, *43*, S136.

60. Pople, J. A.; Segal, G.A., *J. Chem. Phys.*, **1966**, *44*, 3289.

61. Pople, J. A.; Beveridge, D. L.; Dobosh, P. A., *J. Chem Phys.*, **1967**, *47*, 2026.

62. Dixon, R. N., *Mol. Phys.*, **1967**, *12*, 83.

63. Baird, N. C.; Dewar, M. J. S., *J. Chem. Phys.*, **1969**, *50*, 1262.

64. Dewar, M. J. S.; Haselbach, E., *J. Am. Chem. Soc.*, **1970**, *92*, 590.

65. Bingham, R. C.; Dewar, M. J. S; Lo, D. H., *J. Am. Chem. Soc.*, **1975**, *97*, 1285.

66. Lewis, D. F. V., *Chem. Rev.*, **1986**, *86*, 1111.

67. Arenas, J.F.; Qurants, J.J.; Ramirez, F.J., *J. Mol. Struct. (Theochem).*, **1988**, *164*, 143.

68. Dewar, M. J. S., *Science*, **1975**, *187*, 1037.

69. Davidson, R.B.; Jorgensen, W.L.; Allen, L.C., *J. Am. Chem. Soc.*, **1970**, *92*, 749.

70. Dewar, M. J. S.; Zoebisch,E. G.; Healy, E. F.; Stewart, J. J. P., *J. Am. Chem. Soc.*, **1985**, *107*, 3902.

71. Stewart, J. J. P., *J. Comput. Chem.* , **1989**, *10*, 209.

72. Dewar, M. J. S.; Healy, E. F; Holder, A. J.; Yuan, Y-C, *J. Comput. Chem.*, **1990**, *11*, 541.

73. Stewart, J. J. P., *J. Comput. Chem.*, **1990**, *11*, 543.

74. Buß, V.; Messinger, J.; Heuser, N., *QCPE Bulletin*, **1991**, *11*, 5.

75. Dewar, M. J. S.; Storch, D. M., *J. Am. Chem. Soc.* , **1985**, *107*, 3898.

76. Halgren, T. A.; Kleifer, D. A.; Lipscomb, W. N., *Science*, **1976**, *190*, 591.

77. Dewar, M. J. S., *Chem. Britain*, **1975**, *187*, 1037.

78. Kutzelnigg, W., *J. Mol. Struct. (Theochem).*, **1988**, *181*, 33.

79. Lindholm, E., *Tetrahedron*, **1988**, *44*, 7464.

80. Thiel, W., *Tetrahedron*, **1988**, *44*, 7393.

81. Martin, J. G.; Hill, R. K., *Chem. Rev.*, **1961**, *61*, 537.

82. Avram, M.; Mateescu, G.; Nenitzescu, C. D., *Ann. Chem.*, **1960**, *363*, 174.

83. Winstein, S.; Shatavsky, M.; Norton, C.; Woodward, R. B., *J. Am. Chem. Soc.*, **1955** , *77*, 4183.

84. McLean, S.; Haynes, P., *Tetrahedron*, **1965**, *21*, 2313.

85. Corey, E. J.; Weinshenker, N. M.; Schaaf, T. K.; Huber, W., *J. Am. Chem. Soc.*, **1969**, *91*, 5675.

86. Williamson, K. L.; Hsu, Y-F, L.; Lacko, R.; Youn, C. H., *J. Am. Chem. Soc.*, **1969**, *91*, 6129.

87. Mel'nikov, N. N.; Volodkovich, S. D., *Zh. Obsch. Khim.*, **1958**, *28*, 3342.

88. Williamson, K. L; Hsu, Y-F. L., *J. Am. Chem. Soc.*, **1970**, *92*, 7385.

89. Anh, N. T., *Tetrahedron*, **1973**, *29*, 3227.

90. Breslow, R.; Hoffman, J. M.; Perchonok, C., *Tetrahedron Lett.*, **1973**, 3723.

91. Fukui, K.; Inagaki, S.; Fujimoto, H., *J. Am. Chem. Soc.*, **1976** , *98*, 4054.

92. Jones, D. W., *J. Chem. Soc., Chem. Commun.*, **1980**, 739.

93. Macaulay, J.; Fallis, A. G., *J. Am. Chem. Soc.*, **1988**, *110*, 4074.

94. Macaulay, J.; Fallis, A. G., *J. Am. Chem. Soc.*, **1990**, *112*, 1136.

95. Cieplak, A. S.; Tait, B. D.; Johnson, C. R., *J. Am. Chem. Soc.*, **1989**, *111*, 8447. Cieplak, A. S.; Tait, B. D.; Johnson, C. R., *J. Am. Chem. Soc.*, **1987**, *109*, 5875.

96. Fleming, I.; Williams, R. V., *J. Chem. Soc., Perkin Trans. I*, **1981**, 684.

97. Houk, K. N.; Brown, F. K.; Burnell, D.J.; Valenta, Z., *J. Org. Chem.*, **1987**, *52*, 3050.

98. Burnell, D. J.; Valenta, Z., *J. Chem. Soc., Chem. Commun.*, **1985**, 1247.

99. Simmons, H. E.; Fukunaga, T., *J. Am. Chem. Soc.*, **1967**, *89*, 5208. Simmons, H. E.; Dordon, M.D.; Fukunaga, T., *J. Am. Chem. Soc.*, **1976**, *98*, 8401.

100. Holmberg, K.; Kirudd, H.; Westin, G., *Acta Chem. Scand.*, **1974**, *B28*, 913.

101. Yates, P.; Auksi, H., *Can. J. Chem.*, **1981**, *59*, 2510.

102. Shultz, A. G.; Dittami, J. P.; Lavieri, F. P.; Salowey, C.; Sundararman, P.; Szymula, M., *J. Org. Chem.*, **1984** , *49*, 4429.

103. Maat, L.; Peters, J. A.; Prazeres, M. A., *Recl. Trav. Chim. Pays-Bas*, **1985**, *104*, 205.

104. Knaus, E. E.; Pasutto, F. M.; Giam, C. S.; Swinyard, E. A., *J. Heterocyclic Chem.*, **1976**, *13*, 481.

105. Krow, G. R.; Carey, J. T.; Zacharies, D. E.; Knaus, E. E., *J. Org. Chem.*, **1982**, *47*, 1989.

106. Tolstikov, G. A.; Lerman, B. M.; Galin, F. Z., *Zh. Org. Khim.*, **1975**, *11*, 1348.

107. Coxon, J. M.; O'Connell, M.J.; Steel, P. J., *J. Org. Chem*, **1987**, *52*, 7426.

108. Pandey, B.; Zope, U. R.; Ayyangar, N. R., *Synth. Commun.*, **1989**, *19*, 585.

109. Prinzbach, H.; Grund, C.; Fessner, W-D., *Tetrahedron Lett.*, **1989**, *30*, 3133. Prinzbach, H; Fessner, W-D.; Grund, C.; Pinkos, R.; Melder, J-P.; Artschwager-Perl, U.; Klärner, F-G., *Tetrahedron Lett.*, **1989**, *30*, 3137.

110. Ginsburg, D., *Tetrahedron*, **1983**, *39*, 2095.

111. Korat, M.; Tatarsky, D.; Ginsburg, D., *Tetrahedron*, **1972**, *28*, 2315.

112. Ginsburg, D., *Tetrahedron*, **1974**, *30*, 1487.

113. Amith, C.; Ginsburg, D., *Tetrahedron*, **1974**, *30*, 3415.

114. Ashkenazi, P.; Vogel, E.; Ginsburg, D., *Tetrahedron*, **1978**, *34*, 2167.

115. Kaftory, M.; Peled, M.; Ginsburg, D., *Helv. Chim. Acta*, **1979**, *62*, 1326.

116. Kalo, J.; Ginsburg, D.; Bloomfield, J. J., *Tetrahedron*, **1978**, *34*, 2153.

117. Kalo, J.; Ginsburg, D., *Tetrahedron*, **1978**, *34*, 2155.

118. Böhm, M. C.; Gleiter, R. G., *Tetrahedron*, **1980**, *36*, 3209.

119. Landheer, I.; Ginsburg, D., *Tetrahedron*, **1981**, *37*, 133.

120. Kalo, J.; Photis, J. M.; Paquette, L. A.; Vogel, E.; Ginsburg, D., *Tetrahedron*, **1976** , *32*, 1013.

121. Paquette, L. A.; Kakihana, T.; Hansen, J. F.; Philips, J. C., *J. Am. Chem. Soc.*, **1971**, *93*, 152.

122. Trost B. M; Belletire, J. L.; O'Krongly, D., *J. Am. Chem. Soc.*, **1980**, *102*, 7595.

123. Tripathy, R.; Carroll, P. J.; Thornton, E. R, *J. Am. Chem. Soc.*, **1990**, *112*, 6743.

124. Houk, K. N.; Trost, B. M.; Tucker, J. A., *J. Am. Chem. Soc.*, **1990**, *112*, 5465.

125. Franck, R.W.; John, T.V.; Olejniczak, K., *J. Am. Chem. Soc.*, **1982**, *104*, 1106.

126. Franck, R. W.; John, T. V., *J. Am. Chem. Soc.*, **1983**, *48*, 3269.

127. Primeau, J. L.; Anderson, R. C.; Fraser-Reid, B., *J. Am. Chem. Soc.*, **1983**, *105*, 5874.

128. Schmidlin, T.; Burckhardt, P. E.; Waespec-Sarcevic, N.; Tamm, C., *Helv. Chim. Acta*, **1983**, *66*, 450.

129. Boger, D.L; Patel, M.; Takusagawa, F., *J. Org. Chem.*, **1985**, *50*, 1911.

130. Tolbert, L. M.; Ali, M. B., *J. Am. Chem. Soc.*, **1981**, *103*, 2104.

131. Grée, R.; Kessabi, J.; Mosset, P.; Martelli, J.; Carrie, R., *Tetrahedron Lett.*, **1984**, *25*, 3697.

132. Franck, R. W.; Argarde, S.; Subramanium, C. S.; Frechet, D. M., *Tetrahedron Lett.*, **1985**, *26*, 3187.

133. McDougal, P. G.; Rico, J. G.; VanDerveer, D., *J. Org. Chem.*, **1986**, *51*, 4492.

134. Reitz, A. B.; Jordan, A. D.; Maryhoff, B. E., *J. Org. Chem.*, **1987**, *52*, 4800.

135. Kozikowski, A. P.; Nieduzak, T. R.; Konoike, T.; Springer, J. P., *J. Am. Chem. Soc.*, **1987**, *109*, 5167.

136. Kozikowski, A. P.; Jung, S. H.; Springer, J. P., *J. Chem. Soc., Chem. Commun.*, **1988**, 167.

137. Tripathy, R.; Franck, R. W.; Onan, K. D., *J. Am. Chem. Soc.*,**1988**, *110*, 3257.

138. Kaila, N.; Franck, R. W.; Dennenburg, J. J., *J. Org. Chem.*, **1989**, *54*, 4206.

139. Kahn, S. D.; Hehre, W. J., *J. Am. Chem. Soc.*, **1987**, *109*, 663.

140. Grabley, S.; Kluge, H.; Hoppe, H-U., *Angew. Chem., Int. Ed. Engl.*, **1987**, *26*, 664.

141. Burnouf, C.; Lopez, J. C.; Calvo-Flores, F. G.; Labordem, M.; Olesker, A.; Lukacs, G., *J. Chem. Soc., Chem. Commun.*, **1990**, 823.

142. Fisher, M. J.; Hehre, W. J.; Kahn, S. D.; Overman, L. E., *J. Am. Chem. Soc.*, **1988**, *110*, 4625. Fisher, M. J.; Overman, L. E., *J. Org. Chem.*, **1988**, *53*, 2630.

143. Watson, W. H., *"Stereochemistry and Reactivity of Systems Containing π Electrons"*, Verlag Chemie International, Deerfield Beach, FL, **1983**.

144. Ermer, O.; Bell, P.; Mason,S.A., *Angew. Chem., Int. Ed. Engl.* **1989**, *28*, 1239.

145. Wipff, G.; Morkuma, K., *Tetrahedron. Lett.* **1980**, *21*, 4445.

146. Alder, K.; Flock, F. H; Janssen, P., *Chem. Ber.*, **1956**, *89*, 2689.

147. Sugimoto, T.; Kobuke, Y.; Furukawa, J., *J. Org. Chem.*, **1976**, *41*, 1457.

148. Watson, W. H.; Galloy, J.; Bartlett, P. D.; Roof, A. A. M., *J. Am. Chem. Soc.*, **1981**, *103*, 2022.

149. Bartlett, P.; Wu, C., *J. Org. Chem.*, **1985**, *50*, 4087.

150. Paquette, L. A; Gugelchuck, M.; Hsu, Y-L., *J. Org. Chem.*, **1986**, *51*, 3864.

151. Paquette, L. A; Kunzer, H.; Green, K. E; Lucchi, O.; Licini, G.; Pasquato, L.; Valle, G., *J. Am. Chem. Soc.*, **1986**, *108*, 3453.

152. Bartlett, P. D.; Wu, C., *J. Org. Chem.*, **1984**, *49*, 1880.

153. Paquette, L. A.; Carr, R. V. C.; Charumilind, P.; Blount, J. F., *J. Org. Chem.*, **1980**, *45*, 4922.

154. Paquette, L. A.; Green, K. A.; Hsu, L-Y., *J. Org. Chem.*, **1984**, *49*, 3650.

155. Vogel, P.; Hagenbuch, J-P.; Pinkerton, A.; Schwarzenbach, D., *Helv. Chim. Acta*, **1981**, *64*, 1818.

156. Vogel, P.; Mahaim, C., *Helv. Chim. Acta*, **1982**, *65*, 866.

157. Vogel, P.; Avenati, M., *Helv. Chim. Acta*, **1983**, *66*, 1279.

158. Paquette, L. A.; Carr, R. V.C.; Böhm, M. C.; Gleiter, R., *J. Am. Chem Soc.* , **1980**, *102*, 1180. Gleiter, R.; Paquette, L.A., *Acc. Chem. Res.* , **1983**, *16*, 328.

159. Heilbronner, E.; Schmelzer, A., *Helv. Chim. Acta*, **1975**, *58*, 936.

160. Böhm, M. C.; Carr, R. V. C.; Gleiter, R.; Paquette, L. A., *J. Am. Chem. Soc.*, **1980**, *102*, 7218.

161. Paquette, L.A.; Gugelchuck, M., *J. Org. Chem.*, **1988**, *53*, 1835.

162. Paquette, L. A.; Charumilind, P.; Böhm, M. C.; Gleiter, R.; Bass, L. A.; Clardy, J., *J. Am. Chem. Soc.*, **1983**, *105*, 3136. Paquette, L.A.; Charumilind, P.; Böhm, M. C.; Gleiter, R.; Hayes, P.C.; Blount, J.F., *J. Am. Chem. Soc.*, **1983**, *105*, 3148.

163. Paquette, L. A.; Kravetz, T. M; Hsu, L-Y., *J. Am. Chem. Soc.*, **1985**, *107*, 6598.

164. Houk, K. N.; Brown, F. K., *J. Am. Chem. Soc.*, **1985**, *107*, 1971.

165. Houk, K. N.; Brown, F. K., *J. Am. Chem. Soc.*, **1984**, *106*, 4609.

166. Ipaktschi, J.; Herber, J.; Kalinowski, H-O.; Boese, R., *Chem. Ber.*, **1990**, *123*, 305.

167. Mehta, G.; Karra, S. R., *J. Org, Chem.*, **1989**, *54*, 2975. Mehta, G.; Padma, S.; Pattabhi, V.; Pramanik, A.; Chandrasekhar, J., *J. Am. Chem. Soc.*, **1990**, *112*, 2942.

168. Burket, U.; Allinger, N. L., *"Molecular Mechanics"*, ACS Monograph, **1982**, *177*.

169. O' Connell, M. J., Ph.D. Thesis, University of Canterbury, **1987**.

170. The calculations were performed using MMX 88 and associated parameters as availiable from Serena Software, 489 Serena Lane, Bloomington, IN 47401.

171. Steliou, K. S., BAKMDL **1989** , based on the orginal program by W. C. Still.

172. Houk, K. N.; Paddon-Row, M. N.; Rondan, N. G.; Wu, Y-D.; Brown, F. K.; Spellmeyer, D. C.; Metz, J. T.; Li, Y.; Loncharich, R., *Science*, **1986**, *231*, 1108. Houk, K. N.; Tucker, J. A.; Dorigo, A. E., *Acc. Chem. Res.*, **1990**, 23, 107.

173. Menger, F. M., *Adv. Mol. Model.*, **1989**, *1*, 189. Sherrod, M. J.; Menger, F. M., *J. Am. Chem. Soc.*, **1989**, *111*, 2611.

174. Paddon-Row, M. N.; Rondan, N. G.; Houk, K. N., *J. Am. Chem. Soc.*, **1982**, *104*, 7162.

175. Houk, K. N.; Dorigo, A.; *J. Am. Chem. Soc.*, **1987**, *109*, 3968.

176. Sasaki, T.; Eguchi, S.; Kiriyama, T.; Hiroaki, O., *Tetrahedron*, **1974**, *30*, 2707.

177. Marchand, A. P.; LaRoe, W. D.; Sharma, G. V. M.; Suri, S. C.; Reddy, D. S., *J. Org. Chem.*, **1986**, *51*, 1622.

178. Mehta, G.; Srikishna, A., *Tetrahedron*, **1981**, *37*, 4545.

179. Smith, E. C; Barborak, J. C., *J. Org. Chem.*, **1976**, *41*, 1433.

180. Coxon, J. M.; Fong S. T.; Steel P. J., *Tetrahedron Lett.*, **1990**, *31* , 5357.

181. Ensley, H. E.; Mahadevan, S., *Tetrahedron Lett.*, **1989**, *30*, 3255.

182. Shen, K-W.; Kuebler, N.A., *Tetrahedron Lett.* ,**1973**, 2145.

183. Marchand, A. P.; Kaya, R., *J. Org. Chem.*, **1983**, *48*, 5392.

184. Pandey, B.; Zope, U. R.; Ayyangar, N. R., *J. Chem. Soc., Chem. Commun.*, **1990**, 107.

185. Chow, T.J.; Wu, T-K.; Shih H-J., *J. Chem. Soc., Chem. Commun.*, **1989**, 490. Bishop, R.; Lee, G-H., *Aust. J. Chem.*, **1987**, *40*, 249. Bishop, R., *Aust. J. Chem.*, **1984**, *37*, 319.

186. Marchand, A.P.; Huang, C.; Kaya, R.; Baker, A.D.; Jemmis, E. D.; Dixon, D. A., *J. Am. Chem. Soc*, **1987**,*109*, 7095.

187. Jensen, F.; Foote, C. S., *J. Am. Chem. Soc.*, **1987**, *109*, 6376.

188. Underwood, G. R.; Ramamoorthy, B., *J. Chem. Soc., Chem. Commun.*, **1970**, 12.

189. Hutchins, R. O.; Masilamani, D.; Maryanoff, C. A., *J. Org. Chem.*, **1976**, *41*, 1071.

190. Gao, Y.; Sharpless, K. B., *J. Am. Chem. Soc.*, **1988**, *110*, 7538.

191. Carlsen, P. H. J.; Katsuki, T.; Martin, V.S.; Sharpless, K. B., *J. Org. Chem.*, **1981**, *49*, 3936.

192. Garner, H. K.; Lukas, H. J., *J. Am. Chem. Soc.*, **1950**, *72*, 5497.

193. S.T. Fong, Ph. D. Thesis, University of Canterbury, **1991**.

194. Corey, E. J.; Winter, R. A. E., *J. Am. Chem. Soc.*, **1963**, *85*, 2677. Block, E., *Organic Reactions*, **1984**, *30*, 457.

195. Benedict, D.R.; Bianchi, T. A.; Cate, L. A., *Synthesis*, **1979**, 428.

196. Supraneni, C. R.; Gilardi, R., *J. Org. Chem.*, **1986**, *51*, 2382.

197. Pandey, B.; Dalvi, P. V., *J. Org. Chem.*, **1989**, *54*, 2969.

198. Mehta, G.; Singh, V., *Tetrahedron Lett.*, **1978**, 4591.

199. Smith, C. M., *Intl. J. Quantum Chem.*, **1990**, *37*, 773.

200. Dewar, M. J. S.; Healy, E. F.; Stewart, J. J. P., *J. Chem. Soc., Faraday Trans. II*, **1984**, 227.

201. MOPAC, version 6.0. Quantum Chemistry Program Exchange (QCPE), Program Number 455, **1990**.

202. Fox, M. A.; Cardona, R.; Kiwiet, N. J., *J. Org. Chem.*, **1987**, *52*, 1469.

203. Komornicki, A.; McIver, J. W., *Chem Phys. Lett.*, **1971**, *10*, 303. Komornicki, A.; McIver, J. W., *J. Am. Chem. Soc.*, **1971**, *94*, 2625.

204. Stewart, J. J. P.; Davis, L. P.; Burggraf, L. W., *J. Comput. Chem.*, **1987**, *8*, 1117.

205. Houk, K. N.; Gandour, R. W.; Strozier, R. W.; Rondan, N. G.; Paquette, L. A., *J. Am. Chem. Soc.*, **1979**, *101*, 6797.

206. Bach, R. D.; Wolber, G. J.; Schlegel, H. B., *J. Am. Chem. Soc.*, **1985**, *107*, 2837.

207. Hoffmann, R.; Imamura, A.; Hehre, W. J., *J. Am. Chem. Soc.*, **1968**, *90*, 1499.

208. Gleiter, R., *Angew. Chem., Int. Ed. Engl.*, **1974**, *13*, 696. Hoffmann, R., *Acc. Chem. Res.*, **1971**, *4*, 1.

209. Heilbronner, E.; Schmelzer, A., *Helv. Chim. Acta.*, **1975**, *58*, 936.

210. Edmiston, C.; Ruedenberg, K., *Rev. Mod. Phys.*, **1963**, *35*, 457.

211. Gleiter, R.; Zimmermann, H.; Fessner, W-D; Prinzbach, H., *Chem Ber.*, **1985**, *118*, 3856.

212. Dhaneswar, N. N.; Tavale, S. S.; Guru Row, T. N.; Zope, U. R.; Pandey, B.; Ayyangar, N. R., *Acta Crystallogr.*, **1988**, *C44*, 2191.

213. Back, R. A., *Rev. Chem. Int.*, **1984**, *5*, 293.

214. Corey, E. J.; Mock, W. L.; Pasto, D. J., *Tetrahedron Lett.*, **1961**, *11*, 347. Hünig, S.; Müller, H-R.; Thier, W. *Tetrahedron Lett.*, **1961**, 353.

215. Corey, E. J.; Pasto, D. J; Mock, W. L., *J. Am. Chem. Soc.* , **1961**, *83*, 2957.

216. Willis, C.; Back, R. A.; Parsons, J. M.; Purdon, J. G., *J. Am. Chem. Soc.*, **1977**, *99*, 4451. Craig, N. C.; Kliewer, M. A.; Shih, N. C., *J. Am. Chem. Soc.*, **1979**, *101*, 2480.

217. Dykstra, C. E., *"Ab Initio Calculation of the Structures and Properties of Molecules"*, Elsevier B. V., Amsterdam, **1988**.

218. Agrafiotis, D. K.; Rzepa, H. S., *J. Chem. Soc., Chem. Commun.*, **1987**, 902. Agrafiotis, D. K.; Rzepa, H. S., *J. Chem. Soc., Perkin. Trans. II*, **1989**, 475.

219. Gaviña, F.; Luis, S. V.; Costero, A. M. *React. Polym.*, **1987**, *6*, 291. Gaviña, F.; Gil, P.; Palzón, B., *Tetrahedron Lett.*, **1979**, *15*, 1333.

220. Clennan, E. L.; Earlywhite, A. D., *J. Am. Chem. Soc.*, **1987**, *109*, 7105.

221. Grierson, L.; Perkins, M. J.; Rzepa, H. S., *J. Chem. Soc., Chem. Commun.*, **1987**, 1779. Rzepa, H. S., *J. Chem. Res.,(S)*, **1988**, 254.

222. Chung, W-S; Turro, N. J.; Srivastava, S.; Li, H.; le Noble, W. J., *J. Am. Chem. Soc.*, **1988**, *110*, 7882.

223. Mehta, G. A.; Khan, F. A., *J. Am. Chem. Soc.*, **1990**, *112*, 6141.

224. Kleingeld, J. C.; Nibbering, N. M. M.; Grabowski, J. J.; DePuy, C. H.; Fukada, E. K.; McIver, R. T., *Tetrahedron Lett.*, **1982**, *23*, 4755. Johlman, C.L.; White, R. L.; Sawyer,

D. T.; Wilkins, C. L., *J. Am. Chem. Soc.*, **1983**, *105*, 2091.

225. Dewar, M. J. S.; Storch, D. M., *J. Chem. Soc., Chem. Commun.*, **1985**, 94.

226. Madura, J. D.; Jorgensen, W. L., *J. Am. Chem. Soc.*, **1986**, *108*, 2517. Jorgensen, W. L., *Acc. Chem. Res.*, **1989**, *22*, 184.

227. Williams, I. H.; Maggoria, G. M.; Schowen, R. L., *J. Am. Chem. Soc.*, **1980**, *102*, 7831. Williams, I. H.; Splanger, D.; Femec, D. A.; Maggiora, G. M; Schowen, R. L., *J. Am. Chem. Soc.*,**1983**, *105*, 31.

228. Ventura, O. N.; Coitiño, E. L.; Irving, K.; Iglesias, A.; Lledós, A., *J. Mol. Struct. (Theochem).*, **1990**, *210*, 427.

229. Kinns, M.; Sanders, J. K. M., *J. Magn. Reson.*, **1984**, *56*, 518.

230. Perpic-Dumont, M.; Reynolds, W. F.; Enriquez, R. G., *Magn. Reson. Chem.*, **1988**, *26*, 358.

231. Kushner, A. S., *Tetrahedron Lett.*,**1971**, 3275.

232. Coxon, J. M., Gibson J. R, *Aust. J. Chem.*, **1981**, *34*, 2577.

233. Aylward, G. H.; Findlay, T. J. V., *"SI Chemical Data"*, Second edition, **1974**.

234. Haasnoot C. A. G.; De Leeuw F. A.A. M.; Altona, C.,*Tetrahedron*, **1980**, *36*, 2783.

235. Garbisch, E. W., *J. Am. Chem. Soc.*, **1964**, *86*, 5561.

236. Ounsworth, J.P.; Weiler, L., *J. Chem. Educ.*, **1987** *64*, 568.

Acknowledgments.

I wish to thank several people for the help and support I have received during the period of study which this thesis records.

Firstly my thanks go to the supervisor of my research, Dr J. M. Coxon, who created a research environment which was both stimulating and challenging while encouraging independence of thought and action. Doctors P. J. Steel and R. G. A. R. Maclagan also provided invaluable help with aspects of this work.

I would also like to thank my fellow students Siew Fong, for sharing her experience in the chemistry of cage compounds, and Andrew Burritt for stimulating discussions and taking the colour photographs which appear in this thesis.

Finally I am indebted for the love and support I have received from my family especially over the period in which this thesis was under preparation. In particular I wish to thank my parents, Shirley and Dugald McDonald and my wife, Bea Cheer